



University  
of Glasgow

Chick, Helen Elizabeth (2011) *Assessing the potential of non-integrating lentiviral vectors for cardiovascular gene therapy*. PhD thesis.

<http://theses.gla.ac.uk/3045/>

Copyright and moral rights for this thesis are retained by the author

A copy can be downloaded for personal non-commercial research or study

This thesis cannot be reproduced or quoted extensively from without first obtaining permission in writing from the Author

The content must not be changed in any way or sold commercially in any format or medium without the formal permission of the Author

When referring to this work, full bibliographic details including the author, title, awarding institution and date of the thesis must be given

# **Assessing the Potential of Non-Integrating Lentiviral Vectors for Cardiovascular Gene Therapy**

**Helen Elizabeth Chick  
B.Sc. (Hons)**

Submitted in the fulfilment of the requirements of the degree of  
Doctor of Philosophy (Ph.D.) in the College of Medical, Veterinary  
and Life Sciences, University of Glasgow

British Heart Foundation Glasgow Cardiovascular Research Centre,  
Institute of Cardiovascular and Medical Sciences, College of Medical,  
Veterinary and Life Sciences, University of Glasgow

June 2011

© H. E. Chick 2011

## Author's Declaration

I declare that this thesis has been written entirely by myself and is a record of work performed by myself. This thesis has not been submitted previously for a higher degree. The research was carried out in the Institute of Cardiovascular and Medical Sciences, University of Glasgow, under the supervision of Professor Andrew H. Baker.

Helen E. Chick

June 2011

## Acknowledgments

I would like to thank my supervisor, Professor Andrew H. Baker for his advice, guidance and expertise throughout my studies. I would also like to acknowledge Professor Adrian J. Thrasher for his expertise towards this Ph.D. I would also like to thank the British Heart Foundation for the funding of this work.

Big thanks to all the fantastic friends I have made during my time at the BHF GCRC. I would especially like to thank Dr. Robert McDonald and Dr. Angela Bradshaw for their constant help, support, advice and guidance during the last 3 years. I would like to acknowledge the help of Dr. Angelika Kritz and Dr. Nicole Kane for getting me through the first months. I would also like to thank Dr. Raul Alba for his expertise in molecular techniques. Thank you to Nicola Britton and Gregor Aitchison for their technical expertise and to everyone else on the fourth floor of the BHF GCRC past and present.

Most importantly, I want to thank Jennifer MacLachlan, Stacy Wood, Alison Teyhan, Luisa Frei, Aiste Monkeviciute, Allen Kelly and Natalie Fox for listening, putting up with me, providing fantastic and sensible advice and being awesome friends. I couldn't have made it through my Ph.D. without all of you! Many thanks belong to my Ph.D. buddies within the BHF GCRC and the university, for their support, advice and friendship, and reminders of life and fun outside post-graduate studies. Thanks are also due to my friends from home (Street/Glastonbury, Somerset), University of Surrey (acquired from my undergraduate years) and GlaxoSmithKline (in particular Dr. Irene Papanicolaou) for their support and encouragement.

Finally, special thanks to my family for all their support throughout my studies, and in particular my Mum and my Step-Dad for listening to me, consistently supporting and encouraging me, believing in me and for quoting "always look on the bright-side of life!". Thank you so much and I dedicate this to you both! Last but not least, I also dedicate this thesis to my father, the late Alan Martin Chick, to who nurtured me in the "world of science" when I was a child. This is for you Dad!

# Table of Contents

Author's Declaration .....	2
Acknowledgments .....	3
List of Figures .....	10
List of Tables.....	13
List of Appendices .....	14
List of Publications, Awards and Presentations .....	15
List of Abbreviations, Acronyms and Symbols .....	17
Summary .....	23
1 Introduction.....	26
1.1 General introduction .....	27
1.2 Cardiovascular diseases.....	27
1.2.1 Structure of a blood vessel .....	28
1.2.2 Atherosclerosis .....	29
1.2.3 Revascularisation.....	30
1.2.3.1 Pathogenesis of the neointima formation .....	31
1.3 Therapeutic interventions for acute vascular injury .....	36
1.3.1 Drug-eluting stents.....	36
1.3.2 Molecular interventions .....	37
1.4 Gene therapy.....	38
1.5 Gene therapy clinical trials .....	39
1.6 Gene therapy for CVD.....	40
1.7 Cardiovascular gene therapy clinical trials .....	40
1.8 Requirements of a gene transfer vector to the vasculature .....	42
1.9 Viral vectors .....	46
1.10 Lentiviral vectors .....	46
1.10.1 Retroviruses.....	46
1.10.2 Lentiviruses to lentiviral vectors.....	51
1.10.2.1 Biosafety and improved lentiviral vector performance .....	53
1.10.3 Lentiviral gene therapy applications .....	57
1.10.4 Lentiviral-mediated gene transfer to the vasculature.....	60
1.11 Optimisation of lentiviral vectors .....	62
1.11.1 Promoter alternation .....	63
1.11.2 Pseudotyping.....	65
1.11.3 Integration-deficient lentiviral vectors .....	69

1.11.3.1	Integrase proteins .....	69
1.11.3.2	Development of non-integrating lentiviral vectors .....	72
1.12	Therapeutic genes for the vasculature .....	78
1.12.1	Nogo-B .....	81
1.12.1.1	Functional roles of Nogo-B .....	83
1.12.1.2	Nogo-B has a regulator of vascular remodelling.....	85
1.13	<i>Ex vivo</i> and <i>in vivo</i> gene delivery for vascular injury .....	90
1.14	Aims of Thesis .....	91
2	Materials and Methods.....	92
2.1	Chemicals .....	93
2.2	Cell culture .....	93
2.2.1	Isolation and culture of primary vascular cells .....	93
2.2.1.1	Isolation of vascular endothelial cells from human saphenous veins .....	93
2.2.1.2	Isolation of vascular smooth muscle cells from human saphenous veins .....	96
2.2.1.3	Immunocytochemical characterisation of vascular smooth muscle cells .....	96
2.2.2	Maintenance of established cell lines and primary cells .....	98
2.2.3	Cryopreservation and recovery of cultured cell lines and primary cells .....	99
2.3	Plasmid DNA .....	100
2.3.1	Transformation of competent bacteria .....	100
2.3.2	Glycerol stocks of transformed competent bacteria.....	100
2.4	Plasmid preparation.....	104
2.4.1	Plasmid DNA isolation and purification from bacterial cells.....	104
2.4.1.1	Small scale preparation of plasmid DNA (Miniprep) .....	104
2.4.1.2	Large scale preparation of plasmid DNA (maxiprep) .....	105
2.5	Quantification of nucleic acids .....	107
2.6	Restriction endonuclease digestion .....	108
2.7	Gel electrophoresis.....	108
2.7.1	Agarose gel electrophoresis .....	109
2.8	Cloning of Nogo-B into the lentiviral vector construct plasmid.....	115
2.8.1	Polymerase Chain Reaction (PCR) .....	115
2.8.1.1	Nogo-B strategy for PCR cloning.....	115

2.8.2	PCR or restriction endonuclease digestion product purification from agarose gel.....	116
2.8.3	Intermediate plasmid preparation.....	117
2.8.4	DNA sequencing.....	121
2.8.5	Ligation of Nogo-B cDNA into lentiviral vector construct plasmid	125
2.8.5.1	Dephosphorylation of plasmid DNA ends .....	125
2.8.5.2	Ligation of Nogo-B cDNA into digested lentiviral vector construct plasmid DNA.....	125
2.9	Lentiviral vectors .....	126
2.9.1	Lentiviral vector production.....	126
2.9.2	Concentration of lentiviral vector production .....	127
2.10	Determining lentiviral vector titres.....	128
2.10.1	Visual eGFP titre .....	129
2.10.2	Quantitative Real-Time PCR titre.....	129
2.10.2.1	DNA extraction .....	129
2.10.2.2	TaqMan Quantitative PCR.....	130
2.11	Adenoviral vectors.....	135
2.11.1	Production of adenoviral vectors expressing Nogo-B .....	135
2.11.2	Adenovirus purification using CsCl density gradient purification centrifugation .....	136
2.12	Determining adenoviral vector titres .....	137
2.12.1	Micro-BCA assay .....	137
2.12.2	Titration of adenovirus by end-point dilution assay .....	137
2.13	<i>In vitro</i> infections.....	139
2.13.1	<i>In vitro</i> infections with lentiviral vectors.....	139
2.13.2	<i>In vitro</i> infections with adenoviral vectors .....	139
2.13.3	Fluorescence microscopy.....	139
2.13.4	Protein extraction.....	140
2.13.4.1	Cell lysis.....	140
2.13.4.2	Protein isolation from supernatant.....	140
2.13.5	Determination of protein concentration.....	141
2.13.6	Green Fluorescent Protein (GFP) assay .....	141
2.13.7	Efficiency and longevity of transgene expression of continuous culture .....	142
2.13.8	Western blot analysis .....	142

2.13.8.1	Electrophoresis.....	142
2.13.8.2	Western immunoblotting .....	143
2.13.8.3	Densitometric quantification of protein bands.....	147
2.13.9	Immunocytofluorescence .....	147
2.13.10	Confocal microscopy.....	148
2.13.11	Scratch-wound mediated cell migration assay.....	149
2.13.12	3-(4, 5-Dimethylthiazol-2-yl)-2, 5-diphenyltetrazolium bromide (MTT) assay .....	149
2.13.13	Caspase-3/7 assay.....	150
2.14	Statistical analysis.....	151
3	Optimisation of Lentiviral Vectors for Vascular Cell Gene Transfer.....	153
3.1	Introduction .....	154
3.2	Results.....	158
3.2.1	Promoter alternation for lentiviral-mediated transgene expression in human primary vascular cells .....	158
3.2.1.1	The SFFV promoter compared to the UCOE promoter for lentiviral-mediated transgene expression in HeLa cells: efficiency and longevity. ....	158
3.2.1.2	The SFFV promoter compared to the UCOE promoter for lentiviral-mediated transgene expression in VECs: efficiency and longevity .....	164
3.2.1.3	The SFFV promoter compared to the UCOE promoter for lentiviral-mediated transgene expression in VSMCs: efficiency and longevity .....	167
3.2.2	Pseudotyping lentiviral vectors .....	172
3.2.2.1	Pseudotyped-lentiviral transduction efficiency on rat neuronal cells .....	172
3.2.2.2	Pseudotyped-lentiviral transduction efficiency on human vascular cells.....	175
3.2.3	Non-integrating lentiviral vectors for gene transfer in vascular cells .....	182
3.2.3.1	Non-integrating lentiviral-mediated gene delivery in vascular endothelial cells.....	182
3.2.3.2	Non-integrating lentiviral-mediated gene transfer in vascular smooth muscle cells.....	189

3.3	Discussion .....	195
4	<i>In Vitro</i> Assessment of Lentiviral Gene Transfer of Nogo-B in Human Vascular Smooth Muscle Cells .....	201
4.1	Introduction .....	202
4.1.1	Nogo-B, a regulator of vascular remodelling.....	202
4.2	Results.....	204
4.2.1	Cloning of cDNA encoding Nogo-B into a lentiviral vector construct plasmid .....	204
4.2.2	Effect of integrating lentiviral gene transfer of Nogo-B on vascular smooth muscle cells migration and proliferation .....	211
4.2.2.1	Integrating lentiviral-mediated Nogo-B over-expression.....	211
4.2.2.2	Assessment of the effects of int-LV-Nogo-B on VSMC migration .....	216
4.2.2.3	Assessment of the effects of int-LV-Nogo-B on VSMC proliferation.....	218
4.2.3	Effect of non-integrating lentiviral gene transfer of Nogo-B on vascular smooth muscle cells migration and proliferation.....	221
4.2.3.1	Non-integrating lentiviral-mediated Nogo-B over-expression	222
4.2.3.2	Assessment of the effects of NILV-Nogo-B on VSMC migration ... ..	225
4.2.3.3	Assessment of the effects of NILV-Nogo-B in VSMC proliferation .....	228
4.3	Discussion .....	231
5	Analysis of the Mechanism of Action of Nogo-B .....	237
5.1	Introduction .....	238
5.1.1	Association of Nogo-B with VSMC apoptosis and ER-stress .....	238
5.1.2	The association of Nogo-B with signal transduction.....	241
5.2	Results.....	243
5.2.1	Assessment of the effects of lentiviral-mediated Nogo-B over-expression on VSMC apoptosis.....	243
5.2.2	Over-expression of Nogo-B co-localised with the ER.....	245
5.2.3	Assessment of the effects of Nogo-B over-expression on BiP.....	248
5.2.4	Assessment of the effects of Nogo-B over-expression on VSMC intracellular signalling mechanism .....	250
5.3	Discussion .....	261

6	General Discussion .....	267
	List of References .....	275
	Appendices .....	306

## List of Figures

Figure 1.1. The structure of a normal blood vessel. ....	29
Figure 1.2 Pathogenesis of the neointima formation (NIF). ....	33
Figure 1.3. Pathogenesis of vascular bypass graft failure. ....	34
Figure 1.4. Basic features of genomes of retroviruses. ....	49
Figure 1.5. Retroviral replication cycle. ....	50
Figure 1.6. The genome (proviral DNA) structure of a wild-type HIV-1 lentivirus. .....	51
Figure 1.7. A schematic representation of lentiviral vector production. ....	54
Figure 1.8. A schematic representation of the plasmids used in the second generation lentiviral vector production. ....	55
Figure 1.9. A schematic representation of lentiviral vector infection/transduction within a target cell of either dividing or non-dividing status. ....	59
Figure 1.10. A schematic representation of the optimisation of lentiviral vectors. .....	62
Figure 1.11. A schematic diagram of the integration process. ....	71
Figure 1.12. Structure of the lentiviral integrase protein. ....	72
Figure 1.13. Representation of the non-integration process. ....	75
Figure 1.14. The three major spliced isoforms from the Reticulon-4/Nogo gene. .....	83
Figure 1.15. The involvement of Nogo-B in vascular maintenance and remodelling. ....	89
Figure 2.1. Immunocytochemistry for smooth muscle (SM)-actin in HSV SMCs. ...	98
Figure 2.2. Plasmid DNA maps including restriction endonuclease recognition sites. ....	114
Figure 2.3. Overview of the StrataClone™ blunt PCR cloning protocol. ....	120
Figure 3.1. Illustration of the enhancer-less ubiquitously acting chromatin opening element (UCOE). ....	156
Figure 3.2. Transgene expression efficiency and longevity in HeLa cells mediated by lentiviral vectors under the control of the SFFV or UCOE promoter. ....	161
Figure 3.3. Representative micrographs of the efficiency and longevity of eGFP transgene expression in HeLa cells mediated by lentiviral vectors under the control of the SFFV or UCOE promoter. ....	163

Figure 3.4. Transgene expression efficiency and longevity in VECs mediated by lentiviral vectors under the control of the SFFV or UCOE promoter.....	166
Figure 3.5. Transgene expression efficiency and longevity mediated by SFFV or UCOE promoters in VSMCs.....	170
Figure 3.6. Representative micrographs of the efficiency of eGFP transgene expression in VSMCs mediated by lentiviral vectors under the control of the SFFV or UCOE promoter. ....	171
Figure 3.7. Transduction efficiency of pseudotyped int-LVs on B50s.....	173
Figure 3.8. Representative micrographs of the transduction efficiency and longevity of transgene expression mediated by pseudotyped int-LVs in B50s...	174
Figure 3.9. Transduction efficiency of pseudotyped int-LVs on VECs.....	177
Figure 3.10. Representative micrographs of the transduction efficiency of pseudotyped int-LVs on VECs. ....	181
Figure 3.11. Efficiency and longevity of eGFP expression in VECs mediated by NILVs. ....	185
Figure 3.12. Representative micrographs of the efficiency and long-term eGFP transgene expression in VECs mediated by NILVs.....	188
Figure 3.13. Efficiency and longevity of eGFP expression in VSMCs mediated by NILVs. ....	192
Figure 3.14. Representative micrographs of the efficiency and long-term eGFP transgene expression in VSMCs mediated by NILVs. ....	194
Figure 4.1. Nogo-B attenuates neointima formation in acute vascular injury...	203
Figure 4.2. Plasmid map of lentiviral vector construct/transfer plasmid consisting of the multiple cloning site (MCS).....	206
Figure 4.3. Schematic diagram of the cloning of Nogo-B cDNA into the lentiviral vector construct plasmid. ....	207
Figure 4.4. Plasmid maps of complete lentiviral construct/transfer plasmids for full-length and mutant Nogo-B. ....	208
Figure 4.5. Confirmation for the successful cloning of the complete full-length and mutant lentiviral construct/transfer plasmids.....	210
Figure 4.6. Int-LV-full-length Nogo-B and int-LV-mutant Nogo-B transduction of HeLa cells.....	212
Figure 4.7. Int-LV-full-length Nogo-B and int-LV-mutant Nogo-B transduction in VSMCs. ....	213

Figure 4.8. Int-LV-full-length Nogo-B and int-LV-mutant Nogo-B infection in VSMCs indicated by immuno-fluorescence. ....	215
Figure 4.9. Effect of int-LV-Nogo-B on VSMC migration. ....	217
Figure 4.10. Effect of int-LV-Nogo-B on VSMC proliferation. ....	219
Figure 4.11. Representative images of the effect of int-LV-Nogo-B on VSMC proliferation. ....	220
Figure 4.12. Production of LVs. ....	221
Figure 4.13. Western blot analysis of NILV-Nogo-B transduction in VSMCs. ....	223
Figure 4.14. NILV-Nogo-B transduction in VSMCs indicated by immunocytofluorescence. ....	224
Figure 4.15. Effect of NILV-Nogo-B on VSMC migration. ....	226
Figure 4.16. Representative images of the effect of NILV-Nogo-B on VSMC migration. ....	227
Figure 4.17. Effect of NILV-Nogo-B on VSMC proliferation. ....	229
Figure 4.18. Representative images of the effect of NILV-Nogo-B on VSMC proliferation. ....	230
Figure 5.1. Effect of Nogo-B over-expression mediated by LVs on VSMC apoptosis. ....	244
Figure 5.2. Nogo-B over-expression co-localisation with the ER in VSMCs indicated by immunocytofluorescence. ....	247
Figure 5.3. Effect of Nogo-B over-expression on BiP expression levels in VSMCs. ....	249
Figure 5.4. Optimisation for the percentage of serum to induce VSMC quiescence with low p-Akt and p-ERK 1 & 2 activity. ....	252
Figure 5.5. Optimisation for time points of 15 % serum-stimulation in VSMCs with high p-Akt and p-ERK 1 & 2 activity. ....	254
Figure 5.6. Ad-Nogo-B transduction in VSMCs indicated by immunocytofluorescence. ....	256
Figure 5.7. Effect of Nogo-B over-expression on p-Akt activity levels in VSMCs. ....	258
Figure 5.8. Effect of Nogo-B over-expression on p-ERK 1 & 2 activity levels in VSMCs. ....	260
Figure 5.9. Mechanism of action of Nogo-B on VSMC phenotypic effects. ....	266

## List of Tables

Table 1.1 Summary of characteristics of each gene delivery vector for the vasculature. ....	45
Table 1.2. Therapeutic genes which are key to the NIF inhibition.....	80
Table 2.1. Media used to culture these cells in this study. ....	95
Table 2.2. Plasmid DNA used to produce lentiviral vectors. ....	103
Table 2.3. Restriction endonucleases used in plasmid DNA diagnostic digestions. ....	110
Table 2.4. Primers design for Nogo-B strategy for PCR cloning. ....	116
Table 2.5. Primers for sequencing in StrataClone PCR Cloning Vector pSC-B-amp/kan (ampicillin/kanamycin) with either full-length Nogo-B or mutant Nogo-B cDNA insert.....	123
Table 2.6. Primers for sequencing the lentiviral vector construct plasmid with either the full-length Nogo-B or mutant Nogo-B cDNA insert. ....	124
Table 2.7. Antibodies used for Western immunoblotting.....	146
Table 3.2. Pseudotyped LV protein concentration titres. ....	175

## List of Appendices

Appendix 1. Sequences for full-length Nogo-B and mutant (soluble) Nogo-B. ..	308
Appendix 2. DNA sequencing for the full-length Nogo-B lentiviral construct plasmid.....	312
Appendix 3. DNA sequencing for the mutant (soluble) Nogo-B lentiviral construct plasmid.....	314

## List of Publications, Awards and Presentations

### Publication

Helen E. Chick, Ali Nowrouzi, Robert A. McDonald, Nicole M. Kane, Raul Alba, Manfred Schmidt, Adrian J. Thrasher, Andrew H. Baker. Integrase-deficient lentiviral vectors mediate efficient gene transfer to human vascular smooth muscle cells with minimal genotoxic risk. In preparation for *Atherosclerosis, Thrombosis and Vascular Biology*.

### Presentations

Chick, H. E., McDonald, R. A., Kritz, A. B., Kane, N. M., Alba, R., Sessa, W. C., Thrasher, A. J., and Baker, A. H. Effect of Nogo-B Overexpression in Vascular Smooth Muscle Cell Migration and Proliferation Mediated by Integration-Deficient Lentiviral Vectors. 17<sup>th</sup> Germany Society of Gene Therapy (GSGT) Annual Conference 2010. *Human Gene Therapy*, volume 21, issue 9 and pages 1170-1178. October 2010.

Chick, H. E., McDonald, R. A., Kritz, A. B., Kane, N. M., Alba, R., Sessa, W. C., Thrasher, A. J., and Baker, A. H. Analysing the Effect of Nogo-B Overexpression in Vascular Smooth Muscle Cell Proliferation and Migration Induced by Non-Integrating or Integrating Lentiviral Vectors. 7<sup>th</sup> British Society of Gene Therapy (BSGT) Annual Conference 2010. *Human Gene Therapy*, volume 21, issue 4 and pages 507-525. April 2010.

Chick, H. E., McDonald, R. A., Kritz, A. B., Kane, N. M., Alba, R., Sessa, W. C., Thrasher, A. J., and Baker, A. H. The Overexpression of Nogo-B Mediated by Lentiviral Vectors in Acute Vascular Injury. Scottish Society for Experimental Medicine (SSEM) autumn meeting 2009, Glasgow. Website: <http://www.ssem.org.uk/downloads.asp>.

Chick, H. E., McDonald, R. A., Kritz, A. B., Kane, N. M., Alba, R., Sessa, W. C., Thrasher, A. J., and Baker, A. H. Overexpression of Nogo-B Mediated by Lentiviral Vectors in Acute Vascular Injury. Biomedical Faculties' Post-Graduate Open-Day, University of Glasgow, autumn 2009.

## Awards

University of Glasgow Biomedical Faculties' Open-Day: poster prize 2009.

BSGT young researcher travel award to attend the GSGT.

## List of Abbreviations, Acronyms and Symbols

293 cells	HEK cell line
293T cells	HEK transformed cell line
3'	3 prime end
35K	broad spectrum CC-chemokine binding protein 35/ Vaccina virus strain Lister 35 kDa protein
5'	5 prime end
$\alpha$	alpha
$\beta$	beta
$\Delta$ <i>att</i> site	attachment site deletion
$\Delta$ U3	deletion in U3 region
$\gamma$ c	gamma chain
$\lambda$ max	wavelength of maximum absorption
$\mu$ g	microgram
$\mu$ g/ml	microgram per millilitre
$\mu$ l	microlitre
$\mu$ M	micromolar (micromoles per litre)
$\Psi$	packaging signal
$\Psi \Delta$	packaging signal deletion
$\times g$	relative centrifugal force
AAV	adeno-associated virus
ABC	avidin-biotinylated complex
ADA-SCID	adenosine deaminase-deficient severe combined immunodeficiency
Ad	adenoviral vector
Ad5	adenoviral vector serotype 5
Ad-eGFP	adenoviral vector expressing/gene transfer of eGFP
Ad-Nogo-B	adenoviral vector expressing/gene transfer of Nogo-B
AIDS	acquired immune deficiency syndrome
ALD	adrenoleukodystrophy
amp	ampicillin
ampR	ampicillin resistance
ANOVA	analysis of variance
APS	ammonium persulphate
ARKct	adrenergic receptor kinase
ATF6	transcriptional factor activating transcription factor 6
<i>att</i> site	attachment site
AU	arbitrary units
B50	rat cortical neuronal cell line
BCA	bicinchoninic acid
Bcl-2	B-cell lymphoma 2
Bcl-xL	B-cell lymphoma-extra large
bFGF	basic fibroblast growth factor
BiP	binding immunoglobulin protein
BMI1	BMI1 polycomb ring finger proto-oncogene
BMM	bone-marrow-derived monocyte/macrophage
BMT	bone marrow transplantation
bp	base pairs
BP	band pass
BrdU	bromodeoxyuridine
BSA	bovine serum albumin

C2C12 cell line	mouse myoblast cell line
C-terminal	carboxyl terminal domain
CABG	coronary artery bypass grafting
CAG	cytomegalovirus immediate early enhancer/chicken beta-actin
CBP	cyclic adenosine monophosphate-response element binding protein
CBX3	chromobox homolog 3 gene
CC-CK	CC-chemokine
CCD	charged-coupled device
CCND2	G1/S-specific cyclin-D2 proto-oncogene
CCR5	CC chemokine receptor type 5
CD4	cluster of differentiation 4 glycoprotein
Cdc42	cell division control protein 42 homolog (Rho kinase family monomeric G-proteins)
cDNA	complementary DNA
CHD	coronary heart disease
CHOP	C/EBP homologous protein
CIS	common integration site
cm	centimetres
CMV	Cytomegalovirus
CNS	central nervous system
cPPT	central polypurine tract
CsCl	caesium chloride
CSF-1	colony stimulating factor-1
ct	cycle-threshold
CVD	cardiovascular disease
CXCR4	CXC chemokine receptor type 4
d	day
dNTP	deoxynucleotide triphosphate
ddNTP	dideoxynucleotide triphosphate
dH <sub>2</sub> O	deionised water
DAB	diaminobenzidine
DAPI	4', 6-diamidino-2-phenylindole
DEPC	diethylpyrocarbonate
DES	drug-eluting stent
DMEM	Dulbecco's Modified Eagle's Medium
DMSO	dimethyl sulphoxide
DNase	deoxyribonuclease
DNA	deoxyribonucleic acid
E2F	elongation 2 transcriptional factor
EbolaZ	Ebola Zaire
EC	endothelial cell
ECL	enhanced chemiluminescent
ECM	extracellular matrix
EC-SOD	extracellular superoxide dismutase
EDTA	ethylenediamine tetra-acetic acid
EF1 $\alpha$	elongation factor 1 $\alpha$
EGF	epidermal growth factor
eGFP	enhanced green fluorescent protein
ELISA	enzyme-linked immunosorbent assay
eNOS	endothelial nitric oxide synthase
EOR	ER overload response

ER	endoplasmic reticulum
ERK	extracellular signal-regulated kinase
FACS	fluorescence-activated cell sorting
FAM	fluorescein amidite
FCS	fetal calf serum
GAPDH	glyceraldehyde-3-phosphate dehydrogenase
g/l	gram per litre
g/mole	gram per mole
g/molecule	gram per molecule
GP64	Baculovirus gp64
GRP78	glucose-regulated protein 78 kDa
h	hour
HEK	human embryonic kidney
HeLa cells	human cervical carcinoma cell line
HIV-1	human immunodeficiency virus 1
HMGA2	high-mobility group AT-hook 2 proto-oncogene
HNRPA2B1	heterogeneous nuclear ribonucleoprotein A2/B1 gene
HNTV	Hantavirus/Hantaan
HRP	horse radish peroxidase
HSC	haematopoietic stem cells
HSVEC	human saphenous vein endothelial cell
HSVSMC	human saphenous vein smooth muscle cell
IFN- $\gamma$	interferon-gamma
IL	interleukin
IL-1 $\beta$	interleukin-1 beta
IL2RG	IL-2 receptor gamma gene
iNOS	inducible nitric oxide synthase
int-LV	integrating lentiviral vector
int-LV-eGFP	integrating lentiviral vector expressing/gene transfer of eGFP
int-LV-Nogo-B	integrating lentiviral vector expressing/gene transfer of Nogo-B
int-LV-full-length Nogo-B	integrating lentiviral vector expressing/gene transfer of full-length Nogo-B
int-LV-mutant Nogo-B	integrating lentiviral vector expressing/gene transfer of mutant (soluble) Nogo-B
int-LV-SFFV	SFFV-driven integrating lentiviral vector
int-LV-UCOE	UCOE-driven integrating lentiviral vector
IRE1	inositol-requiring kinase 1
ISR	in-stent restenosis
iu/ml	infectious unit of LV per ml
JAK3	janus kinase 3
JNK	c-JUN NH <sub>2</sub> -terminal kinase
kan	kanamycin
KAT	Kuopio angiogenesis trial
kbp	kilo base pairs
kDa	kilo Dalton
l	litre
lacZ	lacZ gene encoding for $\beta$ -galactosidase
LAM-PCR	linear amplification-mediated PCR
LB	Luria-Bertani
LMO2	LIM-domain only 2 proto-oncogene

LV	lentiviral vector
M	molar (moles per litre)
mAmp	milliamp
MAPK	mitogen-activated protein kinase
MCS	multiple cloning site
MDS1-EVI1	myelodysplasia syndrome 1-ecotropic viral integration site 1 gene
MEM	minimum essential media
mg/l	milligram per litre
MI	myocardial infarction
min	minute
miR	microRNA
ml	millilitre
MLV	murine leukaemia virus
MLV-A	murine leukaemia virus-amphotropic
MLV-E	murine leukaemia virus-ecotropic
mM	millimolar (millimoles per litre)
MMP	matrix metallo-proteinase
MOI	multiplicity of infection
mRNA	messenger RNA
MTT	3-(4,5-dimethylthiazol-2-yl)-2, 5-diphenyltetrazolium bromide
N-terminal	amino-acid terminal domain
Nef	negative replication factor
ng	nanogram
ng/ $\mu$ l	nanogram per microlitre
Ng-BR	Nogo-B receptor
NIF	neointima formation
NILV	non-integrating lentiviral vector
NILV-eGFP	non-integrating lentiviral vector expressing/gene transfer of eGFP
NILV-Nogo-B	non-integrating lentiviral vector expressing/gene transfer of Nogo-B
nm	nanometre
nM	nanomolar (nanomoles per litre)
NO	nitric oxide
Nogo	neurite outgrowth inhibitor
Nogo-66	neurite outgrowth inhibitor -66 loop
Nogo-B	neurite outgrowth inhibitor isoform B
OD	optical density
ODU	units of optical density
p53	tumour suppressor protein 53
p56	tumour suppressor protein 56
PAGE	polyacrylamide gel electrophoresis
p-Akt	phosphorylated-Akt
PB	primer binding site
PBS	phosphate buffered saline
PCI	percutaneous coronary interventions
PCR	polymerase chain reaction
PDGF	platelet derived growth factor
PDGFR	platelet derived growth factor receptor
PDI	protein disulphide isomerase
PEI	polyethylenimine

p-ERK	phosphorylated-extracellular signal-regulated kinase
PERK	protein kinase-like ER kinase
PFA	paraformaldehyde
PGK	phosphoglycerate kinase 1
PI3K	phosphatidylinositol-3-kinase
PIC	pre-integration complex
PMA	phorbol 12-myristate 13-acetate
pmol/ $\mu$ l	picomole per microlitre
PNS	peripheral nervous system
PPT	polypurine tract
PRDM16	PR domain containing 16 gene
PREVENT	project of <i>ex vivo</i> vein graft engineering via transfection
qPCR	quantitative PCR
R	repeat region
Rac	Ras-related C3 botulinum toxin substrate (Rho kinase family monomeric G-proteins)
Rb	retinoblastoma protein
Rev	regulatory viral protein
RFU	relative fluorescent unit
RHD	reticulon homology domain
Rho	Ras homolog gene family protein (Rho kinase family monomeric G-proteins)
RhoA	Ras homolog gene family protein, member A (Rho kinase family monomeric G-proteins)
RLU	relative luminescence unit
RNA	ribonucleic acid
RPE65	retinal pigment epithelium-specific 65 kDa protein
rpm	revolutions per minute
RRE	rev response element
RRM	ready reaction mix
RRV	ross river virus
RT	room temperature
RTK	receptor tyrosine kinase
RTN	reticulon protein
SAP	shrimp alkaline phosphatase
SDS	sodium dodecyl sulphate
sec	seconds
S.E.M	standard error of the mean
SETBP1	SET binding protein 1 gene
SFFV	spleen focus forming virus
SIN	self-inactivating
SM	smooth muscle
SM-actin	smooth muscle-actin
SMC	smooth muscle cell
SM-MHC	SM-myosin heavy chain
SOC	super optimal broth with catabolite repression
SOD	superoxide dismutase
SPRI	solid phase reversible immobilization
SV-40	simian virus-40
SVG	saphenous vein graft
TAMRA	tetramethylrhodamine
Tat	transactivator of transcription
TBE	tris/borate

TBS-T	tris buffered saline-tween
TEMED	tetramethylethylenediamine
Th2	T-lymphocyte helper 2
Tie2	tyrosine kinase 2
TIMP	tissue inhibitors of matrix metalloproteinases
T <sub>m</sub>	melting temperature
TM	transmembrane
TNF- $\alpha$	tumour necrosis factor-alpha
TUNEL	terminal deoxynucleotidyl transferase dUTP nick end labelling
U	unit of restriction enzyme activity
U3	unique 3' region
U5	unique 5' region
UCOE	ubiquitously acting chromatin opening element
UPR	unfolded protein response
UTR	untranslated region
UV	ultraviolet light
V	voltage
v/v	volume per volume
VEC	vascular endothelial cell
VEGF	vascular endothelial growth factor
Vif	viral infectivity factor
Vpr	viral protein R
Vpu	viral protein U
VSMC	vascular smooth muscle cell
VSV-g	vesicular stomatitis virus glycoprotein
w	week
w/v	weight per volume
WAS	Wiskott-Aldrich syndrome
WPRE	woodchuck post-transcriptional regulatory element
X-gal	5-bromo-4-chloro-3-indolyl- $\beta$ -D-galactopyranoside

## Summary

Vascular smooth muscle cell (VSMC) migration and proliferation are important hallmarks in the development of the neointima formation (NIF) following acute vascular injury, contributing significantly to the pathogenesis of post-angioplasty restenosis, in-stent restenosis (ISR) and low lumen patency of coronary artery bypass grafting. At present there are a finite number of pharmacological treatments in use for the prevention of the NIF, such as drug-eluting stents (DES) for ISR and more are under development. Vascular gene delivery strategies have been extensively explored. There is a requirement to identify and provide a safe and effective gene transfer strategy for therapeutic gene delivery to attenuate NIF in the clinical setting. Lentiviral vector (LV)s are efficient in transducing vascular cells and have been considered as useful vectors for delivering therapeutic interventions to reduce the NIF following acute vascular injury *in vivo*. Non-integrating LV (NILV)s offer additional potential for LVs in vascular gene therapy. Nogo-B is a member of the reticulon 4 family of transmembrane proteins, and is expressed in vascular endothelial cell (VEC)s and VSMCs. Nogo-B is a regulator in vascular maintenance and remodelling. Nogo-B has a favourable profile for the prevention of the NIF, because this protein acts as a positive and negative regulator of VECs and VSMCs, respectively. This effect is facilitated by Nogo-B mediated chemo-attraction of VECs, and the antagonism of migration and proliferation of VSMCs in response to platelet derived growth factor (PDGF) and/or serum. Nogo-B is down-regulated following vascular injury, which correlates with the development of NIF. Previously, it was demonstrated that adenoviral-mediated Nogo-B gene transfer facilitated over-expression of Nogo-B, and rescued the injury-induced NIF in two distinct and appropriate *in vivo* models of acute vascular injury (the murine wire-injury model and the porcine vein grafting model).

The aim of this thesis was to assess the potential of NILVs for application to vascular gene therapy, by over-expression of Nogo-B. First, second generation self-inactivating (SIN) LVs were optimised (in terms of promoter alternatives, pseudotyping and integration-deficiency) for transgene expression in human vascular cells. Second, the effects of Nogo-B over-expression on human VSMC migration and proliferation, mediated by NILVs were assessed *in vitro* and

compared to its integrating counterparts. Third, the mechanism of action of Nogo-B on human primary VSMCs was explored *in vitro*.

LVs were evaluated for efficiency and/or longevity in vascular cell gene transfer *in vitro* with regards to alternative internal heterologous promoters, pseudotyping and integration-proficiency versus integration-deficiency. Undoubtedly, both promoters, spleen focus forming virus (SFFV) and enhancer-less ubiquitously chromatin opening element (UCOE) evoked efficient and longevity of [vesicular stomatitis virus glycoprotein (VSV-g) pseudotyped] integrating-LV (int-LV)-mediated eGFP transgene expression in VECs and VSMCs. However in contrast to the UCOE promoter, the SFFV promoter was significantly higher in terms of transgene expression in VECs and VSMCs, and thereby was used in subsequent experiments. Interestingly, int-LVs pseudotyped with Rabies, Baculovirus glycoprotein 64 or Ebola Zaire glycoprotein envelope, demonstrated their potential usefulness in efficient VEC transduction and subsequent eGFP transgene expression. Importantly, VSV-g pseudotyped NILVs were efficient in mediating the expression of eGFP in VECs and VSMCs. Thereafter, these selected VSV-g pseudotyped NILVs under the control of the SFFV promoter were used for therapeutic gene transfer analysis in VSMCs *in vitro*.

A new gene delivery vector, NILV expressing Nogo-B (NILV-Nogo-B) was constructed and analysed *in vitro* for its therapeutic potential in the prevention of NIF associated with acute vascular injury. The Nogo-B cDNA was cloned into a LV construct plasmid (consisting of the SFFV promoter) for the generation of int-LV expressing Nogo-B (int-LV-Nogo-B) and NILV-Nogo-B. Indeed, in contrast to their LV expressing eGFP (LV-eGFP) control vector and un-infected VSMCs (endogenous Nogo-B level), NILV-Nogo-B mediated efficient Nogo-B over-expression in human VSMCs, which led to significant phenotypic effects on migration and proliferation with similar effects to int-LV-Nogo-B. NILV-Nogo-B-mediated gene transfer was as effective as its integrating counterparts in reducing VSMC migration. Interestingly, NILV-Nogo-B was at least as good as int-LV-Nogo-B in inhibiting VSMC proliferation.

The mechanism of action of Nogo-B associated with phenotypic effects on VSMC migration and proliferation was evaluated *in vitro*. Previous reports have implicated Nogo-B as being a pro-apoptotic protein, and therefore the effect of

LV-mediated gene transfer of Nogo-B on VSMC apoptosis was assessed. Evidently, neither int-LV-Nogo-B nor NILV-Nogo-B significantly induced VSMC apoptosis. Over-expression of Nogo-B mediated by int-LV was observed co-localised with the endoplasmic reticulum (ER) in VSMCs. A published report indicated that the over-expression of Nogo-B induced ER-stress mediated apoptosis. Results suggested that Nogo-B over-expression did not significantly induce ER-stress signalling in VSMCs. Interestingly, Nogo-B over-expression significantly reduced ERK 1 & 2 activation in VSMCs, but not Akt signalling transduction pathway, and therefore this could have possible implications in phenotypic effects on VSMC migration and proliferation.

Taken together, this thesis demonstrated that SFFV-driven VSV-g pseudotyped NILVs are efficient for vascular cell gene transfer at least *in vitro*. Additionally, this thesis supports the use of NILV-Nogo-B as a candidate for therapeutic application for the prevention of NIF associated with acute vascular injury during revascularisation *in vivo*. In conclusion, this study addresses important implications for the use of NILVs as a potential therapeutic vector in vascular cell gene delivery studies.

# 1 Introduction

## 1.1 General introduction

Revascularisation procedures are initially effective methods in relieving the symptoms of angina and prolonging survival. Despite this, the development of the neointima formation (NIF) following acute vascular injury is a major contributory factor in post-angioplasty restenosis, in-stent restenosis and coronary artery bypass vascular graft failure. Furthermore, the increasing numbers of revascularisation techniques in the foreseeable future inevitably means that the magnitude of this clinical problem will continue to rise unless novel solutions are explored. There is always on-going need for research, development and target validation of new and far more effective therapies in cardiovascular medicine. At present, there are limited numbers of effective pharmacological treatments for the prevention of the NIF. Vascular gene therapy is one such strategy which has been extensively explored over the years. However, there still remains a need to identify and provide a safe and effective delivery strategy for therapeutic genes to prevent the NIF during acute vascular injury in this clinical setting. Lentiviral vectors (LVs) and their integration-deficient counterparts are potentially suitable gene transfer systems for vascular gene therapy.

## 1.2 Cardiovascular diseases

Cardiovascular diseases (CVDs) refers to a group of disorders affecting the heart and circulatory system and these include: hypertension, coronary heart disease (CHD) [associated with myocardial infarction (MI)], cerebrovascular disease (associated with stroke), peripheral vascular disease and many more diseases that are associated with the cardiovascular system. Although there have been many significant advances in therapeutic interventions for CVDs which have helped to control symptoms and reduce the risk of further health problems, CVDs are still the most common cause of premature death in both men and women worldwide. An estimated 17.1 million people die worldwide from CVDs per year, which represents 29 % of all global deaths (<http://www.who.int>, 2009). It is estimated that CVDs cause approximately 38 % of all deaths in the UK, accounting for approximately 200,000 deaths each year (<http://www.bhf.org.uk>, 2008, <http://www.heartstats.org>, 2009a). It is estimated by 2030 almost 23.6 million people worldwide will die from CVDs, but

mainly from CHD and stroke (<http://www.who.int>, 2009). CHD by itself is the UK's most common cause of death before the age of 75. Current figures for the UK indicate that around 2.5 million people are living with CHD, which accounts for approximately 94,000 deaths every year. CHD still has the highest mortality rate compared to any other human disease such as cancer within the developed world (<http://www.bhf.org.uk>, 2008, <http://www.heartstats.org>, 2010b). Moreover, CHD mortality is higher in Scotland than any other part of the UK, with the highest in the west of Scotland (<http://www.heartstats.org>, 2010a). These current statistics are surprising considering the significant improvements to the management of associated risk factors and medical interventions. With respect to these current issues, there remains a need for research and development of new and more effective therapies in cardiovascular medicine for the prevention and treatment of CVDs. This is why cardiovascular gene therapy is continually under intensive investigation and more so in recent years.

### ***1.2.1 Structure of a blood vessel***

The structure of a normal blood vessel wall consists of three morphologically distinct layers: the tunica intima (inner layer), the tunica media (middle layer) and the tunica adventitia (external layer) (Figure 1.1). The intima consists of a continuous endothelial monolayer (relatively quiescent) that forms a protective barrier between the vessel wall and the blood, and overlies the following: a thin layer of basement membrane, an extracellular proteoglycan rich matrix and an internal elastic lamina. Basement membranes contain type IV collagen, heparan sulphate proteoglycans such as perlecan and syndecans, and laminin. Altogether, these components help maintain VSMCs contractile phenotype state (relatively quiescent). The media layer is mainly composed of vascular smooth muscle cells (VSMCs), surrounded by their own basement membrane, and densely packed into an extracellular matrix (ECM). The ECM consists of types I and III collagen, fibronectin, and chondroitin/dermatan sulphate proteoglycans (such as verican). Medial VSMC dilate or contract the vessel, following responses to intimal cues. The media layer is seated on external elastic lamina. The adventitial layer consists of fibroblasts and VSMCs in a loose interstitial matrix, which also contains small blood vessels and lipids. All layers support the structural integrity of a blood vessel (Figure 1.1) (Newby and Zaltsman, 2000).

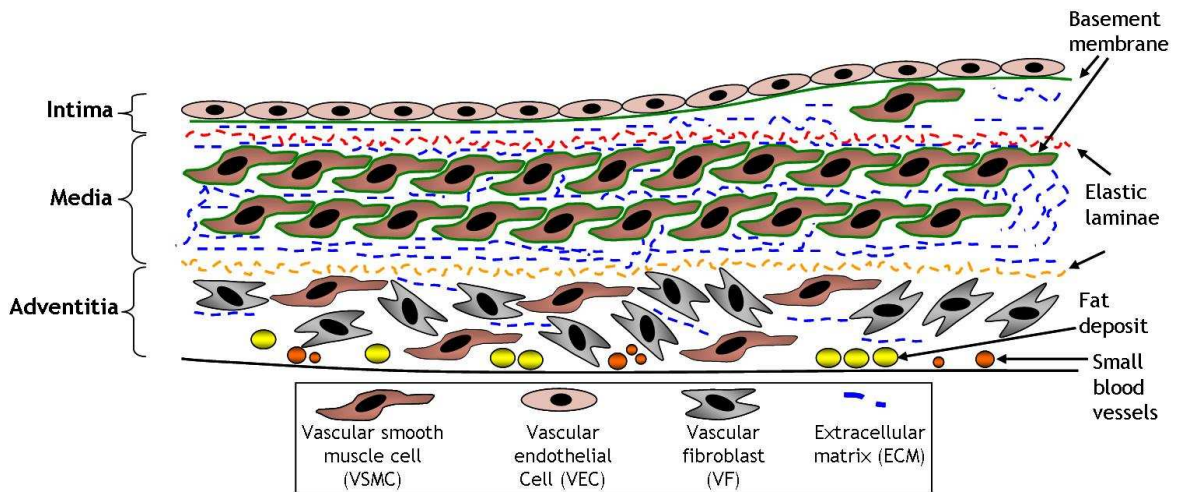


**Figure 1.1. The structure of a normal blood vessel.**

This schematic diagram highlights the three morphologically distinct layers of a normal blood vessel. The intima consists of a continuous endothelial monolayer, which overlies the following: a basement membrane, an extracellular proteoglycan rich matrix and internal elastic laminae. The media layer mainly consists of VSMCs surrounded by basement membrane and densely packed into an ECM. The media layer overlies on external elastic laminae. The Adventitia layer consists of VFs and VSMCs in a loose ECM. Adapted from Newby and Zaltsman (2000).

### 1.2.2 Atherosclerosis

Atherosclerosis is one of the known underlying causes of CHD. Atherosclerosis (origin is from the Greek words ‘athero’ meaning gruel or paste and ‘sclerosis’ meaning hardness) is a progressive disease which involves the formation of an atherosclerotic plaque within the vasculature and has a very complex aetiology. Atherogenesis (fatty streak lesions) occurs naturally with increasing age and mainly within large and medium-sized blood vessels such as the aorta, iliac, coronary, femoral and cerebral arteries. Fatty streak lesions are precursors of more complex advanced lesions within the vasculature. Only a small fraction of individuals will experience advanced atheroma plaque developments (complex advanced lesions) associated with modifiable risk factors (for example obesity, hypertension or hyperglycaemia in diabetes mellitus) and/or un-modifiable risk factors (for example age, gender or genetic determinants/family history of CVD, can predispose individuals). These complex advanced lesions cause mechanical obstruction within the lumen of the blood vessel and mediate tissue ischaemia such as myocardial ischaemia (angina) or cerebral ischaemia. These complications predispose individuals to have a MI or stroke, respectively (Ross, 1999, Lusis, 2000, Glass and Witztum, 2001, Libby and Theroux, 2005, Libby et al., 2011).

### **1.2.3 *Revascularisation***

Angina is caused by occlusive advanced atherosclerotic lesions in the coronary arteries (CHD), which requires revascularisation strategies to re-establish the blood flow. These surgical interventions include coronary artery bypass grafting surgery (CABG) and percutaneous coronary interventions (PCIs) such as balloon catheter angioplasty or stent placement (<http://www.bhf.org.uk>, 2010b, <http://www.bhf.org.uk>, 2010a). CABG involves an autologous blood vessel from the chest (i.e. internal mammary artery), leg (i.e. saphenous vein) or arm (i.e. radial artery), which is used to bypass a blockage within the coronary artery. This blood vessel is attached from the aorta and past the point of blockage within the coronary artery, which gives rise to improved blood supply to the heart (<http://www.bhf.org.uk>, 2010b). During a balloon catheter angioplasty procedure, a cardiac catheter with a tightly folded balloon around it, is inserted and inflated in the narrow area of the coronary artery. This expansion diminishes the impeding blockage, hence widening the artery. Balloon-angioplasty may be followed by intravascular implantation of a short tube of expandable bare metal mesh (known as a stent) to prevent elastic re-coil of the artery (<http://www.bhf.org.uk>, 2010a).

Successful revascularisation therapy can provide great clinical benefit in CHD by treating angina and preventing MI, heart failure, and even death, and therefore increasing life expectancy (<http://www.bhf.org.uk>, 2010a, <http://www.bhf.org.uk>, 2010b). However, the long-term clinical effectiveness of a revascularisation procedure (PCI or CABG treated patients) can be (in some cases) greatly compromised due to an abnormal vascular remodelling process associated with a response to acute vascular injury, and this subsequently results in neointima formation (NIF) at the site of therapeutic intervention. The NIF contributes to the pathogenesis of post-angioplasty restenosis, in-stent restenosis (ISR) and vascular conduit bypass graft failure. The long-term clinical success of a revascularisation procedure is therefore limited by the occurrence of the NIF, which results in recurrent symptoms, such as angina, and possible clinical complications including MI and heart failure. As a consequence, a repeated revascularisation procedure is required, which can impose a major burden on healthcare resources (Mehta et al., 1997, Tsui and Dashwood, 2002, Weintraub, 2007, <http://www.bhf.org.uk>, 2010a). Restenosis is characterised by

the re-occurrence of stenosis (re-occlusion) after a successful PCI. Restenosis occurs in 10-30 % of intravascular stent placements and in 30-50 % of patients receiving balloon-angioplasty interventions, both within 6 months to 1 year post-surgery (Weintraub, 2007). Vascular conduit graft failure is a significant clinical problem in CABG treated patients, with a 15-30 % failure rate within one year post-surgery (Mehta et al., 1997, Buxton and Fuller, 2004, Cho et al., 2006). This increases to approximately 50 % after 10 years (Mehta et al., 1997, Buxton and Fuller, 2004) and a further 15 years results in a failure rate of up to 80 % (Shah et al., 2003, Buxton and Fuller, 2004).

### **1.2.3.1 Pathogenesis of the neointima formation**

In a normal blood vessel (under normal conditions), the vascular endothelium plays an essential role in vessel wall structural integrity and functions as a protective barrier (VECs are tightly packed in a continuous monolayer) between the vessel wall and the blood flow. Fully differentiated medial VSMCs are quiescent and exhibit very low levels of proliferative and apoptotic activities, and as a result are rarely induced to migrate and proliferate to re-establish vascular structural integrity (Newby and Zaltsman, 2000).

The major hallmarks that contribute to the NIF following acute vascular injury involve damage to the endothelial monolayer (depletion of VECs), an increase in VSMC migration and proliferation and ECM deposition (Ross et al., 1977, Ross, 1993, Ross, 1995, Ross, 1999, Newby and Zaltsman, 2000). Acute vascular injury mediates a combination of changes in the vasculature, these include vascular structural integrity, stretch forces, shear stress and flow stress, and as a consequence contributes to the NIF associated with an interplay of vascular remodelling events (Newby and Zaltsman, 2000, Mitra et al., 2006, Muto et al., 2010). Briefly, vascular injury induces endothelial dysfunction (injury) and/or medial damage, which mediates the exposure of sub-endothelial connective tissue, and this subsequently disturbs blood flow causing platelet adherence, aggregation and release of platelet-derived growth factor (PDGF) (also released from dedifferentiated VSMCs). As a consequence, PDGF acts as a chemo-attractant mediating phenotypically modified medial VSMCs (from differentiated to dedifferentiated state) to migrate into the intimal layer where they proliferate and produce ECM proteins (Figure 1.2). Moreover, the alteration in

the regulation of ECM also contributes to the NIF. The up-regulation and activation of matrix metalloproteinases (MMPs) contributes to the remodelling of the ECM following acute vascular injury. Subsequently, this up-regulates the degradation of the ECM, and increases medial VSMC migration and proliferation in the intimal layer. In addition, the down-regulation of basement membrane components (type IV collagen, heparin sulphate proteoglycans and laminin) surrounding VSMCs, facilitates the migration of medial VSMCs into the intimal layer following acute vascular injury. Furthermore, VSMCs increase their production of ECM components such as type I collagen, elastin and fibronectin, and PDGF greatly stimulates further collagen and proteoglycan synthesis; all of which contributes to more ECM deposits within the NIF (Figure 1.2) (Newby and Zaltsman, 2000, Raines, 2004b, Mitra et al., 2006, Newby, 2006). There are many growth factors involved in the NIF following response to acute vascular injury (Newby and Zaltsman, 2000, Berk, 2001, Mitra et al., 2006). In terms of CABG, the NIF acts as a precursor for the development of superimposed/accelerated atherosclerosis in vascular bypass graft failure (Figure 1.3) (Bryan and Angelini, 1994, Newby and Zaltsman, 2000, Muto et al., 2010).

VSMCs are not terminally differentiated and are able to modulate their phenotype in response to changing environmental cues. During vascular injury (also occurs with atherosclerosis), VSMCs switch from a contractile (differentiated) to a synthetic (de-differentiated) phenotype, commonly referred to as phenotypic switching (Newby and Zaltsman, 2000, Mitra et al., 2006). Expression of a repertoire of contractile factors (a complex interplay of multiple molecular and cellular regulatory components) contributes to the up-regulation of SMC-specific/-selective marker genes, for example smooth muscle (SM) alpha ( $\alpha$ ) -actin, SM-myosin heavy chain (MHC) and SM22- $\alpha$ , which are required for VSMC specialised contractile function, and exhibit low rate of proliferation and low synthetic activity. Indeed, molecular and cellular regulation of VSMC differentiation is modified during vascular injury, which results in the down-regulation of SMC-specific marker genes, bringing about the phenotypic switching into the synthetic state associated with induced migration and proliferation phenotypic effects (Owens, 1995, Yoshida and Owens, 2005).

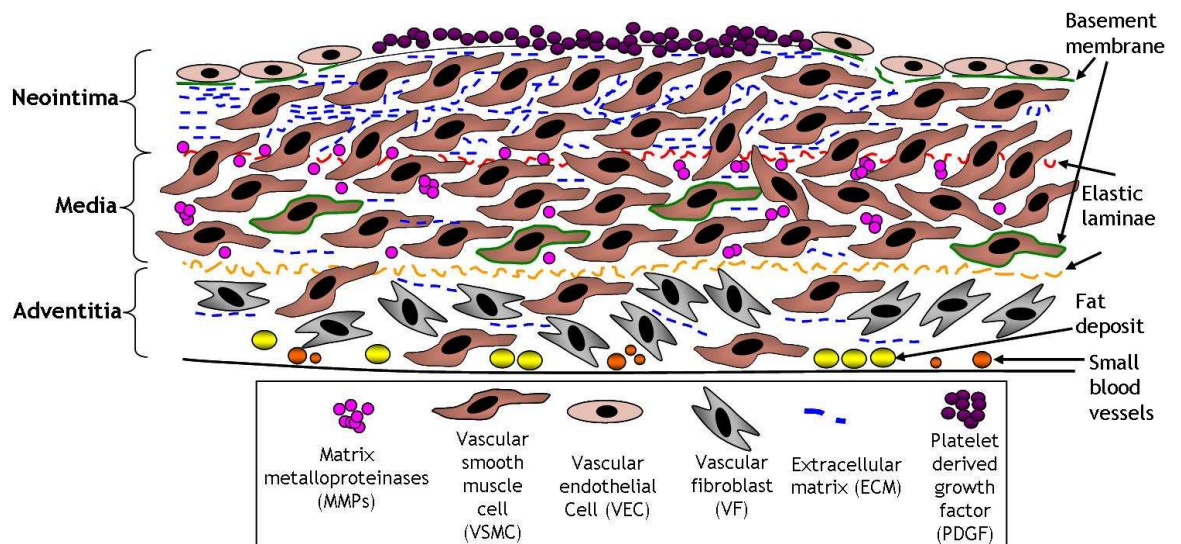


**Figure 1.2 Pathogenesis of the neointima formation (NIF).**

This schematic diagram highlights the events in NIF after acute vascular injury. Vascular injury induces endothelial dysfunction (injury) and/or medial damage, which results in the exposure of sub-endothelial connective tissue. The disruption of blood flow causes platelet adherence, aggregation and release of PDGF. PDGF acts as a chemo-attractant promoting phenotypically modified medial VSMCs to migrate into the intimal layer, where these VSMCs proliferate and produce ECM protein. The up-regulation and activation of MMPs contributes to the remodelling of the ECM following vascular injury and up-regulates the degradation of the ECM, which facilitates medial VSMC migration and proliferation in the intimal layer. The down-regulation of basement membrane components surrounding VSMCs promotes the migration of medial VSMCs. Adapted from Newby and Zaltsman (2000) (Raines, 2004b, Newby, 2006).

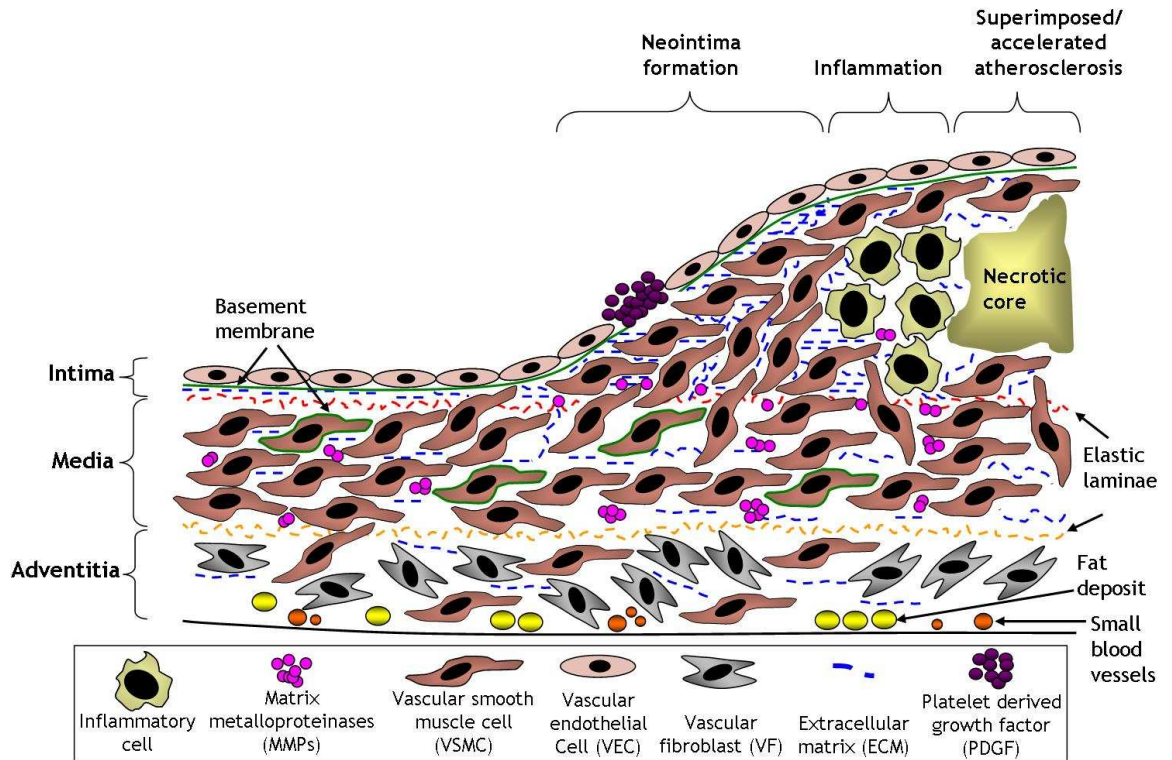


**Figure 1.3. Pathogenesis of vascular bypass graft failure.**

Surgical injury, wall stretch and shear stress facilitates endothelial injury/damage, which subsequently mediates the neointima formation (NIF). NIF encourages a response to inflammation, involving infiltration and interaction of inflammatory cells, macrophage-foam cell formation and accumulation, and ECM production and deposition. Over time, these foam cells die and contribute their lipid-filled contents to necrotic core of the lesion. Thus, the NIF associated with vascular bypass graft failure, forms a template for the development of superimposed/accelerated atherosclerosis. Adapted from George et al., (2006) (Bryan and Angelini, 1994, Newby and Zaltsman, 2000, Muto et al., 2010).

Animal models of vascular injury and human autopsy specimens have been used to define mechanisms/components which contribute to the NIF and to assist with the development of therapeutic strategies to prevent human NIF (Angelini et al., 1992, Lindner et al., 1993, Groves et al., 1995, Kumar and Lindner, 1997, De Scheerder et al., 1999, Schwartz and Henry, 2002, Schwartz et al., 2004, Popov et al., 2008). In a murine wire-injury model, it is well-established that NIF is evident at 2 weeks post-injury. This involves the proliferation of medial VSMCs within days, migration of VSMCs to the intima by 1 week and expansion of the NIF by 3-4 weeks post-injury (Lindner et al., 1993). After approximately 4 weeks post-injury, the repair of the endothelium is complete and VSMCs return to a normal differentiated state with a very low cell turnover (Lindner et al., 1993). In a porcine vein graft model using a saphenous vein as a conduit, NIF is evident between 1-4 weeks post-injury (consisting of migration and proliferation, and a large amount of extracellular matrix) and a slower NIF occurs 4-39 weeks after grafting (Angelini et al., 1992). Both models share key elements and stages associated with the NIF (Angelini et al., 1992, Lindner et al., 1993). In addition, the response to acute vascular injury in humans with regards to precise times of each stage during the vascular remodelling process remains unclear (Weintraub, 2007).

Despite the occurrence of the NIF, revascularisation procedures are still the ideal choice for treatment and prevention of CHD, with improved clinical outcomes outweighing the risks (Hueb et al., 2007, Hueb et al., 2010, Yamaji et al., 2010). The total number of these surgical interventions carried out to treat CHD increases every year. It was reported by the British Cardiovascular Intervention Society in 2008, that 80331 PCIs and 22846 CABG operations were performed in the UK alone (<http://www.heartstats.org>, 2009b). PCIs are considered as the surgical intervention of choice because these procedures are less invasive (<http://www.heartstats.org>, 2010c). The increasing use of revascularisation procedures in the foreseeable future undoubtedly means that this clinical problem (NIF following acute vascular injury) will continue to increase unless novel therapeutic strategies to limit restenosis and increase patency rates are explored and developed (George et al., 2006).

## 1.3 Therapeutic interventions for acute vascular injury

### 1.3.1 *Drug-eluting stents*

Drug-eluting stents (DESs) have significantly reduced the incidence of ISR compared to bare metal bare stents since their introduction in 2002. DESs have become popular in the management of CHD because of the relief of symptoms in most patients and improved survival in those with the most severe disease (Lange and Hillis, 2010). After the DES is inserted, the anti-proliferative agent is gradually released into the blood vessel wall by contact transfer and takes effect over the time course of hours to months, and as a result provides a sustained reduction of the NIF during the acute vascular injury response. This effect is mediated by the cell-cycle inhibition of injured/phenotypically modified vascular cells, especially medial VSMCs (Lange and Hillis, 2010).

The first generation of DESs released sirolimus (Morice et al., 2002, Schofer et al., 2003) or paclitaxel (Stone et al., 2004b, Stone et al., 2004a). These were designed to arrest medial VSMC proliferation, and as a consequence reduce the NIF, the incidence of restenosis and the need for re-intervention; improving clinical outcome (Costa and Simon, 2005). However, data demonstrated that these anti-proliferative compounds were very potent and had long-term effects on other cell types, especially VECs. Paclitaxel inhibited VEC migration, and both paclitaxel and sirolimus inhibited VEC proliferation (Parry et al., 2005). Most importantly giving rise to delayed healing characterised by persistent fibrin deposition and incomplete/delayed re-endothelialisation, which resulted in a risk of late-stent thrombosis (occurs 30 days or more after DES implantation) (Joner et al., 2006, Finn et al., 2007). In spite of the risk, DESs improve clinical outcome in terms of restenosis and therefore the risk does not outweigh the benefits (Jensen et al., 2007). Due to the delayed re-endothelialisation, a dual anti-platelet therapy with aspirin and clopidogrel (for inhibition of platelet aggregation and thrombus formation) is required by at least several months during the perceived endothelial regeneration period (King et al., 2008, Kushner et al., 2009), thereby increasing clinical outcome and improving the therapeutic index of DESs. The second generation of DESs such as the everolimus-eluting stents are more effective in inhibiting ISR and reducing the incidence of late-stent thrombosis, when comparing them to the first generation such as

paclitaxel-eluting stents (Stone et al., 2010). These second generation DESs are currently used in clinical practice and have been since 2006 in the UK (Lange and Hillis, 2010).

Currently there still remains a need to develop innovative new therapies, which combine the beneficial effects of stenting with agents that mediate only the desired effect on vascular cell pathobiology, and therefore, dramatically reduce the incidence of ISR and thrombosis, and greatly improve clinical outcome. Research and development of molecular or gene delivery systems for the prevention of the NIF during acute vascular injury associated with the stent implantation procedure, represents a novel and compelling alternative, which is worthy of investigation.

### **1.3.2 Molecular interventions**

Cell-cycle progression is controlled by a repertoire of cell-cycle regulatory genes for example *c-myc*, *c-myb*, *cdc2* and many others. Therefore, these cell-cycle regulatory genes have roles in cell proliferation. In quiescent cells, the elongation 2 transcriptional factor (E2F) is bound in a protein complex [includes retinoblastoma (Rb) protein] which prevents its binding to its consensus E2F-binding sequence in the promoter regions of cell-cycle regulatory genes. This prevents the stimulation of these cell-cycle regulatory genes/proteins involved in cell-cycle progression (Ehsan and Mann, 2000, Mann and Dzaou, 2000). In proliferating cells (cell-cycle progression), E2F is released from its protein complex (by phosphorylation), and as a result activates cell-cycle regulatory gene expression (Ehsan and Mann, 2000, Mann and Dzaou, 2000).

A strategy to block the function of the transcription factor E2F, involved a double-stranded E2F “decoy” oligonucleotide that consisted of the consensus E2F-binding site. As a consequence, this prevented the interaction of the E2F with the E2F-binding sequence in the promoter regions of cell-cycle regulatory genes, thereby inhibiting their activation and blocking VSMC proliferation and the NIF following acute vascular injury (Morishita et al., 1995). An *ex vivo* study in a rabbit vein graft model demonstrated that vein grafts treated intraoperatively with E2F “decoy” (also known as edifoligide), substantially inhibited the NIF and subsequently inhibited accelerated/ superimposed

atherosclerosis (Ehsan et al., 2001). Based on these promising experimental results, the project of *ex vivo* vein graft engineering via transfection (PREVENT) clinical trials (I to IV) were undertaken (Mann et al., 1999, SoRelle, 2001, Alexander et al., 2005a, Alexander et al., 2005b, Conte et al., 2005, Conte et al., 2006) and to date have provided the most extensive investigations within the molecular therapy approach in the prevention of vascular bypass graft failure.

Despite these promising preliminary clinical results from single-centre phases I and II (PREVENT I and II) in peripheral limb vein grafts and CABG respectively (Mann et al., 1999, SoRelle, 2001), this E2F “decoy” therapy was ineffective in preventing lower extremity vein graft and CABG failure in two large phase III multicentre clinical phases (PREVENT III and IV, respectively) (Alexander et al., 2005b, Conte et al., 2006). These results demonstrated that the edifoligide regime was not efficient in the reduction of the NIF.

## 1.4 Gene therapy

Gene therapy is defined as the insertion/delivery of a gene into an individual’s cell or tissue to correct inherited or acquired pathology by gene replacement, gene over-expression or gene silencing, and therefore to ultimately achieve beneficial/therapeutic effects (<http://www.dh.gov.uk/ab/GTAC/Genetherapy/>, 2011). Gene therapy was originally conceived for the treatment of inherited monogenic disorders such as Duchene’s muscular dystrophy, cystic fibrosis, sickle cell anaemia, severe combined immunodeficiency (SCID) and haemophilia A or B, where gene replacement (replacement of the non-functional gene with the “wild-type”/functional gene) “should” restore a normal phenotype. Gene therapy approaches are also applied to the treatment of acquired diseases including cardiovascular diseases (CVDs) and cancer, and have enormous potential to provide novel and alternative therapeutic interventions for diseases which are currently lacking in suitable therapies. However, the success of gene therapy is restricted by the limited number of suitable vectors for each application and limitations in delivery to the target site, and therefore will depend on further research into optimisation (Edelstein et al., 2004, Edelstein et al., 2007).

## 1.5 Gene therapy clinical trials

Since 1989 to 2010, 1703 gene therapy clinical trials have been approved worldwide (<http://www.wiley.com/legacy/wileychi/genmed/clinical/>, 2011b). Approximately 68.7 % of gene therapy clinical trials have used viral vectors as their vector of choice, whereas approximately 25.1 % have been approved and conducted with the use of non-viral vectors (<http://www.wiley.com/legacy/wileychi/genmed/clinical/>, 2011c). There have been many successful gene therapy clinical phase I/II trials, for example for the treatment of X-linked SCID which is a monogenic disorder of the immune system that occurs exclusively in males. This occurs due to a mutation in the gene that encodes for the common gamma chain ( $\gamma_c$ ) within the receptors (of early lymphoid progenitor cells) for interleukin (IL)-2, IL-4, IL-7, IL-9, IL-15 and IL-21, which gives rise to the absence of janus kinase 3 (JAK3) signal transduction. Thus, the early lymphoid progenitor cells in patients with X-linked SCID are defective in cytokine signalling, resulting in the absence of T-lymphocytes and natural killer (NK) cells, dysfunctional B-lymphocytes and hypogammaglobulinemia. This condition is also commonly known among the general public as “bubble boy” syndrome. Patients with X-linked SCID suffer from recurrent infections, failure to thrive and may die within the first year of life due to an impaired adaptive immune response. In the absence of an effective treatment, allogenic bone marrow transplantation (BMT) has become the therapeutic intervention. However, BMT can be associated with incomplete reconstitution of B-lymphocyte function and/or severe complications such as graft-versus-host disease (Santilli et al., 2008). In addition, gene therapy is another therapeutic intervention that has been explored since 1996 for its possible clinical application. Gene therapy clinical trials were initiated after successful preclinical data of retroviral mediated gene transfer of the functional  $\gamma_c$  gene in lymphoid cells (with a mutated  $\gamma_c$  gene), which resulted in restored receptor expression and function (Candotti et al., 1996, Cavazzana-Calvo et al., 1996, Hacein-Bey et al., 1996, Taylor et al., 1996, Hacein-Bey et al., 1998, Whitwam et al., 1998, Lo et al., 1999, Soudais et al., 2000). *Ex vivo* retroviral gene transfer of the correct  $\gamma_c$  gene in CD34 positive cells [haematopoietic stem cells (HSC)] in X-linked SCID patients, have shown long-term benefits with developed and functional T and B-lymphocytes and NK cells in the normal ranges

of a normal healthy patient (Cavazzana-Calvo et al., 2000, Hacein-Bey-Abina et al., 2002, Gaspar et al., 2004, Hacein-Bey-Abina et al., 2010). Unfortunately, there have been a few cases of adverse events with the onset of leukaemia in these X-linked SCID treated patients, caused by insertional mutagenesis mediated retroviral vectors, which resulted in the expression of endogenous proto-oncogenes (Hacein-Bey-Abina et al., 2003a, Hacein-Bey-Abina et al., 2003b, Hacein-Bey-Abina et al., 2008, Howe et al., 2008). However, these risks are counterbalanced by outstanding results demonstrated in these clinical gene therapy trials, because of the benefits observed and disease-free remission many years after gene delivery in the majority of these patients.

## 1.6 Gene therapy for CVD

Gene therapy for CVD became a new and exciting discipline for the prevention and treatment of a multitude of CVDs, ignited by the earliest successful evidence of *in vivo* vascular gene transfer and expression in VECs by Nabel *et al.* in 1989 (Nabel et al., 1989, Nabel et al., 1990, Nabel et al., 1991). Since that time, intensive investigations (preclinical and clinical trials) have explored viral and non-viral gene delivery vectors for many CVD applications, and these include: complex polygenic traits such as hypertension; acute vascular injury including restenosis and vascular graft bypass failure; ischaemic disease including myocardial or peripheral ischaemia, as well as monogenic disorders (familial hypercholesterolaemia) (Gaffney et al., 2007, Rissanen and Yla-Herttuala, 2007).

## 1.7 Cardiovascular gene therapy clinical trials

In terms of gene therapy clinical trials for CVDs, 144 out of 1703 (8.5 %) have been carried out so far worldwide and this is the second most frequently studied target (<http://www.wiley.com/legacy/wileychi/genmed/clinical/>, 2011a). Pro-angiogenic gene therapy clinical trials for the coronary artery and peripheral vascular disease are the most explored area of cardiovascular gene therapy with several completed clinical trials. This pro-angiogenic gene therapy approach involves the stimulation of neovascularisation (also known as therapeutic angiogenesis). This strategy involves enhancing the development of blood vessels to bypass occluded arteries. Angiogenic growth factors such as vascular

endothelial growth factor (VEGF) are associated with VEC proliferation and migration, which subsequently results in accelerated endothelial repair and tube formation (Gaffney et al., 2007, Rissanen and Ylä-Herttuala, 2007).

To date, clinical investigations carried out in Finland by Seppo Ylä-herttuala *et al.*, have explored VEGF gene transfer mediated by either viral (for example adenovirus) or non-viral vectors in phase I/II trials in patients with severe vascular diseases for pro-angiogenesis and/or anti-restenosis (Laitinen et al., 2000, Makinen et al., 2002, Hedman et al., 2003, Hedman et al., 2009). These studies have demonstrated that these vector delivery systems are well tolerated, safe and feasible for gene transfer (Laitinen et al., 2000, Makinen et al., 2002, Hedman et al., 2003, Hedman et al., 2009). In terms of anti-restenosis, VEGF gene transfer induced nitric oxide (NO) production from the endothelium, which subsequently reduced VSMC proliferation and migration and platelet aggregation, and therefore inhibited the NIF in a preclinical model of vascular disease (Laitinen et al., 1997). However, disappointing results were found in the clinical setting for the prevention of restenosis (Laitinen et al., 2000, Hedman et al., 2003). The clinical importance of this study demonstrates that the most appropriate and efficient gene delivery vector system and therapeutic transgene is critical in design and utility to target restenosis in vascular gene therapy. As a consequence, this may explain why previous work has failed for example transient transgene expression, gene transfer vectors of either non-viral or non-integrating viral systems and better choice of therapeutic gene (Hedman et al., 2011). Therefore, this is an area of interest for this study in terms of vascular gene transfer for the inhibition of NIF following acute vascular injury with an aim to improve or provide an alternative gene delivery vector system coupled with a better choice of therapeutic gene which will be discussed further in this thesis. Nevertheless, in the Kuopio Angiogenesis Trial (KAT) (phase II), a significant improvement in myocardial perfusion was observed in patients treated with adenoviral-mediated VEGF gene transfer in ischaemic hearts (Hedman et al., 2003). Furthermore, another study (phase II) demonstrated that patients with peripheral arterial occlusive disease who received either adenoviral- or plasmid DNA- mediated VEGF gene transfer had improved vascularity (Makinen et al., 2002).

There have been many positive preclinical and phase I/II pro-angiogenic gene therapy trials worldwide. In addition, a number of clinical phase II/III trials have been undertaken, but no advancement to clinical practice due to low gene transfer efficiency (Rissanen and Yla-Herttuala, 2007, Karvinen and Yla-Herttuala, 2010, Hedman et al., 2011). However, overall, many investigations have indicated that pro-angiogenic growth factor gene therapy has the potential to be useful in the clinical setting for CHD and peripheral vascular disease in the foreseeable future.

## **1.8 Requirements of a gene transfer vector to the vasculature**

There are many different types of gene transfer vector systems that have the potential for being useful in vascular gene therapy. Overall, viral vectors have the ability to mediate efficient gene transfer and transgene expression in the vasculature, compared to non-viral vectors which elicit relatively low-levels of gene transfer efficiency and transgene expression (Baker, 2004, Gaffney et al., 2007, Rissanen and Yla-Herttuala, 2007, Karvinen and Yla-Herttuala, 2010). However, safety risks (immunogenicity and toxicity profiles) arise with viral vectors, compared to non-viral vectors (Baker, 2004, Rissanen and Yla-Herttuala, 2007). Another important quality to be considered is the cloning capacity available in the vector genome for the insertion of the transgene cassette. Non-viral vectors have a large cloning capacity, whereas for viral vectors this is determined by the amount of genome that can be excised whilst preserving vector infectivity status (Thomas et al., 2003).

The choice of the most appropriate gene transfer vector for delivery and efficient transgene expression is a critical component in the design and utility for many gene therapy applications. The following are important vector features/characteristics to be considered for vascular gene therapy (for an ideal vector):

- Highly efficient transduction (viral) or transfection (non-viral) for vascular cells with limited gene transfer to non-target cells.

- Ability to mediate gene transfer and transgene expression in dividing and non-dividing cells.
- Ability to mediate sustained transgene expression during the acute vascular injury.
- The level of gene delivery clearly must be sufficient to achieve therapeutic benefit in absence of toxicity, eliciting host immune response (lack of immunogenicity is desirable) and any other potentially deleterious side effects.
- The ease in high vector titre productions at clinical grade.
- Episomal (non-integration) or integration maintenance of transgene without deleterious side effects (such as insertional mutagenesis can occur after integration into the host's genome).
- The vector should have a sufficient cloning capacity.

Table 1.1 illustrates characteristics of each gene transfer vector for the vasculature (Thomas et al., 2003, Baker et al., 2005, Baker et al., 2006, George et al., 2006, Gaffney et al., 2007, Rissanen and Yla-Herttuala, 2007, Waehler et al., 2007, White et al., 2007, Karvinen and Yla-Herttuala, 2010). To date, none of the current vectors fulfil all these qualities required for use in vascular gene therapy (Rissanen and Yla-Herttuala, 2007, Karvinen and Yla-Herttuala, 2010). In addition, viral and non-viral vectors have the ability to be modified to increase their selectivity and efficiency to the vascular tissue, which includes methods of "tropism alternation" such as modifications of the capsid (targeted peptides) or pseudotyping (with different serotype capsids/envelopes) and peptide-targeted liposome/plasmid DNA complexes, respectively (Baker, 2004, Baker et al., 2005, White et al., 2007, White et al., 2008). There is a requirement to identify and provide a safe and effective gene transfer strategy for therapeutic gene delivery to attenuate the NIF following acute vascular injury. Thus, this current study will address an alternative vector system, NILVs, which is an area of interest.

Vector	Cloning capacity	Immunogenicity	Vector genome forms	Advantages	Disadvantages
Plasmid DNA	Unlimited size	Low	Episomal	<ul style="list-style-type: none"> <li>• Safe (limited toxicity)</li> <li>• Ease of production</li> <li>• Ability to transfect dividing and non-dividing cells</li> </ul>	<ul style="list-style-type: none"> <li>• Low transfection efficiency</li> <li>• Non-specific transfection</li> <li>• Poor nuclear trafficking</li> <li>• Transient transgene expression</li> </ul>
Adenoviral vector (serotype 5)	Approximately 8 kbp	High	Episomal	<ul style="list-style-type: none"> <li>• Efficient vascular transduction</li> <li>• High titre production at clinical grade</li> <li>• Ability to transduce dividing and non-dividing cells</li> <li>• Well characterised <i>in vivo</i></li> </ul>	<ul style="list-style-type: none"> <li>• Transient transgene expression</li> <li>• High degree of hepatic tropism following systemic delivery</li> <li>• Viral gene products induce inflammatory and immunogenic responses</li> </ul>
Adeno-associated virus (AAV) (serotype 2)	Approximately 4.5 kbp	Low	Episomal or integrative maintenance	<ul style="list-style-type: none"> <li>• Relatively easy to produce high titres for clinical application</li> <li>• Improved vascular transduction efficiency mediated by AAV pseudotyping/targeting peptides</li> <li>• Good safety profile</li> <li>• Ability to transduce dividing and non-dividing cells</li> <li>• Wild-type virus is non-pathogenic in humans</li> <li>• Sustained transgene expression</li> </ul>	<ul style="list-style-type: none"> <li>• Relatively a low level of vascular transduction efficiency</li> <li>• Partially integrative, with minimal risk of insertional mutagenesis</li> <li>• Limited cloning capacity</li> <li>• After systemic delivery majority of transduction found in the liver</li> </ul>

Vector	Cloning capacity	Immunogenicity	Vector genome forms	Advantages	Disadvantages
Retroviral vector	Approximately 8 kbp	Low	Integrative	<ul style="list-style-type: none"> <li>• Persistent transgene expression</li> <li>• Efficient vascular transduction</li> </ul>	<ul style="list-style-type: none"> <li>• Inability to transduce non-dividing cells</li> <li>• Relatively low-titre productions</li> <li>• Integration may mediate the risk of insertional mutagenesis and oncogenesis</li> </ul>
Lentiviral vector	Approximately 8 kbp	Low	Integrative	<ul style="list-style-type: none"> <li>• Ability to transduce dividing and non-dividing cells</li> <li>• Easy to pseudotype with heterologous envelope glycoproteins</li> <li>• Long-term transgene expression</li> <li>• Efficient vascular transduction</li> </ul>	<ul style="list-style-type: none"> <li>• Difficult to produce high-titres for clinical grade</li> <li>• Integrative- therefore raises safety issues with insertional mutagenesis and oncogenesis</li> </ul>

Table 1.1 Summary of characteristics of each gene delivery vector for the vasculature.

## 1.9 Viral vectors

To date, adenoviral vectors [typically serotype 5(Ad5)] are widely used in gene therapy applications [approximately 23.8% of the total gene therapy clinical trials approved have used adenoviral vectors (<http://www.wiley.com/legacy/wileychi/genmed/clinical/>, 2011c)]. In addition, for cardiovascular gene therapy these vectors hold promise for their use in gene transfer of pro-angiogenic factors (previously mentioned in section 1.7). In terms of vascular gene therapy for the prevention of the NIF, adenoviral vectors are the most commonly used vectors for gene transfer in preclinical studies and clinical trials, and are so far the most promising vectors for the potential use in this clinical setting (Gaffney et al., 2007, Rissanen and Yla-Herttuala, 2007, Karvinen and Yla-Herttuala, 2010). However, Ad5 vector mediates a high degree of hepatic tropism following systemic delivery, which is an undesirable characteristic for many clinical applications in gene therapy. This has led to the successful use of adenoviral vectors in *ex vivo* transduction prior to vein grafting (George et al., 2000, Baker et al., 2006, Kritz et al., 2008) and *in vivo* stent-based delivery (gene-eluting stent) (Johnson et al., 2005, Sharif et al., 2008) in preclinical studies. In addition, recent developments in other vectors have highlighted their potential utility in vascular gene therapy, for example lentiviral vectors (LVs).

## 1.10 Lentiviral vectors

### 1.10.1 Retroviruses

The *retroviridae* family consists of many genera of retroviruses, these include: alpharetroviruses, betaretroviruses, gammaretroviruses, deltaretroviruses, epsilonretroviruses (for all the above, the term oncoretroviruses are still commonly used), spumaviruses and lentiviruses (Federico, 2003, Cann, 2005, Bartholomae et al., 2010), all of which are under development for use in many applications in gene therapy (Bartholomae et al., 2010, Mátrai et al., 2010). All retroviruses have evolved to use their host as a continuous reservoir of viral replication because of their permanent integration into the host genome. Oncoretrovirus infections cause diseases such as cancer, which are mostly benign. Lentiviruses (lenti is the latin word for “slow”) infections are

characterized by relatively long incubations periods, followed by severe and usually fatal disease such as cancer (Federico, 2003).

As previously mentioned, the first gene delivery system to be used successfully for *in vivo* gene transfer into the vasculature was a retroviral vector, namely an amphotrophic murine gamma-retroviral vector (Nabel et al., 1989, Nabel et al., 1990, Nabel et al., 1991). To date, approximately 20.5 % and 1.7 % of the world's gene therapy clinical trials (since 1989 to present) have used retroviral vectors and LVs as their platform vector, respectively (<http://www.wiley.com/legacy/wileychi/genmed/clinical/>, 2011c).

Retroviruses are small envelope RNA viruses. All retroviruses are composed of two single-stranded positive-sense RNAs (except spumaviruses), with a genome that does not serve directly as messenger RNA (mRNA) immediately after infection. Each RNA strand comprises of three basic essential genes: *gag* (encodes structural proteins), *pol* (encodes enzymes such as reverse transcriptase, integrase and protease) and *env* (encodes the viral envelope glycoprotein). The genomic RNA is capped at the 5' region and polyadenylated at the 3' region as expected for a RNA molecule that is expressed by cellular transcription machinery (retrovirus production) (Figure 1.4). The retrovirus particle is comprised of the diploid RNA genome complexed with nucleocapsid proteins (encoded by the *gag* gene), reverse transcriptase, integrase and protease (required for *gag-pol* cleavage and maturation of viral particles), which are encapsulated into a retrovirus capsid (encoded by the *gag* gene), followed by matrix proteins (encoded by the *gag* gene) which assist with the formation of the envelope comprised of viral envelope glycoproteins (encoded by the *env* gene) and host cell-membrane. A glycoprotein comprises of a transmembrane domain and a surface domain (Buchsacher and Wong-Staal, 2000, Palu et al., 2000, Bartholomae et al., 2010).

The replication cycle of the *retroviridae* is shown in Figure 1.5. The virus genome is converted into double stranded DNA molecule by reverse transcriptase in the cytoplasm of the host cell and transported into the cell nucleus in association with matrix proteins and integrase, and this known as the pre-integration complex (PIC). The double stranded DNA molecule is then incorporated into the host's genome by the integrase enzyme. Thereafter,

retroviruses replicate via an integrated DNA intermediate, known as a provirus DNA, as part of the host cell's genome by cellular transcriptional machinery. A provirus DNA is longer than a RNA template due to duplication of direct repeat sequences at the 5 prime end (5') and 3 prime end (3') of the sequence; these elements are known as the long terminal repeats (LTRs) (Figure 1.4). These LTRs are necessary for integration into the host genome, expression of viral genes, and defines the 5' and 3' ends of the provirus DNA (Buchschacher and Wong-Staal, 2000, Palu et al., 2000, Bartholomae et al., 2010).

The retrovirus genome contains essential viral sequences, such as the direct repeat sequences with elements required for reverse transcription, integration and gene expression. The RNA genome comprises the following direct repeat sequences: 5' end (in this order) begins with a repeat region (R) followed by a unique 5' region (U5), and 3' end of the RNA genome terminates with the unique 3' region (U3) followed by a 3' R element (Figure 1.4). During reverse transcription the U3 and U5 regions are duplicated in the proviral DNA and are known as the LTRs. Both LTRs are comprised of the proviral U3, R and U5 regions (in this order) and the arrangements of these regions are required for viral gene expression (Figure 1.4). Attachment (*att*) sites in the 5' and 3' LTRs are essential for proviral DNA integration (Figure 1.4). The U3 region at the 5' LTR contains a viral enhancer-promoter region which facilitates the initiation of transcription at the U3/R junction (Figure 1.4). The proviral genome contains a transcription termination signal at the 3' LTR. In addition, there are other elements within the retroviral RNA genome which are required for reverse transcription, integration and gene expression. The primer binding site (PB) in the 5' end of the RNA genome is essential for reverse transcription for the initiation of the negative-strand DNA synthesis mediated by host's cell derived tRNA primer (Figure 1.4). The polypurine tract (PPT) within the 3' end of the RNA genome is copied to generate a PPT primer site, which is essential to initiate the synthesis of the positive-strand DNA (Figure 1.4). Moreover, another important element within the viral genome is the packaging sequence/signal, which aids the viral RNA to be distinguished from other RNAs generated by the host cell and for RNA encapsidation (Buchschacher and Wong-Staal, 2000, Palu et al., 2000, Buchschacher, 2001). Simple gammaretroviruses for example murine leukaemia viruses (MLV) are the most commonly used retroviruses as delivery vector

systems (Bartholomae et al., 2010). For the rest of this thesis gammaretroviruses will be referred to as retroviruses/retroviral vectors unless otherwise stated.

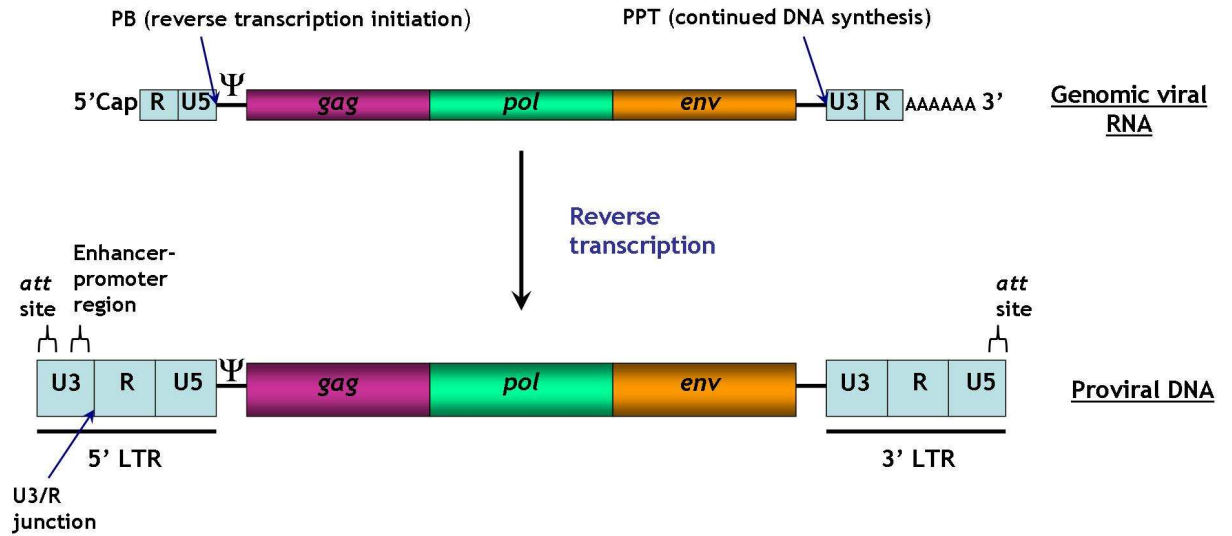


**Figure 1.4. Basic features of genomes of retroviruses.**

Positive sense strands of viral RNA genome is comprised of the *gag*, *pol* and *env* genes, with direct repeat sequences at the 5' and 3' regions: 5' R U5 and 3' U3 R. Primer binding site (PB) is essential for reverse transcription and the polypurine tract (PPT) is necessary for positive-strand DNA synthesis (PPT primer site on negative-strand DNA). This genomic viral RNA is capped (cap) at the 5' and polyadenylated (AAAAAA) at the 3' (by cellular transcription machinery during retroviral production). During reverse transcription the U3 and U5 are duplicated in the proviral DNA and give rise to two identical long terminal repeats (LTRs, U3 R U5 region) at the 5' and 3' regions. Attachment (*att*) sites are required for integration. Enhancer-promoter region and the U3/R junction are required for transcription. Ψ packaging signal/sequence. R, repeat region; U3, unique 3' region; U5, unique 5' region (Palu et al., 2000, Buchschacher, 2001).

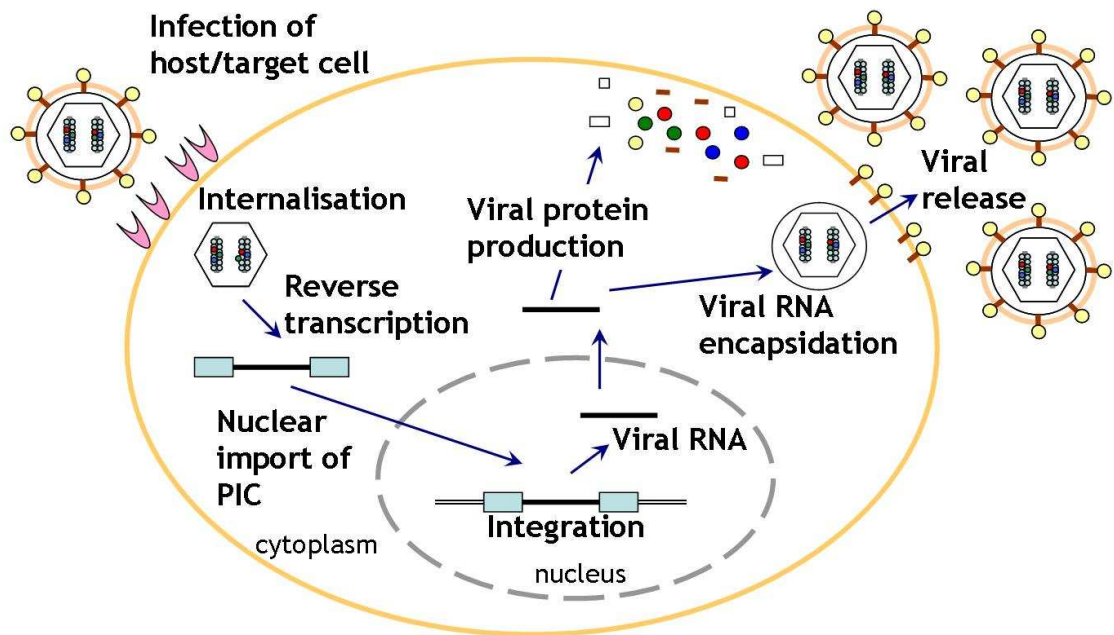


**Figure 1.5. Retroviral replication cycle.**

Infection begins when a retrovirus enters its target (host) cell through interactions between the envelope glycoprotein and the cellular receptor. Viral-cell membrane fusion mediates release of viral core into cell cytoplasm. Viral RNA is reverse transcribed into double-stranded DNA by reverse transcriptase and then transported to the cell nucleus mediated by the pre-integration complex (PIC). Viral DNA is permanently integrated into the host's genome by integrase, and thereafter retroviruses replicate via an integrated DNA intermediate (known as a proviral DNA) as part of the host cell's genome by cellular transcriptional machinery. Proviral DNA is transcribed into viral RNA and translated to produce viral structural proteins and enzymes. These all assemble to form the new virion core (viral RNA encapsidation) and obtain the viral glycoprotein envelope as they bud from the host cell-membrane (Buchschacher and Wong-Staal, 2000, Palu et al., 2000, Bartholomae et al., 2010).

### 1.10.2 Lentiviruses to lentiviral vectors

Lentiviruses are a subclass of retroviruses and these include human immunodeficiency virus type-1 (HIV-1), simian immunodeficiency virus (SIV), feline immunodeficiency virus (FIV) and equine infectious anaemia virus (EIAV). HIV-1 glycoprotein (gp120 and gp41) envelope targets immune cells, primarily CD4<sup>+</sup> expressing T lymphocytes, macrophage and dendritic cells by utilising CD4 (cluster of differentiation 4 glycoprotein) and chemokine co-receptors CCR5 (C-C chemokine receptor type 5) or CXCR4 (CXC chemokine receptor type 4) (Waki and Freed, 2010). The lentivirus HIV-1 genome is very similar to the basic genome organisation of all retroviruses and integrates into the host's genome (see section 1.10.1). In addition, lentiviruses encode two regulatory proteins Tat and Rev essential for viral replication, and four accessory proteins Vif, Vpr, Vpu and Nef necessary for viral replication and/or pathogenesis. The majority of these regulate replication of HIV-1 during its latent period of infection [pre-acquired immune deficiency syndrome (AIDS)] and active AIDS (Federico, 2003, Seelamgari et al., 2004). The genome structure of wild-type HIV-1 lentivirus proviral DNA is shown in Figure 1.6. For the rest of this thesis HIV-1-derived LV is referred to as LV, unless otherwise stated.

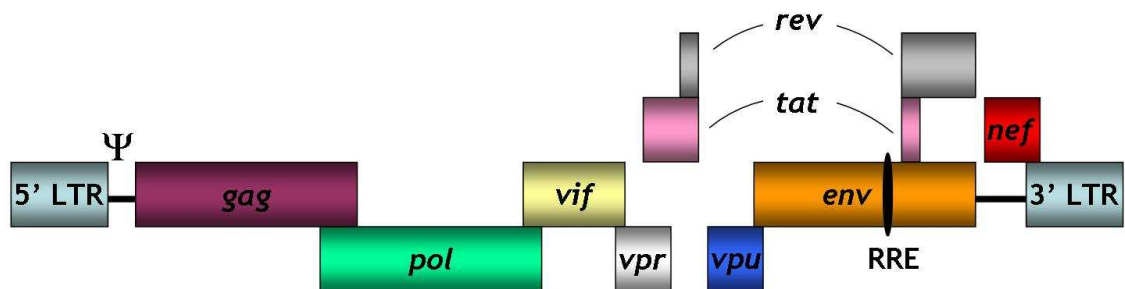


**Figure 1.6. The genome (proviral DNA) structure of a wild-type HIV-1 lentivirus.**

The *gag*, *pol* and *env* genes encode: structural proteins; integrase, protease and reverse transcriptase, and envelope glycoprotein, respectively. *Tat* (transactivator of transcription) and *rev* (regulatory viral protein) genes encode regulatory proteins essential for viral replication. *Vif* (viral infectivity factor), *vpr* (viral protein R), *vpu* (viral protein U) and *nef* (negative replication factor) genes encode accessory proteins essential for viral replication and/or pathogenesis.  $\Psi$ , packaging sequence. LTR, long terminal repeats (Buchschacher and Wong-Staal, 2000, Federico, 2003, Sinn et al., 2005b).

Lentiviruses have the ability to transduce dividing and non-dividing cells, and therefore offer one greater advantage over (gamma)retroviruses as gene transfer vector systems. Retroviruses possess low transduction efficiency for non-dividing cells in comparison to dividing cells. This is because the translocation of the

retrovirus PIC into the nucleus requires the dissolution of the nuclear membrane during mitosis. Unlike retroviruses, lentiviruses mediate gene transfer through the nuclear envelope and into the nucleus of non-dividing cells, which is facilitated by the PIC associated with integrase, matrix protein, Vpr and central polypurine tract (cPPT) (Heinzinger et al., 1994, Naldini et al., 1996b, VandenDriessche et al., 2002). This major attribute led to the development of LVs for their use in gene therapy. These LVs have been genetically engineered to express a therapeutic/marker gene and are devoid of their virulent endogenous viral proteins. Like that of retroviral vectors, the designs of LVs are based on the separation of cis- and trans- acting elements, and therefore are replication-defective. Similar to retroviral vectors, LV gene transfer provides long-term transgene expression because it integrates the gene into the host's genome and will subsequently replicate as part of the target cell's DNA (Naldini et al., 1996b).

Briefly, for retroviral vectors and LVs, their viral vector constructs are generated by deleting their viral genes (*gag*, *pol* and *env*) and replacing them with a transgene of interest under the control of a chosen alternative internal heterologous promoter element. Essential viral sequences known as *cis*-acting elements remain within the construct (transfer plasmid) because they are essential for vector production, reverse transcription, integration and transgene expression such as the two LTRs, PB, PPT, packaging sequence and sequences involved with integration of the proviral DNA (*att* sites). Other viral genes are required for vector production and function (such as the envelope, reverse transcriptase, integrase, matrix proteins and other structural proteins) and these are inserted into separate plasmids or stably integrated into the DNA of a packaging cell line to provide helper functions in *trans*. These viral genes exist in *trans* to improve safety of these vectors, by significantly reducing the possibility of recombination events, which may give rise to replication-component recombinant retroviral vectors or LVs. These vectors are generated by the introduction of the construct/transfer plasmid into either a packaging cell line or a transient co-transfection method with helper plasmids, both providing a single cycle of vector propagation (Buchsacher and Wong-Staal, 2000, Sinn et al., 2005b, Bartholomae et al., 2010, Matrai et al., 2010, Mátrai et al., 2010).

### 1.10.2.1 Biosafety and improved lentiviral vector performance

Most replication defective LVs are produced by transient co-transfection of three plasmids in human embryonic kidney (HEK) 293T cells mediated by polyethylenimine (PEI). This involves the following plasmids: a packaging plasmid, a construct/transfer plasmid (containing the internal heterologous promoter and the gene of interest) and an envelope plasmid (described in Figure 1.7) (Sinn et al., 2005b, Cockrell and Kafri, 2007, Escors and Breckpot, 2010, Matrai et al., 2010). LVs are most commonly pseudotyped with the vesicular stomatitis virus (*Rhabdoviridae*) glycoprotein (VSV-g) envelope. This is because of its broad tropism and stability of vector particles and high-titre stocks during production (Cockrell and Kafri, 2007, Escors and Breckpot, 2010, Matrai et al., 2010). LVs have been developed over the years for biosafety to prevent the emergence of replication-competent wild-type human HIV-1 recombinants and are referred to as ‘generations’ with association to the modified packaging plasmid (*trans*-acting element modifications) (Cockrell and Kafri, 2007, Escors and Breckpot, 2010, Matrai et al., 2010). The first generation comprised of *gag* and *pol* genes, viral regulatory genes *tat* and *rev* and accessory genes *vif*, *vpr*, *vpu* and *nef* in the packaging plasmid (Naldini et al., 1996a). In contrast, the second generation of LVs were engineered to be multiple attenuated. This second generation packaging system involved the deletion of four accessory genes *vif*, *vpr*, *vpu* and *nef*, which had no effect of vector titres and transduction efficiency. Furthermore, this packaging system improved safety because if any recombination events occurred, these replication-competent LVs would be devoid of virulence factors (Zufferey et al., 1997). The Tat and Rev proteins regulate transgene expression (Dull et al., 1998, Buchschacher and Wong-Staal, 2000). Figure 1.8 illustrates the basic *cis*- and *trans*-acting elements within the plasmids used for the production of the second generation LVs (elements mentioned in this figure are discussed later in this section). It was this generation system that was used in this research thesis. The third generation is the latest LVs. The packaging system no longer has the *tat* gene, and the *rev* gene is encoded not in the packaging plasmid, but in a fourth plasmid. This enhances the unlikely possibility of wild-type replication-competent recombinants generation (Dull et al., 1998, Zufferey et al., 1998).

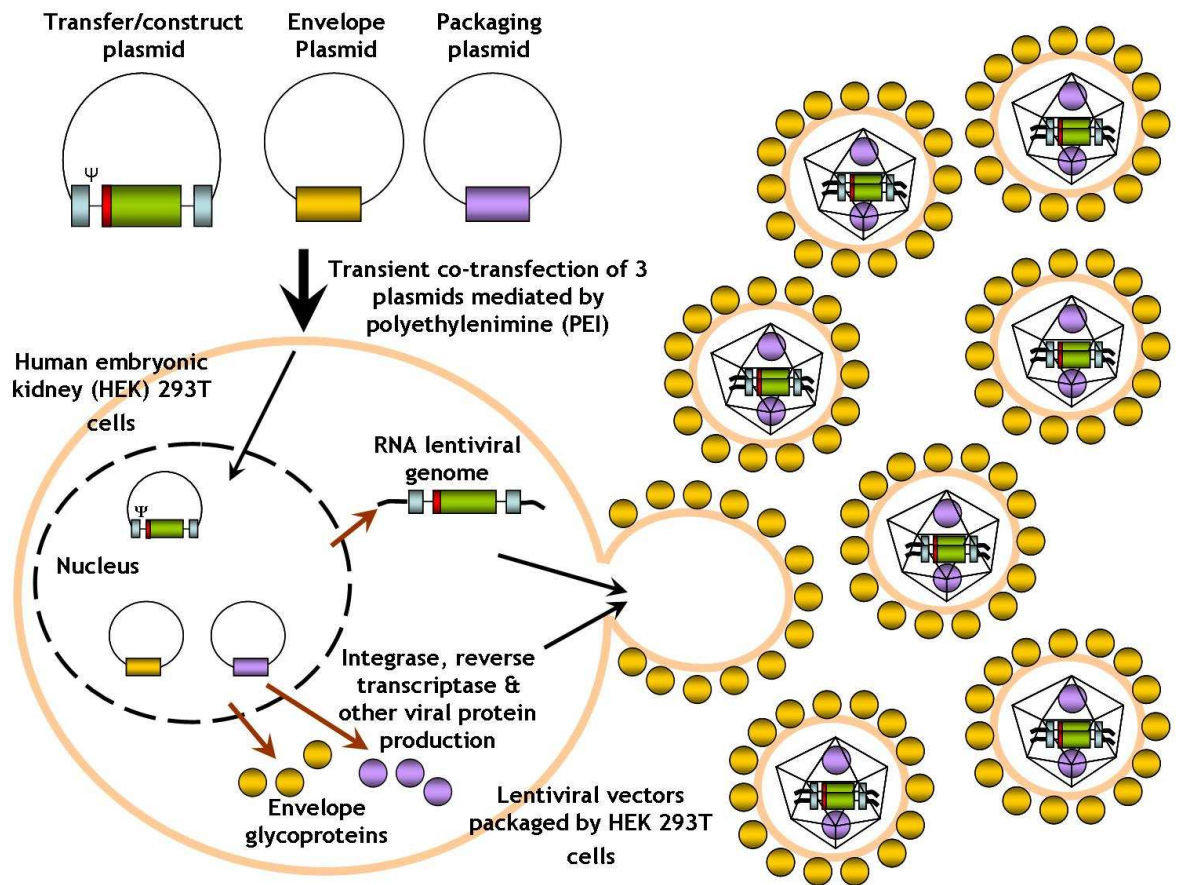


**Figure 1.7. A schematic representation of lentiviral vector production.**

Replication defective lentiviral vectors are produced by a transient co-transfection of three plasmids in human embryonic kidney (HEK) 293T cells mediated by polyethylenimine (PEI). This includes the following three plasmids: a packaging plasmid, a construct/transfer plasmid (comprising of the promoter and the gene of interest) and an envelope plasmid. These plasmids are incorporated into the nucleus. It is here where the transgene is transcribed from the transfer plasmid to make lentiviral vector RNA. Plus, the envelope glycoprotein and viral proteins (including integrase and reverse transcriptase) are transcribed and translated from their corresponding plasmids. Subsequently, this produces functional proteins which are either packaged into the vector particle or are used during the production of these vectors. Lentiviral vectors are packaged by the HEK 293T cells (packaging signal involved in this process,  $\Psi$ ), which is shed from the cell membrane into the cell's supernatant. The important components of these vectors are the vector RNA genome, the lentiviral enzymes integrase and reverse transcriptase. Lentiviral vectors can be harvested from the supernatant and used to infect target cells to mediate gene transfer. Viral genes in *trans*-acting are not carried along with the vector because they lack the *cis*-acting sequences required for propagation, thus rendering these vectors replication-defective. Adapted from Verma and Somia (1997) (Zufferey et al., 1997, Buchsacher and Wong-Staal, 2000).

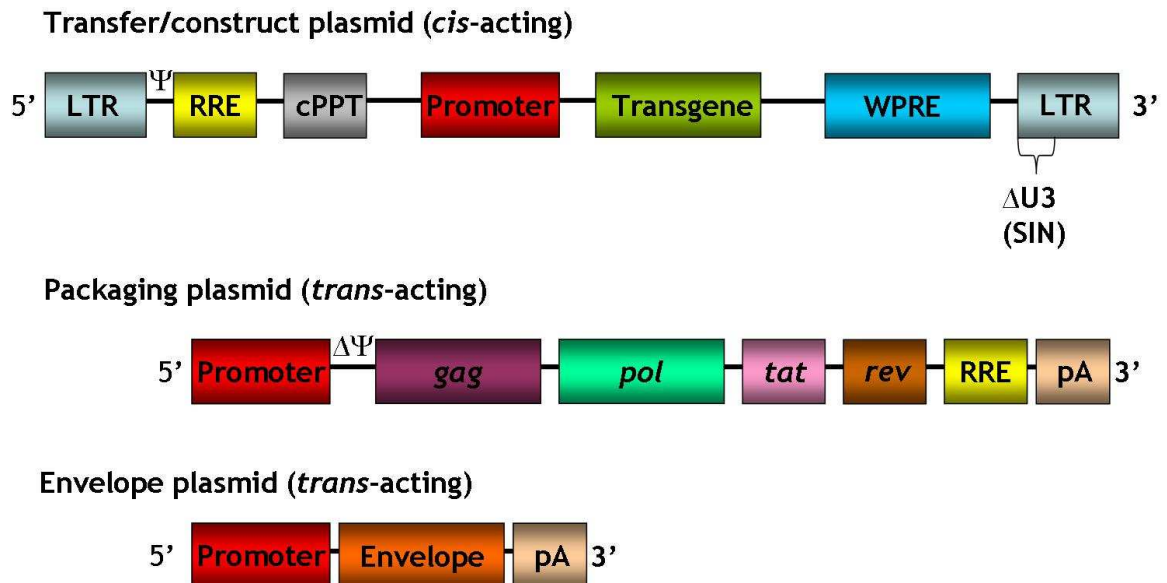


**Figure 1.8.** A schematic representation of the plasmids used in the second generation lentiviral vector production.

This second generation packaging system of these self-activating (SIN) lentiviral vectors involves the basic *cis*- and *trans*- acting elements within three different plasmids. The transfer/construct plasmid comprises of the following and its *cis*-acting elements: an expression cassette with the gene of interest under the control of an internal heterologous promoter element; Rev responsive element (RRE); Woodchuck post-transcriptional regulatory element (WPRE) and *cis*-acting factors [packaging sequence ( $\Psi$ ), primer binding site (not shown), polypurine tract (not shown), central polypurine tract (cPPT), attachment (*att*) sites (not shown) and long terminal repeats (LTRs)], which are necessary for lentiviral vector production and/or transgene expression. SIN lentiviral vectors were generated by partial deletion in the U3 region, which involved removing the sequence encoding the viral enhancer-promoter ( $\Delta$ U3). The packaging plasmid contains *trans*-acting elements (minus four accessory genes *vif*, *vpr*, *vpu* and *nef*) required for one round of packaging during the lentiviral vector production and/or transgene expression and this includes: the *gag* gene for structural proteins; the *pol* gene for lentiviral enzymes integrase and reverse transcriptase; genes *tat* and *rev* for viral production and transgene expression (all under the control of an internal heterologous viral promoter). Moreover, this plasmid contains a deletion in the packaging sequence ( $\Delta$  $\Psi$ ). The Rev protein binds to the RRE to enhance RNA nuclear export. The envelope plasmid (*trans*-acting) consists of the glycoprotein envelope gene under the control of an internal heterologous promoter sequence. pA, polyadenylation signal (Cochrane et al., 1990, Zufferey et al., 1997, Dull et al., 1998, Zufferey et al., 1998, Zufferey et al., 1999, Sirven et al., 2000, Vigna and Naldini, 2000, Demaison et al., 2002, VandenDriessche et al., 2002, Logan et al., 2004, Cockrell and Kafri, 2007).

The transfer plasmid consists of an expression cassette with the gene of interest under the control of an internal heterologous promoter element, plus *cis*-acting factors which are essential for packaging; reverse transcription and integration (see section 1.10.2). This transfer plasmid has undergone further modifications to improve biosafety (rendering them more replication-defective) and LV performance (Escors and Breckpot, 2010, Matrai et al., 2010). Self-inactivating (SIN) LVs have been engineered by deleting transcriptional regulatory sequences (homogenous viral enhancer-promoter unit), which abolishes the risk of replication-competent recombinants, vector mobilization and host gene transactivation (enhancer-mediated mutagenesis). During reverse transcription, the U3 regions in the 3' and 5' LTRs of the integrated provirus DNA are

generated from the U3 region in the 3' end of the viral RNA genome. The U3 region is important in the 5' LTR of proviral DNA because it contains the LV enhancer-promoter sequence. A modification in the U3 region within the 3' end of the viral RNA genome was introduced [incorporated in the transfer plasmid (Figure 1.8)], which involved a deletion in the enhancer-promoter sequences. During reverse transcription, this deletion was transferred to the 5' LTR of the proviral DNA, hence no viral enhancer-promoter sequences. As a result, this mediates transcriptional inactivation of the 5' LTR, which prevents the production of full-length vector RNA within the target cells/tissue. This modified element minimises the production risk of replication-competent recombinant LVs in transduced target cells/tissue. It is the internal heterogeneous promoter that controls the expression of the transgene. Efficient self-inactivation does not influence vector titre or impair transgene expression. This deletion spares but weakens the 3'-polyadenylation region which is essential for transgene expression (Zufferey et al., 1998). These SIN LVs have enhanced biosafety and have increased the utility of LVs in gene therapy studies over the years (Matrai et al., 2010). For the rest of this thesis, SIN LVs are referred to as LVs unless otherwise stated.

There have been several *cis*-acting element additions to the transfer plasmid, which have demonstrated improvements in LV performance, these include the following: woodchuck hepatitis virus post-transcriptional regulatory element (WPRE); Rev-responsive element (RRE) and central polypurine tract or central flap (cPPT) element. The WPRE mediates the enhancement of viral genomic transcript packaging and thus increases LV titres. Furthermore, this element increases expression of transgenes by regulating the polyadenylation (increased mRNA stability), RNA export (enhanced nuclear export) and translation (Zufferey et al., 1999, Demaison et al., 2002, Sinn et al., 2005b). The RRE remains in or is reintroduced into the LVs because it facilitates Rev-mediated export of RNA from the nucleus into the cytoplasm. Therefore, this element enhances LV titres and increases transgene expression. Furthermore this element is also present on the packaging (*trans*-acting) plasmid (Cochrane et al., 1990, Dull et al., 1998, Buchschacher and Wong-Staal, 2000, Sinn et al., 2005b). The cPPT is normally deleted from the transfer plasmid because it is present in the middle of the HIV genome embedded in the *pol* gene. However, this element is important and thus

reinserted. This cPPT element increases LV titres, enhances the nuclear translocation of the vector genome (PIC), increases total amount of vector genome integrated into the host chromosome and improves gene transfer performance of the vector (Sirven et al., 2000, Demaison et al., 2002, VandenDriessche et al., 2002, Logan et al., 2004, Sinn et al., 2005b). LVs have been indicated to be highly efficient in transduction and mediate enhanced transgene expression in human HSCs with these incorporated elements into the LV transfer plasmid (Demaison et al., 2002). These additional *cis*-acting elements in the SIN second generation LVs will be used in the context of vascular gene delivery within this thesis.

### **1.10.3 Lentiviral gene therapy applications**

Many advantageous characteristics enable LVs to be ideal vectors for gene transfer. LVs resemble retroviral vectors in their ability to provide long-term transgene expression mediated by integration into the target host cell genome. In addition, LVs have the ability to transduce non-dividing cells as well as dividing cells, because these vectors do not depend on the dissolution of the nuclear membrane during mitosis (Naldini et al., 1996b). LVs mediate a relatively low inflammatory response and lessened immunogenicity, thus offer an excellent opportunity for *in vivo* gene transfer with efficient and sustained transgene expression over a long duration (Abordo-Adesida et al., 2005). It is relatively easy to pseudotype LVs with a heterologous viral envelope protein, such as the VSV-g protein which broadens the viral vector tropism and enables this LV to be robust (can be easily concentrated by centrifugation) (Matrai et al., 2010). LVs have a large cloning capacity of approximately 8-10 kbp (Kumar et al., 2001, Matrai et al., 2010). However, LVs are integrative in a semi-random manner, harbouring common integration sites (CIS) within proto-oncogenes (Modlich et al., 2009, Cavazzana-Calvo et al., 2010) with similarities to retroviral vectors (Hacein-Bey-Abina et al., 2003b, Ott et al., 2006, Deichmann et al., 2007, Schwarzwaelder et al., 2007, Hacein-Bey-Abina et al., 2008, Modlich et al., 2009). Therefore, LVs raise safety issues with insertional mutagenesis and oncogenesis (Modlich et al., 2009, Cavazzana-Calvo et al., 2010, Matrai et al., 2010), but with lower frequencies [LV hotspots reflect a benign integration bias rather than oncogenic selection (Biffi et al., 2011)] compared to other retroviral vectors (Montini et al., 2006, Matrai et al., 2010, Biffi et al., 2011). As a

consequence, it is important for integration site analysis to be carried out for monitoring of CIS (Schmidt et al., 2007, Gabriel et al., 2009, Schmidt et al., 2009). LV titres are relatively low compared to other viral vectors (Matrai et al., 2010). In addition, a recent report presented a simple and inexpensive LV production method using caffeine to increase titres of LVs for clinical grade (Ellis et al., 2011). Furthermore, LVs can be engineered to express one or more transgenes and thus aids its appeal as a gene delivery vector (Sinn et al., 2005b). Figure 1.9 illustrates LV-mediated gene transfer, reverse transcription, integration and transgene expression within a target cell of either dividing or non-dividing.

LVs have the potential to achieve permanent therapeutic benefit in the clinic for the following diseases/disorders/applications: neurological (Naldini et al., 1996a, Naldini et al., 1996b, Rahim et al., 2009), haematological (Cavazzana-Calvo et al., 2010, Ward et al., 2011), immunodeficiencies (Mortellaro et al., 2006, Charrier et al., 2007, Marangoni et al., 2009, Zhou et al., 2010), stem cell manipulation (Gropp et al., 2003, Lombardo et al., 2007), somatic cell reprogramming (Chang et al., 2009), liver (Matrai et al., 2011), muscular (Apolonia et al., 2007, Talbot et al., 2010), lung (Buckley et al., 2008), ocular (Yanez-Munoz et al., 2006) and CVD (Dishart et al., 2003a, Cefai et al., 2005, Qian et al., 2006, Yang et al., 2010), and other applications to cells/tissues which are otherwise difficult to transduce (Matrai et al., 2010). Several clinical trials have been approved and are ongoing or being prepared with LV as the vehicle of choice for many gene therapy applications, for example  $\beta$ -thalassemia (Cavazzana-Calvo et al., 2010), adrenoleukodystrophy (ALD) (Cartier et al., 2009), Parkinson's disease (EIAV-LV) (<http://www.oxfordbiomedica.co.uk/>, 2011, Stewart et al., 2011) and Wiskott-Aldrich syndrome (WAS) (Galy et al., 2008).

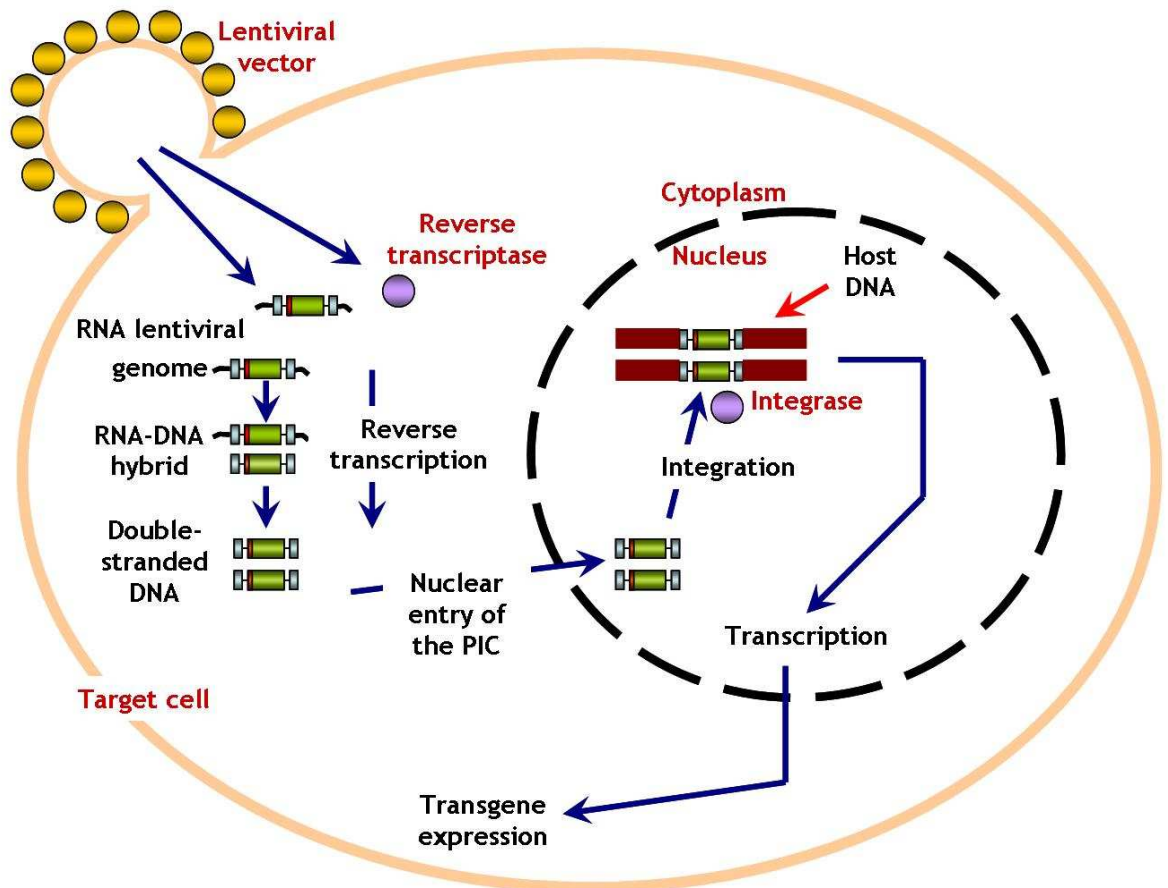


**Figure 1.9. A schematic representation of lentiviral vector infection/transduction within a target cell of either dividing or non-dividing status.**

A lentiviral vector infects the target cell, which allows the RNA vector genome to enter. The lentiviral enzyme reverse transcriptase converts the RNA vector genome into a RNA-DNA hybrid, then into the linear double-stranded DNA molecule, during reverse transcription. The lentiviral vector DNA associated with the pre-integration complex (PIC) is then translocated into the nucleus. The lentiviral vector DNA is then integrated into the host's cell genome, facilitated by the lentiviral enzyme integrase. Finally, the transgene is expressed by the host-cell machinery. Adapted from Verma and Somia (1997).

#### **1.10.4 Lentiviral-mediated gene transfer to the vasculature**

LVs offer an alternative yet promising option for therapeutic vascular gene transfer into the vasculature (George et al., 2006, Gaffney et al., 2007, White et al., 2007), because it is largely comprised of relatively slow dividing vascular cells in a disease state (Gordon et al., 1990) and even during the acute vascular injury response (Westerband et al., 1997, Hilker et al., 2002). LVs have demonstrated to be highly efficient in transduction of VSMCs and VECs (Dishart et al., 2003a, Cefai et al., 2005, Qian et al., 2006, Yang et al., 2010). The VSV-g pseudotyped LV at a short exposure time of 30 minutes *in vitro* demonstrated comparable transduction efficiencies in human VECs and VSMCs to adenoviral vectors (Dishart et al., 2003a, Cefai et al., 2005). Dishart *et al.*, indicated that LVs mediated significantly higher transgene expression in VSMCs compared to adenoviral vectors. However, in terms of VECs, the transduction efficiency was vice versa (Dishart et al., 2003a). In addition, Cefai *et al.*, demonstrated that LVs transduced VECs and VSMCs with greater efficiency compared to adenoviral vectors (Cefai et al., 2005). Taken together, these two investigations evidently show that LVs are efficient in transducing human VSMCs (Dishart et al., 2003a, Cefai et al., 2005). VSV-g pseudotyped LV gene transfer of TIMP-3 mediated efficient transduction and over-expression in human VSMCs, which reduced migration and induced apoptosis of these cells *in vitro* and this was comparable to adenoviral vector gene transfer (Dishart et al., 2003a). VSV-g pseudotyped LV-mediated VEGF gene transfer promoted human VEC proliferation and sprouting *in vitro* (Cefai et al., 2005).

LVs have demonstrated their usefulness in delivering therapeutic genes into the vasculature *in vivo* and thus reducing the NIF (Qian et al., 2006, Yang et al., 2010). Hanta pseudotyped LV-mediated gene delivery of the therapeutic gene human extracellular superoxide dismutase (EC-SOD) mediated over-expression and prevented NIF in a rabbit model of acute vascular injury. These results indicated LVs are efficient in transduction of the vasculature via a catheter-mediated delivery of this vector and had no significant effect on inflammation and toxicity (Qian et al., 2006). LV-mediated gene transfer of small interfering RNA of CREB binding protein (CBP) via a catheter-mediated delivery was investigated in a rat model of acute vascular injury. Results indicated a

reduction in the NIF and the promotion of re-endothelialisation (Yang et al., 2010). LV-mediated gene transfer of broad spectrum CC-CK binding protein 35k [also known as Vaccinia virus strain Lister 35 kilo Dalton (kDa) protein (35k)] demonstrated a reduction in atherosclerosis progression *in vivo* and the potential benefits of long-term LV transduction (Bursill et al., 2009).

A low titre production of LVs remains problematic for clinical application for example vascular gene therapy (Matrai et al., 2010). Regardless, LVs are attractive for vascular gene therapy because these vectors could potentially mediate efficient and sustained transgene expression in the vasculature (Dishart et al., 2003b, Baker et al., 2006, George et al., 2006, Gaffney et al., 2007, White et al., 2007). LVs mediate semi-random integration into the host's chromosome and thus may potentially induce the risk of insertional mutagenesis, which could lead to oncogenesis in the vasculature (see section 1.10.3). LVs have the potential to mediate gene transfer of a therapeutic gene into the vasculature within a short time exposure, which is required in this clinical setting (Dishart et al., 2003a, Cefai et al., 2005, George et al., 2006, White et al., 2007). LV gene transfer demonstrated relatively low inflammation in the vasculature (Cefai et al., 2005). NILVs and LVs appeal for many gene therapy applications (see section 1.11.3 for more detail), especially in the vasculature (George et al., 2006, White et al., 2007). To date, a number of studies have used LVs for gene transfer into the vasculature, and in addition none have used NILVs which is an area of interest for this study.

## 1.11 Optimisation of lentiviral vectors

LVs are relatively versatile in optimising for various gene therapy applications, by improving vector performance and safety. These include envelope alternation (pseudotyping), promoter alternation (to drive transgene expression) and non-integration or integration (packaging plasmid) (Figure 1.10). Optimisation of LVs can greatly improve efficiency and long-term transgene expression in target cells and tissue. Promoter alternation, pseudotyping and non-integration will be discussed further in this section.

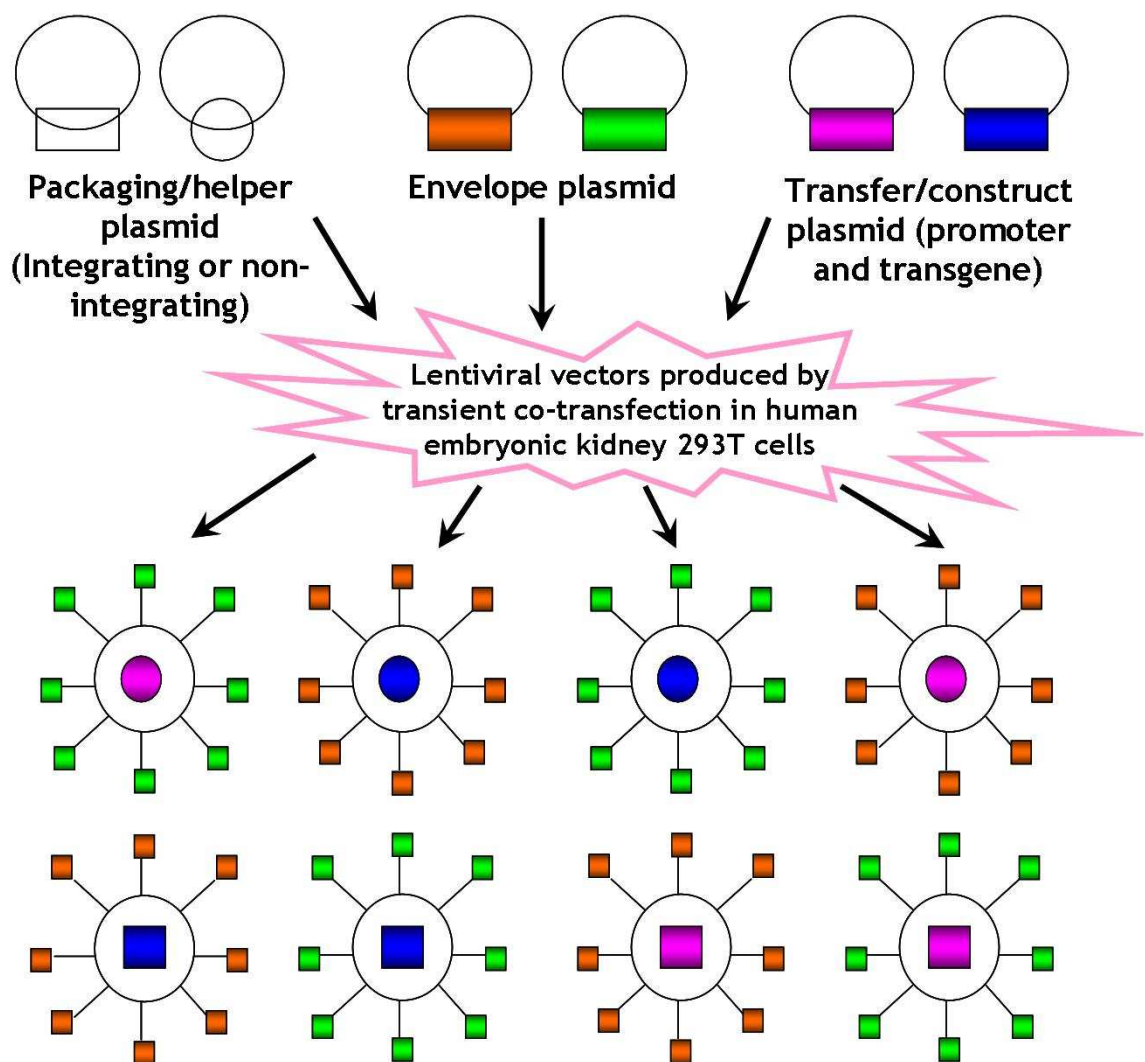


**Figure 1.10. A schematic representation of the optimisation of lentiviral vectors.**

Lentiviral vectors are relatively versatile in optimising for application, by improving vector performance and safety. Lentiviral vectors can be modified by the interchange of the packaging plasmid for integration or mutated-integration genes, alternation of the viral envelope plasmid (pseudotyping) and transfer/construct plasmid for the chosen internal heterologous promoter to drive the expression of the transgene of interest. Circle or square for packaging plasmid = integration-proficient or integration-deficient. Orange or green = glycoprotein envelope. Pink or blue = lentiviral vector genome.

### **1.11.1 Promoter alternation**

The control of transgene expression after LV gene transfer is mediated by an internal heterologous promoter. Many studies continue to validate and refine ideal promoters to improve safety and performance of LVs as gene transfer vehicles for particular disease applications. These promoters can be ubiquitous or cell-type specific. Cell- and tissue- specific promoters are advantageous because they have the ability to confine expression to targeted cells or tissues, while maintaining sufficient levels of transgene expression to achieve a desired effect. Moreover, they are less prone to promoter inactivation, and thus provide stability and longevity of transgene expression (Sinn et al., 2005b, Escors and Breckpot, 2010). Regulatory promoters are favourable since they have the potential to regulate transgene expression, which is appealing for many gene therapy applications such as monogenic disorders (Sinn et al., 2005b, Zhang et al., 2007, Escors and Breckpot, 2010). Another example includes regulated gene expression levels and relatively rapid onset of transgene transcription mediated by LVs, which would be desirable for acute vascular injury.

LVs have been shown to be efficient delivery vehicles for gene transfer to the vasculature. Past studies have demonstrated LV-mediated transgene expression in the vasculature facilitated by various internal heterologous promoters, and these include the following: cytomegalovirus (CMV), CMV immediate early enhancer/chicken beta-actin (CAG) promoter, phosphoglycerate kinase 1 (PGK) (housekeeper-derived) promoter, tyrosine kinase 2 (Tie2, angiotensin receptor) promoter and elongation factor-1 $\alpha$  (EF1 $\alpha$ ) (housekeeper-derived) promoter. As mentioned previously (section 1.11.2), HNTV-pseudotyped LVs mediated efficient gene transfer and the over-expression of human EC-SOD in the vasculature facilitated by the PGK promoter, following acute vascular injury (Qian et al., 2006). A study by Dishart *et al.*, demonstrated that the CMV promoter facilitated stronger LV-mediated transgene expression in VECs and VSMCs, compared with the CAG and PGK promoter (Dishart et al., 2003a). In addition to these findings, another study indicated that the CMV promoter elicited greater LV-mediated transgene expression in comparison to EF1 $\alpha$  promoter in VECs and VSMCs (Cefai et al., 2005). Moreover, the PGK promoter facilitated relatively lower transcriptional activity compared to CMV and EF1 $\alpha$  promoters in vascular cells. This study also observed that the endothelium-

specific Tie2 promoter facilitated significant cell-specific LV-mediated transgene expression in VECs, although a reduced level was achieved compared to the CMV promoter (Cefai et al., 2005). In addition, an investigation reported that adenoviral-mediated gene transfer of an anti-proliferative hybrid transgene and its expression under the control of a cell-specific human SM  $\alpha$ -actin promoter inhibited VSMC proliferation and the NIF (Wills et al., 2001). However, smooth muscle cell specific promoters such as the human SM  $\alpha$ -actin promoter have not been explored in the context of LV-mediated transgene expression in the vasculature.

It was reported that an internal spleen focus forming virus (SFFV) promoter (enhancer region of the SFFV, U3-LTR) elicited a higher level and long-term transgene expression in human haematopoietic cells *in vivo* mediated by LVs, compared to the CMV promoter (Demaison et al., 2002). In the context of the vasculature, LV mediated transgene expression facilitated by the SFFV promoter has not yet been tested, and this may have the potential to improve the level of transgene expression.

All enhancer elements associated with internal regulatory elements have the potential to enhance insertional mutagenesis associated with LV-mediated gene transfer (Hacein-Bey-Abina et al., 2003b, Ott et al., 2006, Zhang et al., 2007, Howe et al., 2008). Ubiquitously acting chromatin opening element (UCOE) is an enhancer-less regulatory element, which consists of a methylation-free CpG island associated with closely spaced dual divergently transcribed promoters of house-keeping genes [derived from the human *HNRPA2B1-CBX3* (heterogeneous nuclear ribonucleoprotein A2/B1-chromobox homolog 3) house-keeping gene locus] and maintains a chromatin-opening function, and thus is resistant to transcriptional silencing (irrespective of tissue/cell-type and integration site position effects) (Williams et al., 2005, Zhang et al., 2007). As a result, UCOEs allow closely-associated promoters of transgene expression to function with increased efficiency, stability, consistency and longevity (Williams et al., 2005). In comparison to viral SFFV promoter (an enhancer-associated viral promoter, prone to insertion-site position effects and transcriptional silencing), UCOE facilitated higher, consistent and stable transgene expression in haematopoietic cells (mediated by LV gene transfer) and was resistant to transcriptional silencing, while the minimal, enhancer-less re-composite house-keeping gene

promoters were less likely to induce LV-mediated insertional mutagenesis (Zhang et al., 2007). Unlike the SFFV promoter element, the stability of transgene expression from the UCOE element in a LV system is mediated by resistance to DNA methylation induced silencing (Zhang et al., 2010). Altogether, LV-mediated transgene expression via the enhancer-less UCOE regulatory element is favourable since it has the potential to regulate transgene expression, resist transcriptional silencing and overcome integration-site position effects such as insertional mutagenesis (may aid a better safety profile). Therefore, this regulatory element is desirable for many gene therapy applications, especially for acute vascular injury and has not been tested in the vasculature. In summary, there is a continuous need to validate and refine ideal promoter elements to improve safety and performance of LVs as gene transfer vehicles and indeed for acute vascular injury.

### **1.11.2 Pseudotyping**

A LV can be pseudotyped with an envelope protein derived from a virus other than the parent vector genome (heterologous glycoprotein envelope). Pseudotyping the LV can broaden or narrow the tropism of these vectors to different cells or tissue types. Each envelope glycoprotein preferentially interacts with specific cell/tissue types and their receptors, and therefore may potentially narrow or broaden transduction. *Rhabdovirus* VSV-g (as mentioned previously) is the most commonly used viral envelope protein for pseudotyping LVs because it aids in high titre productions, typically broadens the tropism (cellular membrane mediated endocytosis) and enhances transduction to a variety of cells. However one major drawback is the induction of cytotoxicity which may limit this pseudotyped LV and its potential use in the clinic. The challenge is finding an envelope glycoprotein in pseudotyping the LV successfully for enhancing transduction and/or cell/tissue-specific targeting (Cronin et al., 2005, Sinn et al., 2005b, Cockrell and Kafri, 2007, Escors and Breckpot, 2010, Matrai et al., 2010). Various other viral envelopes have been used to pseudotype LVs and have demonstrated their potential in transduction efficiency in targeted cell/tissue types with limited cytotoxicity, for example rabies, Ross River virus, Ebola-Zaire, baculovirus gp64, murine leukaemia virus (MLV) -amphotropic and -ecotropic and Hantavirus (Cronin et al., 2005, Sinn et al., 2005b, Escors and Breckpot, 2010, Matrai et al., 2010).

Rabies virus belongs to the *Lyssavirus* genus and predominantly infects the central nervous system (CNS) and causes inflammation of the brain and eventually death. A few animal model studies have demonstrated the use of rabies (glycoprotein envelope) pseudotyped LVs for efficient transduction and sustained transgene expression within cells of the central nervous system (CNS) (Mazarakis et al., 2001, Kato et al., 2007, Rahim et al., 2009). Two of these studies observed that rabies pseudotyped LVs successfully mediated gene transfer in neurones *in vivo* due to retrograde axonal transport, whereas this function did not occur with VSV-g pseudotyped LVs (Mazarakis et al., 2001, Kato et al., 2007). In addition, a recent study demonstrated rabies pseudotyped NILV-mediated gene delivery efficiently transduced neurones in adult rats *in vivo* (Rahim et al., 2009). These preclinical studies support the use of rabies pseudotyped LVs as effective vectors for gene therapy applications, especially for the treatment of inherited and acquired neurological disorders.

Ross River virus (RRV) belongs to the virus genus *Alphaviruses* and causes polyarthritis. RRV glycoprotein envelope has a broad tropism for various species and many cell types (Jakobsson et al., 2006). This viral envelope protein has been implicated to have potential utility for various cell types, for example LV pseudotyped with RRV envelope demonstrated higher transduction efficiency in murine hepatocytes, kupffer cells, astrocytes and oligodendrocytes and induced less cytotoxicity, compared with VSV-g pseudotyped LV *in vivo* (Kang et al., 2002). RRV pseudotyped LVs have demonstrated efficient transduction of neurons and glial cells when injected into different structures in the rat brain, plus these vectors had the ability to transduce human neuronal progenitor cells *in vitro* (Jakobsson et al., 2006).

Ebola Zaire (EbolaZ) virus belongs to the family of *filoviruses* and is transmitted through bodily fluids causing lethal haemorrhagic fever. One of the main targets is endothelial cells (Sanders, 2004). The examination of *in vivo* tropism of EbolaZ pseudotyped LVs compared to VSV-g pseudotyped LVs, indicated these vectors were more efficient in transduction of myocytes and equally the same for cardiomyocytes (MacKenzie et al., 2002). EbolaZ pseudotyped LVs were injected into murine muscle *in utero* and these vectors were found to transduce muscle satellite/stem cells. Subsequently, regenerated muscle after injury demonstrated transgene expression had originated from transduced satellite

cells (MacKenzie et al., 2005). EbolaZ pseudotyped LVs have demonstrated their effectiveness in efficient transduction of the airway epithelia in *in vitro* and *in vivo* models (Kobinger et al., 2001, Sinn et al., 2003). Altogether, these investigations indicate that EbolaZ pseudotyped LV-mediated gene transfer may hold promise for the treatment of respiratory diseases (i.e. cystic fibrosis), muscular diseases and CVDs.

Baculovirus glycoprotein 64 (GP64) belongs to the *Baculovirus* family and have species-specific tropisms among many invertebrates. LVs pseudotyped with GP64 glycoprotein envelope have shown narrower tropism, lack of cytotoxicity and higher vector titre productions with greater stability (Kumar et al., 2003, Schaubert et al., 2004, Cronin et al., 2005). GP64 pseudotyped LVs in comparison to VSV-g pseudotyped LVs, have been proven to efficiently transduce a variety of cell lines but with a slightly more restricted tropism and a poor ability to transduce haematopoietic cell types. Moreover, the GP64 pseudotyped LV was demonstrated to be an attractive alternative to the VSV-g pseudotyped LV with comparable transduction efficiency in mouse liver tissue *in vivo* (Schauber et al., 2004). In addition, GP64 pseudotyped LV-mediated gene transfer indicated greater transduction efficiency of mouse nasal epithelia than observed with VSV-g pseudotyped LV (Sinn et al., 2005a). Furthermore, a study concluded that LVs pseudotyped with GP64 provided efficient cell-specific, high-level transgene expression in fetal and neonatal airway epithelial cells in the murine lung, compared to LVs pseudotyped with VSV-g. GP64 pseudotyped LV mediated long-term transgene expression in the mouse lung after neonatal administration (Buckley et al., 2008). In addition, GP64 pseudotyped LVs mediated efficient transduction levels in cells of the astrocytic lineage in adult rats (Rahim et al., 2009) In summary, these studies suggest that GP64 pseudotyped LVs have the potential to provide modality for treatment in liver and lung diseases.

Murine leukaemia virus (MLV) are *oncoretroviruses* (part of the *gammaretrovirus* genus) and have the ability to infect and cause cancer in mice. MLV-amphotropic envelope (MLV-A) has a broad host range compared to MLV-ecotropic envelope (MLV-E). MLV-A pseudotyped LVs infected human skin tissues (epidermal and dermal layers) with higher efficiency compared to VSV-g pseudotyped LVs, at low virus titres (Kunicher et al., 2008). These particular pseudotyped LVs were highly efficient in gene transfer to specific cells of the CNS such as the striatum

and thalamus, compared to VSV-g pseudotyped LVs, following injection into separate brain regions of adult mice (Watson et al., 2002). LVs pseudotyped with the MLV-A envelope protein were more efficient in transducing human adult cord blood CD34<sup>+</sup> cells and superior in establishing human haematopoiesis in immunodeficient mice, compared to VSV-g pseudotyped LVs (Hanawa et al., 2002). Altogether, these investigations propose that MLV-A pseudotyped LVs may be effective in gene therapy applications for skin diseases, neurological disorders and immunodeficiencies.

LVs pseudotyped with MLV-E glycoprotein envelope effectively transduce pluripotent human embryonic stem cells (Koch et al., 2006). Thus, this particular pseudotyped LV has the potential to provide an alternative to the VSV-g pseudotyped LV-mediated gene transfer in stem cell manipulation.

Hantavirus (HNTV) is collectively a family of viruses which cause fatal respiratory disease and haemorrhagic fever with renal syndrome in humans (Bahr et al., 2004, Muranyi et al., 2004). A study investigated the transduction of VECs with LVs pseudotyped different strains of Hantavirus (Qian et al., 2006). *In vitro* data from this study indicated that the Hantaan strain mediated higher transduction efficiency for VECs (bovine aortic VECs and human umbilical vein VECs), compared to VSV-g pseudotyped LVs. *In vivo* locally delivered HNTV pseudotyped LVs were highly efficient in transduction of vascular cells in a rabbit model of acute vascular injury and greatly targeted the site of vascular injury. Furthermore, *in vivo* results demonstrated that transduction efficiency of this pseudotyped LV was evidently superior compared to VSV-g pseudotyped LV and adenoviral vector, following local delivery. In addition, HNTV pseudotyped LV gene transfer of human EC-SOD mediated over-expression and reduced the NIF in a rabbit acute vascular injury model 6 weeks after delivery. These findings suggest the potential use of this particular HNTV pseudotyped LV for therapeutic gene transfer into the vasculature for the prevention of the NIF (Qian et al., 2006).

In summary, all these preclinical investigations have demonstrated that cell targeting can be enhanced/modified with pseudotyped LVs (plus possibly with limited cytotoxicity), in comparison to VSV-g. All pseudotyped-LVs mentioned have yet to be tested in the context of acute vascular injury (with an exception

to HNTV glycoprotein envelope) and offer additional potential for these vectors in vascular gene therapy.

### **1.11.3 Integration-deficient lentiviral vectors**

As previously mentioned, LVs mediate integration and long-term transgene expression and have the potential to be very useful for diseases/disorders, in which permanent cell correction is required by gene therapy, for example monogenic disorders including WAS (Charrier et al., 2007, Galy et al., 2008, Marangoni et al., 2009), adenosine deaminase-deficient (ADA)-SCID (Mortellaro et al., 2006) and X-linked SCID (Zhang et al., 2007, Zhou et al., 2010, Almarza et al., 2011). Despite this, one of the major limitations of using integrating LV (int-LV) gene transfer is the occurrence of semi-random integration, which can potentially lead to oncogenesis associated with insertional mutagenesis as observed in a clinical trial (Hacein-Bey-Abina et al., 2003b, Hacein-Bey-Abina et al., 2008) and previously described in section 1.5. Importantly, disease applications involving non-dividing (post-mitotic or quiescent) cells for LV-mediated gene transfers do not require integration and these include the retina, brain, liver and skeletal muscle. These shortcomings led to a major advancement in LVs, the development of non-integrating LVs (NILVs). These NILVs mediate gene transfer with minimal host genome integration, whilst retaining similar transduction efficiency of their integrating counterparts (still harness lentiviral-mediated gene transfer to non-dividing and dividing cells) and provide stable transgene expression. NILVs offer enormous potential for the utility of LVs in clinical gene therapy (Vargas et al., 2004, Nightingale et al., 2006, Philippe et al., 2006, Yanez-Munoz et al., 2006, Apolonia et al., 2007, Philpott and Thrasher, 2007, Rahim et al., 2009).

#### **1.11.3.1 Integrase proteins**

After reverse transcription in the cytoplasm, the lentiviral double-stranded DNA is associated with the PIC, which facilitates nuclear entry (see section 1.10.2.1). The integrase protein (approximately 32-45 kDa in size and encoded in the *pol* gene) is a major component of the PIC and catalyses the proviral double-stranded DNA integration into the host chromosome (Philpott and Thrasher, 2007, Wanisch and Yanez-Munoz, 2009, Banasik and McCray, 2010). Moreover, it

is known that there are two different circular non-integrated lentiviral double-stranded DNA molecules (episomes) present naturally in a cell after lentivirus infection. Extrachromosomal lentiviral DNA exists and accumulates in the nucleus in the following three forms: double-stranded linear DNA (precursor to the integrated provirus); intramolecular homologous recombination between LTRs forming an episome with a single LTR (1-LTR circle) and intramolecular non-homologous end joining of the LTRs forming an episome with two adjacent LTRs (2-LTR circle). The levels of 1-LTR episomes are greater than the 2-LTR episomes. Both episomes are stable and have the ability to facilitate transgene expression, but lack replication signals i.e. origin of replication, and thus dilute during cell division and do not persist in dividing cells (Butler et al., 2002, Pierson et al., 2002, Philpott and Thrasher, 2007, Wanisch and Yanez-Munoz, 2009, Banasik and McCray, 2010). The integration process of proviral DNA is slightly inefficient and as a result these episomes normally persist in cells infected by retroviruses, retroviral vectors, lentiviruses and LVs, but at a relatively low level (Wanisch and Yanez-Munoz, 2009).

A representation of the integration process is shown in Figure 1.11. The integrase protein has 3 functional domains: the N-terminal zinc finger domain, the core catalytic domain and the C-terminal DNA-binding domain (Figure 1.12). The core catalytic amino-acid triad motif consists of amino-acids D64, D116 and E152 (DDE motif, known as the catalytic triad) in lentiviruses and retroviruses and is absolutely necessary for integration. The process of integration begins with viral DNA binding via the C-terminal domain of the integrase protein. Integrase binds to the U3 and U5 *att* sites within the LTRs of the double-stranded linear lentiviral DNA. The integrase protein facilitates the 3' process, which involves the cleavage of the 3' terminal dinucleotides within both LTRs. As a result, this generates a 3' hydroxyl group (OH) at each end of the viral DNA, which are absolutely essential for the catalytic process mediated by the catalytic domain (important positions are D64, D116 and E152). Integrase then binds and brings together the genomic DNA and the viral DNA, thereby initiating integration. The integration reaction occurs when these 3' hydroxyl groups attack the phosphodiester bonds on the opposite strands of the target DNA. As a consequence, this process mediates transfer and the joining of the double-

stranded viral DNA into the host's DNA (Philpott and Thrasher, 2007, Banasik and McCray, 2010).

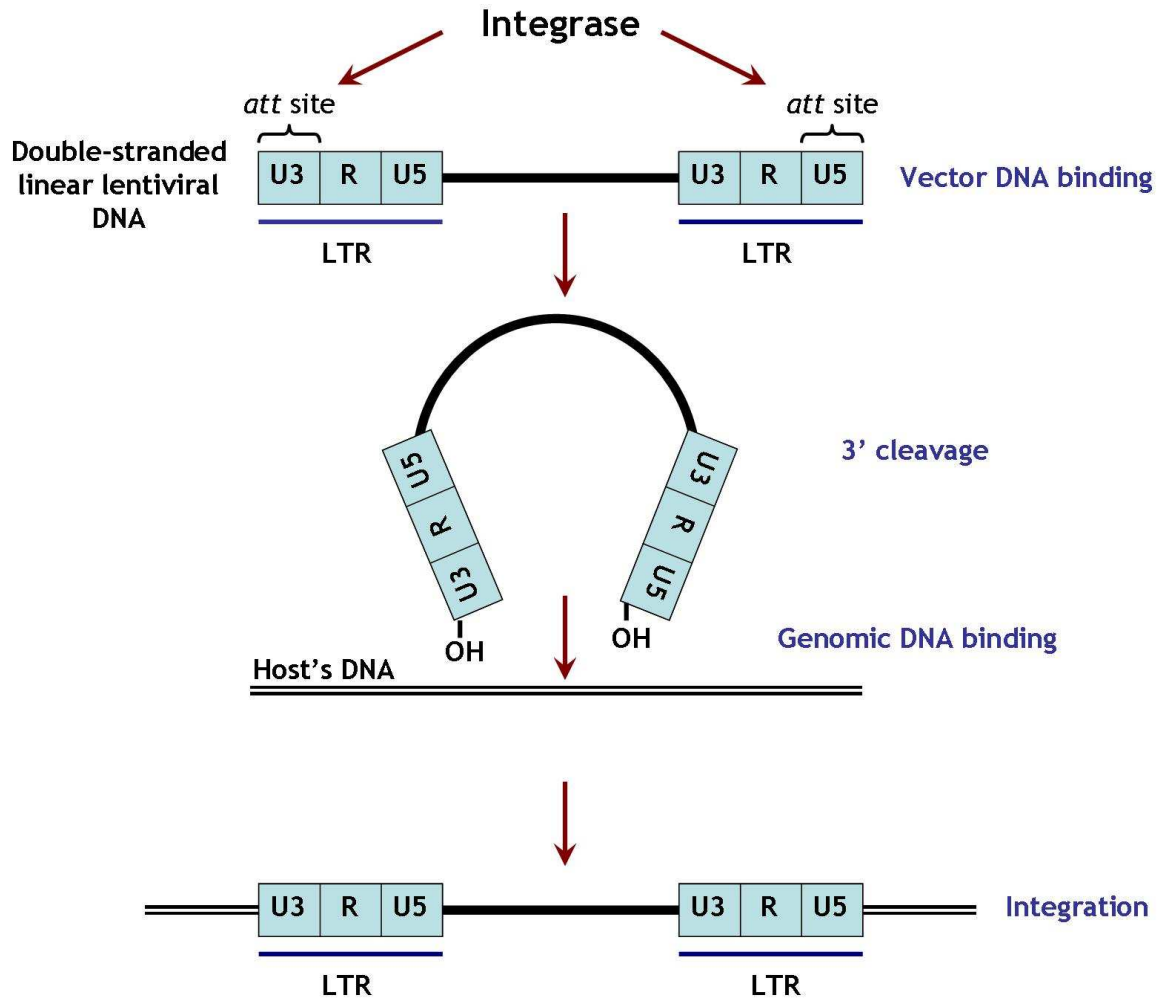


**Figure 1.11. A schematic diagram of the integration process.**

Integrase binds to the double-stranded linear lentiviral DNA via U3 and U5 *att* sites within the LTRs. Integrase facilitates the cleavage of 3' terminal dinucleotides within both LTRs and as a result generates a 3' hydroxyl group (OH) at each end of the viral DNA which are necessary for the catalytic process. Integrase then binds and brings together the host's DNA and the viral DNA. The integration reaction occurs when 3' hydroxyl groups attack phosphodiester bonds on the opposite strands of the host's DNA, and thereby mediating transfer and joining of the viral DNA into the genomic DNA (Philpott and Thrasher, 2007, Banasik and McCray, 2010).

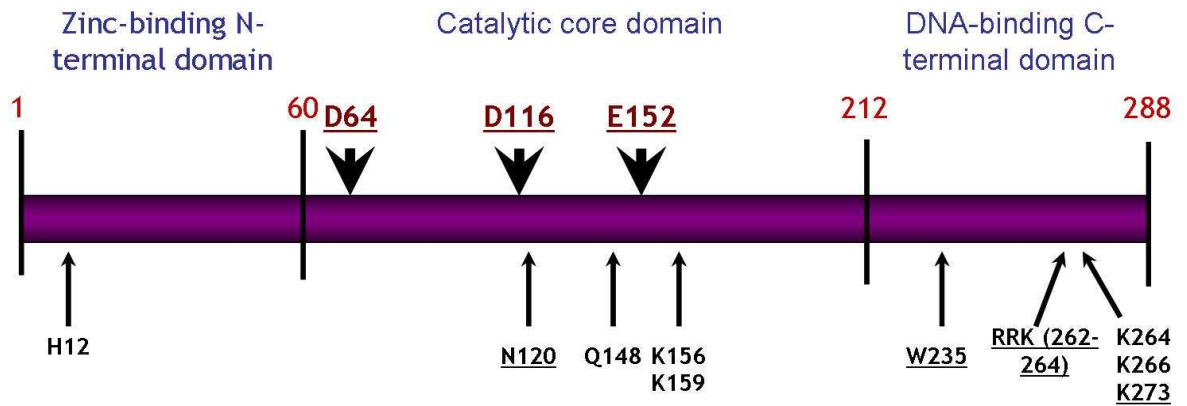


**Figure 1.12. Structure of the lentiviral integrase protein.**

A schematic representation of the three functional domains of integrase which comprise of the following: the zinc-binding N-terminal domain, the catalytic core domain and the DNA-binding C-terminal domain. Arrows illustrate the amino acids that give rise to class I integrase mutations, thereby rendering lentiviral vectors, non-integrating. Residues D64, D116 and E152 (in bold red and underlined), generates the DDE catalytic triad which is absolutely essential for integration. A point mutation in any of these residues affects the catalytic triad and thus blocks integration. A point mutation in any one of these residues: N120, W235, RRK (262-264) and K273 (in black and underlined), affects the binding of integrase to the genomic DNA, thereby inhibiting integration (Philpott and Thrasher, 2007, Banasik and McCray, 2010).

### 1.11.3.2 Development of non-integrating lentiviral vectors

In general, NILVs are integration-deficient due to mutations in the integrase gene. The integrase protein has pleiotropic effects in PIC nuclear translocation and integration, thus many mutants to this protein will have an effect on several viral functions as well as integration. Integration-deficient LVs and retroviral vectors are created, by introduction of specific point mutations in the gene which encodes for the integrase protein via the packaging plasmid. Integrase mutations can be divided into two classes. Class I integrase mutations result in normal DNA synthesis, integration failure and accumulation in the cell nucleus as double-stranded DNA episomes. However, class II integrase mutations (in the N-terminal domain) have pleiotropic effects (defects in assembly, reverse transcription and a lack of integration) and cause limited transgene expression. Thus, class II mutations are not considered for NILV-mediated transgene expression, whereas class I mutations are more appropriate (Philpott and Thrasher, 2007, Wanisch and Yanez-Munoz, 2009, Banasik and McCray, 2010). There are a large number of class I integrase point mutations, which affect different steps of the integration process, thereby giving rise to NILV-mediated gene transfer and transgene expression (Figure 1.12 & Figure 1.13). The most common class I integrase mutations used in NILVs are point mutations in the catalytic triad. A point mutation in any of these residues (D64, D116 and E152,

the DDE catalytic triad) inactivates the catalytic function of integrase and prevents integrase function, thus rendering integration deficiency (Figure 1.12). In addition, other integrase residues can bear a point mutation rendering the integrase protein ineffective, thereby inhibiting integration (Figure 1.12), these include the following:

- Position Q148 in the core domain: blocks vector DNA binding via the *att* site and strand transfer (class I).
- Residues N120, K156 & K159 in the core domain: impairs the binding of the integrase to the genomic DNA (class I).
- The W235 residue and the RRK (262-264) motif in the DNA-binding C-terminal domain: inhibits integrase binding to the target host genomic DNA (class I).
- The K264/K266/K273 triad in the DNA-binding C-terminal domain: impairs target DNA binding and strand transfer (class I).
- The H12 residue in the zinc-binding N-terminal domain: blocks integrase multimerization function (class II).

(Apolonia et al., 2007, Philpott and Thrasher, 2007, Wanisch and Yanez-Munoz, 2009, Banasik and McCray, 2010). The most common mutant residue used in studies to date, which facilitates the inactivation of integrase, is the D64 residue known as the D64V mutant [a single amino acid change, aspartic acid to valine at position D64 in the HIV-1 integrase protein sequence (Naldini et al., 1996a)] (Nightingale et al., 2006, Yanez-Munoz et al., 2006, Apolonia et al., 2007, Rahim et al., 2009).

A CA dinucleotide in the 3' strand of the *att* site of the viral DNA is required for 3' cleavage mediated by integrase during the integration process (Philpott and Thrasher, 2007, Wanisch and Yanez-Munoz, 2009, Banasik and McCray, 2010). Instead of the mutational inactivation of the integrase protein, NILVs can also be developed by mutating (for example replacing conserved CA with TG dinucleotides) these *att* sites at the U3 and U5 ends of the viral genome via the transfer/construct plasmid and thereby blocking integration (Nightingale et al., 2006, Apolonia et al., 2007).

These class I integrase and/or *att* site mutants prevent the integration process of the double stranded viral DNA molecule. Instead two circular forms of non-integrated double-stranded viral DNA are generated from the linear form, giving rise to 1-LTR and 2-LTR episomes. These episomes accumulate in the nucleus. These viral DNA circular forms are transcriptionally active and facilitate transgene expression (Figure 1.13) (Philpott and Thrasher, 2007, Wanisch and Yanez-Munoz, 2009, Banasik and McCray, 2010).

In post-mitotic cells these episomal forms are stably maintained. However, these episomes lack replication signals and as a consequence dilute during cell division and do not persist in dividing cells. NILVs retain the high transduction efficiency of their integrating counterparts, with reduced host genome integration and risks associated with insertional mutagenesis. NILV-mediated transgene expression is as efficient as their integrating counterparts in non-dividing cells and at the initial infection of dividing cells (Nightingale et al., 2006, Philippe et al., 2006, Yanez-Munoz et al., 2006, Apolonia et al., 2007, Philpott and Thrasher, 2007, Rahim et al., 2009, Wanisch and Yanez-Munoz, 2009).

NILVs increases bio-safety not only in terms of having the ability to be integration-deficient, but also less likely to generate replication-competent-recombinants. Ideally NILVs require both integrase and *att* site mutations for clinical application in order to: minimise integration if vector mobilization occurs; enhance the reduction in the risk of replication-competent-recombinant generation, and limit the emergence of residual integration frequency (Philippe et al., 2006, Wanisch and Yanez-Munoz, 2009, Matrai et al., 2010).

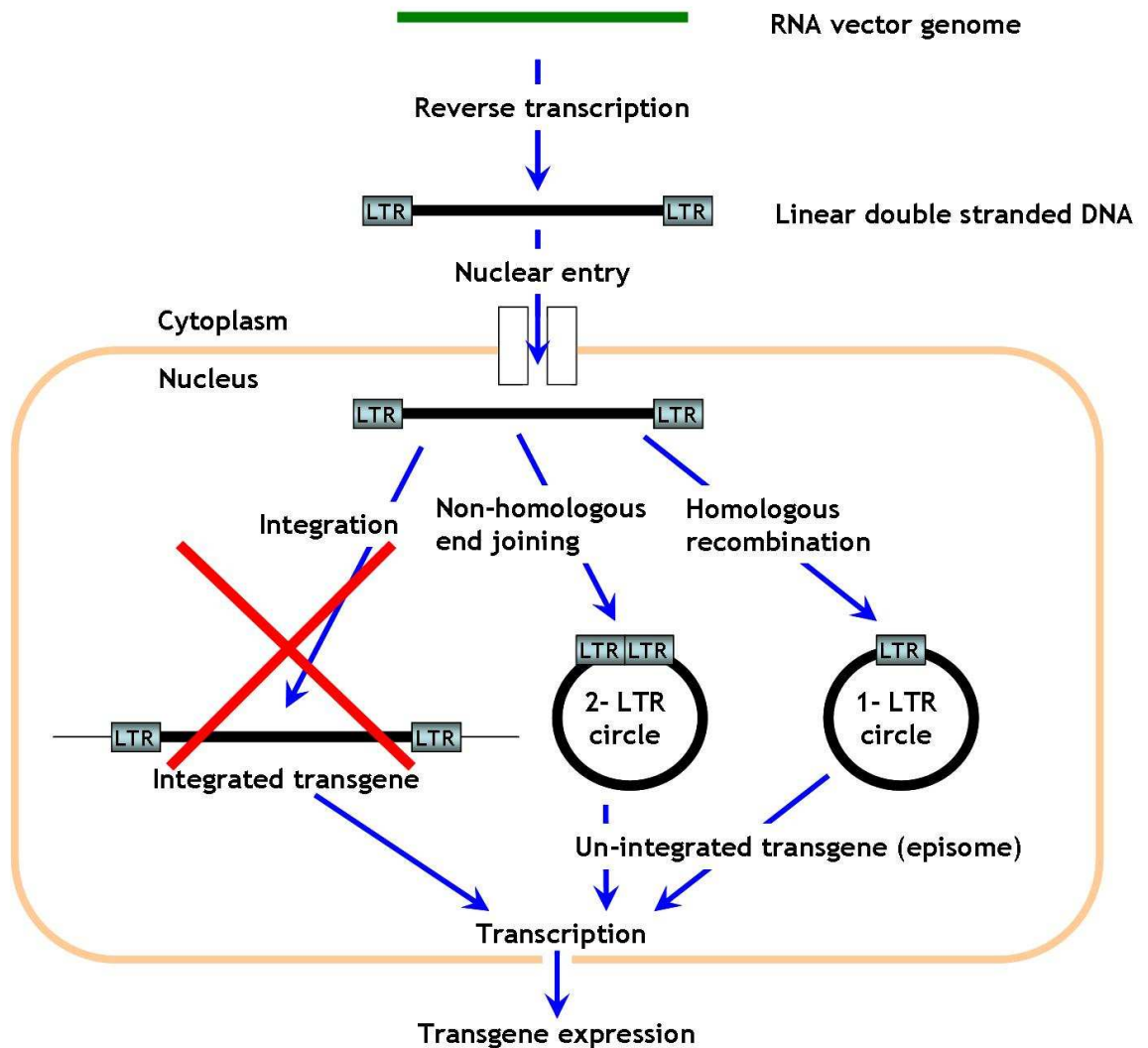


**Figure 1.13. Representation of the non-integration process.**

Class I integrase and/or *att* site mutants prevent the integration process of the linear double stranded viral DNA molecule. Instead two circular forms of non-integrated double-stranded viral DNA are formed from the linear form and accumulate in the nucleus. These episomes are generated either by intramolecular homologous recombination between LTRs forming an episome with a single LTR (1-LTR circle) and intramolecular non-homologous end joining of the LTRs forming an episome with two adjacent LTRs (2-LTR circle). These circular forms of viral DNA are transcriptionally active and facilitate transgene expression. However, these episomes lack replication signals and as a consequence dilute during cell division. Adapted from Philpott and Thrasher (2007) (Wanisch and Yanez-Munoz, 2009, Banasik and McCray, 2010).

NILVs are by definition relatively integration-defective, but this is not absolute because of residual integration, which is suggested to occur by background cellular recombination events (mediated through DNA nicks located anywhere in the vector episome) and not by integrase. Consequently, all NILVs mutations possess residual integration efficiencies (Philpott and Thrasher, 2007, Wanisch and Yanez-Munoz, 2009). In contrast to their integrating counterparts, the most commonly used D64V mutant possesses approximately a  $10^3$ -fold reduction in integration efficiency as well as N120L and W235E mutants. Mutants K264R,

Q148A and K264, 266, 273R gave rise to residual integration rates of 3-, 13- and 14-fold lower than integrating LVs (int-LV). The residual integration rate of the *att* site mutant was approximately 200-fold lower than the wild-type vector (Apolonia et al., 2007). The D64V mutant has also been demonstrated to decrease integration by 10<sup>4</sup>-fold lower than the wild-type HIV-1 vector (Leavitt et al., 1996). In addition, residual integration frequencies were also evident in NILV combination mutants (mutations in the *att* site and integrase gene) with no further reduction compared to integrase mutants alone (for example D64V mutant) (Nightingale et al., 2006, Apolonia et al., 2007).

A number of studies have demonstrated the potential use of NILVs for gene transfer (Vargas et al., 2004, Nightingale et al., 2006, Philippe et al., 2006, Yanez-Munoz et al., 2006, Apolonia et al., 2007, Rahim et al., 2009). Vargas *et al.*, demonstrated that NILVs (D116N mutant) with the incorporation of the simian virus-40 (SV-40) origin of replication in their genome, have the ability to retain transgene expression in 293T cells (dividing cells) that contain the SV-40 large T antigen. Thus, this study implied the potential application of NILVs for gene transfer in dividing cells (Vargas et al., 2004). Mutations in the *att* sites and the integrase protein (D64V mutation) mediated a high and stable transduction efficiency, but transgene expression was transient in dividing haematopoietic cells after one month post-transduction, due to the dilution of lentiviral episomes (1-LTR and 2-LTR) during cell division (Nightingale et al., 2006). Class I integrase mutation in the RRK motif generated NILVs with efficient transduction for dividing and non-dividing cells *in vitro*, but provided transient transgene expression in dividing cells. In contrast, these vectors mediated long-term and stable transgene expression in non-dividing cells (neural cells) *in vitro* and (murine brain tissue) *in vivo*, which were as efficient as int-LVs (Philippe et al., 2006). The D64V mutant NILV exhibited highly efficient gene transfer and sustained transgene expression *in vivo* in the retina and brain tissue of mice, which was as efficient as the int-LV-mediated gene transfer. In addition, NILV-mediated gene transfer of rpe65 (retinal pigment epithelium-specific 65 kDa protein) facilitated functional rescue of congenital blindness in a murine model of autosomal recessive retinitis pigmentosa (due to mutations in the *rpe65* gene) (Yanez-Munoz et al., 2006). In addition, it is known that D64V mutant NILVs have similar transduction efficiencies as int-LVs (Yanez-Munoz et al., 2006), whereas

RRK motif mutant NILVs exhibit lower transduction efficiencies compared to their integrating versions (Philippe et al., 2006). NILVs with class I point mutations in the integrase or mutations in the integrase *att* sites on the vector DNA genome or in combination, demonstrated efficient transduction and integration deficiency *in vitro*. In additions, these NILVs exhibited transient transgene expression in dividing cells, whereas non-dividing cells retained transgene expression overtime. Evidently, four different NILVs [the D64V mutant, the mutant which comprised of a deletion in the *att* site ( $\Delta att$  site), D64V $\Delta att$  mutant, and the D64VN120LW235E $\Delta att$  mutant] retained high transduction efficiency and longevity of transgene expression in murine muscle tissue *in vivo*, similar to their integrating counterparts (Apolonia et al., 2007). Recently, Rahim *et al.*, reported NILVs (D64V mutants) mediated efficient transduction and long-term transgene expression in tissues of the central nervous system (CNS) in rodents *in vivo*. Moreover, NILVs were as effective as their integrating versions *in vivo*, suggesting implications for these vectors in clinical gene therapy applications for neurological disorders (Rahim et al., 2009).

Permanent transgene expression is not necessarily important during acute vascular injury. Many studies have reported that transient transgene expression mediated by adenoviral vectors can provide sufficient therapeutic benefits (George et al., 2000, Wan et al., 2004, Johnson et al., 2005, Kritz et al., 2008). An alternative to int-LV-mediated transgene expression is NILVs. NILVs exhibited by the D64V mutant [high transduction efficiency and lower residual integration efficiency (Leavitt et al., 1996, Apolonia et al., 2007)] have yet to be tested for their therapeutic use in the context of the acute vascular injury response and offer additional potential for these vectors in vascular gene therapy. VSMCs are vascular cells which slowly divide. Therefore it is suggested the NILV-mediated episomal transgene would be diluted slowly, but persist for the duration required (George et al., 2006, White et al., 2007).

Taken together, optimisation of LVs is an area of interest for this study. LVs used within this thesis will be optimised in terms of alternative promoters, pseudotyping and integration-deficiency for human vascular gene delivery.

## 1.12 Therapeutic genes for the vasculature

The end point of any vector development and optimisation is to express a gene that will exert a therapeutic effect within its aimed target (target validation). The complexity of vascular response to injury has given rise to a wide range of potential targets for therapeutic intervention in the vasculature. Therapeutic strategies aimed to prevent the NIF, include the following associated factors:

- Reduction in VSMC migration and/or proliferation.
- Inhibition in the degradation of the ECM (pre-exists) and/or inhibition in the up-regulation of newly formed ECM deposits (thus ECM modulation).
- VSMC apoptosis.
- Acceleration of re-endothelialisation and improvement of endothelial function.
- Inhibition in vasculature inflammation.
- Anti-thrombosis

To date, there are many therapeutic genes that have been/are being investigated (involving many different vectors) to prevent the NIF after acute vascular injury and to name but a few are listed in Table 1.2. The ideal therapeutic gene would target the major contributors to pathogenesis of the NIF and mediate an effect by phenotypic modulation of VSMC (migration and/or proliferation) and acceleration of re-endothelialisation, therefore possessing a key strategy to the regulation of vasculature remodelling and maintenance, and inhibition of thrombosis (George et al., 2006, Gaffney et al., 2007).

One of the major hallmarks in the process of the NIF after acute vascular injury is ECM degradation by MMPs, which consequently results in medial VSMC migration into the intima. The activity of these proteins is strongly inhibited by TIMPs (Baker et al., 2002, Newby, 2007, Raffetto and Khalil, 2008). Studies have explored gene transfer of TIMP-1, 2 and 3 mediated by either adenovirus or AAV. Over-expression of these TIMPs in preclinical vascular injury models have

demonstrated inhibition of medial VSMC migration, which mediated a reduction in the NIF (George et al., 1998a, George et al., 1998b, George et al., 2000, Hu et al., 2001, Ramirez Correa et al., 2004).

TIMP-3 is a candidate therapeutic gene that has been extensively studied because of its ability to bind to the MMPs, which inhibits ECM degradation, blocks VSMC migration and induces VSMC apoptosis mediated by its bystander effect. Preclinical studies have demonstrated that the over-expression of TIMP-3 inhibited vascular remodelling at 28 days post-infection, thus reduced NIF in the following acute vascular injury models of disease: *ex vivo* adenoviral gene transfer porcine saphenous vein graft (SVG) model and human SVG organ culture model (George et al., 2000); *ex vivo* non-viral gene transfer mediated by microbubble-facilitated ultrasound delivery in a porcine SVG model (Akowuah et al., 2005) and *in vivo* gene-eluting stent-based adenoviral-mediated delivery in a porcine vascular injury model (ISR model) (Johnson et al., 2005).

The tumour suppressor protein 53 (p53) is another candidate therapeutic gene because it reduces VSMC migration and it is pro-apoptotic. These characteristics are key to the NIF inhibition. It has been shown that adenoviral gene transfer of wild-type p53 mediated over-expression, which resulted in inhibition of the NIF in an *ex vivo* organ culture model of a human vein graft and in an *in vitro* human saphenous SMC isolated culture. This effect was induced by modulation of VSMC migration and an induction of apoptosis (George et al., 2001). Moreover, a further study demonstrated that *ex vivo* adenoviral-mediated gene transfer of p53 prior to grafting an *in vivo* porcine vein graft model, resulted in an increased lumen size and inhibition of the NIF at 28 days post-infection (Wan et al., 2004). For Nogo-B, see section 1.12.1.2 for information on its therapeutic potential in acute vascular injury, which is an area of interest within this study. However, there are still many more potential therapeutic genes, which are key to the NIF inhibition.

Therapeutic genes	Anti-VSMC migration	Anti-VSMC proliferation	ECM modulation	Pro-apoptotic	Pro-re-endothelialisation	Anti-inflammatory	Bystander effect
TIMP-1	✓		✓				✓
TIMP-2	✓	✓	✓				✓
TIMP-3	✓		✓	✓			✓
p53	✓			✓			
β-ARK <sub>ct</sub>		✓					
Nogo-B	✓	✓			✓		✓?
p56 and p56/E2F		✓					
35k						✓	✓

**Table 1.2. Therapeutic genes which are key to the NIF inhibition.**

These include the following: tissue inhibitors of matrix metalloproteinases (TIMP)-1(Baker et al., 1998, George et al., 1998b, Ramirez Correa et al., 2004), TIMP-2 (Baker et al., 1998, George et al., 1998a, Hu et al., 2001), TIMP-3 (Baker et al., 1998, George et al., 2000, Dishart et al., 2003a), tumour suppressor protein 53 (p53) (George et al., 2001), carboxyl terminus of the β-adrenergic receptor kinase (β-ARK<sub>ct</sub>) (Iaccarino et al., 1999, Luo et al., 2004), neurite outgrowth inhibitor isoform B (Nogo-B)(Acevedo et al., 2004, Kritz et al., 2008), retinoblastoma protein (Rb) also known as tumour suppressor protein 56 (p56) and p56/elongation 2 transcriptional factor (E2F) (Wills et al., 2001) and broad spectrum CC-chemokine (CK) binding protein 35k also known as Vaccinia virus strain Lister 35KDa protein (35k)(Ali et al., 2005). ECM, extracellular matrix; VSMC, vascular smooth muscle cells.

### **1.12.1 Nogo-B**

Nogo-B belongs to a superfamily of transmembrane (TM) proteins associated with the endoplasmic reticulum (ER), called the reticulons (RTN). The reticulon family is a large (greater than 300 family members) group of evolutionary conservative membrane-associated proteins found in many eukaryotes, and absent only in archaea and bacteria (Oertle et al., 2003b, Oertle and Schwab, 2003, Voeltz et al., 2006, Yang and Strittmatter, 2007).

All RTN proteins are typically between 200-1200 amino-acids in length and contain a reticulon homology domain (RHD). This RHD domain is a highly conserved region at the carboxyl (C)-terminal domain (approximately 200 amino acids in length) and is comprised of a hydrophilic loop (60-70 amino acids long and known as the 66-amino-acid loop region) flanked by two hydrophobic regions (each 28-36 amino acids in length and membrane embedded known as TMs), followed by a short C-terminal hydrophilic stretch (approximately 50 amino acids long). Each RTN protein has a specific amino acid (N)-terminal domain (Oertle and Schwab, 2003, Voeltz et al., 2006, Yan et al., 2006, Yang and Strittmatter, 2007, Teng and Tang, 2008).

There are four independent mammalian RTN genes which encode RTN proteins 1-4 (RTN1, RTN2, RTN3 and RTN4 also known as Nogo). RTN1-3 were identified prior to RTN4/Nogo. Each gene can give rise to a range of different transcripts (various isoforms differ greatly in their N-terminal domain, with varying length). Each RTN gene and its isoforms have similar but also diverse intracellular and extracellular functions and have a ubiquitous expression pattern in different tissue (mediated by their divergent N-terminal domain), but all have their close association with the ER (mediated through its highly conserved RHD) (Oertle and Schwab, 2003, Voeltz et al., 2006, Yan et al., 2006, Yang and Strittmatter, 2007, Teng and Tang, 2008).

The RHD especially the TM domains are important in the RTN protein association with/translocation into the ER and ER-associated functions. RTNs are primarily localised to the ER (greater than 95%). A small fraction of these RTN proteins also associate with other cellular structures within a cell, such as the cell membrane. It is possible that RTN proteins have cellular functions in ER

morphogenesis (involved in bending and shaping the ER membrane), intracellular trafficking (reticulum-Golgi apparatus trafficking), vesicle formation, membrane morphogenesis, apoptosis and cell division (Oertle and Schwab, 2003, Voeltz et al., 2006, Yan et al., 2006, Yang and Strittmatter, 2007, Teng and Tang, 2008).

RTN-4/Nogo is encoded by a single gene on human chromosome 2 (2p16). There are three major spliced variants/isoforms, known as Nogo-A (RTN-4A), Nogo-B (RTN-4B) and Nogo-C (RTN-4C) (Figure 1.14) (Teng and Tang, 2008). The name Nogo originates from the longest isoform, Nogo-A; a potent inhibitor of neurite outgrowth and axon regeneration after CNS injury, hence the name neurite outgrowth inhibitor (Nogo) (Yan et al., 2006, Yang and Strittmatter, 2007, Teng and Tang, 2008). All three Nogo isoforms have an N-terminus of varying length and (Figure 1.14) various functional roles. Nogo-A and -B have a common N-terminus for the first 184 amino acids (Oertle and Schwab, 2003, Teng and Tang, 2008). Nogo-A (longest Nogo isoform, 250 kDa) is highly expressed in the CNS (Chen et al., 2000, Huber et al., 2002) and has been extensively studied with its myelin-associated neurite outgrowth inhibitory effect (negative regulator in regeneration of the adult CNS after injury), associated with neurological disorders (Teng and Tang, 2008, Schwab, 2010). Nogo-B (45-55 kDa) is expressed ubiquitously, which includes the CNS, peripheral nervous system (PNS), spleen, skeletal muscle, testis, lung, intestine, gall bladder, kidney, heart and vessel walls (Huber et al., 2002, Acevedo et al., 2004). Nogo-B has gained more interest over the recent years because of its diverse biological roles, such as in the modulation of vascular maintenance and remodelling (Acevedo et al., 2004, Kritz et al., 2008), and its pro-apoptotic function in cancer (Li et al., 2001). Nogo-C (shortest Nogo isoform, 25 kDa) is expressed in CNS and skeletal muscle, and very little is known about its function (Huber et al., 2002, Teng and Tang, 2008). All three Nogo spliced variants contain an ER retention sequence at the C-terminal domain (Dodd et al., 2005).

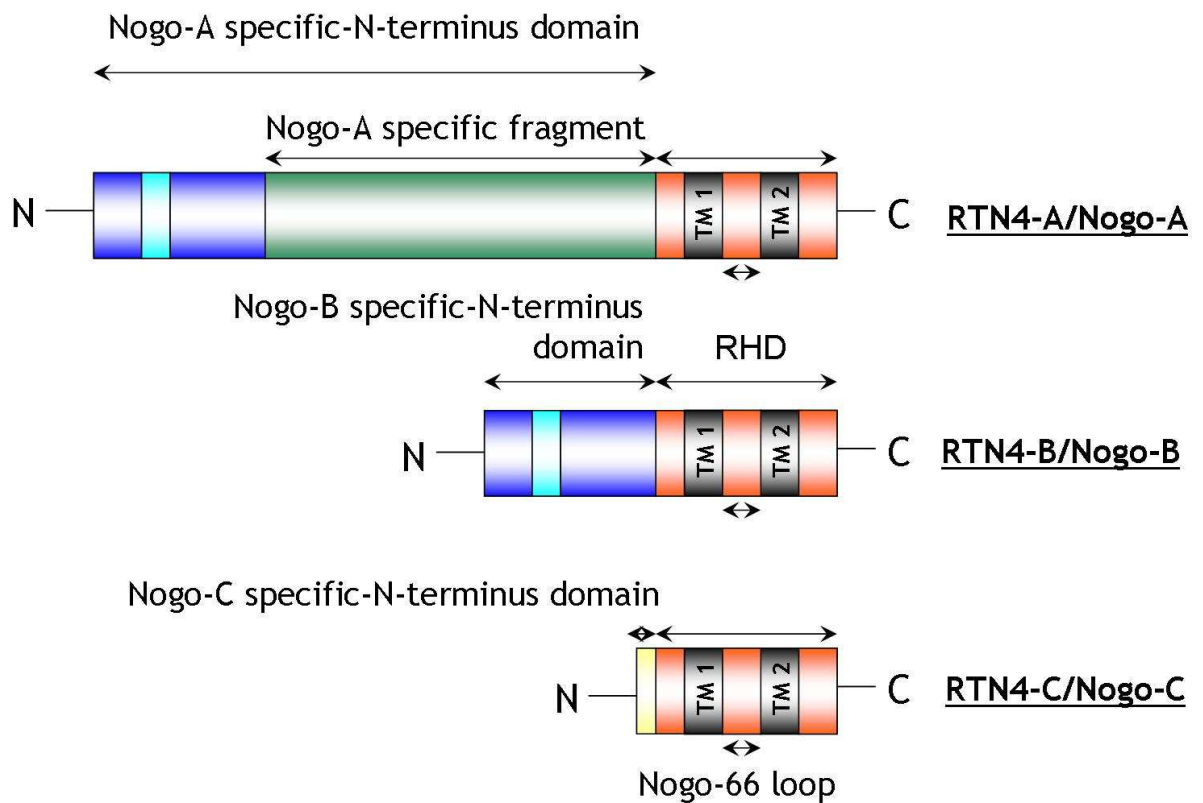


**Figure 1.14. The three major spliced isoforms from the Reticulon-4/Nogo gene.**

Three spliced variants are known as Nogo-A (RTN-4A), Nogo-B (RTN-4B) and Nogo-C (RTN-4C). The conserved carboxyl (C)-terminus encodes the reticulon-homology domain (RHD). This RHD is comprised of a hydrophilic 66-amino acid loop domain (Nogo-66 loop) flanked by two hydrophobic regions which forms the transmembrane (TM1 or TM2) domains and this followed by a short C-terminal hydrophilic stretch. Each RTN protein has a specific amino acid (N) -terminal domain. The Nogo-A specific N-terminal fragment and Nogo-66 loop mediate the inhibition of neurite outgrowth. Nogo-A mediates its effect through the engagement of the extracellular Nogo-66 loop with the axonal cell-surface Nogo-66 receptor/Nogo receptor. Nogo-B has a common N-terminus with Nogo-A for the first 184 amino acids, but does not bear a sequence involved with the induction of a strong inhibitory activity of neurite outgrowth. Little is known about Nogo-C. All three Nogo isoforms have an N-terminus of varying length, diverse tissue expression and various functional roles. Adapted from Oertle and Schwab (2003) (Voeltz et al., 2006, Yan et al., 2006, Yang and Strittmatter, 2007, Teng and Tang, 2008).

### 1.12.1.1 Functional roles of Nogo-B

Nogo-B [spliced variant of Nogo-A lacking a region involved in strong inhibitory activity for neurite out-growth (Oertle et al., 2003a)] has been shown to function as a potent pro-apoptotic protein in various cancer cells, whereas normal cells are relatively resistant (Li et al., 2001). Nogo-B interacts with anti-apoptotic members of the B-cell lymphoma-2 (Bcl-2) family [Bcl-2 and B-cell lymphoma-extra large (Bcl-x<sub>L</sub>)]. This is mediated when the over-expression of Nogo-B prevents the translocation of Bcl-2 and Bcl-x<sub>L</sub> to the mitochondria from the ER, which reduces their anti-apoptotic effect (Tagami et al., 2000, Watari and Yutsudo, 2003). Moreover, the transcription of Nogo-B has been shown to be suppressed in certain cancer types (i.e. lung cancer), therefore this protein may

also act as a tumour suppressor (Li et al., 2001). The Drs protein (tumour suppressor) can interact with Nogo-B, and subsequently induce apoptosis (Tambe et al., 2004). In contrast, one study indicated that the stable over-expression of Nogo-B in certain types of cancer did not significantly induce a pro-apoptotic effect, compared to wild-type control (Oertle et al., 2003c). Nogo-B over-expression may also have the ability to induce ER-stress mediated apoptosis through ER-specific pathways (see section 5.1.1) (Kuang et al., 2006).

Nogo-B has recently been reported to have more biological roles. Endothelial Nogo-B induces adhesion signalling and promotes leukocyte transendothelial migration and diapedesis, therefore plays a key part in the acute inflammation response (Di Lorenzo et al., 2010). Nogo-B was demonstrated to be expressed highly in renal injury from human and murine specimens, and a positive regulator of macrophage recruitment to the obstructive kidney in a murine model of this disease. Therefore, Nogo-B could potentially be a novel biomarker of diverse renal injuries (Marin et al., 2010). Recently, it was reported that Nogo-B displays endogenous expression in the lung epithelium. Data suggested that Nogo-B has a major role as a negative regulator of allergic-driven T-lymphocyte helper 2 (Th2) cells in the asthmatic lung, as supported by the genetic gain and loss of function in a murine model (Wright et al., 2010). Another study indicated that endogenous levels of Nogo-B are important in the airway remodelling in chronic asthma (down-regulated in the airway of chronic asthmatic mice), and in the regulation of migration (Nogo-B necessary for migration) and contraction (increased contractility after Nogo-B down-regulation) of airway smooth muscle cells (Xu et al., 2011). Nogo-B has been identified as a positive regulator of liver fibrosis and cirrhosis in hepatic injury, mediated through the activation of the transforming growth factor-beta (TGF- $\beta$ )/Smad2 signalling pathways in myofibroblasts (Zhang et al., 2011).

The use of Nogo-A/B knockout mice demonstrated the endogenous role of Nogo-B in inflammatory tissue repair and its essential function in chemotaxis of macrophages and associated wound-healing/tissue repair after limb ischaemia. Moreover, Nogo-B influenced and regulated the activation of Ras-related C3 botulinium toxin substrate (Rac), followed by F-actin polymerisation and cell migration of monocytes/macrophages (Yu et al., 2009). A recent study also

demonstrated that Nogo-B may influence human monocyte-derived macrophage migration via association with cytoskeletal structures and cytoskeletal intracellular signalling pathways [actin, Ras homolog gene family, member A (RhoA) and Rac] (Schanda et al., 2011).

Collectively, Nogo-B is an important regulator in wound-healing, tissue repair and/or inflammation during renal injury, asthma, hepatic injury and peripheral vascular disease/limb ischemia.

### **1.12.1.2 Nogo-B has a regulator of vascular remodelling**

Nogo-B has therapeutic potential in the vascular setting (Acevedo et al., 2004, Miao et al., 2006, Pan et al., 2007, Paszkowiak et al., 2007, Rodriguez-Feo et al., 2007, Kritz et al., 2008, Lee et al., 2009, Yu et al., 2009, Zhao et al., 2010). Previous studies have documented high levels of Nogo-B in VECs, VSMCs (Acevedo et al., 2004) and monocytes/macrophages (Paszkowiak et al., 2007, Rodriguez-Feo et al., 2007, Yu et al., 2009). VSMCs have two variants of Nogo-B: Nogo-B1 and Nogo-B2 (Acevedo et al., 2004). Nogo-B protein acts as a positive and negative regulator of vascular cells, respectively by mediating the chemoattraction of VECs and antagonising migration and proliferation of VSMCs in response to PDGF-BB (Figure 1.15) (Acevedo et al., 2004, Kritz et al., 2008). Nogo-B protein expression is predominantly found in a reticular pattern [due to its ER retention sequence in the C-terminus domain (Raines, 2004a, Dodd et al., 2005)] with a small fraction (approximately 2% of the total Nogo-B protein per vascular cell) localised within the cell membrane of vascular cells (Acevedo et al., 2004). Moreover, the N-terminus of Nogo-B has been found to be located extracellularly (Acevedo et al., 2004). Nogo-B may have two special topological patterns. This is because, the two long TM domains may span the plasma membrane once or twice, and thus could locate the Nogo-66 loop either inside or outside the vascular cell (Figure 1.15) (Acevedo et al., 2004).

Endogenous Nogo-B expression is important for vascular maintenance and remodelling (Acevedo et al., 2004), as well as cardiac function (Bullard et al., 2008). Nogo-B expression is down-regulated following acute vascular injury. Indeed, mice deficient in Nogo-A/B demonstrated accelerated rates of NIF after acute vascular injury, which were attenuated/rescued by adenoviral gene

transfer of Nogo-B (Acevedo et al., 2004). Recently, it was shown that the NIF was rescued in a porcine vein graft model and a wire injured mouse model mediated by adenoviral gene transfer of Nogo-B, and this was associated with a reduction in VSMC proliferation (Kritz et al., 2008). In terms of VSMCs, mechanistically it is known that the N-terminus of Nogo-B blocks PDGF-BB induced VSMC migration *in vitro* (Acevedo et al., 2004, Kritz et al., 2008). This effect may occur through competitive binding antagonism of the PDGF receptor (PDGFR) or functional blockade of PDGF signalling downstream of the receptor (Acevedo et al., 2004). However, it is unknown if this is the functional domain which mediates phenotypic effects of VSMC proliferation. It has been suggested that the Nogo-B phenotypic effects on VSMC migration and/or proliferation, maybe facilitated through modulation of signal transduction from the cell surface and/or it may mediate its effect by ER-specific activities (such as the regulation of the structure of the ER network in association with cytoskeletal structures, and/or possible ER-stress mediated apoptosis) (see Figure 1.15) (Raines, 2004a), all of which will be discussed further in chapter 5.

Nogo-B expression is down-regulated in human arterial atherosclerotic plaques (Rodriguez-Feo et al., 2007, Lee et al., 2009), stenotic lesions (Rodriguez-Feo et al., 2007), and lesions of aortic aneurysms (Pan et al., 2007). The reduction of Nogo-B protein may contribute to plaque formation, destabilisation and vascular abnormalities (Pan et al., 2007, Rodriguez-Feo et al., 2007, Lee et al., 2009). Nogo-B has been shown to be reduced in the intima and media, but up-regulated in the adventitia under conditions of injury-induced NIF and has been regarded as a biomarker for injury-induced NIF (Paszkwiaik et al., 2007). Shear-stress and low-flow induced inward remodelling differs mechanistically, and is distinct from injury-induced NIF, and is associated by an endothelium-dependent compensatory mechanism and infiltration of inflammatory cells (Tronc et al., 1996). The injury-induced NIF can only partially account for lumen loss during restenosis, and additionally the rearrangement within the vasculature following shear-stress and low-flow induced inward remodelling could explain the reduction of lumen (Paszkwiaik et al., 2007). It has been shown that intimal Nogo-B is reduced and no change in medial and adventitial Nogo-B levels during inward remodelling. Inward remodelling differs mechanistically from vascular injury in terms of Nogo-B expression and therefore Nogo-B is not a

marker/mediator of inward remodelling (Paszowski et al., 2007). However, low-flow induced inward remodelling along with vascular injury-induced NIF enhanced NIF associated with reduced Nogo-B expression levels in the intimal and medial layers and increased Nogo-B expression in macrophage within the adventitial layer. Thus, Nogo-B is a regulator in vascular remodelling and also vascular inflammation (Paszowski et al., 2007). Nogo-B was demonstrated to contribute to vascular apoptosis. High levels of Nogo-B were located in macrophage/foam cell-rich areas of human carotid plaques (contribute to lipid-rich necrotic cores), and therefore may induce VSMC apoptosis (Rodriguez-Feo et al., 2007). Additionally, it is also important to consider validating vascular beds in terms of cell turnover and macrophage recruitment in the adventitial layer in the gene delivery of Nogo-B in ISR and CABG animal models. Mechanistically, how Nogo-B inhibits NIF in response to acute vascular injury is unknown, but mechanisms will be addressed in chapter 5.

The lack of Nogo-receptor (Nogo-receptor binds to the Nogo-66 loop) expressed in VECs and VSMCs (Acevedo et al., 2004), led to the identification of a Nogo-B receptor (Ng-BR), which is highly expressed in blood vessels, VECs and in the heart (Miao et al., 2006). This receptor is presumed to be localised at the cell surface membrane and the ER (Miao et al., 2006, Harrison et al., 2009). Ng-BR is specific for the N-terminus of Nogo-B (Miao et al., 2006). N-terminus of Nogo-B promotes the adhesion and chemotaxis of VECs, and negatively regulates PDGF-BB-induced migration of VSMCs (Figure 1.15) (Acevedo et al., 2004). Ng-BR has been described to be essential for Nogo-B- and vascular endothelial growth factor (VEGF)- stimulated VECs migration in vascular remodelling and angiogenesis, via the activation and phosphorylation of Akt of the phosphatidylinositol 3-kinase (PI3K) pathway (Figure 1.15) (Miao et al., 2006, Zhao et al., 2010).

Ng-BR (transmembrane receptor) consists of an intrinsically unstructured ectodomain (with no secondary and tertiary structures) and a partially folded cytoplasmic domain (with secondary structures and weak tertiary structures). It has been suggested that this Ng-BR is very rare (Li and Song, 2007). Plus, the intrinsically unstructured protein ectodomain may be favourable and facilitate specialised biological functions, such as signal transduction, cytoskeletal organisation, protein-DNA recognition, endocytosis and maintenance/production

of membrane structures. Thus, this transmembrane receptor may possess a disordered function due to its structure (Li and Song, 2007). This receptor has been demonstrated to have implications in the regulation of intracellular cholesterol trafficking (Harrison et al., 2009) and dolichol biosynthesis (Harrison et al., 2011), as well as in vascular remodelling and angiogenesis (Figure 1.15) (Miao et al., 2006, Zhao et al., 2010).

Circulating Nogo-B (secreted Nogo-B) levels are detectable in human plasma, however the mechanism of secreting this transmembrane protein is unclear (Rodriguez-Feo et al., 2007). As mentioned the soluble N-terminal domain of Nogo-B (soluble Nogo-B) promotes vascular cell adhesion and modulates migration (Acevedo et al., 2004). Taken together, Nogo-B is presumed to also exert its effects on VECs and VSMCs migration through a bystander effect.

In summary, Nogo-B is a candidate therapeutic gene for the inhibition of the NIF, due to its characteristics [positive and negative regulator of VEC migration and VSMC migration and proliferation, respectively, and has a possible bystander effect (if soluble) (see Table 1.2)] which are key to the regulation of the vascular remodelling and maintenance during the acute vascular injury response.

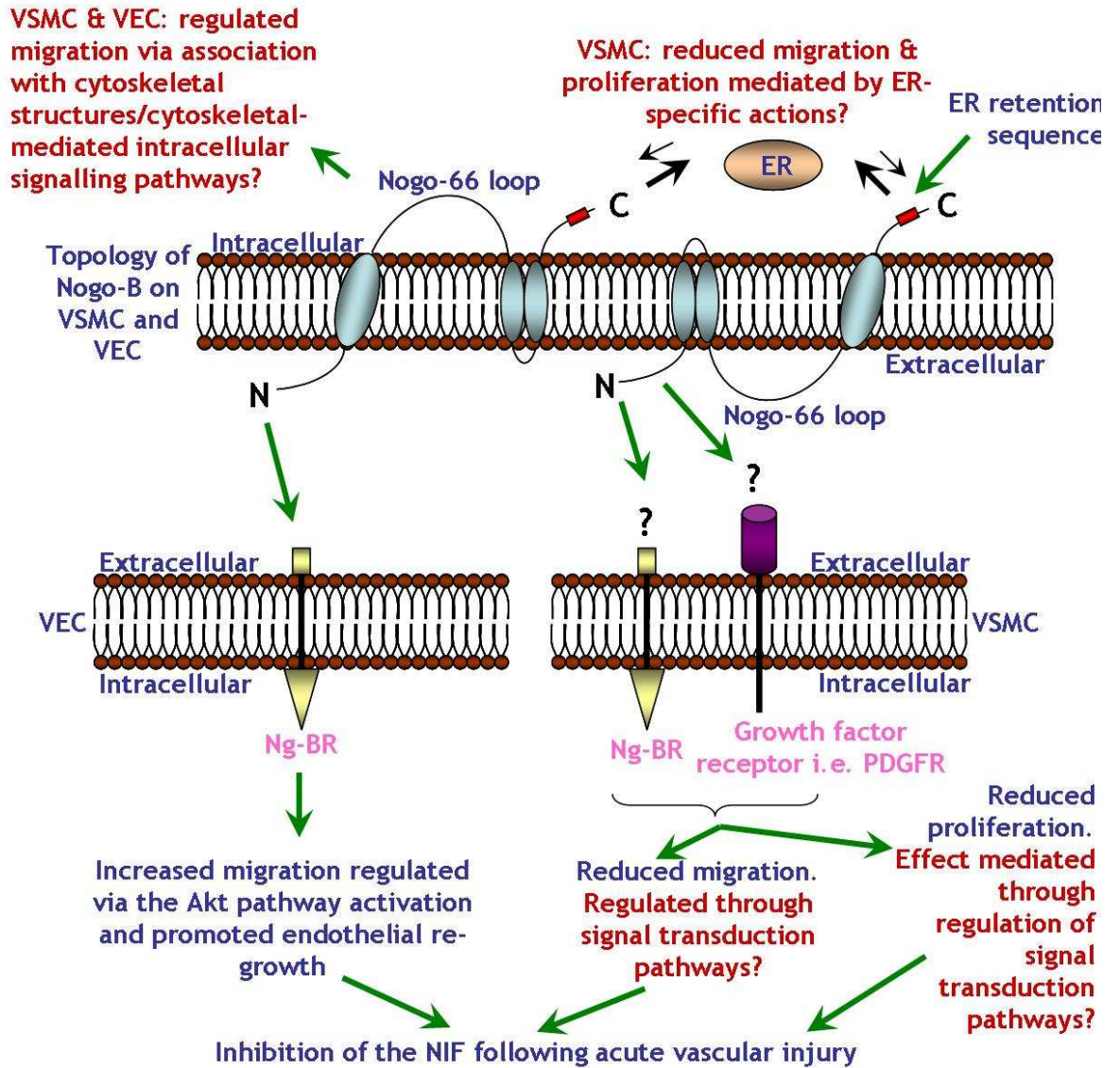


**Figure 1.15. The involvement of Nogo-B in vascular maintenance and remodelling.**

Nogo-B protein acts as a positive regulator of vascular endothelial cell (VEC) migration and a negative regulator of vascular smooth muscle cell (VSMC) migration and proliferation. ER, endoplasmic reticulum; NIF, neointima formation; PDGFR, platelet-derived growth factor receptor; Ng-BR, Nogo-B receptor. Adapted from Raines (2004a) (Acevedo et al., 2004, Miao et al., 2006, Kritz et al., 2008, Yu et al., 2009, Zhao et al., 2010, Schanda et al., 2011).

### 1.13 *Ex vivo* and *in vivo* gene delivery for vascular injury

A number of gene transfer vectors (coupled with a specific therapeutic gene key to the NIF) have been explored for local delivery to the vasculature during revascularisation (in preclinical vascular injury models such as human, pig, rabbit and mouse) mediated through catheters (Luo et al., 2004, Numaguchi et al., 2004, Qian et al., 2006, Nakano et al., 2007), direct injection (Ramirez Correa et al., 2004, Kritz et al., 2008) or prior to grafting (George et al., 2000, Hu et al., 2001, Kritz et al., 2008). Subsequently, these methods have demonstrated efficient transduction and effective inhibition of the NIF during the acute vascular injury response.

CABG is particularly well suited to *ex vivo* gene delivery because of the access of vascular tissue before grafting, thus enhancing the safety profile of this potentially useful therapy. During a CABG gene therapy procedure, *ex vivo* vascular gene delivery would involve a harvested autologous blood vessel (most commonly a saphenous vein) from a patient, which would then be incubated with the gene transfer vector of choice (carrying the desired therapeutic gene) before grafting. This clinical window would be narrow and between 10-30 minutes, thus it would be necessary to use an efficient gene delivery vector to mediate gene transfer into the vasculature. This genetically engineered vascular conduit graft would then be re-introduced into the patient and subsequently express the therapeutic transgene (Baker et al., 2006, George et al., 2006). In a pig model of vascular bypass grafting surgery, *ex vivo* delivery of an adenoviral vector expressing Nogo-B in an autologous saphenous vein demonstrated significant inhibition of the NIF, in comparison to the control adenoviral vector treated vein (Kritz et al., 2008).

## 1.14 Aims of Thesis

The principle aim of this thesis was to assess NILV-mediated gene transfer to facilitate over-expression of Nogo-B in VSMCs and assess the phenotypic effects, as a potential therapeutic strategy for the prevention of the NIF following acute vascular injury. This was achieved through the following assessments:

- Optimisation of LVs for human vascular cell gene transfer *in vitro*, in terms of alternative promoters, vector pseudotyping and integration-deficiency.
- Analysis of the effect of Nogo-B over-expression on human primary VSMC migration and proliferation, mediated by NILVs or int-LVs *in vitro*.
- Analysis of the mechanism of action of Nogo-B on human VSMCs *in vitro*.

## **2 Materials and Methods**

## 2.1 Chemicals

All Chemicals, unless otherwise stated, were obtained from Sigma-Aldrich (Poole, Dorset, UK) and were of the highest grade obtainable. All cell culture reagents were obtained from Gibco® (Invitrogen, Paisley, UK) unless otherwise stated. Dulbecco's calcium and magnesium free phosphate buffered saline (PBS) (sterile) was obtained from Lonza (Slough, UK). All primers and probes (oligonucleotides) were obtained from MWG-Biotech (Ederberg, Germany). Nuclease-free water [not diethylpyrocarbonate (DEPC)-treated] was purchased from Ambion® (Applied-Biosystems/Ambion, Warrington, UK).

## 2.2 Cell culture

All primary cell isolations and cell cultures were performed in sterile conditions using biological safety class II vertical laminar flow cabinets. Cells were grown in 37°C incubators maintained at 5 % CO<sub>2</sub> and 95 % air. Details of media used for growth and maintenance for each established cell line and primary cells are shown in Table 2.1.

### 2.2.1 *Isolation and culture of primary vascular cells*

Freshly obtained saphenous veins from patients that had undergone coronary artery bypass grafting (CABG) surgery were stored in sterile saline solution by the Glasgow Golden Jubilee National Hospital, until collection. Samples were cleaned of excess connective tissue under sterile conditions. The study complies with the Declaration of Helsinki and was approved by the West of Scotland Research Ethics Committee 1 (Reference number: 06/S0703/110). All participants gave written informed consent.

#### 2.2.1.1 **Isolation of vascular endothelial cells from human saphenous veins**

Human saphenous vein endothelial cells (HSVECs) were isolated on the day of surgery by standard collagenase digestion, based on a modified version of the protocol described (Jaffe et al., 1973). In summary, saphenous veins were gently perfused with wash media [Dulbecco's Modified Eagle's Medium (DMEM) (with 1 g/L D-glucose, 110 mg/L sodium pyruvate and phenol red and without L-

glutamine) supplemented with 1 % (v/v) penicillin, 100 µg/ml streptomycin and 2mM L-glutamine], to flush out remaining blood. Veins were cannulated with a sterile small surgical crocodile clip at one end, infused with wash media supplemented with 2 mg/ml of type IV collagenase (Sigma-Aldrich and sterile-filtered) and cannulated on the opposite side. Type IV collagenase was used because the endothelial monolayer is seated on a basement membrane consisting of collagen type IV, thus allowing detachment (Newby and Zaltsman, 2000). Vessels were incubated at 37°C in a sterile petri dish (with a lid) in 5 % CO<sub>2</sub> for 15 minutes (min). HSVEC suspensions were obtained by flushing the vein with wash media and collecting flow-through in a sterile petri dish. Veins were refilled with collagenase solution, incubated at 37°C for a further 10 min, flushed through and EC suspension collected and pelleted by centrifugation at 2,000 x g for 5 min at room temperature (RT). HSVECs were resuspended in 5 ml of 20 % complete EC media (Table 2.1), placed in a 25 cm<sup>2</sup> tissue culture (T-25) flask and incubated at 37°C in 5 % CO<sub>2</sub>. After 24 hours (h) incubation culture media was removed, HSVECs were washed twice in PBS (to remove remaining non-adherent red blood cells and debris) and fresh 20 % complete EC media added. Culture media was changed every 3-4 days (d) and these cells were used up to passage of 5. In culture, these HSVECs had a cobble like morphology (Jaffe et al., 1973). Three individual preparations of HSVECs were used in this thesis.

Cell type	Description	Composition of cell culture media used	Detaching reagent
HeLa cells (American Type Culture Collection [ATCC]- LGC Standards, Middlesex, UK)	Human cervical carcinoma cell line.	Minimum Essential Media (MEM) (BioWhittaker, UK) supplemented with 10 % (v/v) fetal calf serum (FCS) (FCSPAA Laboratories, Yeovil, UK), 1% (v/v) penicillin, 100 µg/ml streptomycin, 2 mM L-glutamine and 1 mM sodium pyruvate (Sigma-Aldrich) (10 % complete MEM).	Trypsin-ethylenediamine tetra-acetic acid (EDTA)
293 cells (ATCC-LGC Standards)	Human Embryonic Kidney (HEK) cell line.	10 % complete MEM.	Citric saline
293T cells (ATCC-LGC Standards)	HEK transformed cell line (contains adenoviral and simian virus (SV)-40 DNA sequences).	10 % complete MEM.	Citric saline
B50 cells (European Collection of Cell Cultures [ECACC], Health Protection Agency, Salisbury, UK)	Rat cortical neuronal cell line.	Dulbecco's Modified Eagle Medium (DMEM) 1x (with 1 g/L D-glucose and 110 mg/L sodium pyruvate and without L-glutamine and phenol red) supplemented with 10 % (v/v) FCS, 1 % (v/v) penicillin, 100 µg/ml streptomycin and 2 mM L-glutamine (10 % complete DMEM).	Trypsin-EDTA
Vascular smooth muscle cells (VSMCs)	Primary vascular smooth muscle cells isolated from human saphenous vein.	Smooth muscle cell (SMC) growth media 2 (PromoCell, Heidelberg, Germany) with the addition of the supplement mix (containing 5 % [v/v] FCS, 0.5 ng/ml human epidermal growth factor, 2 ng/ml human basic fibroblast growth factor and 5 µg/ml human insulin), plus 10 % (v/v) FCS (for a 15% [v/v] FCS final concentration), 1 % (v/v) penicillin, 100 µg/ml streptomycin and 2 mM L-glutamine (15 % complete SMC media).	Trypsin-EDTA
Vascular endothelial cells (VECs)	Primary vascular endothelial cells isolated from human saphenous vein.	Large vessel endothelial cell (EC) basal medium (TCS cellworks Ltd, Buckingham, UK) supplemented with a large vessel endothelial cell growth supplement pack (containing hydrocortisone, human epidermal growth factor, human fibroblast growth factor with heparin and an antibiotic supplement [containing 25 mg/ml gentamicin and 50 µg/ml amphotericin B]) with the addition of 20 % (v/v) FCS, 1 % (v/v) penicillin and 100 µg/ml streptomycin and 2 mM L-glutamine (20 % complete EC media).	Trypsin-EDTA

Table 2.1. Media used to culture these cells in this study.

### **2.2.1.2 Isolation of vascular smooth muscle cells from human saphenous veins**

Following HSVEC isolation, vessels were stored overnight at 4°C in sterile-filtered dissection media [DMEM (with 1 g/L D-glucose, 110 mg/L sodium pyruvate and phenol red and without L-glutamine) supplemented with 1 % (v/v) penicillin, 100 µg/ml streptomycin, 2 mM L-glutamine and 15 mM Hepes buffer]. The following day human saphenous vein smooth muscle cells (HSVSMCs) were obtained from medial explants extracted from these veins, according to the method described (Southgate and Newby, 1990). Briefly, segments of veins were cleaned of fat and connective tissue, subsequently cut longitudinally and pinned luminal side up on a layer of sylgard [(184 encapsulating resin from BDH, Poole, Dorset, UK) set in a glass petri dish]. A rubber policeman was used to remove the endothelial layer, if the vein had not undergone HSVEC isolation. The medial layer was scored at 1 cm intervals with a sterile scalpel, segments of tunica media were then peeled off from the adventitial layer with a pair of forceps. Segments were cut into 1 mm<sup>2</sup> size squares using a McIlwain tissue chopper. Segments were washed twice in dissection media, followed by a wash in 15 % complete SMC media (Table 2.1) and then incubated at 37°C in 5 % CO<sub>2</sub> in minimal media until adhesion to the T-25 flask (approximately 24 h). Subsequently, explants were cultured in 15 % complete SMC media at 37°C in 5 % CO<sub>2</sub>. HSVSMCs were seen migrating from explants. Culture media was changed every 5-7 d and these cells were used up to passage of 8. In culture, these HSV SMCs had a hill and valley morphology (Chamley-Campbell et al., 1979). Twenty seven individual preparations of HSVSMCs were used in this thesis.

### **2.2.1.3 Immunocytochemical characterisation of vascular smooth muscle cells**

HSVSMCs were identified by immunocytochemistry staining for smooth muscle actin (SM-actin). At passage 1, HSVSMCs were harvested and seeded in 8-well culture slides (BD Biosciences, Oxford, UK), and incubated at 37°C in 5 % CO<sub>2</sub>. Media was removed from HSVSMCs once they had reached 80-90 % confluence, washed twice in PBS at RT for 5 min each and fixed in 4 % (w/v) paraformaldehyde (PFA) at RT for 10 min. HSVSMCs were washed in PBS three times, permeabilised in 0.1 % (v/v) triton x-100 in PBS at RT for 10 min, followed by three further PBS washes. HSVSMCs were incubated with 0.3 % H<sub>2</sub>O<sub>2</sub> in PBS at

RT for 10 min to block endogenous peroxidases, followed by three PBS washes. HSVSMCs were incubated in 10 % rabbit serum and 1 % (w/v) bovine serum albumin (BSA) in PBS (blocking solution) at RT for 30 min to block non-specific binding of antibodies. HSVSMCs were then incubated with 1.4 µg/ml of monoclonal mouse anti-human SM-actin IgG2a (clone 1A4) (Dako, Glostrup, Denmark) primary antibody or with appropriate isotype-matched mouse primary antibody (Dako) at 4°C for 16-18 h in blocking solution, and then washed once in 0.1 % (v/v) tween20 in PBS to remove unbound primary antibodies, followed by two PBS washes. Next, HSVSMCs were incubated with 2.85 µg/ml of polyclonal rabbit anti-mouse IgG biotinylated (conjugated with biotin) (Dako) secondary antibody in PBS at RT for 1 h and then washed three times in PBS to remove any unbound biotinylated secondary antibodies. For enhanced colour intensity and detection of primary/biotinylated antibody complex, HSVSMCs were incubated with avidin-biotinylated complex (ABC) associated with horseradish peroxidase (HRP) at RT for 30 min [from the Vectastain® ABC elite kit (Vector laboratories, Peterborough, UK) and prepared according to the manufacturer's instructions], followed by three washes in PBS to remove any unbound ABC reagent. Avidin reacts with biotin on the secondary antibodies, forming a larger complex. HSVSMCs were incubated with diaminobenzidine (DAB) solution [consisting of DAB (chromogen) and hydrogen peroxide (substrate)] (Vector laboratories) until cells developed a brown intensity (approximately 1 min) and placed in deionised water to stop the reaction. The HRP enzyme catalyses the substrate/chromogen reaction to form a brown colour. HSVSMCs were then counter-stained with Harris haematoxylin for nucleus staining for 30 seconds (sec), washed in running water, dehydrated in ascending ethanol concentrations (70 %, 95 % and 100 %) and incubated twice in Histoclear (each for 7 min), before mounting in DPX. HSVSMCs were visualised using bright-field microscopy using Olympus BX40 microscope (Olympus®, Essex, UK) at either 100 × or 400 × magnification. Micrographs were acquired using Hitachi HV-C20A CCD camera (Hitachi®, Maidenhead, UK) for digital imaging with ImagePro (MediaCybernetics®, Bethesda, MD, USA). Nuclei appeared blue/purple and areas where the primary antibody had bound appeared brown. After immuno-staining, approximately 90 % of these isolated and cultured HSVSMCs stained positive for the SM-actin marker (Figure 2.1).

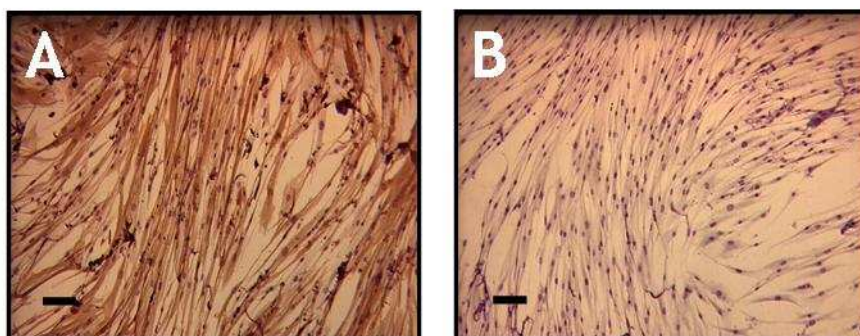


**Figure 2.1. Immunocytochemistry for smooth muscle (SM)-actin in HSV SMCs.** Immunocytochemistry was carried out on VSMCs in permeabilised conditions. (A) monoclonal mouse anti-human SM-actin IgG2a primary antibody (1.4 µg/ml) was used to detect SM-actin. (B) Isotype-matched mouse IgG2a primary antibody was used to indicate no non-specific binding of the anti-human SM-actin antibody. A polyclonal rabbit anti-mouse IgG biotinylated (2.85 µg/ml) secondary antibody was used, followed by avidin-biotinylated complex associated with horseradish peroxidase and diaminobenzidine (DAB) which produced a brown colour for positive staining. 100 µm scale bar applicable to both panels (magnification × 100).

### **2.2.2 Maintenance of established cell lines and primary cells**

Cells were grown as a monolayer and media was replenished every 3-4 d. Cells were routinely passaged at approximately 80 % confluence to prevent loss of surface contact and overgrowth. To passage, cells were washed twice in PBS and incubated in a minimal volume of trypsin-EDTA or citric-saline (as stated in Table 2.1) at 37°C in 5 % CO<sub>2</sub>, for approximately 5 min or until the majority of cells had detached from the flask. The action of trypsin-EDTA or citric saline was blocked by the addition of an equal volume of complete media containing serum (rich source of trypsin inhibitors). Cells were pelleted by centrifugation at 480 x g for 5 min, supernatant removed and resuspended in fresh complete media for passaging or plating.

For intracellular signal transduction assays the following culture media was also used: serum-free media/ 0 % serum complete SMC media [MEM supplemented with 1 % (v/v) penicillin, 100 µg/ml streptomycin, 2 mM L-glutamine and 1 mM sodium pyruvate] and 1 % serum complete SMC media [MEM supplemented with 1 % (v/v) FCS, 1 % (v/v) penicillin, 100 µg/ml streptomycin, 2 mM L-glutamine and 1 mM sodium pyruvate]. A 30 min incubation with 50 µM Phorbol 12 myristate 13-acetate (PMA) (Sigma-Aldrich) in 0 % serum complete SMC media was used as a positive control of the activation of ERK 1 & 2 intracellular signal transduction in VSMCs.

For plating, cells were counted using a haemocytometer (Hausser Scientific, Horsham, Pa. USA) for the required cell density. A cover-slip was placed on the haemocytometer grid and 10  $\mu$ l of the cell suspension was applied to the grid under the cover-slip. The number of cells per ml was determined by counting the number of cells in 4 sets of 16 corner squares, followed by the average number of cells in 1 set of 16 corner squares and multiplied by  $10^4$ . To determine the volume of cell suspension required for a specific cell density/well, the following equation was used:

$$\left( \frac{\text{cell density required}}{\text{number of cells} \times 10^4 / \text{ml in cell suspension}} \right) = \text{ml of cell suspension required/ well.}$$

### ***2.2.3 Cryopreservation and recovery of cultured cell lines and primary cells***

Cells were harvested as described above (section 2.2.2) and resuspended at a density of approximately  $1-2 \times 10^7$  cells/ml for primary cells or  $1-2 \times 10^6$  cells/ml for cell lines in cryo-preservation media [complete cell culture media supplemented with 10 % (v/v) dimethyl sulphoxide (DMSO) (removed ice crystal formation and partially solubilised the cell membrane) and sterile-filtered]. 1 ml of the cell suspensions were aliquoted into sterile 2 ml cryo-preservation vials and cooled at a constant  $-1^\circ\text{C}/\text{min}$  at  $-80^\circ\text{C}$  using isopropanol. Vials were then transferred to liquid nitrogen and stored indefinitely until required.

For resuscitation, cryo-preserved cells were removed from liquid nitrogen, thawed at  $37^\circ\text{C}$  in minimal time required (approximately 1-2 min) and then added drop-wise to 10 ml of pre-warmed complete culture media (Table 2.1). Cells were then pelleted (section 2.2.2), supernatant discarded (to remove DMSO), resuspended in complete culture media and transferred to a T-25 flask. Cells were then incubated overnight at  $37^\circ\text{C}$  and the complete culture media changed.

## 2.3 Plasmid DNA

### 2.3.1 Transformation of competent bacteria

All bacterial culturing was performed in sterile conditions using biological safety class II vertical laminar flow cabinets. Cells were grown in 37°C incubators. DNA is a hydrophilic molecule and is naturally repelled by the cell membrane. As a result, bacteria have to be made 'competent' by producing small pores in the bacterial cell wall and membrane, by suspending the cells in ice cold 50 mM CaCl<sub>2</sub> repeatedly. Competent *E.coli* cells were used to transform plasmid DNA; these were JM109 cells (Promega, Southampton, UK), XL-1 blue cells or XL-10 gold cells (both from Stratagene-Agilent Technologies, Wokingham, UK) (Table 2.2). Competent bacterial cells were thawed gently on ice for approximately 5 min. 50 µl of competent cells were transferred into pre-cooled 1.5 ml micro-centrifuge tubes and incubated on ice for 10 min with shaking every 2 min. For XL-10 gold cells, an additional 2 µl of β-mercaptoethanol was added to increase transformation efficiency. To each 50 µl aliquot, 1 µl of unknown concentration or approximately 10 ng-50 ng of plasmid DNA was added, mixed and kept on ice for 30 min, allowing the plasmid DNA to bind to the cell wall and membrane and enter through the small pore. Cells were then subjected to heat shock at 42°C for 40 sec and immediately returned to ice for a further 2 min. Cells were removed from the ice and 1 ml of RT SOC (Super Optimal broth with Catabolite repression) media (20g/l bactotryptone, 5 g/l yeast extract, 10 mM NaCl, 2.5 mM KCl and 20 mM glucose) was added to each aliquot, followed by 1 h incubation at 37°C in an orbital shaker at 180 rpm, to allow the expression of the newly acquired plasmid DNA. 20 µl or 200 µl of bacterial transformation cultures were spread onto Luria-Bertani (LB) agar plates (10 g/l bactotryptone, 5 g/l bacto yeast extract, 5 g/l NaCl and 15 g/l agar and pH 7.5) with 100 µg/ml of ampicillin [all DNA plasmids used in the study were ampicillin resistant (as described in Table 2.2)]. Plates were kept in a 37°C incubator overnight, to allow the growth of antibiotic resistant transformant colonies.

### 2.3.2 Glycerol stocks of transformed competent bacteria

For archiving of plasmid DNA transformant colonies (Table 2.2), glycerol stocks were generated. A single colony was picked from a freshly spread/streaked (LB

agar plate with ampicillin and amplified in 5 ml of LB broth with 100 µg/ml of ampicillin for 8 h (for mid-log phase) at 37°C with shaking at 180 rpm. Glycerol stocks consisted of 30 % (v/v) sterile glycerol and 70 % (v/v) of plasmid DNA transformant bacteria in 2 ml sterile cryo-preservation vials. Glycerol stocks were mixed thoroughly by vortexing and stored at -80°C until required for streaking on LB agar plate with ampicillin.

DNA plasmid name	Description of DNA plasmid	Plasmid specificity	Reference	Antibiotic resistance	Competent bacteria used in transformation
pHR'SIN-cPPT-SFFV-eGFP-WPRE	Lentiviral vector construct with spleen focus forming virus (SFFV) promoter and cDNA encoding enhanced green fluorescent protein (eGFP)	Lentiviral vector construct plasmid	Demaison et al., 2002	Ampicillin	JM109
pHR'SIN-cPPT-UCOE-eGFP-WPRE	Lentiviral vector construct with enhancer-less ubiquitously acting chromatin opening element (UCOE) promoter and cDNA encoding eGFP	Lentiviral vector construct plasmid	Zhang, et al., 2007	Ampicillin	XL-10 gold
pCMV delta R8.74	Wild-type integrase gene	Second-generation packaging plasmid	Yanez-Munoz et al., 2006	Ampicillin	JM109
pCMV delta R8.74 D64V	Integrase-deficient gene (D64V point mutation)	Second-generation packaging plasmid	Yanez-Munoz et al., 2006	Ampicillin	JM109
pMD.G2	Vesicular stomatitis virus-glycoprotein envelope (VSV-g)	Envelope plasmid	Zhang et al., 2007	Ampicillin	JM109
pHCMVwhvGP64	Baculovirus gp64 glycoprotein envelope (GP64)	Envelope plasmid	Sinn et al., 2005	Ampicillin	JM109
pEZGP	Ebola Zaire glycoprotein envelope	Envelope plasmid	Sinn et al., 2003	Ampicillin	JM109

DNA plasmid name	Description of DNA plasmid	Plasmid specificity	Reference	Antibiotic resistance	Competent bacteria used in transformation
pRRV-E2E1	Ross River Virus glycoprotein envelope (RRV)	Envelope plasmid	Kang et al., 2002	Ampicillin	JM109
pHIT456(MLV-A)	Murine Leukaemia Virus-Amphotropic glycoprotein envelope (MLV-A)	Envelope plasmid	Lodge et al., 1998	Ampicillin	JM109
pEcoMLVenv	Murine Leukaemia Virus-Ecotropic glycoprotein envelope	Envelope plasmid	Koch et al., 2006	Ampicillin	JM109
pHNTV-M	Hantavirus glycoprotein envelope (HNTV)	Envelope plasmid	Qian et al., 2006	Ampicillin	XL-1 blue
pLP-RVG	Rabies glycoprotein envelope	Envelope plasmid	Rahim et al., 2009	Ampicillin	JM109
pHR'SIN-cPPT-SFFV-MCS-WPRE	Lentiviral vector construct with SFFV promoter and multiple cloning site (MCS)	Lentiviral vector construct plasmid	Ward et al., 2011	Ampicillin	JM109
pHR'SIN-cPPT-SFFV-fulllengthNogo-B-WPRE	Lentiviral vector construct with SFFV promoter and cDNA encoding full length Nogo-B	Lentiviral vector construct plasmid	See Chapter 4	Ampicillin	JM109
pHR'SIN-cPPT-SFFV-mutantNogo-B-WPRE	Lentiviral vector construct with SFFV promoter and cDNA encoding mutant Nogo-B	Lentiviral vector construct plasmid	See Chapter 4	Ampicillin	JM109

Table 2.2. Plasmid DNA used to produce lentiviral vectors.

SIN, self-inactivating; cPPT, central polypurine tract; WPRE, woodchuck post-transcriptional regulatory element.

## 2.4 Plasmid preparation

### 2.4.1 *Plasmid DNA isolation and purification from bacterial cells*

Plasmid DNA was isolated and purified using either the QIAprep® Miniprep kit or the QIAGEN® plasmid purification Maxi kit (Qiagen, Crawley, UK) from bacterial cells.

#### 2.4.1.1 Small scale preparation of plasmid DNA (Miniprep)

The QIAprep® Miniprep kit was used for fast and cost-effective isolation, and purification of approximately 20 µg of plasmid DNA. In this protocol, bacteria were lysed under alkaline [sodium hydroxide (NaOH)/ sodium dodecyl sulphate (SDS)] conditions, and then applied to the QIAprep spin columns which consisted of a silica gel membrane that mediated the binding of DNA in the presence of a high-salt buffer, followed by several washes to remove impurities and finally pure plasmid DNA was eluted in low-salt buffer.

This small scale isolation and purification of plasmid DNA was carried out according to the manufacturer's instructions. Briefly, a single colony was picked from a freshly spread or streaked LB agar plate with ampicillin, and amplified in 5 ml of LB broth with ampicillin for 12-16 h (stationary phase) at 37°C in an orbital shaker at 180 rpm. Harvested bacterial cells were centrifuged at 6800 x g for 3 min at RT. Pelleted bacterial cells were resuspended in 250 µl of P1 buffer [containing Tris-HCl (pH 8.0) and EDTA] with 100 µg/ml of ribonuclease A (RNase A) to allow degradation of bacterial RNA. EDTA chelates divalent metals (i.e. Mg<sup>2+</sup> and Ca<sup>2+</sup>) and the removal of these cations destabilises the bacterial cell wall, which allows P2 buffer to reach the peptidoglycan cell wall for degradation. EDTA chelates Mg<sup>2+</sup> ions, which are required for function of deoxyribonucleases (DNases), and therefore prevents any degradation of plasmid DNA during isolation. Tris-HCl provides isotonic conditions to stop the bacterial cells bursting open during re-suspension. 250 µl of P2 lysis buffer [containing NaOH (alkaline conditions) and SDS] was then added for bacterial cell lysis and mixed thoroughly by inverting 4-6 times. NaOH loosens the cell wall. SDS is a detergent which disrupts the cell membrane by denaturing cell membrane proteins. Subsequently, this results in the release of plasmid DNA and sheared

cellular DNA from these cells. NaOH denatures cellular DNA by producing linearization and separation of strands. NaOH also denatures RNA, whereas plasmid DNA is circular and remains topologically constrained and intact. Taken together, the addition of lysis buffer (NaOH/SDS) aids in the denaturing of proteins, RNA and cellular DNA and the release of plasmid DNA from bacterial cell lysates. Lysis buffer was then neutralised with the addition of 350  $\mu$ l of N3 buffer (containing guanidine hydrochloride and acetic acid) and mixed immediately by inverting 4-6 times. N3 buffer adjusts the conditions to high-salt binding and causes cellular debris, protein, cellular DNA and SDS to precipitate; leaving the plasmid DNA in solution. Samples were subjected to centrifugation at 17900 x g for 10 min at RT, supernatant (containing plasmid DNA, along with some RNA and protein contaminants) was then transferred to the QIAprep spin column to allow binding of plasmid DNA to the silica gel membrane, followed by centrifugation at 17900 x g for 1 min at RT and flow-through was discarded. The bound plasmid DNA was washed with 500  $\mu$ l of buffer PB (containing guanidine hydrochloride and isopropanol) to remove endonucleases, RNA and protein, and centrifuged at 17900 x g for 1 min at RT and flow-through was discarded. A further wash with 750  $\mu$ l of buffer PE (containing ethanol) was used to remove salts, RNA and protein and to ensure DNA-silica membrane bonds remain intact, followed by centrifugation at 17900 x g for 1 min at RT and flow-through was discarded. Plasmid DNA was subjected to additional centrifugation at 17900 x g for 1 min at RT to remove residual wash buffer. Next, plasmid DNA was finally eluted after 1 min incubation with 50  $\mu$ l of nuclease-free water, followed by centrifugation at 17900 x g for 1 min at RT.

#### **2.4.1.2 Large scale preparation of plasmid DNA (maxiprep)**

The QIAGEN® plasmid purification Maxi kit was used for fast isolation and purification of approximately 500  $\mu$ g plasmid DNA (transfection grade/ultrapure plasmid DNA). This protocol is based on the same principles of alkaline bacterial cell lysis as mentioned in section 2.4.1.1 plasmid DNA miniprep. However, in this procedure, bacterial cell lysates were applied into anion-exchange-based QIAGEN-tip 500 columns. This anion-exchange chromatography is based on the interaction of negatively charged plasmid DNA under appropriate low-salt and pH conditions, with a positively charged solid phase of the anion-exchange matrix (within the column). RNA, proteins and low molecular weight impurities were

removed by a medium salt wash and finally plasmid DNA was eluted under high-salt conditions (via a high concentration of counter ions i.e. chloride).

This large scale isolation and purification of plasmid DNA was carried out according to manufacturer's instructions. Briefly, a single colony was picked from a freshly streaked LB agar plate with ampicillin, and used to inoculate a starter culture of 5 ml of LB broth with ampicillin for 8 h at 37°C in an orbital shaker at 180 rpm. This starter culture was then diluted into 500 ml of LB broth with ampicillin, for amplification during 12-16 h at 37°C in an orbital shaker at 180 rpm. Bacterial cells were harvested by centrifugation at 6000 x g for 15 min at 4°C. Bacterial pellet was resuspended in 10 ml P1 buffer with RNase A, and then lysed by the addition of 10 ml P2 lysis buffer (NaOH/SDS), mixed thoroughly by vigorously inverting 4-6 times and incubated at RT for 5 min. Next, 10 ml of chilled buffer P3 was added, mixed immediately and thoroughly by vigorously inverting 4-6 times, and incubated on ice for 20 min. Buffer P3 is a neutralisation buffer containing acidic potassium acetate. This incubation step triggers precipitation of potassium dodecyl sulphate, which traps denatured proteins, cellular DNA and cell debris, and leaves plasmid DNA in solution. Bacterial cell lysate was then centrifuged at 20000 x g for 30 min at 4°C and the supernatant (containing the plasmid DNA, along with RNA, protein and low molecular weight contaminants) was removed. A QIAGEN-tip 500 was equilibrated by addition of 10 ml buffer QBT [containing 750 mM NaCl, 50 mM MOPS (pH 7.0), 15 % (v/v) isopropanol and 0.15 % (v/v) Triton® X -100] and allowed to empty by gravity flow at RT. The supernatant was transferred to anion-exchange-based QIAGEN®-tip and allowed to enter the resin by gravity flow. This step allows plasmid DNA to selectively bind to the column under low-salt and pH conditions. The QIAGEN-tip was washed twice with 30 ml of buffer QC, a medium-salt wash [containing 1.0 M NaCl, 50 mM MOPS (pH 7.0), 15 % (v/v) isopropanol], at RT. QC buffer removes residual RNA, proteins, metabolites and other low-molecular weight impurities. The plasmid DNA was then eluted from the QIAGEN-tip by addition of 15 ml buffer QF, a high-salt buffer [containing 1.25 M NaCl, 50 mM Tris-HCl (pH 8.5), 15 % (v/v) isopropanol], at RT. Plasmid DNA was then precipitated by adding 10.5 ml of isopropanol at RT. Isopropanol-based DNA precipitation also aids in the concentration and desalting of plasmid DNA. Precipitated plasmid DNA was mixed and centrifuged

immediately at 15000 x g for 30 min at 4°C. Supernatant was then removed and the pellet washed by an addition of 5 ml of 70 % (v/v) ethanol and centrifuged at 15000 x g for 10 min at RT. Next, supernatant was removed and the pellet was air-dried for 5 min at RT. Plasmid DNA was then re-dissolved in 200 µl of nuclease-free water before quantification of yield and measurement of purity by NanoDrop™ (section 2.5). Ethanol removes precipitated salts and replaces isopropanol because it is more volatile, therefore allows plasmid DNA to re-dissolve in nuclease-free water easier.

## 2.5 Quantification of nucleic acids

DNA was quantified using NanoDrop™ 1000 Spectrophotometer and ND-1000 v3.1.0 software (Thermo Scientific, Loughborough, UK). This apparatus detects and measures the pulse light produced by a xenon flash lamp that passes through the sample, using a linear charged-coupled device (CCD) array. The wavelength of maximum absorption of light by RNA and DNA is 260 nm [UltraViolet light (UV) spectrophotometry at  $260\text{nm}=\lambda_{\text{max}}$  (wavelength of maximum absorption)] due to conjugated double bonds present in their constituent bases. The absorption properties of nucleic acids are used for detection, quantification and for purity measure. The amount of DNA was calculated and based on the modified Beer-Lambert equation, with ng/µl as units. The equation is as follows:

$$c = (A \times \epsilon) / b$$

$c$  = the nucleic acid concentration in ng/µl

$A$  = the absorbance in arbitrary units (AU)

$\epsilon$  = the wavelength-dependent extinction coefficient in ng/µl

$b$  = the path-length in cm

The extinction coefficients used for nucleic acids are as the following:

Doubled-stranded DNA: 50 ng/µl

Single-stranded DNA: 33 ng/µl

RNA: 40 ng/ $\mu$ l

The purity of the nucleic acid was determined and assessed by calculating  $A_{260}:A_{280}$  ratio. A ratio of 1.8-2 was considered pure and a value below 1.6 indicates protein contamination.

## 2.6 Restriction endonuclease digestion

Restriction endonuclease digestion is a procedure that cuts double stranded DNA by the action of type II restriction endonucleases. Restriction endonucleases produce either 'sticky' ends or 'blunt' ends, facilitating the ligation of nucleotide sequences with complementary 'sticky' ends or 'blunt' ends respectively, which then generates recombinant plasmid DNA molecules. Restriction endonuclease digestions were used for general diagnostics during plasmid DNA isolation and purification (section 2.4) or for preparation of plasmid DNA for cloning procedures (section 2.8). For general plasmid DNA diagnostic digests (Table 2.3 and Figure 2.2), 250-500 ng of plasmid DNA was digested in a 50  $\mu$ l single or double restriction endonuclease digestion reaction, containing 10 U (unit of restriction enzyme activity) (1  $\mu$ l) of each specific restriction enzyme (Promega Southampton, UK) and 5  $\mu$ l of the appropriate 5  $\times$  reaction buffer (Table 2.3). The total reaction volume of 50  $\mu$ l was made up with nuclease-free water. For preparing plasmid DNA for lentiviral vector cloning procedures in this thesis (section 2.8), 1-10  $\mu$ g of plasmid DNA was digested in a 50 $\mu$ l restriction endonuclease digestion reaction (with *Bam*HI & *Xho*I). Each restriction endonuclease digestion reaction was then mixed gently, centrifuged briefly and incubated at 37°C for 2 h. Completed reactions were analysed via agarose gel electrophoresis (section 2.7).

## 2.7 Gel electrophoresis

Gel electrophoresis is used to separate nucleic acids (section 2.7.1) or proteins (section 2.13.8.1) using crosslinked polymers within an electrical current. DNA molecules and protein are negatively charged. When applying electrical current, samples migrate through the gel from the cathode towards the anode, and separation is dependent on their molecular size through the crosslinked polymers (the pores of the gel). The two main types of gel are agarose and acrylamide.

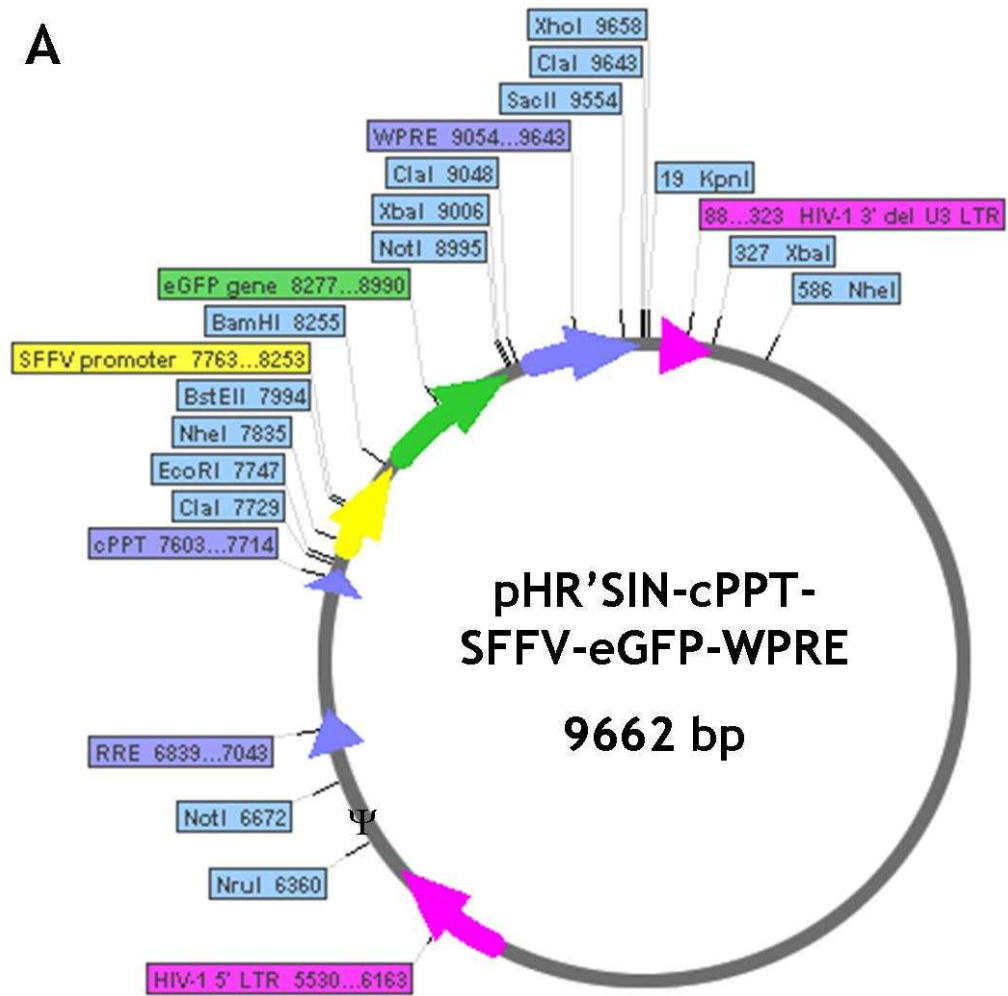
### **2.7.1 Agarose gel electrophoresis**

Agarose gel electrophoresis is typically used for analysing polymerase chain reaction (PCR) fragments or restriction endonuclease digest reactions. Complete reaction samples (section 2.6) were electrophoresed through a 1 % (w/v) agarose (Invitrogen) gel in 1 x Tris/Borate/EDTA (TBE) [89 mM Tris-base, 89 mM boric acid, 2 mM EDTA, pH 8.0, (Fisher Bioreagents, Loughborough, UK)] and ethidium bromide (10ng/ml). Samples and DNA size markers [100 base pairs (bp) and/or 1 kilobase pairs (kbp) DNA ladders, depending on the size of the fragment of interest (Promega)] were mixed with 6x blue/orange loading dye for a 1 x final concentration [0.4 % orange G, 0.03 % bromophenol blue, 0.03 % xylene cyanol FF, 15 % Ficoll® 400, 10 mM Tris-HCl (pH 7.5) and 50 mM EDTA (pH 8.0) (Promega)] ready for loading into the gel electrophoresis pre-cast-wells/lanes and for tracking migration during electrophoresis (xylene cyanol FF migrates at approximately 4 kbp, bromophenol blue at approximately 300 bp and orange G at approximately 50 bp). Agarose gels were electrophoresed at a constant voltage (V) of 90 to 100 V with a running buffer of 1 x TBE. Plasmid DNA were visualised using Molecular Imager® ChemiDoc™ XRS+ Imaging System with Image Lab™ software by UV transillumination (Bio-Rad Laboratories, Hemel Hempstead, UK).

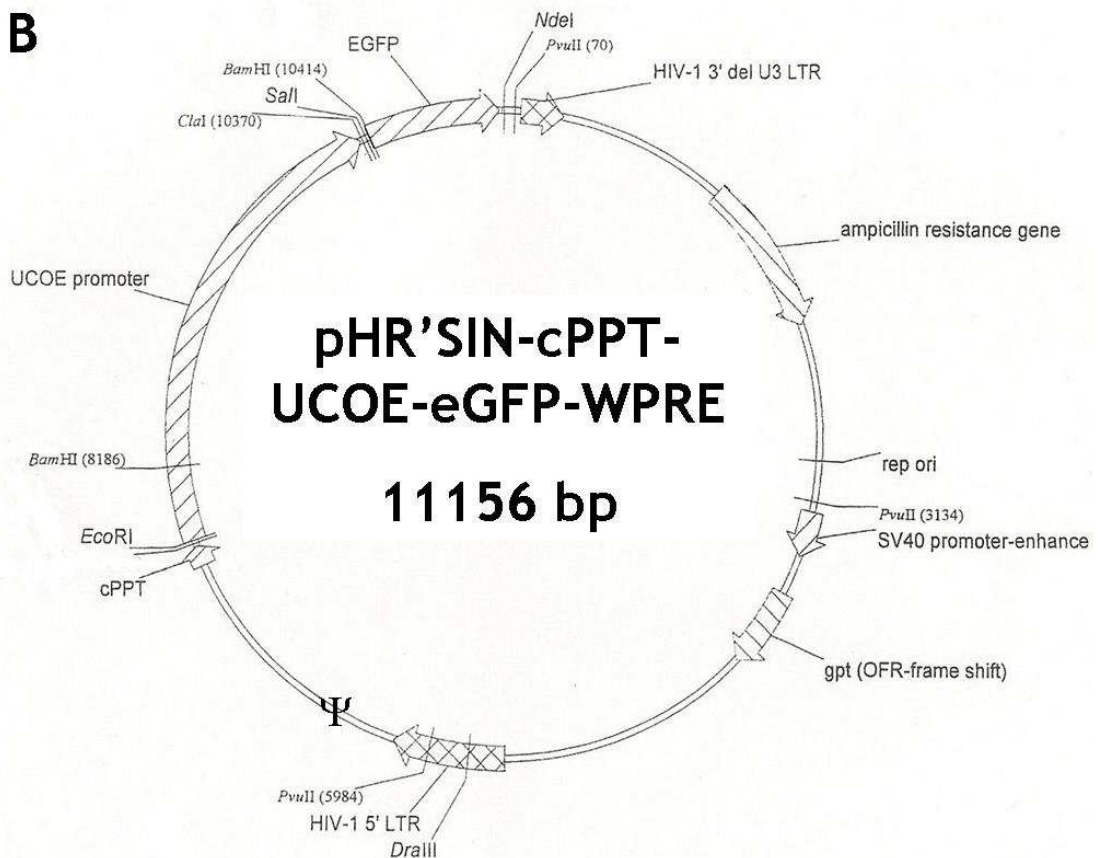
Plasmids DNA	Size of plasmid DNA, base pairs (bp)	Plasmid DNA diagnostic restriction endonuclease digest (Promega)	Buffer used in digestion (Promega)	Plasmid DNA fragments (bp)
pHR'SIN-cPPT-SFFV-eGFP-WPRE	9662	<i>Xba</i> I <i>Nhe</i> I	Buffer D Buffer B	1100 & 8600 2200 & 7500
pHR'SIN-cPPT-UCOE-eGFP-WPRE	11156	<i>Pvu</i> II	Buffer B	5914, 3064 & 2850
pCMV delta R8.74	11921	<i>Pvu</i> I & <i>Sal</i> I	Buffer D	8663 & 3258
pCMV delta R8.74 D64V	11921	<i>Pvu</i> I & <i>Sal</i> I	Buffer D	8663 & 3258
pMD.G2	5824	<i>Nde</i> I	Buffer D	3651, 1556 & 617
pLP-RVG	5736	<i>Eco</i> RI	Buffer H	2927 & 1345
pEcoMLVEnv	9761	<i>Nde</i> I & <i>Pvu</i> I	Buffer D	1438 & 8323
pHR'SIN-cPPT-SFFV-MCS-WPRE	8931	<i>Bam</i> HI & <i>Xho</i> I <i>Sac</i> II <i>Nhe</i> I <i>Xba</i> I	Buffer C Buffer C Buffer B Buffer D	8921 & 10 8931 7246 & 1685 7970 & 961
pHR'SIN-cPPT-SFFV-fulllengthNogo-B-WPRE	10084	<i>Bam</i> HI & <i>Xho</i> I <i>Sac</i> II <i>Nhe</i> I <i>Xba</i> I	Buffer C Buffer C Buffer B Buffer D	8921 & 1163 8535 & 1549 7246 & 2838 9123 & 961
pHR'SIN-cPPT-SFFV-mutantNogo-B-WPRE	9535	<i>Bam</i> HI & <i>Xho</i> I <i>Sac</i> II <i>Nhe</i> I <i>Xba</i> I	Buffer C Buffer C Buffer B Buffer D	8921 & 614 8535 & 1000 7246 & 2289 8574 & 961

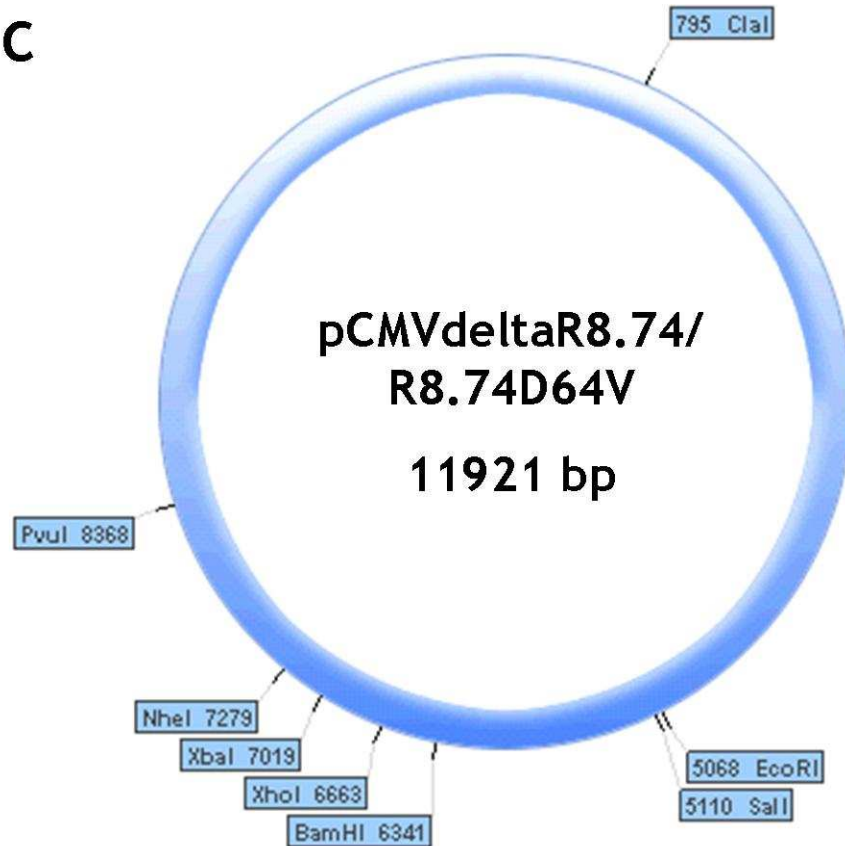
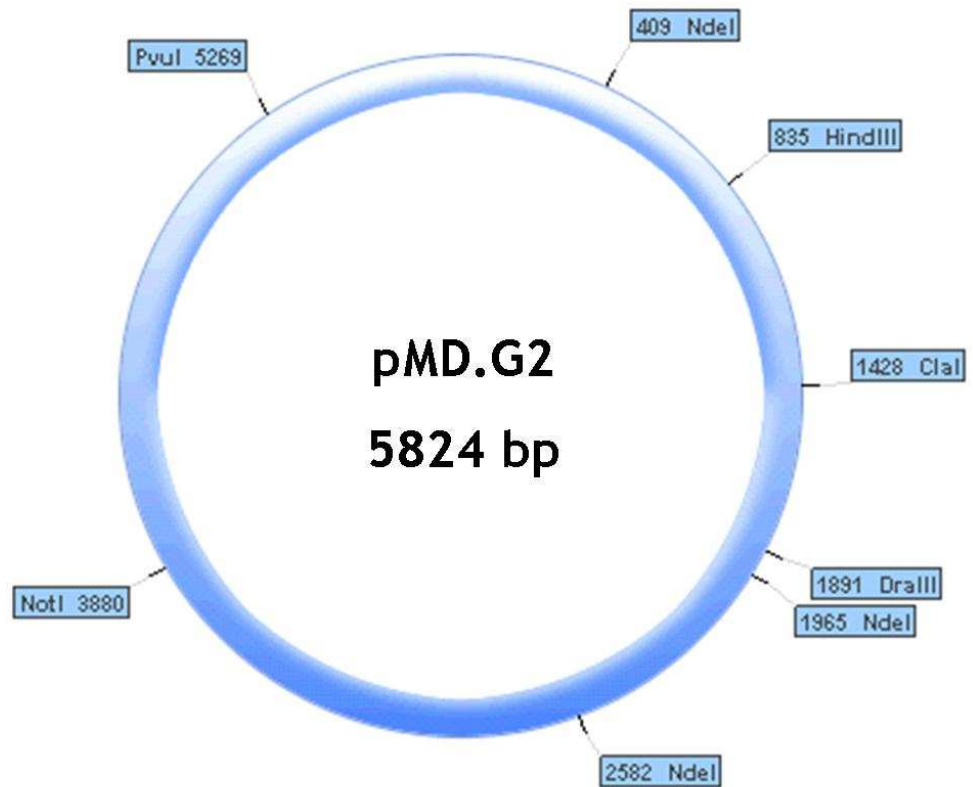
Table 2.3. Restriction endonucleases used in plasmid DNA diagnostic digestions.

**A**



**B**



**C****D**

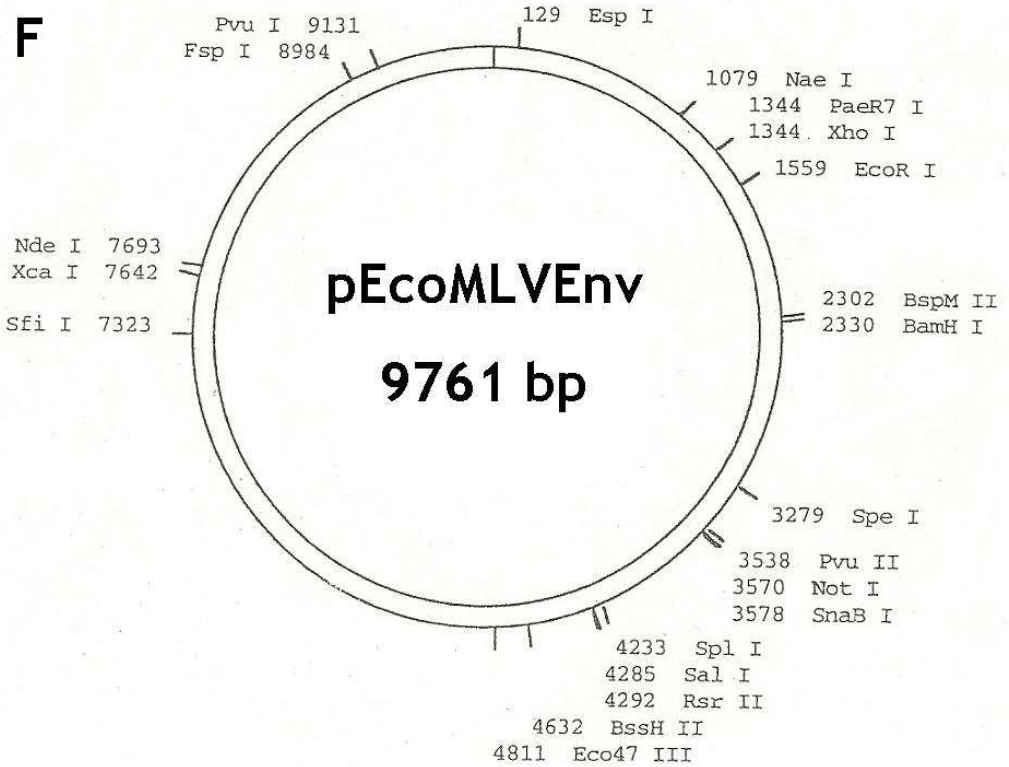
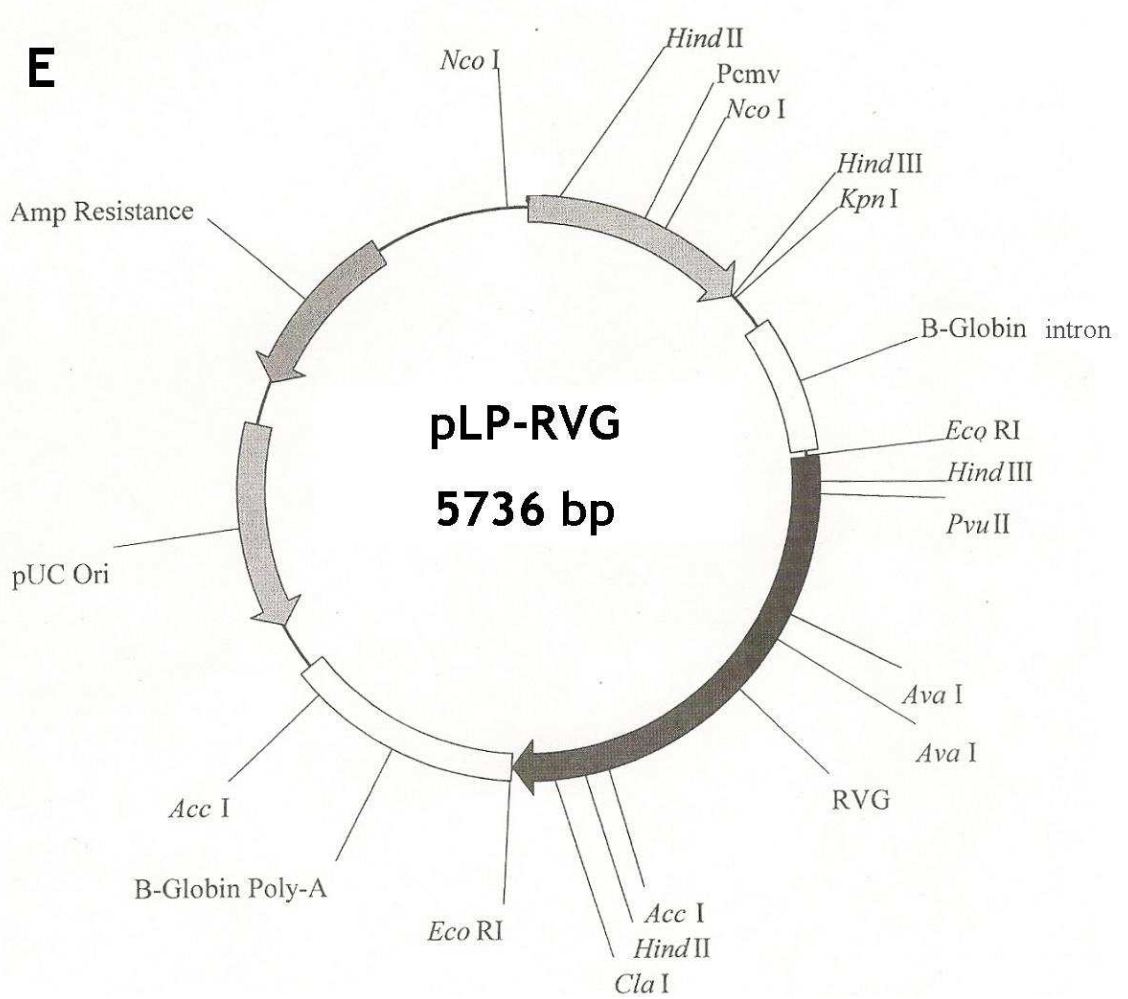


**Figure 2.2. Plasmid DNA maps including restriction endonuclease recognition sites.**

(A) pHR'SIN-cPPT-SFFV-eGFP-WPRE (lentiviral vector construct) plasmid, (B) pHR'SIN-cPPT-UCOE-eGFP-WPRE (lentiviral vector construct) plasmid, (C) pCMV delta R8.74/R8.74D64V (second-generation packaging) plasmid, (D) pMD.G2 [vesicular stomatitis virus-glycoprotein (VSV-g)] plasmid, (E) pLP-RVG (rabies glycoprotein) plasmid and (F) pEcoMLVEnv [murine leukaemia virus-ecotropic (MLV-E) glycoprotein] plasmid. LTR, long terminal repeat; bp, base pairs; cPPT, central polypurine tract; WPRE, Woodchuck post-transcriptional regulatory element; SFFV, spleen focus forming virus promoter; UCOE, enhancer-less ubiquitously acting chromatin opening element; eGFP, enhanced green fluorescent protein; RRE, Rev responsive element;  $\Psi$ , packaging sequence/signal; HIV-1 3' del U3 LTR, partial deletion in the U3 region of the 3' LTR; RVG, rabies virus glycoprotein.

## 2.8 Cloning of Nogo-B into the lentiviral vector construct plasmid

Nogo-B was the transgene of interest; cDNA of Nogo-B was cloned into lentiviral vector construct/transfer plasmid DNA for the production of lentiviral vectors expressing Nogo-B (section 2.9). Full-length Nogo-B-haemagglutinin tagged cDNA (insert 1.2 kbp between *KpnI* and *XbaI* restriction sites) in a pcDNA3 plasmid (full-length Nogo-B) and Nogo-B 1-200 (soluble/mutant Nogo-B) cDNA (insert 603 bp between *HindIII* and *XhoI* restriction sites) in a pSectag2 plasmid with a myc-6xhistidine tag, were sent concentrated on filter paper [sent from William Sessa's lab, University of Yale, USA (Acevedo et al., 2004)] and reconstituted into 50 µl of nuclease-free water. The full-length Nogo-B plasmid and mutant (soluble) Nogo-B plasmid (both ampicillin resistant) were transformed into XL-10 gold and XL-1 blue competent bacterial cells, respectively (section 2.3.1). Ampicillin resistant transformant colonies were then amplified, and plasmid DNA isolated and purified using QIAprep Miniprep kit (section 2.4.1.1).

### 2.8.1 Polymerase Chain Reaction (PCR)

#### 2.8.1.1 Nogo-B strategy for PCR cloning

Forward and reverse oligonucleotide primers were designed, each complementary to both 3' prime ends of the double stranded cDNA target sequence of either full-length or mutant Nogo-B (as described in Table 2.4 for primer design and labelled red), with added restriction enzyme recognition sites *BamHI* and *XhoI* at 5' ends of PCR primers (labelled blue) (see Appendix 1 for complete cDNA sequences of full-length Nogo-B and mutant Nogo-B). With regards to the justification of selected primers for mutant Nogo-B: the forward primer was the same design used for full-length Nogo-B, and the reverse primer was designed 600 bp downstream from the start codon with an addition of a stop codon. Oligonucleotide primers were resuspended in nuclease-free water (Ambion-Applied Biosystems, Warrington, UK) to a concentration of 10 pmol/µl. For the amplification of plasmid PCR targets, Herculase® II fusion DNA polymerase (Stratagene-Agilent Technologies) was used according to the manufacturer's instructions. Herculase® II fusion DNA polymerase was used because of its special enzyme formulation and optimised buffer system, which ensures high-fidelity PCR (excellent 3' to 5' proof-reading exonuclease activity)

and successful amplification of difficult GC-rich targets. ArchaeMaxx® polymerase enhancing factor was also included, which provides superior yield and excellent reliability with shorter cycling times. Briefly, for each 50 µl PCR reaction, the following was added: 50 ng of plasmid DNA, 1 µl of Herculanase II fusion DNA polymerase, 0.5 µl dNTP mix (each dNTP added at 25 mM), 10 µl of 5 x Herculanase II reaction buffer [final concentration of 2 mM Mg<sup>2+</sup> (a cofactor for this thermostable DNA polymerase, and excessive Mg<sup>2+</sup> aids stabilisation of double-stranded DNA and inhibits denaturation of DNA products at each cycle)], 1 µl of each primer (forward and reverse) (Table 2.4) added at 10 pmol/µl (10 µM) and then made up to 50 µl volume with nuclease-free water.

Each PCR reaction was completed in a Tetrad high-throughput PCR machine and carried out according to the manufacturer's instructions. Each PCR reaction was subjected to 1 cycle of initial denaturation at 95°C for 1 min and then followed by 40 cycles of the following: 30 sec at 95°C for denaturation, 30 sec at 65°C for primer annealing to the template plasmid DNA and 1.15 min at 74°C for optimal polymerisation (chain extension). Finally, each PCR reaction was subjected to ligation at 74°C for 5 min and 12°C thereon. PCR products were then isolated using 1 % agarose gel electrophoresis (section 2.7.1) for 1.5 h. PCR products at approximately 1.2 kbp and 603 bp for full-length Nogo-B and mutant Nogo-B, respectively, were visualised alongside a 100 bp and 1 kbp DNA ladder using UV transillumination and then excised from the 1 % agarose gel using a clean scalpel.

PCR primers		Sequence	Annealing temperature at °C (T <sub>m</sub> )
Full-length Nogo-B	Forward	5'-TCAGGGATCCATGGAAGACCTGGACCAGTC-3'	70
	Reverse	5'-CGGACTCGAGTCAAGCGTAGTCTGGGACG-3'	72
Mutant Nogo-B	Forward	5'-TCAGGGATCCATGGAAGACCTGGACCAGTC-3'	70
	Reverse	5'-ATTACTCGAGATCACACCACTCCAGTCTTCTTAAT-3'	67

Table 2.4. Primers design for Nogo-B strategy for PCR cloning.

### 2.8.2 PCR or restriction endonuclease digestion product purification from agarose gel

PCR products or excised DNA fragments following restriction endonuclease digestions were subjected to extraction and purification to eliminate excess

nucleotides, primers or enzyme reaction reagents. The Wizard® SV Gel and PCR Clean-Up System (Promega) was used because of its fast silica membrane-based system which is designed to isolate and purify up to 40 µg DNA fragments between 100 bp to 10 kbp. This kit was used following the manufacturer's instructions. Briefly, following separation of PCR products or excised DNA fragments by agarose gel electrophoresis, each gel portion containing the DNA segment of interest at the correct size was cut with a clean scalpel and transferred into a clean 1.5 ml micro-centrifuge tube. Next, 10 µl of membrane binding solution [containing 4.5 M guanidine isothiocyanate and 0.5 M potassium acetate (pH 5.0) (chaotropic salts)] was added per 10 mg of gel slice, vortexed and incubated at 65°C for 10 min until the gel was fully dissolved. The SV mini-column was inserted into a collection tube. Each dissolved gel mixture was then transferred to a SV mini-column, incubated at RT for 1 min to allow binding of DNA to the silica-membrane within the column and then subjected to centrifugation at 16000 x g for 1 min to discard flow-through containing agarose gel contaminants and excess nucleotides, primers and enzyme reaction reagents. Each mini-column was washed twice with washing solution [containing 10 mM potassium acetate (pH 5.0), 16.7 µM EDTA (pH 8.0) and 80 % ethanol] with 700 µl and 500 µl, respectively, and each wash was subjected to centrifugation at 16000 x g for 1 min to discard flow-through. Ethanolic wash buffer eliminates impurities, washes away chaotropic salts from the silica-membrane and ensures DNA-silica membrane bonds remain intact. Next, each mini-column was centrifuged at 16000 x g for 5 min, flow-through discarded and subjected to centrifugation at 16000 x g for 1 min at RT with the micro-centrifuge tube lid open to allow evaporation of any residual ethanol. Each mini-column was transferred to a clean 1.5 ml micro-centrifuge tube, and DNA bound to the silica-membrane of the mini-column was incubated with 50 µl of nuclease-free water for 1 min at RT and then centrifuged at 16000 x g for 1 min at RT to elute gel-purified DNA. DNA was stored at 4°C or -20°C, depending on when required.

### ***2.8.3 Intermediate plasmid preparation***

The StrataClone™ Blunt PCR Cloning kit was used to clone blunt-ended PCR products of either full-length Nogo-B or mutant Nogo-B into an intermediate plasmid. This StrataClone™ Blunt PCR Cloning kit provided highly efficient, 5 min cloning of blunt-ended PCR products.

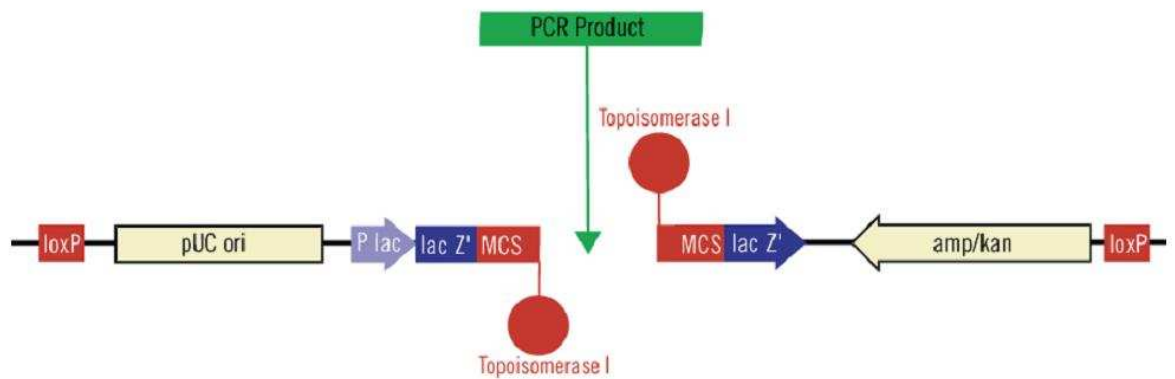
The StrataClone™ Blunt PCR Cloning kit was used according to manufacturer's instructions. Briefly, each StrataClone™ blunt-ended PCR cloning reaction mixture was prepared by combining the following components and in this order and mixed gently by repeated pipetting: 3 µl of StrataClone™ Cloning Buffer (optimal conditions for DNA topoisomerase I and Cre recombinase to function), 2 µl of approximately 50 ng of blunt-ended PCR product or StrataClone™ Blunt Control Insert, and then 1 µl StrataClone™ Vector Mix. The StrataClone™ Vector Mix [StrataClone PCR Cloning Vector pSC-B-amp/kan (ampicillin/kanamycin)] contains two blunt-ended DNA arms, each charged with topoisomerase I on one end and containing a *loxP* recognition sequence on the other end (Figure 2.3). Blunt-ended PCR products were efficiently ligated between these two topoisomerase I-charged vector arms in a 5 min RT reaction, and then placed on ice (Figure 2.3).

This linear molecule was then transformed into StrataClone™ SoloPack competent cell line engineered to transiently express Cre recombinase. Cre recombinase catalyses the recombination between the two *loxP* recognition sequences on the ends of the linear molecule and creates a circular DNA molecule, which is proficient for replication in bacterial cells grown in LB broth with ampicillin. StrataClone™ SoloPack competent cells were used according to manufacturer's instructions. Briefly, for each transformation reaction, an aliquot of StrataClone™ SoloPack competent cells were thawed on ice for approximately 5 min and then gently mixed. Per transformation reaction, 1 µl of the completed StrataClone™ blunt-ended PCR cloning reaction mixture (of either the blunt-ended PCR product or StrataClone™ Blunt Control Insert) was added to StrataClone™ SoloPack competent cells. StrataClone™ Blunt Control Insert transformation reactions were completed to ensure efficiency of DNA topoisomerase I and Cre-induced recombination activity and this was performed in duplicate. For transformation efficiency of these component bacterial cells, extra transformations were performed with or without pUC18 control DNA, in duplicate. For the pUC18 transformation control, the provided pUC18 DNA was diluted in sterile deionised water (dH<sub>2</sub>O) at a 1:10 dilution and then 1 µl of diluted pUC18 DNA to an aliquot of StrataClone™ SoloPack competent cells. Transformation reactions were gently mixed and incubated on ice for 20 min. Next, each transformation reaction was heat-shocked at 42°C for 45 sec,

followed by an addition of 250  $\mu$ l of pre-heated (42°C) SOC media and then these transformation reactions were incubated at 37°C for 1 h with agitation. For blunt-ended PCR product, StrataClone™ Blunt Control Insert or pUC18 control, 5  $\mu$ l, 25  $\mu$ l or 100  $\mu$ l of each transformation mixture was plated on LB agar plates with ampicillin and 5-bromo-4-chloro-3-indolyl- $\beta$ -D-galactopyranoside (X-gal) (containing 40  $\mu$ l of 2 % X-gal on each plate). Plus, 30  $\mu$ l of pUC18 control (with or without plasmid) or 25  $\mu$ l of the StrataClone™ Blunt Control Insert transformation reactions were plated on LB agar-ampicillin plates. All plates were then incubated at 37°C overnight.

Blue-white screening of blunt-ended PCR product transformation reactions were carried out. Positive transformant colonies with the StrataClone blunt-ended PCR Cloning Vector pSC-B-amp/kan plasmid appeared white (not blue). This is because, the insertion of a blunt-ended PCR product within the *lacZ'* gene cassette prevents its function, and therefore produces no  $\beta$ -galactosidase for the X-gal substrate present on these LB agar-ampicillin plates.

Incubate blunt PCR product with topoisomerase I-charged vector arms (5 min)



Transform StrataClone competent cells expressing Cre recombinase

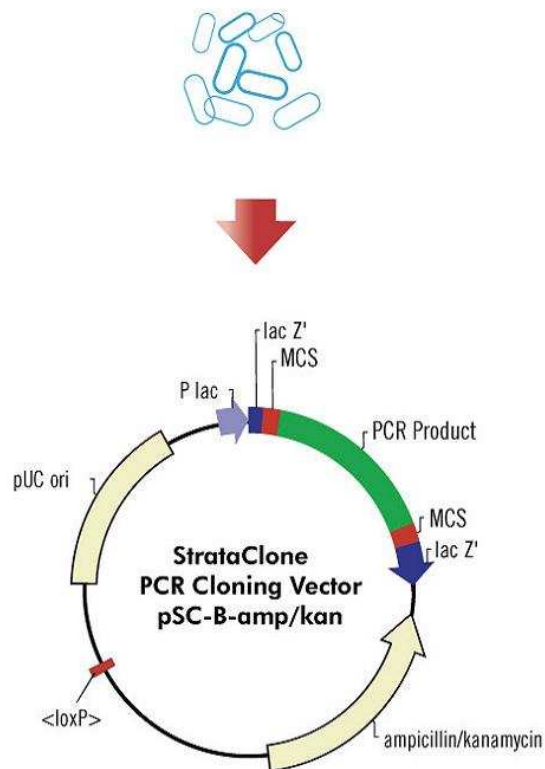


**Figure 2.3. Overview of the StrataClone™ blunt PCR cloning protocol.**

Amp/kan, ampicillin/kanamycin; *lacZ'*, *lacZ'* gene encoding  $\beta$ -galactosidase; MCS, multiple cloning site. Diagram adapted from StrataClone™.

#### **2.8.4 DNA sequencing**

Determination of a DNA sequence was completed using the 2', 3'-dideoxynucleotide triphosphate (ddNTP) sequencing technique. This procedure is based on the use of ddNTPs and each of the four ddNTPs is labelled with a specific fluorophore. These ddNTPs have a missing hydroxyl group at the 3' position, making it impossible for another nucleotide to bind. This resulted in a series of different size DNA fragments, which are visualised through the last nucleotide incorporated as a fluorescent labelled ddNTP. The DNA analyser utilised a laser beam focused in a constant position on the capillary electrophoresis, to excite the fluorescence caused by the fluorophore labelled ddNTP. According to the different wavelength that each fluorophore emitted, the analyser then translated the information from these four different nucleotides and generated a DNA sequence (Brown, 2010).

In order to confirm the cDNA of full-length Nogo-B and mutant Nogo-B were correct and had the correct orientation in either the StrataClone PCR Cloning Vector pSC-B-amp/kan or the lentiviral vector construct plasmid (pHR'SIN-cPPT-SFFV-fulllengthNogo-B-WPRE or pHR'SIN-cPPT-SFFV-mutantNogo-B-WPRE), DNA sequencing was carried out. Plasmid DNA was isolated from amplified single colony of competent bacteria (section 2.4) and each insert was sequenced with individual reactions for either forward or reverse strand sequencing. For each sequencing reaction the following was added per well on a 96-well plate: 200 ng of plasmid DNA; 2  $\mu$ l of each specific forward or reverse primer (at 2  $\mu$ M) (Table 2.5 and Table 2.6); 1  $\mu$ l of v3.1 Ready Reaction Mix (RRM) [consisting of DNA polymerase, dNTPs (deoxynucleotide triphosphates) and labelled ddNTPs] and 5  $\mu$ l of 5  $\times$  v3.1 sequencing buffer [the two latter from the BigDye<sup>®</sup> Terminator v3.1 cycle sequencing kit (Applied Biosystems, MA, USA)], and then each reaction was made up to a final volume of 20  $\mu$ l with nuclease-free water.

Each forward or reverse sequencing reaction was completed in a Tetrad high-throughput PCR machine and carried out according to the manufacturer's instructions. Each sequencing reaction was subjected to 96°C for 45 sec to denature, 50°C or 55°C for annealing depending on melting temperature ( $T_m$ ) of forward or reverse primer (Table 2.5 and Table 2.6) for 25 sec and 60°C for 4

min to extend the DNA sequenced fragment until the addition of ddNTP terminator.

For each sequence reaction, a sequence clean-up was performed to efficiently eliminate sequencing reaction contaminants that reduce signal strength during analysis of the DNA sequence. The sequencing reaction was cleaned with Agencourt® CleanSEQ® (Beckman Coulter®, Takeley, UK), following the manufacturer's instructions. Briefly, 10 µl of RT Agencourt® CleanSEQ® (contained paramagnetic beads) was added to each sequencing reaction, followed by the addition of 62 µl of 85 % ethanol for precipitation of DNA sequencing products. Each sequencing reaction was mixed and centrifuged at 220 x g for 10 sec at RT to allow selective binding of sequencing strands to paramagnetic beads. The plate was then placed on a Agencourt® solid phase reversible immobilisation (SPRI) magnetic plate for 2 min at RT, to allow separation of the sequencing strands from unincorporated dyes, nucleotides, salts and other contaminants. With the plate on the magnet, the plate was then inverted on tissue paper and the contaminants in the cleared solution were discarded. Next, 150 µl of 85 % ethanol wash was added to each well, mixed well and incubated at RT on the magnet for another 2 min. The plate was inverted on tissue paper and centrifuged to 80 x g for 10 sec at RT, to remove any remaining contaminants. The plate was then left to air-dry for 10 min at RT to remove any remaining ethanol present. To each sequencing reaction, 40 µl of nuclease-free water was added, re-suspended and placed on the magnet for 2 min at RT, to allow elution of purified DNA sequencing products from these paramagnetic beads. The 20 µl of purified sequencing product was transferred to a bar-coded 96-well plate and analysed using an ABI PRISM® 3730 DNA analyser using Sequencing analysis v5.2 software (Applied Biosystems, MA, USA).

Sequencing primers for M13 binding site	Melting temperature at °C ( $T_m$ )	Sequencing annealing temperature (°C)	
StrataClone PCR Cloning Vector pSC-B-amp/kan with either full length Nogo-B or mutant Nogo-B cDNA insert	Forward 5'-GGAAACAGCTATGACCATG-3'	53	50
	Reverse 5'-GTAAAACGACGGCCAGTG-3'	54	50

Table 2.5. Primers for sequencing in StrataClone PCR Cloning Vector pSC-B-amp/kan (ampicillin/kanamycin) with either full-length Nogo-B or mutant Nogo-B cDNA insert.

Sequencing primers		Melting temperature at °C (T <sub>m</sub> )	Sequencing annealing temperature (°C)
pHR'SIN-cPPT-SFFV-fulllengthNogo-B-WPRE	Forward 5'-CAATCAGCCTGCTTCTCG-3'	58	55
	Reverse 5'-ATGCCTGCAGGTCGACTCTAG-3'	60	55
	Forward 5'-GCAGTCTCGCCCTCCAAG-3'	60	55
	Reverse 5'-GAGAGCCAAAATCAGTAGTGTCAG-3'	60	55
pHR'SIN-cPPT-SFFV-mutantNogo-B-WPRE	Forward 5'-CAATCAGCCTGCTTCTCG-3'	58	55
	Reverse 5'-ATGCCTGCAGGTCGACTCTAG-3'	60	55

Table 2.6. Primers for sequencing the lentiviral vector construct plasmid with either the full-length Nogo-B or mutant Nogo-B cDNA insert.

## 2.8.5 *Ligation of Nogo-B cDNA into lentiviral vector construct plasmid*

### 2.8.5.1 Dephosphorylation of plasmid DNA ends

To prevent re-circularisation and re-ligation of the linearised lentiviral vector construct plasmid DNA during ligation reaction, it was important to remove the 5' phosphate groups. Shrimp Alkaline Phosphatase (SAP) (Promega) was added to catalyse the removal of 5' phosphate groups after the restriction endonuclease digestion and prior to ligation reaction, and was carried out according to the manufacturer's instructions. Per de-phosphorylation reaction (using the completed 50 µl restriction endonuclease digestion reaction containing the lentiviral vector construct plasmid) the following was added: 10 U of SAP per 5 µg of plasmid DNA backbone, 5 µl of SAP buffer (at a 10 × concentration) and 4 µl of nuclease-free water. Each reaction was incubated for 1 h at 37°C, followed by heat-inactivation of the SAP for 15 min at 65°C. Subsequently, the lentiviral vector construct backbone was isolated by using 1 % agarose gel electrophoresis (see section 2.7.1), excised from the agarose gel using a clean scalpel and then subjected to agarose gel extraction and purification (see section 2.8.2).

### 2.8.5.2 Ligation of Nogo-B cDNA into digested lentiviral vector construct plasmid DNA

To ligate cDNA of Nogo-B (phosphorylated) and the de-phosphorylated lentiviral vector construct plasmid DNA, T4 DNA ligase (isolated from bacteriophage T4) (Biolabs) was added and each ligation reaction was carried out according to manufacturer's instructions. T4 DNA ligase catalyses the formation of a phosphodiester bond between juxtaposed 5' phosphate and 3' hydroxyl termini. Ligation reactions were performed at a ratio of 3:1 of insert:vector. To calculate how much insert and the vector to add, to get a 3:1 ratio, the following formula was used:

$$\left( \frac{(\text{ng of vector}) \times (\text{kbp size of insert})}{(\text{kbp size of vector})} \right) \times (\text{ratio}) = \text{ng of insert}$$

For example: ng of cDNA of full-length Nogo-B required

ng of vector = 100 ng

kbp size of insert = full-length of Nogo-B, 1.2

kbp size of the vector = 9

ng of insert =  $[(100 \times 1.2)/9] \times 3 = 40$  ng of cDNA of full-length Nogo-B required

Per ligation reaction the following was also added: 1  $\mu$ l of T4 DNA ligase for 1 U, 1  $\mu$ l of T4 ligase buffer (at a 10  $\times$  concentration) and then made to a final volume of 10  $\mu$ l with nuclease-free water. Next, ligation reactions were incubated at RT for 1 h, before proceeding to transform into competent bacteria to select ampicillin resistant transformant colonies with the complete ligated plasmid (section 2.3.1).

## 2.9 Lentiviral vectors

All second-generation, self-inactivating (SIN) HIV-1 based lentiviral vectors (LV) were produced using a three-plasmid transient transfection system, as previously described (Demaison et al., 2002, Buckley et al., 2008). Details of plasmids used in generating these LVs, are listed in Table 2.2.

### 2.9.1 *Lentiviral vector production*

Low passage 293T cells (Table 2.1) were seeded and grown to approximately 70 % confluence in T-150 flask, and incubated overnight at 37°C in 5 % CO<sub>2</sub>. The next day the three-plasmid transient transfection was set-up in a flow cabinet (with no light on). The following three plasmids were added to 5 ml of Opti-MEM® I reduced serum media with GlutaMax™ I (plus containing: 2400 mg/l sodium bicarbonate, HEPES, sodium pyruvate, hypoxanthine, thymidine, trace elements, growth factors and 1.1 mg/l phenol red) (Invitrogen): 50  $\mu$ g of the SIN HIV-1 based lentiviral vector construct/transfer plasmid encoding for the viral genome; 17.5  $\mu$ g of the envelope plasmid and 32.5  $\mu$ g of the second-generation packaging plasmid (see Table 2.2 for plasmid specificity). The three plasmid mixture was then filter-sterilised through a 0.22  $\mu$ m filter. 10 mM stock of

branched polyethylenimine (PEI) (Sigma-Aldrich) with an average molecular weight of approximately 25000 was prepared. 10 ml of dH<sub>2</sub>O was added to 10 ml of PEI and mixed by vortex. Approximately 10 ml of 12N HCl was added, with 1 ml at a time and vortexed. This was then topped up to 41.2 ml with dH<sub>2</sub>O, mixed by vortex and stored in 10 µl aliquots at -80°C until required. 1 µl of 10 mM of PEI was added to 5 ml of Opti-MEM® I reduced serum media with GlutaMax™ I and filtered through a 0.22 µm filter, for a final concentration of 2 nM of PEI. The three plasmid mix and the 2 nM PEI solution was then mixed together at 1:1 ratio, and incubated for 20 min at RT to allow plasmid DNA and PEI to form polyplexes for transfection. These polyplexes facilitate effective DNA binding and protection from lysosomes and high endosomolytic competence for translocation to the nucleus, hence superior transfection efficacy can be achieved. 293T cells were washed with 10 ml of Opti-MEM® I reduced serum media with GlutaMax™ I to dilute remaining 10 % complete MEM. Next, 10 ml of DNA/PEI polyplexes were added per T-150 flask of 293T cells and were then incubated at 37°C in 5 % CO<sub>2</sub> for 4 h. For a control flask, 10 ml of Opti-MEM® I reduced serum media with GlutaMax™ I was added alone. After this three-plasmid transfection of 4 h, transfection media was removed, 25 ml of fresh 10 % complete MEM media was then added per flask and incubated at 37°C in 5 % CO<sub>2</sub>. Supernatant (containing LVs) was collected at 48 h (this time point collection was stored at 4°C until required and media was replenished with 25 ml of fresh 10 % complete MEM) and 72 h, and then filtered through a 0.22 µm filter to remove cellular debris because of its cytotoxic effect when using in *in vitro* and *in vivo*.

### **2.9.2 Concentration of lentiviral vector production**

It was important to concentrate LV preparations and to resuspend in minimal volume of Opti-MEM® I reduced serum media with GlutaMax™ I, for the use in *in vitro* experiments. First, 14 ml ultra-clear centrifuge tubes (Beckman Coulter Ltd, Buckinghamshire, UK) were sterilised with 70 % (v/v) ethanol, followed by rinsing in sterile PBS and then filtered LV vector supernatants were loaded. These tubes were loaded into a SW-32.1 Ti rotor bucket (Beckman Coulter), placed in the SW32 Ti rotor (Beckman Coulter) and subjected to ultracentrifugation at 90353 x g (23000 rpm) for 1 h and 7 min at 4°C with acceleration at maximum and deceleration at 9, using a Optima L-80 XP

UltraCentrifuge (Beckman Coulter). Immediately after ultracentrifugation, supernatant was decanted from these tubes carefully without disruption to the LV pellet and then left for 2 min to sit upside down on fresh tissue paper to remove as much supernatant as possible. Next, these tubes were placed upright, 50 µl of Opti-MEM® I reduced serum media with GlutaMax™ I was added per tube and left to incubate on ice for 20 min for the LV pellet to resuspend. After 20 min on ice, each tube was subjected to pipetting up and down several times to resuspend LV vector pellet. Finally, concentrated LVs were then aliquoted at 20 µl or 50 µl and stored at -80°C until required.

## 2.10 Determining lentiviral vector titres

Functional titres of concentrated LV vector preparations were determined. 293T cells were seeded in a 12-well plate at a density of  $5 \times 10^4$ /well and incubated overnight at 37°C in 5 % CO<sub>2</sub>. Serial dilutions of concentrated freeze-thawed LV vector [functional LV vectors decrease after freeze-thawing (Higashikawa and Chang, 2001)] stocks were prepared, ranging from  $1 \times 10^2$  to  $1 \times 10^6$  (termed as dilution factor) in 10 % complete MEM media (Demaison et al., 2002). Culture media was changed for 1 ml of fresh 10 % complete media, followed by an addition of either 30 µl or 100 µl of sequential LV vector dilutions and repeated in duplicate. The plate was then incubated in a humidified chamber at 37°C in 5 % CO<sub>2</sub>. After 3 d post-infection, TaqMan quantitative PCR titres (see section 2.10.2) were assessed by quantifying pro-viral LV DNA copy numbers. Only 293T cells transduced with LV vectors expressing enhanced green fluorescent protein (eGFP) were assessed by fluorescence microscopy (see section 2.13.3 and 2.10.1) for a visual eGFP titre.

### 2.10.1 Visual eGFP titre

Expression of eGFP per well was visualised (section 2.13.3) per sequential LV dilutions, and percentage of eGFP visualised was recorded (100 × magnification) per field of view in triplicate and an average was taken. An infectious unit of LVs per ml (iu/ml) was calculated using this equation:

$$\left( \frac{(\% \text{ of visual expression}/100) \times (\text{cell density seeded})}{\text{volume of inoculum (ml)}} \right) \times \text{LV dilution factor}$$

= iu/ml

For example: integrating LV expressing eGFP at a dilution factor of  $1 \times 10^2$  with a volume of inoculum at 0.03 ml gave 82.5 % of eGFP expression when transduced on  $5 \times 10^4$  293T cells.

$$[(0.825) \times (5 \times 10^4)]/0.03 = 1375000$$

$$1375000 \times 100 = 1.375 \times 10^8 \text{ iu/ml}$$

All the sequential dilutions were calculated for iu/ml and used to determine an average functional LV titre (iu/ml) (Demaison et al., 2002, Sastry et al., 2002).

### 2.10.2 Quantitative Real-Time PCR titre

#### 2.10.2.1 DNA extraction

Viral and total genomic DNA was isolated from each well of the LV 12-well plate titration assay using the QIAamp® DNA Mini Kit (QIAGEN). This was due to its rapid purification of high-quality DNA, and complete removal of contaminants and inhibitors of PCR.

QIAamp® DNA Mini Kit was used according to manufacturer's instructions. Briefly, culture media was removed, 293T cells were gently washed with PBS, then 200 µl of PBS was added per well and cells were scraped with a rubber

policeman. Detached cells were transferred into a fresh micro-centrifuge tube and resuspended by pipetting up and down gently. Per tube/sample, 20 µl of proteinase K (a subtilisin-like endolytic protease) was added prior to 200 µl of optimised lysis buffer AL (containing SDS, EDTA and guanidine hydrochloride), and then resuspended and mixed by pulse-vortexing for 15 sec. Proteinase K was used because  $\text{Ca}^{2+}$  is not essential for its function, therefore EDTA and other chelating agents do not interfere with its activity and can be used alongside proteinase K to inactivate  $\text{Ca}^{2+}$ -dependent nucleases in DNA preparations. Guanidine hydrochloride is a chaotropic salt, which allows adsorption of DNA onto the silica-gel membrane of the QIAamp Spin Column [with similar principle to plasmid DNA miniprep isolation (section 2.4.1.1)]. Polysaccharides, RNA, proteins and PCR inhibitors-divalent cations do not adsorb, and thus are removed. Samples were incubated at 56°C for 10 min for optimal lysis. 200 µl of 100 % ethanol was added to each sample, mixed by pulse-vortexing for 15 sec, briefly centrifuged to remove drops from inside the lid and then the complete sample was loaded onto a QIAamp® spin column. Samples were centrifuged at 6000 x g for 1 min at RT to allow the DNA to be adsorbed onto the silica-gel membrane of the spin column and flow-through discarded. Each spin column was washed with 500 µl of buffer AW1 (containing guanidine hydrochloride and ethanol) and centrifuged at 6000 x g for 1 min at RT, followed by a second wash step with 500 µl of buffer AW2 (containing ethanol) and centrifuged at 20000 x g for 3 min at RT. To eliminate any chance of possible buffer AW2 carryover and remaining contaminants, each spin column was centrifuged at 20000 x g for 1 min at RT. Finally, each spin column was placed in a clean micro-centrifuge tube, 50µl of nuclease-free water was added per sample/spin column, left for 5 min at RT to allow DNA to de-adsorb from the silica-membrane, and then centrifuged at 6000 x g for 1 min at RT to elute DNA from the spin column. The quantity of DNA in each sample was quantified by NanoDrop™ (section 2.5), and all samples were diluted to 50 ng/µl.

### 2.10.2.2 TaqMan Quantitative PCR

LV vector genomic copy number was quantified in DNA extracted from 293T cells 3 d post-infection by TaqMan quantitative PCR (qPCR) according to a published protocol for late reverse transcriptase amplicon quantification, and standard curves were generated using lentiviral vector construct plasmid DNA as

described (Butler et al., 2001). Briefly, primers and probe primer: late RT forward, MH531 5'-TGTGTGCCCGTCTGTTGTGT-3' ( $T_m$ : 59.4°C), late RT reverse, MH532 5'-GAGTCCTGCGTCGAGAGAGC-3' ( $T_m$ : 63.5°C) and late RT fluorescent probe 5'-[fluorescein amidite(FAM)]-CAGTGGCGCCCGAACAGGGA-[teramethylrhodamine(TAMRA)]-3' ( $T_m$ : 65.5°C), were used to detect late reverse transcripts (linear double stranded DNA-pre-integration complex) with LTRs at both ends.

For each titre assay, a standard curve of the amplicon being measured was created from its construct lentiviral vector plasmid of interest. Serial dilutions of plasmid copy numbers were generated and ran in triplicate ranging from  $1 \times 10^{12}$  to  $1 \times 10^0$  (dilution factor). Plasmid copy numbers of standards were based upon the following equations:

1. To determine molecular weight of plasmid:

$$(\text{bp}) \times (330 \text{ Daltons} \times 2 \text{ nt/bp}) = \text{Daltons}$$

$$\text{Daltons} = \text{g/mole}$$

2. Determine weight of one copy of plasmid (molecule):

$$\left( \frac{\text{g/mole}}{\text{Avogadro's number (molecules/mole)}} \right) = \text{g/molecule}$$

3. Determine copy number of plasmid per ml in plasmid stock:

$$\left( \frac{\text{concentration of plasmid g/ml}}{\text{g/molecule}} \right) = \text{copy number of plasmid (molecules of plasmid)/ml}$$

## 4. Preparation of top standard:

$$\left( \frac{\text{copy number of plasmid/ml}}{\text{top standard required}} \right) = \text{initial dilution for top standard}$$

$$\left( \frac{1000}{\text{initial dilution factor for top standard}} \right) = \mu\text{l of plasmid stock required for 1 ml of top standard}$$

Top standards were aliquoted and stored at -20°C until required.

For example: pHR'SIN-cPPT-SFFV-eGFP-WPRE plasmid DNA, 9662 bp and plasmid stock at a concentration of 909.3 ng/μl.

1.  $(9662 \times (330 \times 2)) = 6376920 \text{ g/mole.}$
2.  $(6376920 / 6.023 \times 10^{23}) = 1.059 \times 10^{-17} \text{ g/molecule.}$
3.  $(0.0009093 / 1.059 \times 10^{-17}) = 8.59 \times 10^{13} \text{ copy number of plasmid/ml.}$
4.  $(8.59 \times 10^{13} / 1 \times 10^{12}) = 85.9 \text{ initial dilution for } 1 \times 10^{12} \text{ top standard.}$

$(1000/85.9) = 11.64 \mu\text{l of plasmid stock required for 1 ml for } 1 \times 10^{12} \text{ top standard.}$

The following was added to each 12.5 μl volume TaqMan qPCR reaction per well on a 384-well plate: 6.25 μl of 2 x TaqMan universal master mix [containing AmpliTaq Gold® DNA polymerase, dNTPs, passive reference and optimised buffer components (Applied Biosystem)], final concentration of each of the forward and reverse primer at 300 nM, final concentration of the probe primer at 100nM, 125ng of DNA (2.5 μl of 50 ng/μl) or 2.5 μl of plasmid DNA standard, and the remaining volume was made up with nuclease-free water. Each sample and standard was measured in triplicate. A non-template control of 2.5 μl of

nuclease-free water in place of DNA was used to eliminate false positives. The 384-well plate was then placed in Applied Biosystems 7900HT fast real-time PCR system. Each TaqMan qPCR reaction for samples and standards were subjected to the following parameters: initial incubations at 50°C for 2 min and initial denaturing at 95°C for 10 min, followed by 40 cycles of amplification were carried out at 15 sec for denaturing at 95°C and annealing/extending for 1 min at 60°C.

Each TaqMan qPCR reaction exploits the 5' nuclease activity of AmpliTaq Gold® DNA polymerase, to cleave a probe consisting of an oligonucleotide with a reporter dye FAM at the 5' end and a quencher dye TAMRA at the 3' end. During the reaction, cleavage of the probe separated the FAM and the TAMRA, which resulted in an increased fluorescence of the FAM. The amount of late RT amplicons during each cycle was detected directly by measuring the increase in fluorescence of FAM (with excitation/emission at 540nm/575nm), which was quenched by TAMRA and this increase in fluorescence can be measured directly. Acquisition of data occurred when PCR amplification was in the exponential phase (real-time detection).

The raw cycle number [cycle-threshold (Ct)] values for standards and samples and the values of the dilutions of the standards were exported from the SDS v2.3 software (Applied Biosystems™) and imported into GraphPad Prism® v4 (La Jolla, CA, USA). The standard curve of the amplicon (plasmid) copy numbers was sigmoidal (x-axis value was amplicon copy numbers for a given Y-axis value of TaqMan Ct value), therefore amplicon copy numbers of each of the standards was transformed using  $x = \log(x)$  in order to form linear regression to determine/quantify the late reverse transcriptase amplicons in each of the sample diluent of LVs using their Ct values. Amplicon copy numbers determined, were then transformed using inverse log ( $x = 10^x$ ) and exported to an Excel spread sheet for the final calculations.

Infectious viral units per ml (iu/ml) of each sample diluent of LVs were based upon the following sequential equations:

1. **Total DNA extracted** = concentration of DNA (ng/μl) x volume of DNA eluted

2. **Percentage of total cell DNA added to the TaqMan qPCR reaction when using 125 ng** =  $(125 \text{ ng} / \text{total DNA extracted}) \times 100$
3. **Cell number used in TaqMan qPCR reaction** =  $5 \times 10^4 \times (\text{Percentage of total cell DNA added to the TaqMan qPCR reaction when using 125 ng} / 100)$
4. **Amplicon copy number per cell** = Amplicon copy number (calculated from GraphPad Prism) / cell number used in TaqMan qPCR reaction
5. **Infectious viral units per ml (iu/ml)** = Amplicon copy number per cell  $\times ((\text{dilution factor}) \times 1000 / \text{volume } (\mu\text{l}) \text{ of inoculum})$

For example: Integrating LV expressing Nogo-B at a dilution factor of  $1 \times 10^2$  with a volume of inoculum at 0.03 ml gave an amplicon copy number of  $2.66 \times 10^6$  when transduced with  $5 \times 10^4$  293T cells. Concentration of DNA extracted was 491.6 ng/ $\mu\text{l}$  in a volume of 50  $\mu\text{l}$  of nuclease-free water.

1. **Total DNA extracted:**  $491.6 \times 50 = 24580 \text{ ng}$
2. **Percentage of total cell DNA added to the TaqMan qPCR reaction when using 125ng:**  $(125/24580) \times 100 = 0.509 \%$
3. **Cell number used in TaqMan qPCR reaction:**  $5 \times 10^4 \times (0.509\%/100) = 254.272$
4. **Amplicon copy number per cell:**  $2.66 \times 10^6 / 254.272 = 10461.248$
5. **Infectious viral units per ml (iu/ml):**  $10461.248 \times ((100) \times 1000/30) = 3.487 \times 10^7 \text{ iu/ml}$

An average of all the sample diluents of LVs was calculated for the functional LV titre (iu/ml).

## 2.11 Adenoviral vectors

High titre preparations of first-generation, replication-defective serotype 5 adenoviral vectors expressing full-length human Nogo-B-haemagglutinin(HA)-tagged (Ad-Nogo-B) (Acevedo et al., 2004) were produced by large-scale amplification in 293 cells using a plaque pure stock of recombinant Ad-Nogo-B. First-generation, replication-defective serotype 5 adenoviral vectors expressing eGFP (Ad-eGFP) were obtained from Crucell (Leiden, Netherlands).

### 2.11.1 Production of adenoviral vectors expressing Nogo-B

Low passage 293 cells were seeded and grown to 80 % confluence in 24 T-150 flasks. 50 µl of plaque pure stock of Ad5-Nogo-B was added into 500 ml of 10 % complete MEM media (Table 2.1) and 293 cells were then infected with 21 ml per flask. For a control flask of no virus infected 293 cells, 21 ml of 10 % complete MEM media alone was added. Media was changed every 3 d until cytopathic effect of the vector was initiated. 293 cells were then fed with 10 ml of fresh 10% complete MEM media and incubated until all cells were detached from the flask. Once detached, media containing cells from each flask were then collected immediately to avoid prolonged incubation periods of detached cells, which may cause loss of virus titre. Next, the cells were harvested to extract adenoviral vectors (this happened on 5<sup>th</sup> d for this preparation) by centrifugation at 850 x g for 10 min at RT (and supernatant was discarded), and resuspended in 8 ml of PBS between all 24 pellets. An equal volume of Arklone P (trichlorotrifluoroethane) (ICI Ltd, Cheshire, UK) was then added to the falcon tube, followed by inversion for 10 sec and gentle shaking for 5 sec. This step was repeated for 1 min. The solution was subjected to centrifugation at 850 x g for 15 min at RT to form 3 layers. The upper layer consisted of an aqueous solution, containing Ad-Nogo-B, whereas the middle and lower layers contained cellular debris and solvent, respectively. The top aqueous layer (pink layer) was removed, placed into a fresh falcon tube and stored at -80°C until purification by caesium chloride (CsCl) gradient centrifugation.

### **2.11.2 Adenovirus purification using CsCl density gradient purification centrifugation**

A virus extraction with solvents such as Arklone P leaves contaminating cellular debris in the preparation, which is cytotoxic when using *in vitro* and *in vivo*. For this reason a CsCl density gradient was used to separate cellular debris and purify virus preparations. This method is also a simple and efficient method to concentrate adenoviral vector preparations. First, 14 ml cellulose-nitrate ultra-clear centrifuge tubes (Beckman Coulter) were sterilised with 70% (v/v) ethanol, followed by rinsing in sterile dH<sub>2</sub>O. In these tubes, a 3 layer gradient was formed by pipetting a lower layer of 2 ml of sterile CsCl with a density of 1.45 g/cm<sup>3</sup>, followed by careful layering of 3 ml of sterile CsCl with a density 1.32 g/cm<sup>3</sup> and finally 2 ml of sterile 40 % (v/v) glycerol. Next, the crude Ad-Nogo-B preparation was added drop-wise to the top of the gradient and the remaining space was filled with PBS. The tube was loaded into a Sorvall Discovery 90 rotor bucket, placed in the rotor (RPS40T-859) and subjected to ultracentrifugation at 90000 x g for 1.5 h at 4°C with maximum acceleration and zero deceleration, using a Optima L-80 XP UltraCentrifuge (Beckman Coulter).

After ultracentrifugation a discrete white band was formed between the CsCl 1.45 and the CsCl 1.32, which contained the Ad-Nogo-B. This was removed by piercing the tube below the virus band using a 21 gauge needle, and the virus was carefully collected into the syringe in the minimum volume (caution was taken to prevent disruption of the other bands). To further purify and concentrate Ad-Nogo-B preparation, the virus was subjected to dialysis. A sterile Slide-A-Lyser Dialysis Cassette (molecular weight cut-off of 10000 kDa)(PerbioScience UK Ltd, Northumberland, UK) was hydrated for 1 min in sterile dialysis solution consisting of 0.01 M Tris pH 8.0 and 0.001 M EDTA (TE buffer). The extracted virus was transferred to a dialysis cassette for dialysis. The virus was dialysed for approximately 2 h against 2 litres (L) of TE buffer with stirring. After 2 h, the TE buffer was changed for 2 L of fresh TE buffer and the dialysis repeated overnight with stirring. After the overnight dialysis, the TE buffer was changed and supplemented with 10% (v/v) glycerol and dialysis was continued for a further 2 h. Finally, the virus was removed from the dialysis cassette with a needle and syringe, aliquoted into 50 µl volumes and stored at -80°C until required.

## 2.12 Determining adenoviral vector titres

Adenoviral vector (Ad) titres were determined by using two methods: Micro-BCA assay for determining physical virus titres, or by titration of adenoviral vectors by end-point dilution assay for determining functional virus titres.

### 2.12.1 *Micro-BCA assay*

Virus particle titres for Ad-Nogo-B and Ad-eGFP were determined by measuring the protein content of the virus stocks, using the micro-bicinchoninic acid (BCA) protein assay kit (Pierce, Rockford, IL, USA) according to manufacturer's instruction. Briefly, 8 bovine serum albumin (BSA) standards ranging from 0.5 µg/ml to 200 µg/ml were prepared in PBS and 150 µl of each was loaded in duplicate into wells of a clear 96-well plate, plus 150 µl of PBS in duplicate as the blank. Next 1, 3 and 5 µl of virus were added in duplicate and each well was made up to a total volume of 150 µl with PBS. Next, 150 µl of BCA working reagent was added to all samples and standards and then the plate was incubated at 37°C for 2 h (see section 2.13.5 on the principles of the BCA assay). Absorbance (optical density) of each well at 570 nm was measured in a Wallac Victor<sup>2</sup> plate reader (Wallac, Turku, Finland). To calculate the protein content, the blank absorbance was subtracted from the readings of each sample and standard. The amount of protein present in each virus was then calculated from the linear equation based on the standard curve. The physical virus particle titre (vp/ml) was then calculated using the following established formula: 1 µg protein =  $1 \times 10^9$  viral particles (VP)(Von Seggern et al., 1998).

### 2.12.2 *Titration of adenovirus by end-point dilution assay*

Functional titres of Ad-Nogo-B and Ad-eGFP were quantified by the end-point dilution assay, through serial dilutions of adenoviral vectors in 293 cells and their ability to form plaques. These functional titres were calculated as plaque-forming units per ml (pfu/ml). 293 cells were plated in a 96-well plate at 50-60 % confluence. Serial dilutions of adenoviral vectors were prepared at dilutions ranging from  $10^{-2}$  to  $10^{-12}$  in 10 % complete MEM media (Table 2.1). Media in each well of a row was replaced with 100 µl of sequential adenoviral dilutions (10 wells per row). An additional row with 100 µl of media alone to each well of 293

cells was used as a control (no transduction). The plate was then incubated in a humidified chamber at 37°C in 5% CO<sub>2</sub> overnight. Next, media in each well was changed for 200 µl of fresh media and every 2-3 d thereafter until the 8<sup>th</sup> d. On the 8<sup>th</sup> d post-transduction, pfu/ml was calculated according to the visible cytopathic effect at the two lowest adenoviral dilutions, followed by using these sequential equations (Nicklin and Baker, 1999):

**A) The proportionate distance (PD) =**

$$\left( \frac{\% \text{ positive wells above } 50\%-50}{(\% \text{ positive wells above } 50\%) - (\% \text{ positive below } 50\%)} \right)$$

**B) And log ID<sub>50</sub> (infectivity dose) =**

$$[\text{Log dilution above } 50\% + (\text{proportionate distance} \times \text{dilution factor})]$$

For example; for a plate with 9 positive wells at 1<sup>-9</sup> dilution and 2 positive wells at 1<sup>-10</sup> dilution the calculation would be as follows:

$$\text{PD} = (90\% - 50\%) / (90\% - 20\%) = 0.57$$

$$\text{logID}_{50} = -9 + (0.57 \times -1) = -9.57$$

$$\text{TCID}_{50} \text{ (Tissue Culture Infectivity Dose)} = 1 / 10^{-9.57}$$

$$\text{TCID}_{50}/100\mu\text{l} = 10^{9.57} \quad \text{TCID}_{50}/1\text{ml} = 10^{10.57} = 3.27 \times 10^{10} \text{ TCID}_{50}/\text{ml}$$

$$1 \text{ TCID}_{50} \approx 0.7 \text{ pfu}$$

$$\text{Final titre} = (3.27 \times 10^{10}) \times 0.7 = 2.6 \times 10^{10} \text{ pfu/ml}$$

## 2.13 *In vitro* infections

### 2.13.1 *In vitro* infections with lentiviral vectors

Cells were seeded to required density and incubated overnight at 37°C in 5 % CO<sub>2</sub>. A multiplicity of infection (MOI) per cell of LV was calculated on the basis of infective titres (iu/ml) and an accurate cell count prior to infection. LVs were diluted in culture media with 8 µg/ml of polybrene to the desired concentrations based on MOIs required (Dishart et al., 2003a), unless otherwise stated. Cells were transduced with LVs and incubated for 18 h, unless otherwise stated. Next, these cells were washed twice in PBS, maintained in fresh culture media and incubated at 37°C in 5 % CO<sub>2</sub>, until required.

### 2.13.2 *In vitro* infections with adenoviral vectors

Cells were seeded to required density and incubated overnight at 37°C in 5 % CO<sub>2</sub>. A MOI per cell of Ad was calculated on the basis of infective titres (pfu/ml) and accurate cell count prior to infection. Adenoviral vectors were diluted in culture media to the desired concentrations based on MOIs required. Cells were transduced with adenoviral vectors and incubated for 18 h. After, 18 h transduction, cells were washed twice in PBS, maintained in fresh culture media and incubated at 37°C in 5 % CO<sub>2</sub>, until required.

The basic MOI calculation used:

$$\left( \frac{\text{MOI (per cell)} \times \text{number of cells/well}}{\text{titre}} \right) = \mu\text{l/well}$$

### 2.13.3 Fluorescence microscopy

Expression of eGFP was visualised under a Nikon Eclipse TS100 inverted microscope (Nikon®, Surrey, UK), with a Nikon mercury burner light source attachment for fluorescence imaging. Using 200 ×, 100 × or 40 × magnification where stated, micrographs were acquired using QImaging CCD camera

(QImaging®, Surrey, BC, Canada) for digital imaging with Image-Pro software (Media Cybernetics, Bethesda, MD, USA).

Expression of Nogo-B was visualised under an Olympus 1×71 inverted microscope (attached with a slide holder) (Olympus®, Southend-on-Sea, Essex, UK), with an Olympus Th4-200 mercury burner light source attachment for the fluorescence imaging. Using 600 × magnification, micrographs were acquired using the Olympus CCD built-in camera for digital imaging with Cell<sup>^</sup>M imaging software (Olympus).

### **2.13.4 Protein extraction**

#### **2.13.4.1 Cell lysis**

Cell media was removed, cells were gently washed twice in sterile PBS and cell lysates were prepared. Briefly, cells were placed on ice and freshly prepared ice-cold cell lysis buffer was added [containing 50 mM Tris-HCl pH 7.4 (at 4°C), 150mM NaCl, 2 mM EDTA, 2 mM ethylene glycol tetra-acetic acid (EGTA), 0.2 % (v/v) Triton X-100 and 0.3 % (v/v) nonylphenoxypolyethoxylethanol (NP-40)] supplemented with 100 mM phenylmethanesulfonyl fluoride (PMSF) (inhibitor of serine proteases and cysteine proteases), 1 M NaF (inhibitor of serine phosphatases and threonine phosphatases) and 1 x final concentration of complete protease inhibitor cocktail (inhibitors for serine proteases, cysteine proteases and metallo-proteases) (Roche, Welwyn Garden City, UK). In addition, 1 x phosphatase inhibitor cocktail 2 (Inhibitors of tyrosine protein phosphatases, and acid and alkaline phosphatases) (Sigma-Aldrich) was added to cell lysis buffer for phosphorylated-proteins in cell signalling analysis for phosphorylated-ERK1/2 and phosphorylated-Akt in VSMCs (refer to chapter 5). Cell extracts were scraped off, transferred to a micro-centrifuge tube and incubated on ice for 10 min with agitation every 5 min. Extracts were subjected to centrifugation at 12000 x g for 1 min at 4°C. Cell lysates were stored at -20°C when not required immediately.

#### **2.13.4.2 Protein isolation from supernatant**

For quantification of secreted Nogo-B, supernatants from VSMCs and HeLa cells were collected prior to cell lysis and concentrated using 10k [concentration of

protein with a molecular mass greater than 10 kilo Dalton (kDa)] centrifugal filter units (Millipore, Livingston, UK) at 4000 x g centrifugation in a swing bucket rotor at 25°C for 20 min, following the manufacturer's instructions. Each concentrated supernatant was transferred from the filter unit into a micro-centrifuge tube, and stored -20°C until needed for analysis.

### ***2.13.5 Determination of protein concentration***

Protein concentration in cell lysates and supernatants were determined using the bicinchoninic acid (BCA) protein assay (Fisher Scientific, Loughborough, UK), a colourimetric detection and quantification protocol, as per the manufacturer's instructions. Briefly, a standard curve was generated using dilutions of BSA prepared in cell lysis buffer as the following: 2000 µg/ml, 1500 µg/ml, 1000 µg/ml, 750 µg/ml, 500 µg/ml, 250 µg/ml, 125 µg/ml and 25 µg/ml. The BCA working reagent was prepared by mixing BCA reagent A with BCA reagent B at a ratio of 50:1 (A: B). In a 96-well plate, 25 µl of each standard were added in duplicate and each sample added in triplicate. 200 µl of BCA working reagent was added to each well (final ratio of 1:8, respectively) and then the plate was incubated at 37°C for 30 min. During this incubation, the following reactions occur: peptides bonds reduce  $\text{Cu}^{2+}$  ions from the cupric sulphate to  $\text{Cu}^+$  ions (at 37°C); next, two molecules of BCA form a complex with  $\text{Cu}^+$ , which forms a purple coloured product, and absorbs (optical density) light at 570 nm. Finally the amount of  $\text{Cu}^{2+}$  ions reduced is proportional to the amount of protein present. Following incubation, the plate was analysed and optical density (OD) was measured using a Wallac Victor<sup>2</sup> plate reader (Wallac, Turku, Finland) at a wavelength of 570 nm. To calculate the protein concentration, the blank absorbance from 0 µg/ml of BSA (cell lysis buffer alone) was subtracted from the readings of each standard and sample. A standard curve was generated, and sample protein concentrations were determined from the linear equation based on the standard curve.

### ***2.13.6 Green Fluorescent Protein (GFP) assay***

Briefly, infected cells in a 48-well plate were washed in PBS twice, and then lysed in 200 µl cell lysis buffer (section 2.13.4.1). A standard curve was generated using dilutions of recombinant eGFP (Clontech, Basingstoke, UK)

prepared in cell lysis buffer, as the following: 1 µg/ml, 0.5 µg/ml, 0.25 µg/ml, 0.1 µg/ml, 0.05 µg/ml and 0.01 µg/ml. In a pre-cooled 96-well plate, 20 µl of each standard were transferred in duplicate and each sample transferred in triplicate, and subsequently 80 µl of cell lysis buffer was added to each well (final ratio of 1:4, respectively). The plate was then analysed immediately on a Wallac Victor<sup>2</sup> plate reader with emission at 507 nm. Average relative fluorescent unit (RFU) readings for standards and samples were calculated. A linear standard curve was generated to ensure the assay was functioning. Expression of eGFP for all samples were normalised to the total protein amount present determined by a BCA assay (section 2.13.5) on these cell lysates, and the results were then expressed as RFU/mg protein (Nicklin et al., 2001, Dishart et al., 2003a)

### ***2.13.7 Efficiency and longevity of transgene expression of continuous culture***

At appropriate time points post-infection, eGFP expression was monitored by fluorescence microscopy (see section 2.13.3) and subsequently cells were washed in PBS twice prior to cell lysis (see section 2.13.4.1). Cell lysates were scraped, harvested and placed on ice for 10 min, followed by storage at -20°C until required for eGFP quantification (see section 2.13.6). In addition, one replicate per condition was reserved prior to cell lysis and used for assessing transgene expression longevity. Cells were passaged as described in section 2.2.2.

### ***2.13.8 Western blot analysis***

To detect specific proteins and assess levels of protein expression in cell lysates and/or supernatants, sodium dodecyl sulphate polyacrylamide gel electrophoresis (SDS-PAGE) and western immuno-blotting was performed. Denaturing (heating at 95°C) and reducing (use of SDS and β-mercaptoethanol) conditions were used for all proteins analysed.

#### ***2.13.8.1 Electrophoresis***

Each SDS-PAGE gel (18 cm × 16 cm) consisted of a reducing 10 % resolving gel [consisting of 33.3 % (v/v) N, N'-methylene-bis-acrylamide (polyacrylamide 30 %)

(Bio-Rad Laboratories), 11.25 mM Tris-HCl pH 8.8, 0.1 % (v/v) SDS, 1 % (v/v) ammonium persulphate (APS) and 0.1 % (v/v) N, N,N', N'-tetramethylethylenediamine (TEMED)] and reducing 4 % stacking gel [containing 13.3 % (v/v) polyacrylamide (30 %), 3.75 mM Tris-HCl pH 6.8, 0.1 % (v/v) SDS, 1 % (v/v) APS and 0.1 % (v/v) TEMED (the latter two are added for polymerisation to occur)]. Protein samples and controls were prepared prior to gel loading, with 6 x reducing loading buffer for a final concentration of 1 x [consisting of 12 % (w/v) SDS, 36 % (v/v) glycerol, 375 mM Tris-HCl pH 6.8, 0.012 % (w/v) bromophenol blue and 6 % (v/v)  $\beta$ -mercaptoethanol]. Samples and controls were heated at 95°C for 5 min to denature the protein, mildly cooled and loaded into the wells within the gel. Amersham full-range rainbow molecular weight marker (GE healthcare, Buckingham, UK) at a volume of 40  $\mu$ l was added to the gel, as a marker of protein size. Samples were electrophoresed at 100 V through the 4 % stacking gel for approximately 45 min in running buffer (consisting of 25 mM Tris, 0.2 M glycine, 1mM SDS), followed by 200 V for electrophoresis through the resolving gel for approximately 4 h to achieve separation on the gel.

Proteins were transferred onto Hybond-P polyvinylidene difluoride (PVDF) membrane (GE healthcare), using an electric current to promote protein migration from the gel to the membrane (towards the anode) to enable antibody binding and detection. Protein transfer was performed overnight at 80 milliAmp (mA) and 20 V in transfer buffer [consisting of 25 mM Tris, 0.2 M glycine, 20 % (v/v) methanol, 0.01 % (v/v) SDS] at 4°C. To confirm the samples and controls had transferred correctly, the membrane was stained with Ponceau S solution (Sigma-Aldrich) as per the manufacturer's instructions for reversible protein detection. Briefly, the membrane was immersed in Ponceau S staining solution for 5 min to visualise proteins. After staining, the membrane was rinsed with distilled water and rapidly immersed in 0.1 M NaOH for protein bands to disappear within 10-30 sec. Next, the membrane was rinsed with distilled water for 2-3 min; this was then followed by Western immunoblotting.

### **2.13.8.2 Western immunoblotting**

After transfer of proteins to the membrane, antibody detection was performed. Each membrane blocked in tris-buffered saline tween (TBS-T) buffer [consisting of 50 mM Tris-HCl pH 7.4, 150 mM NaCl, 2.7 mM KCl and 0.1 % (v/v) Tween20]

with either 5-10 % (w/v) fat-free milk powder or 5 % (w/v) BSA (see Table 2.7 for blocking solution used for each antibody) for 3 h at 4°C with agitation. After blocking, each membrane was incubated with an appropriate concentration of primary antibody (Table 2.7) diluted in blocking solution at 4°C overnight with shaking. The membrane was washed by two 5 min washes in blocking solution at RT before addition of secondary antibody conjugated with HRP. The secondary antibody was diluted in blocking solution (Table 2.7) and incubated with the membrane for 1 h at RT with shaking. Following secondary antibody incubation, the membrane was washed four times for 15 min in blocking solution and washed a further two times in TBS-T alone. Proteins were visualised using Enhanced Chemiluminescent (ECL) plus detection system (GE healthcare), as per the manufacturer's instructions. ECL plus is a substrate for HRP on immunoblots and the release of luminescence can be exposed to X-ray films. Briefly, for ECL plus, reagent A and B were mixed in a 40:1 ratio and poured onto the membrane. After 5 min the excess ECL plus was drained off and the membrane was wrapped in saran wrap, and placed in an autoradiography cassette. Kodak general purpose medical x-ray films were exposed for various lengths of time, ranging from 1 sec to overnight. Films were developed in a Kodak X-Omat 1000 developer.

Western blotting	Description/Epitope recognised	Primary antibody	Animal raised in	Clone no.	Source	Concentration or dilution (primary antibody)	Blocking solution	Secondary antibody [horseradish peroxidase (HRP) conjugated antibody]	Clone no.	Source
Nogo-B (45-50 kDa)	N-terminus of Nogo-B	Goat polyclonal anti-human Nogo IgG	Goat	N-18	Santa-Cruz Biotechnology®	0.4 µg/ml	10 % (w/v)(non-fat) milk in TBS-T	Donkey anti-goat IgG-HRP	SC-2056	Santa-Cruz Biotechnology
GAPDH (36 kDa)	Glyceraldehyde 3 phosphate dehydrogenase (GAPDH)	Mouse monoclonal IgG1 to GAPDH	Mouse	6C5	Abcam®	0.2 µg/ml	10 % (non-fat) milk in TBS-T	Polyclonal rabbit anti-mouse IgG-HRP	P0260	Dako
p-ERK 1 & 2 (44 kDa & 42 kDa, respectively)	Phosphorylated threonine and tyrosine residues within the regulatory site of active MAP kinase, ERK 1 & 2 (p-ERK 1 & 2)	Mouse monoclonal IgG1 to p-ERK 1 & 2	Mouse	MAPK-YT	Abcam	1 µg/ml	5 % (w/v) BSA in TBS-T	Polyclonal rabbit anti-mouse IgG-HRP	P0260	Dako
ERK1 (44 kDa)	ERK1 of MAP kinase	Rabbit polyclonal IgG to ERK1	Rabbit	ab7947	Abcam	0.4 µg/ml	5 % BSA in TBS-T	Polyclonal swine anti-rabbit IgG-HRP	P0217	Dako
p-Akt (Ser473) (60 kDa)	Akt phosphorylated at serine 473 (p-Akt)	Mouse monoclonal IgG2b to p-Akt	Mouse	587F11	Cell Signalling Technology®, Danvers, MA	1/1000 dilution	5 % (w/v) (non-fat) milk in TBS-T	Polyclonal rabbit anti-mouse IgG-HRP	P0260	Dako

Western blotting	Description/Epitope recognised	Primary antibody	Animal raised in	Clone no.	Source	Concentration or dilution (primary antibody)	Blocking solution	Secondary antibody [horseradish peroxidase (HRP) conjugated antibody]	Clone no.	Source
Akt (pan)(60 kDa)	Total Akt (pan)	Rabbit monoclonal IgG to Akt (pan)	Rabbit	C67E7	Cell Signalling Technology	1/1000 dilution	5 % BSA in TBS-T	Polyclonal swine anti-rabbit IgG-HRP	P0217	Dako
GRP78/BiP (75-78 kDa)	78kDa glucose regulated protein/Binding immunoglobulin Protein (GRP78/BiP)	Rabbit polyclonal IgG to GRP78 BiP	Rabbit	ab21685	Abcam	1 µg/ml	5 % (non-fat) milk in TBS-T	Polyclonal swine anti-rabbit IgG-HRP	P0217	Dako
SM-alpha actin (42 kDa)	Smooth Muscle alpha actin (SM-alpha actin)	Mouse monoclonal IgG2a to SM-alpha actin	Mouse	1A4	Abcam	0.4 µg/ml	10 % (non-fat) milk in TBS T	Polyclonal rabbit anti-mouse IgG-HRP	P0260	Dako

**Table 2.7. Antibodies used for Western immunoblotting.**

TBS-T, tris-buffered saline tween buffer; BSA, bovine serum albumin; ERK, extracellular signal-regulated kinase; MAP Kinase, mitogen-activated protein kinase; Akt, PI3 Kinase-Akt.

### 2.13.8.3 Densitometric quantification of protein bands

To normalise each protein band to a loading control (to ensure that any change in protein level was not due to unequal loading), immuno-detected bands on an X-ray film were scanned to generate a digital image in Bio-Rad quantity one 1-D analysis software (Bio-Rad). The density of each protein band was determined by the software, using the global background subtraction method. Demarcated by boxes using the volume tool, the density of the bands were measured using the analysis for volume report function and expressed in units of optical density per  $\text{mm}^2$  (ODU/ $\text{mm}^2$ ). The adjusted density for each protein band was divided by the equivalent value obtained for the loading control band to give a final density value corrected for loading.

### 2.13.9 Immunocytofluorescence

VSMCs seeded in 4- or 8-well culture chamber slides were washed in PBS at RT twice to remove any remaining culture media, and then fixed in 4 % PFA at RT for 10 min, followed by three washes in PBS at RT for 5 min each. VSMCs were permeabilised for 10 min in 0.1 % (v/v) Triton-X-100 in PBS at RT, followed by another three PBS washes, and then blocked using 10 % (v/v) donkey serum (Sigma-Aldrich) and 1 % (w/v) BSA in PBS (blocking solution) for 30 min to block non-specific binding of antibodies. After blocking, VSMCs were then incubated with primary antibodies in blocking solution for 1 h at RT. 2  $\mu\text{g}/\text{ml}$  of goat polyclonal anti-human Nogo (N-18) IgG (Santa-Cruz Biotechnology, Santa Cruz, CA) was used to indicate Nogo-B expression or its isotype-matched goat IgG control (Sigma-Aldrich). After incubations, VSMCs were washed three times in PBS to remove any unbound primary antibodies, and then incubated with a corresponding secondary antibody: 4  $\mu\text{g}/\text{ml}$  of Alexa-Fluor®-555 (red) donkey anti-goat IgG (Invitrogen) in PBS for 1 h at RT in the dark. Next, VSMCs were washed three times in PBS to remove any unbound secondary antibodies, mounted on coverslips with Prolong-Gold anti-fade reagent with 4', 6-diamidino-2-phenylindole (DAPI) (Invitrogen), and coverslips were sealed with clear nail varnish to prevent drying and movement under the microscope. DAPI was used for nuclear counter-staining. VSMCs were visualised using either fluorescence microscopy (section 2.13.3) or confocal microscopy (section 2.13.10), where

stated. The nucleus appeared blue and the areas where the primary antibody for Nogo-B had bound appeared red.

VSMCs were fixed, permeabilised and blocked in blocking solution, as previously described. These VSMCs were then ready for double immunostaining. After blocking, VSMCs were incubated with the first primary antibody: 10 µg/ml of mouse monoclonal anti-human endoplasmic reticulum (ER) protein disulphide isomerase (PDI) (clone RL90) IgG2a (Abcam, Cambridge, UK) or isotype-matched mouse IgG2a control (Sigma-Aldrich) in blocking solution (10 % donkey serum and 1 % BSA) in PBS for 1 h at RT. Subsequently, VSMCs were washed in PBS three times and then incubated with the first secondary antibody: 4 µg/ml of Alexa-Fluor®-594 (far red) donkey anti-mouse IgG (Invitrogen) secondary antibody in PBS at RT for 1 h in the dark. Next, VSMCs were washed three times in PBS and then incubated with the second primary antibody: 2 µg/ml of goat polyclonal anti-human Nogo (N-18) IgG or isotype-matched goat IgG control in blocking solution for 1 h at RT. After second primary antibody incubation step, VSMCs were washed three times in PBS and incubated with the second secondary antibody: 4 µg/ml of Alexa-Fluor®-488 (green) donkey anti-goat IgG (Invitrogen) secondary antibody in PBS at RT for 1 h in the dark. Subsequently, VSMCs were washed three times in PBS and then mounted on coverslips with Prolong-Gold anti-fade reagent with DAPI, as previously described. VSMCs were visualised using confocal microscopy (section 2.13.10). The nucleus appeared blue, and the areas where the primary antibodies for Nogo-B and ER PDI had bound appeared green and red, respectively.

### **2.13.10 Confocal microscopy**

Immunostaining of Nogo-B and/or ER PDI was/were visualised under a Carl Zeiss LSM 510 Meta confocal microscope (Carl Zeiss®, Welwyn Garden City, UK) with a LSM 510 laser module (Mbq 52ac) for fluorescence imaging. Using magnification × 630, micro-photographs were acquired using a built-in CCD camera for digital imaging with LSM image software under constant exposure time, gain and offset and with approximate optical slice of 1 µm. Channels 420 nm-480 nm band pass (BP), 505 nm-530 nm BP and 550 nm-657 nm BP were chosen for imaging DAPI, both eGFP and Alexa Fluor®-488 and both Alexa Fluor®-555 and -594,

respectively, and used according to the absorption and emission spectra for fluorescence.

### **2.13.11 Scratch-wound mediated cell migration assay**

VSMC migration was assessed by scratch-wound mediated cell migration assay, with reference to a scratch assay protocol written by Liang et al., (2007), with modifications. Briefly, VSMCs were seeded at a density of  $0.5 \times 10^4$  cells per well into 8-well culture slides overnight for 50-60 % confluence prior to LV infection. After 3 d post-infection when VSMCs had reached 100 % confluence, a scratch was created using a p200 pipette tip (for 10 h post-wounding) or p1000 pipette tip (for 22 h post-wounding). VSMCs were washed twice in PBS to remove cell debris and to smooth the edge of the scratch. VSMCs were maintained in 15 % complete SMC media (Table 2.1) and placed in the incubator at 37°C in 5 % CO<sub>2</sub>. Reference lines close to the edge of the scratch were marked and images of the scratch acquired at 0 h and 10 h or 22 h (as stated) using bright-field microscopy (Nikon eclipse TS100 inverted microscope). Images were acquired using a QImaging CCD camera at magnification  $\times 100$  or 40 (as stated). After 10 h or 22 h post-wounding, VSMCs were fixed in 4 % PFA, washed three times in PBS at RT and absolute migration was measured using ImagePro software. Absolute migration measurements involved measuring the furthest distance that these VSMCs had migrated from the wound edge. For each condition (repeated in triplicate), 10 migration distances of 3 fields of view were measured.

### **2.13.12 3-(4, 5-Dimethylthiazol-2-yl)-2, 5-diphenyltetrazolium bromide (MTT) assay**

A 3-(4,5-Dimethylthiazol-2-yl)-2,5-diphenyltetrazolium bromide (MTT) assay was used to determine the proliferation/viability status of VSMCs after the over-expression Nogo-B mediated by LVs 5 d post-infection, and this was carried out using a CellTiter 96® Non-radioactive Cell Proliferation Assay (MTT assay) kit (Promega). This assay directly measures the reduction of the MTT component (tetrazolium) of the dye solution into an insoluble formazan product by the mitochondria of proliferating/viable cells present.

VSMCs were seeded at a density of  $0.5 \times 10^4$  cells (30 % confluence) per well on a 48-well plate and incubated at 37°C in 5 % CO<sub>2</sub> overnight. Next, growth-

arrested/quiescent VSMCs were induced by using serum-free media [MEM supplemented with 1 % (v/v) penicillin, 100 µg/ml streptomycin, 2 mM L-glutamine and 1 mM sodium pyruvate] (Libby and O'Brien, 1983, Fager et al., 1988) for 48 h prior to LV infection (section 2.13.1) (Kritz et al., 2008). After 4 d post-infection, media was removed and 200 µl of fresh 15 % complete VSMC media was added to LV treated and untreated VSMCs. These cells were then placed in a humidified chamber in the incubator at 37°C in CO<sub>2</sub> overnight.

The MTT assay kit was used 5 d post-infection, according to the manufacturer's instruction. Briefly, 30 µl of dye solution was added to each well (15:100 ratio of dye solution to culture media). Blank controls consisted of 200 µl of 15 % complete SMC media, 30 µl of dye solution and no VSMCs; to reduce background contributed by non-specific absorbance of chemical interference of compounds within the media and/or media supplements. After incubation for 4 h at 37°C in 5 % CO<sub>2</sub>, 200 µl of solubilisation/stop solution was then added to each well to solubilise the formazan product and each well was mixed with a fresh p200 tip (avoided bubble formation because this can interfere with accurate readings of absorbance values). Optical density (OD) was quantified using a Wallac Victor<sup>2</sup> plate reader at a wavelength of 570 nm. The average blank control OD reading was subtracted from readings of each sample. OD<sub>570nm</sub> was directly proportional to the number of proliferating/viable VSMCs.

### **2.13.13 Caspase-3/7 assay**

A Caspase-Glo®-3/7 assay kit (Promega) was used to determine VSMC apoptosis after the over-expression Nogo-B mediated by LVs 5 d post-infection. This assay measures the presence of two members of the cysteine aspartic acid-specific protease (caspase) family, caspase -3 and -7, which have key effector roles in apoptosis. The assay involves two steps for the measurement of caspase-3/7 activities. Step one involves a luminogenic caspase-3/7 substrate containing the tetra-peptide sequence DEVD (Z-DEVD-aminoluciferin), which is selective for caspase-3/7 activity and cleaved by caspase-3/7 to release aminoluciferin (a substrate for luciferase). Step two involves aminoluciferin cleavage by luciferase, which generates a luminescent signal ('glow-type' signal).

Prior to caspase-3/7 activity assay, VSMCs were seeded at a density of  $0.25 \times 10^4$  cells (30 % confluence) per well on a white 96-well plate and incubated at 37°C in 5 % CO<sub>2</sub> overnight. Next, VSMC quiescence was induced with serum-free media (section 2.13.12) for 48 h prior to LV infection (section 2.13.1) in 15 % complete SMC media.

The caspase-Glo 3/7 assay kit was used according to the manufacturer's instruction. Briefly, lyophilised Caspase-Glo Substrate®-3 and -7 (Z-DEVD-aminoluciferin) and Caspase-Glo® Buffer (optimised for cell lysis, caspase activity and luciferase activity) were mixed to form a Caspase -Glo®-3/7 Reagent. After 4 d post-infection, media was removed and 100 µl of fresh 15 % complete VSMC media was added to LV treated and untreated VSMCs, and these cells were then placed in a humidified chamber in the incubator at 37°C in 5 % CO<sub>2</sub> overnight. At 5 d post-infection, 100 µl of Caspase -Glo® 3/7 Reagent was added per well. A blank reaction was used in this caspase-3/7 assay, namely a "no-cell" control consisting of 100 µl of 15 % complete SMC media, 100 µl of Caspase -Glo® 3/7 Reagent and no VSMCs; to reduce background luminescence associated with cell culture media and supplements, i.e. caspase-3/7 activities can be detected in FCS. Next, the plate was covered in aluminium foil to protect from light, gently mixed using a plate shaker for 30 sec to aid cell lysis, and then incubated at RT. After 3 h incubation, luminescence [in relative luminescence units (RLU)] was quantified using a Wallac Victor<sup>2</sup> (luminometer function). Luminescence measured was directly proportional to the amount of caspase-3/7 activity present. The "no-cell" control luminescence signal was subtracted from luminescence signal produced by LV and Ad infected VSMCs and un-infected VSMCs. Caspase-3/7 activities for all samples were normalized to the total protein amount present [quantified using the BCA assay on cell lysates from a parallel assay (section 2.13.5)] and the results were expressed as RLU/mg protein.

## 2.14 Statistical analysis

*In vitro* experiments were carried out on three independent occasions and results shown are representative, unless otherwise stated. Results are expressed as the mean ± standard error of the mean (S.E.M) of triplicates, unless otherwise stated. Results were tested for, and shown to exhibit, gaussian distribution by

applying the Shapiro-Wilk normality test to the data. Subsequently, as stated, results were analysed using two-tailed unpaired Student's t-test, or one-way analysis of variance (ANOVA) for Bonferroni's multiple comparisons (using GraphPad Prism). Statistical significance was accepted when  $p < 0.05$ .

### **3 Optimisation of Lentiviral Vectors for Vascular Cell Gene Transfer**

### 3.1 Introduction

LVs are highly efficient for vascular cell gene transfer (Dishart et al., 2003a, Cefai et al., 2005, Qian et al., 2006, Yang et al., 2010) and have been considered useful vectors for delivering therapeutic genes to reduce the NIF caused by acute vascular injury *in vivo* (Qian et al., 2006, Yang et al., 2010). In terms of transduction efficiencies for human vascular cells, LVs are similar to adenoviral vectors in mediating efficient levels of transgene expression at a short exposure time of 30 minutes *in vitro* (Dishart et al., 2003a, Cefai et al., 2005), which is necessary in the clinical setting.

The development of NILVs has greatly increased the therapeutic potential of LVs for a range of conditions, owing to the fact that these vectors mediate gene transfer with a more favourable safety profile since they minimize the risk of insertional mutagenesis (Nightingale et al., 2006, Philippe et al., 2006, Yanez-Munoz et al., 2006, Apolonia et al., 2007, Rahim et al., 2009). Many preclinical studies have shown NILVs to have important implications for gene transfer in dividing cells [Jurkat T lymphocyte cell line, haematopoietic progenitor cells, 293 T cells and mouse myoblast (C2C12) cell line] by mediating transient transgene expression (Nightingale et al., 2006, Philippe et al., 2006, Apolonia et al., 2007) and in non-dividing cells (within muscle, the eye and CNS) by providing long-term and stable transgene expression (Philippe et al., 2006, Yanez-Munoz et al., 2006, Apolonia et al., 2007, Rahim et al., 2009). There are many numbers of class I integrase point mutations and the most common mutant residue used in most studies up to date is the D64V [part of the catalytic triad and facilitates the inactivation of the integrase function, thereby prevents integration (Philpott and Thrasher, 2007, Banasik and McCray, 2010)]. Evidently, studies have indicated that D64V mutant NILVs [with low residual integration frequency of  $10^3$ -fold less than the int-LV (Apolonia et al., 2007)] retain high transduction efficiency of their integrating counterparts (Nightingale et al., 2006, Yanez-Munoz et al., 2006, Apolonia et al., 2007, Rahim et al., 2009). NILVs have yet to be explored in vascular gene therapy and have a potential in this clinical setting especially in the context of acute vascular injury, providing transgene expression can be maintained for an adequate duration required for therapeutic gain.

LVs are relatively versatile and thus optimisation can easily be assessed (which includes promoter modification/specificity, pseudotyping and/or integration-proficiency or integration-deficiency). Past studies have indicated LV-mediated transgene expression in vascular tissue can be facilitated by various internal heterologous promoters and these include the following: viral promoters such as CMV and CAG; housekeeping gene promoters for example PGK and EF1 $\alpha$ , and VEC-specific Tie2 promoter (Dishart et al., 2003a, Cefai et al., 2005, Qian et al., 2006). The CMV promoter mediated stronger LV-mediated transgene expression in VECs and VSMCs, compared to CAG, PGK, EF1 $\alpha$  and Tie2 promoters (Dishart et al., 2003a, Cefai et al., 2005). The SFFV promoter [enhancer-promoter region of the SFFV (U3-LTR) and is a ubiquitous promoter] has the ability to drive a high level and long-term LV-mediated transgene expression in human HSC *in vivo*, contrary to the CMV promoter (Demaison et al., 2002). Since this study, this particular promoter has been highly regarded for many gene therapy application studies involving the eye (Tschernutter et al., 2005, Yanez-Munoz et al., 2006), lung (Buckley et al., 2008), muscle (Apolonia et al., 2007), CNS (Rahim et al., 2009) and haematological disorders (Ward et al., 2011). In relevance to vascular gene transfer, LV-mediated transgene expression elicited by the SFFV promoter has yet to be evaluated in the vasculature.

An enhancer element is associated with an internal regulatory element (enhancer-promoter element) for up-regulation of transgene expression. This enhancer-promoter element has the potential to induce integration-site position effects, such as the transactivation of a proto-oncogene (associated with integration either near or within this gene), and as a consequence mediates a possible risk of insertional oncogenesis (Hacein-Bey-Abina et al., 2003b, Ott et al., 2006, Zhang et al., 2007, Hacein-Bey-Abina et al., 2008, Howe et al., 2008, Modlich et al., 2009). This has been demonstrated in two clinical studies for X-linked SCID, where retroviral-mediated gene transfer presented a high risk of oncogenesis through insertional activation/insertional mutagenesis in the *LMO2* (LIM-domain only 2) locus in HSCs, which was a consequence of the enhancer sequence (Hacein-Bey-Abina et al., 2003b, Hacein-Bey-Abina et al., 2008, Howe et al., 2008). The enhancer-less ubiquitously acting chromatin opening element (UCOE) is derived from the human *HNRPA2B1-CBX3* house-keeping gene locus (Figure 3.1). UCOE, as its name suggests maintains a chromatin-opening

function, and is an enhancer-less regulatory element consisting of a methylation-free CpG island region encompassing two closely spaced dual divergent transcribed *CBX3* and *HNRPA2B1* promoters (Figure 3.1), and therefore is resistant to transcriptional silencing (irrespective of tissue type or integration site position effects) (Williams et al., 2005, Zhang et al., 2007). Unlike the SFFV viral promoter element, UCOE can facilitate highly efficient, consistent, stable and long-term LV-mediated transgene expression, as demonstrated in HSCs. Moreover, UCOE gave rise to the efficient rescue of the IL-2 receptor gamma gene (*IL2RG*) deficiency in a mouse model of X-linked SCID (Zhang et al., 2007). In addition, this UCOE promoter overcomes enhancer-mediated integration-site position effects and potentially reduces the risk of insertional mutagenesis, and thereby aids in a better safety profile (Zhang et al., 2007). This UCOE regulatory element is desirable for many gene therapy applications and has not been tested in the vasculature.

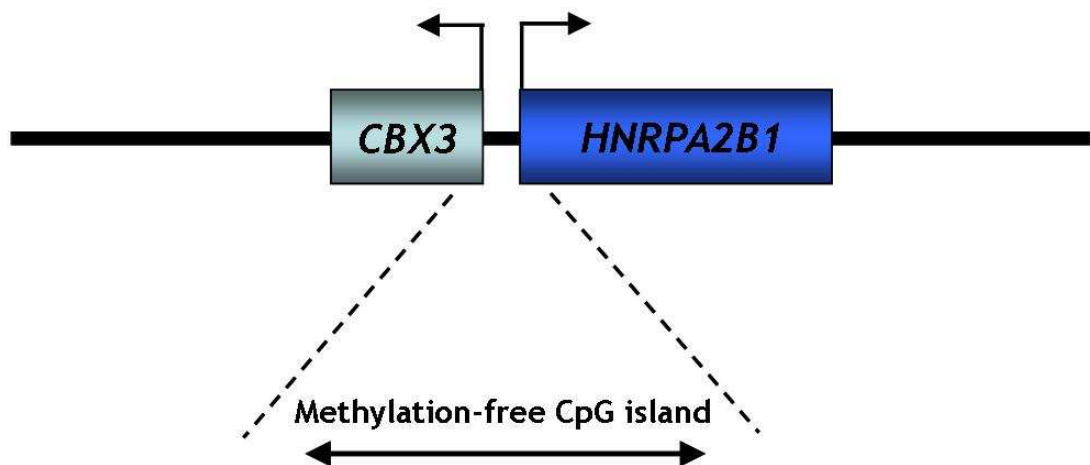


**Figure 3.1.** Illustration of the enhancer-less ubiquitously acting chromatin opening element (UCOE).

This enhancer-less internal regulatory element consists of a methylation-free CpG island region associated with two closely spaced dual divergent *CBX3* and *HNRPA2B1* promoters (derived from human *HNRPA2B1-CBX3* house keeping gene locus). *CBX3*, chromobox homolog 3; *HNRPA2B1*, heterogeneous nuclear ribonucleoprotein A2/B1. Adapted from Zhang et al., (2007).

As mentioned in section 1.11.2, various viral glycoprotein envelopes have been used to pseudotype LVs, as well as the most commonly used VSV-g envelope, and these include the following: rabies (Mazarakis et al., 2001, Kato et al., 2007, Rahim et al., 2009), RRV (Kang et al., 2002, Jakobsson et al., 2006), EbolaZ (Kobinger et al., 2001, Kang et al., 2002, MacKenzie et al., 2002, Sinn et al., 2003, Sanders, 2004, MacKenzie et al., 2005, Jakobsson et al., 2006), GP64 (Schauber et al., 2004, Sinn et al., 2005a, Buckley et al., 2008, Rahim et al., 2009), MLV-A (Hanawa et al., 2002, Watson et al., 2002, Kunicher et al., 2008) MLV-E (Koch et al., 2006) and HNTV (Qian et al., 2006). These glycoproteins have been explored for their potential usefulness in diverse gene therapy applications. All of these pseudotyped LVs mentioned have yet to be explored in the context of acute vascular injury, and could provide an additional advantage for these vectors in this clinical setting depending on the level and selectivity of transgene expression. HNTV pseudotyped LVs have demonstrated their utility in vascular gene delivery, especially in acute vascular injury where these vectors greatly targeted the site of vascular injury compared to VSV-g pseudotyped LVs (Qian et al., 2006).

The aim of this study was to optimise and assess LV-mediated transgene expression in human vascular cells *in vitro*, in terms of the following:

- To define transgene expression levels mediated by alternative internal heterologous promoters, in particular the SFFV promoter and the UCOE promoter in vascular cells.
- To assess the transduction efficiencies of alternative pseudotyped LVs (envelope glycoproteins: rabies, RRV, EbolaZ, GP64, MLV-A, MLV-E and HNTV) in vascular cells.
- To evaluate the potential of NILV-mediated gene transfer (in parallel to their integrating counterparts) for efficiency and longevity of eGFP expression in vascular cells.

## 3.2 Results

### 3.2.1 *Promoter alternation for lentiviral-mediated transgene expression in human primary vascular cells*

Efficiency and longevity of transgene expression facilitated by LV-mediated gene transfer under the control of either the SFFV or UCOE promoter, were evaluated in HeLa cells and primary human vascular cells. HeLa cells were tested along side vascular cells, because they are a well-established and a permissive cell line for LVs. Lentiviral construct plasmids comprising of an eGFP transgene under the control of either a SFFV or UCOE promoter (pHR'SIN-cPPT-SFFV-eGFP-WPRE or pHR'SIN-cPPT-UCOE-eGFP-WPRE, respectively) (Demaison et al., 2002, Zhang et al., 2007), VSV-g envelope (pMD.G2) plasmid (Zhang et al., 2007) and the integration-proficient packaging plasmid (pCMV delta R8.74 wild-type integrase) (Yanez-Munoz et al., 2006) were obtained from Adrian Thrasher's lab [University College London (UCL), UK] and have been described previously (also see Figure 2.2, Table 2.2 and Table 2.3 for more details on plasmids). Int-LVs expressing eGFP under the control of either the SFFV (int-LV-SFFV) or the UCOE (int-LV-UCOE) promoter were produced, and visual eGFP titres of  $4.29 \times 10^8$  iu/ml and  $3.28 \times 10^7$  iu/ml, respectively, were used in this part of the LV optimisation study.

Lysates from HeLa cells, VSMCs and VECs infected with either int-LV-SFFV or int-LV-UCOE or un-infected were assessed for eGFP expression by fluorimetry [measured in relative fluorescent units (RFU)]; at various time points of continuous culture and then normalised to mg of total protein.

#### 3.2.1.1 **The SFFV promoter compared to the UCOE promoter for lentiviral-mediated transgene expression in HeLa cells: efficiency and longevity.**

The SFFV promoter compared to the UCOE promoter for LV-mediated transgene expression efficiency and longevity in HeLa cells is illustrated in Figure 3.2. Results demonstrated that int-LV-UCOE and int-LV-SFFV both mediated efficient and sustained transgene expression in HeLa cells, at a MOI of 10 and 50 from 1 w to 11 w post-infection (Figure 3.2). Representative fluorescent micrographs of

these HeLa cells at 2 w and 4 w post-infection also illustrated these results (Figure 3.3).

At a lower MOI of 10, int-LV-UCOE provided more efficient, stable and consistent long-term transgene expression compared to int-LV-SFFV (Figure 3.2). Figure 3.3 illustrated that int-LV-UCOE at a MOI of 10 4 w post-infection induced more efficient eGFP expression compared to int-LV-SFFV. Int-LV-SFFV at a MOI of 50 mediated a greater increase in eGFP expression, in contrary to int-LV-UCOE at all post-infection time points (Figure 3.2). Fluorescent microscopy also demonstrated that int-LV-SFFV at MOI of 50 enhanced the expression of eGFP greater than int-LV-UCOE in HeLa cells (Figure 3.3).

Data from this assay indicated that int-LV-SFFV at a MOI of 50 facilitated long-term transgene expression from 1 w to 11 w post-infection in HeLa cells (Figure 3.2). Transgene expression mediated by int-LV-SFFV was enhanced at 1 w to 2 w post-infection [ $48.3 \pm 3.9$  RFU ( $\times 10^6$ )/mg protein vs.  $66.3 \pm 5.9$  RFU ( $\times 10^6$ )/mg protein] (Figure 3.2), however a decreased eGFP expression was observed from 2 w to 11 w post-infection (Figure 3.2). Notably, results indicated that int-LV-UCOE at MOI of 50 mediated a relatively stable and consistent transgene expression in HeLa cells, from 1 w to 11 w post-infection (Figure 3.2). Overall at both MOIs, int-LV-UCOE provided efficient, stable and consistent long-term transgene expression, whereas int-LV-SFFV mediated efficient transgene expression which was down-regulated overtime in HeLa cells (Figure 3.2).

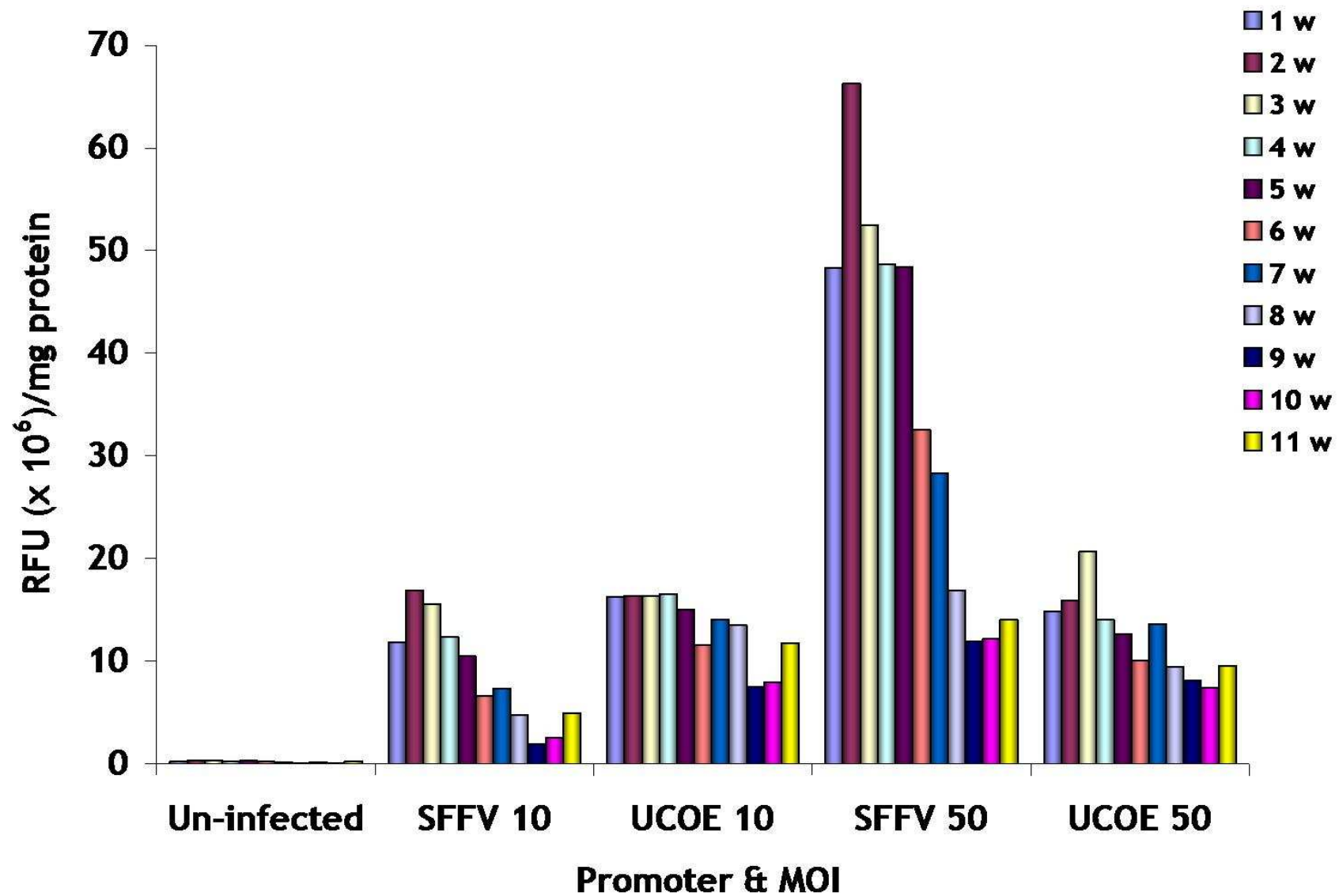


**Figure 3.2. Transgene expression efficiency and longevity in HeLa cells mediated by lentiviral vectors under the control of the SFFV or UCOE promoter.**

HeLa cells were seeded (cell density of  $1 \times 10^4$ /well on a 48-well plate) and infected with int-LV-SFFV or UCOE at a MOI of 10 or 50 (in the presence of 8  $\mu\text{g}/\text{ml}$  of polybrene for 1 h incubation), or un-infected. Efficiency and longevity of eGFP transgene expression were assessed at 1, 2, 3, 4, 5, 6, 7, 8, 9, 10 and 11 weeks (w) post-infection by analysing eGFP expression in HeLa cell lysates by fluorimetry [measured in relative fluorescent units (RFU)], which were then normalised to the total mg of protein (measured by a BCA assay with optical density measured at 570 nm wavelength). Mean value (for technical replicates), repeated in triplicate, and n=1 (cell line population used). UCOE, enhancer-less ubiquitously acting chromatin opening element; SFFV, spleen focus forming virus; MOI, multiplicity of infection; int-LV, integrating lentiviral vector.

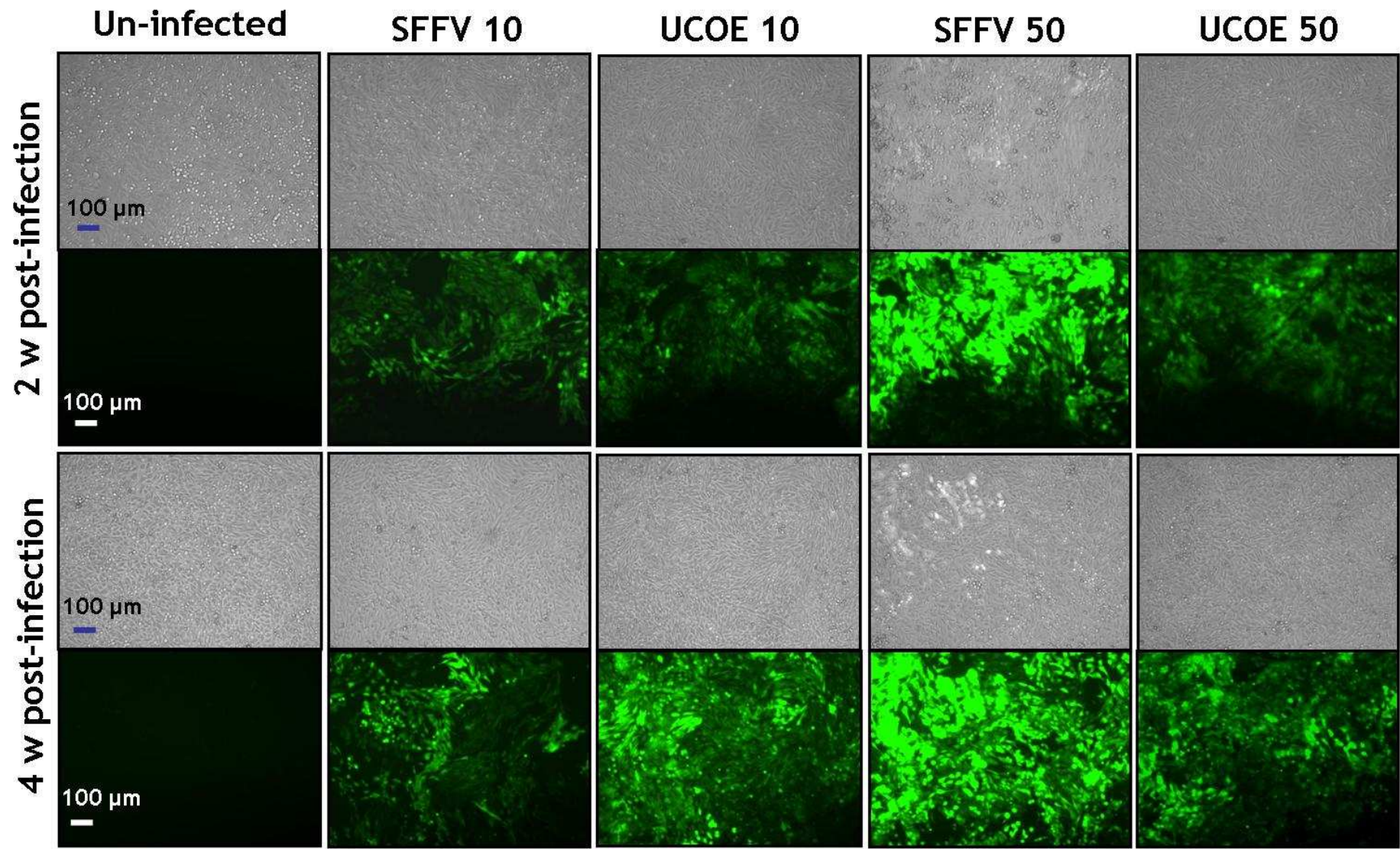


**Figure 3.3. Representative micrographs of the efficiency and longevity of eGFP transgene expression in HeLa cells mediated by lentiviral vectors under the control of the SFFV or UCOE promoter.**

Fluorescent micrographs of eGFP expression in HeLa cells infected with int-LV-SFFV or int-LV-UCOE at a MOI of 10 or 50, or un-infected, at 2 and 4 w post-infection. 100  $\mu\text{m}$  scale bar applicable to all panels (magnification x 100). Representative of n=1 (cell line population used) in triplicate. UCOE, enhancer-less ubiquitously acting chromatin opening element; SFFV, spleen focus forming virus; MOI, multiplicity of infection; int-LV, integrating lentiviral vector.

### 3.2.1.2 The SFFV promoter compared to the UCOE promoter for lentiviral-mediated transgene expression in VECs: efficiency and longevity

Both int-LV-SFFV and int-LV-UCOE at a MOI of 50 facilitated similar long-term efficient transgene expression of eGFP in VECs (Figure 3.4). However, with an exception at 4 w post-infection, this time point indicated int-LV-SFFV mediated higher eGFP expression in comparison to int-LV-UCOE [ $16.60 \pm 0.69$  RFU ( $\times 10^5$ )/mg protein vs.  $6.73 \pm 0.48$  RFU ( $\times 10^5$ )/mg protein, respectively] (Figure 3.4). In terms of longevity, this data indicated that int-LV-SFFV enhanced eGFP transgene expression between 1 w to 3 w and 3 w to 4 w post-infection (long-term) [1 w to 3 w:  $5.88 \pm 0.65$  RFU ( $\times 10^5$ )/mg protein vs.  $12.07 \pm 1.08$  RFU ( $\times 10^5$ )/mg protein, respectively, and 3 w to 4 w:  $12.07 \pm 1.08$  RFU ( $\times 10^5$ )/mg protein vs.  $16.6 \pm 0.69$  RFU ( $\times 10^5$ )/mg protein, respectively] (Figure 3.4). This profile was observed until 5 w post-infection, when transgene expression decreased from 4 w to 5 w [ $16.6 \pm 0.69$  RFU ( $\times 10^5$ )/mg protein vs.  $4.11 \pm 0.32$  RFU ( $\times 10^5$ )/mg protein, respectively] (Figure 3.4). In contrast, int-LV-UCOE induced stable and consistent eGFP transgene expression from 1 w to 5 w post-infection (Figure 3.4). Overall, results have a similar profile to data from HeLa cells (Figure 3.2).

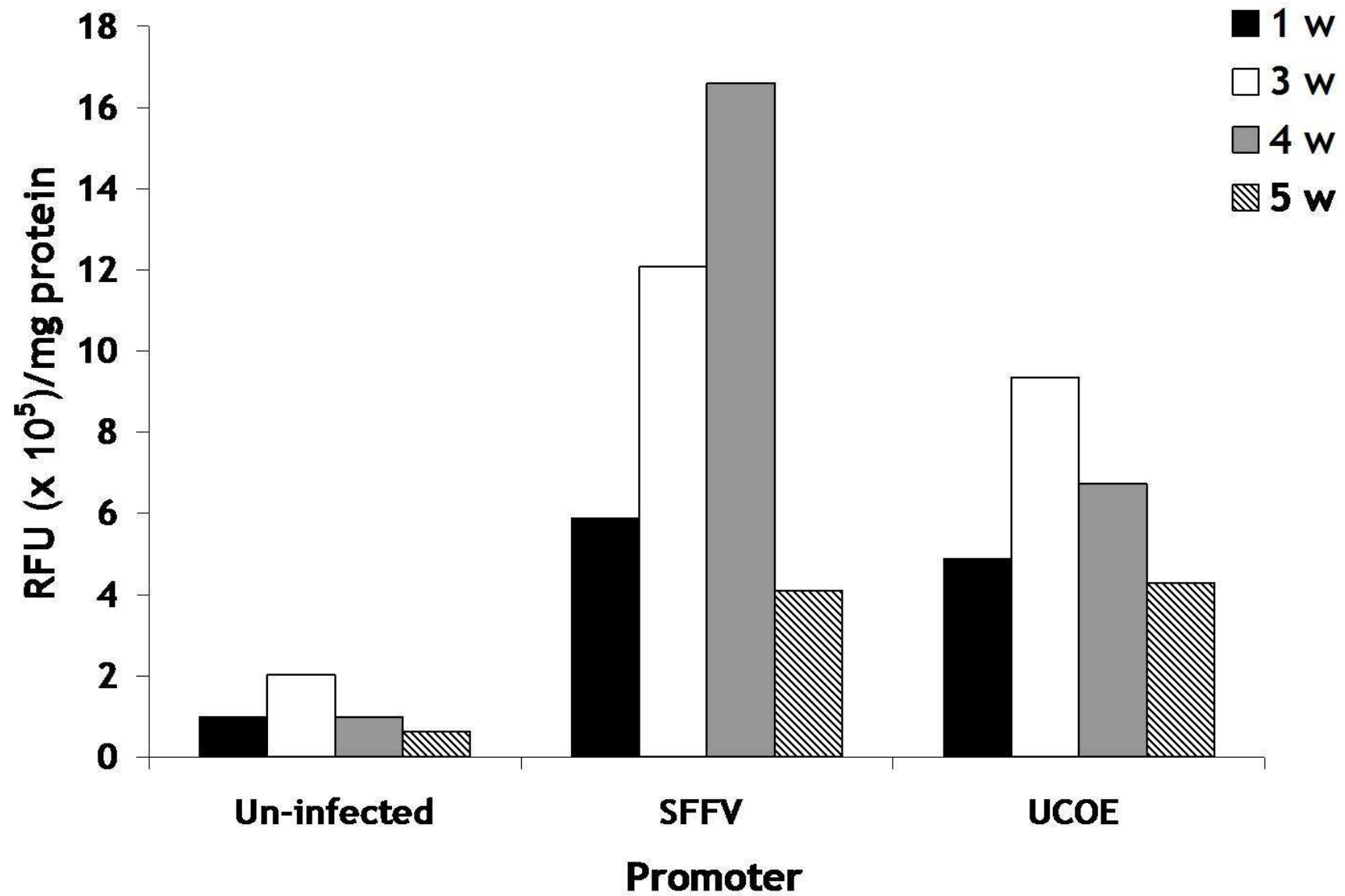


**Figure 3.4. Transgene expression efficiency and longevity in VECs mediated by lentiviral vectors under the control of the SFFV or UCOE promoter.**

Vascular endothelial cells (VECs) were seeded (cell density of  $2 \times 10^4$ /well on a 48-well plate) and infected with int-LV-SFFV or UCOE at a MOI of 25 (in the presence of 8  $\mu\text{g}/\text{ml}$  of polybrene for 1 h incubation) or un-infected. Efficiency and longevity of eGFP transgene expression were assessed at 1, 3, 4 and 5 weeks (w) post-infection by analysing eGFP expression in VEC lysates by fluorimetry [measured in relative fluorescent units (RFU)], which were then normalised to the total mg of protein (measured by a BCA assay with optical density measured at 570 nm wavelength). Mean value (for technical replicates) of patient sample repeated in triplicate and  $n=1$  (cell population/number of individual VEC preparations used). UCOE, enhancer-less ubiquitously acting chromatin opening element; SFFV, spleen focus forming virus; MOI, multiplicity of infection; int-LV, integrating lentiviral vector.

### 3.2.1.3 The SFFV promoter compared to the UCOE promoter for lentiviral-mediated transgene expression in VSMCs: efficiency and longevity

Int-LV-SFFV and int-LV-UCOE at both MOIs tested, provided efficient and long-term transgene expression from 1 w to 8 w post-infection in VSMCs. At a MOI of 50, int-LV-SFFV mediated higher eGFP expression compared to int-LV-UCOE at 1 w [ $11.1 \pm 0.8$  RFU ( $\times 10^6$ )/mg protein vs.  $3.6 \pm 0.2$  RFU ( $\times 10^6$ )/mg protein, respectively], 4 w [ $3.7 \pm 0.2$  RFU ( $\times 10^6$ )/mg protein vs.  $2.2 \pm 0.3$  RFU ( $\times 10^6$ )/mg protein, respectively], 6 w [ $2.3 \pm 0.2$  RFU ( $\times 10^6$ )/mg protein vs.  $0.3 \pm 0.1$  RFU ( $\times 10^6$ )/mg protein, respectively] and 8 w [ $0.9 \pm 0.08$  RFU ( $\times 10^6$ )/mg protein vs.  $0.2 \pm 0.08$  RFU ( $\times 10^6$ )/mg protein, respectively] post-infection (Figure 3.5).

Results from this experiment also demonstrate that transgene expression was sustained over-time mediated by int-LV-SFFV and int-LV-UCOE in VSMCs, from 1 w to 8 w post-infection. Regardless, longevity of transgene expression decreased after 1 w to 8 w post-infection with int-LV-SFFV (Figure 3.5), which was similar in profile to that observed in HeLa cells (Figure 3.2) and VECs (Figure 3.4). In contrast, int-LV-UCOE at a MOI of 50 facilitated an increase in eGFP expression from 1 w to 3 w post-infection [ $3.6 \pm 0.2$  RFU ( $\times 10^6$ )/mg protein vs.  $8.8 \pm 1.5$  RFU ( $\times 10^6$ )/mg protein, respectively], but unfortunately transgene expression was greatly down-regulated from 3 w to 4 w post-infection [ $8.8 \pm 1.5$  RFU ( $\times 10^6$ )/mg protein vs.  $2.2 \pm 0.3$  RFU ( $\times 10^6$ )/mg protein, respectively] (Figure 3.5), which was not seen in HeLa cells (Figure 3.2) and VECs (Figure 3.4). Figure 3.6 illustrated representative fluorescent images of VSMCs at 1 w post-infection, and reiterated that int-LV-SFFV and int-LV-UCOE mediated efficient transgene expression at MOIs of 10 and 50.

In summary, results in this section demonstrated that both int-LV-SFFV and int-LV-UCOE regulate long-term efficient transgene expression in HeLa cells, VECs and VSMCs. In addition, int-LV-SFFV mediated greater efficiency of transgene expression in all three cell types, compared to int-LV-UCOE. Notably, transgene expression facilitated by int-LV-SFFV declined over time in HeLa cells, VECs and VSMCs, whereas int-LV-UCOE provided stable and consistent transgene expression in HeLa cells and VECs but not in VSMCs. However, difficulties were encountered when producing high-titre preparations of int-LV-UCOE ( $3.28 \times 10^7$

iu/ml). Collectively and accordingly, the SFFV promoter was used for the remaining LV experiments in this thesis.

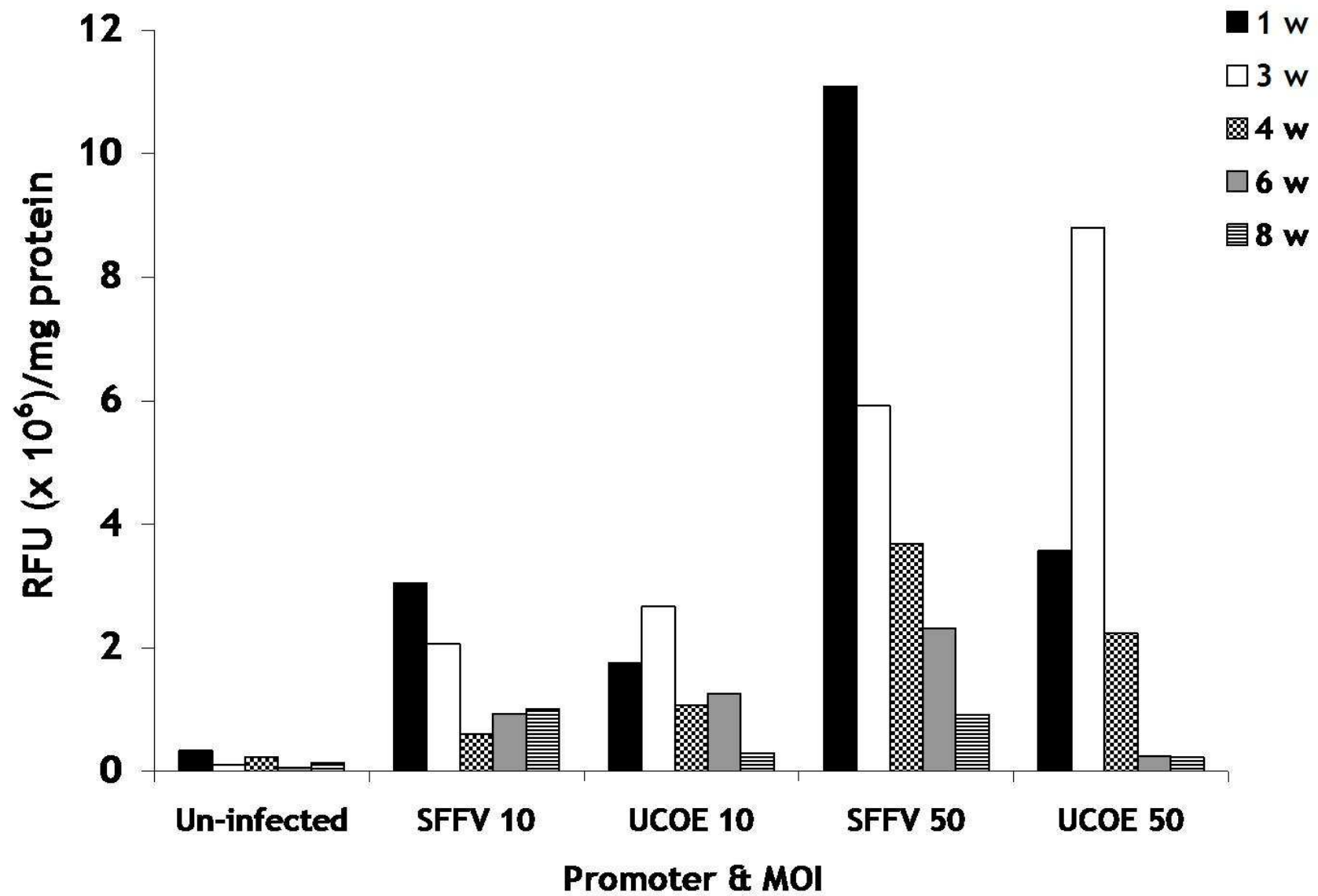


**Figure 3.5. Transgene expression efficiency and longevity mediated by SFFV or UCOE promoters in VSMCs.**

Vascular smooth muscle cells (VSMCs) were seeded (cell density of  $2.5 \times 10^4$ /well on a 48-well plate) and infected with int-LV-SFFV or UCOE (in the presence of 8  $\mu\text{g}/\text{ml}$  of polybrene for 1 h incubation) at a MOI of 10 or 50, or un-infected. Efficiency and longevity of eGFP transgene expression were assessed at 1, 3, 4, 6 and 8 weeks (w) post-infection by analysing eGFP expression in VEC lysates by fluorimetry [measured in relative fluorescent units (RFU)], which were then normalised to the total mg of protein (measured by a BCA assay with optical density measured at 570 nm wavelength). Mean value (for technical replicates) of patient sample repeated in triplicate and n=1 (cell population/number of individual VSMC preparations used). UCOE, enhancer-less ubiquitously acting chromatin opening element; SFFV, spleen focus forming virus; MOI, multiplicity of infection; int-LV, integrating lentiviral vector.

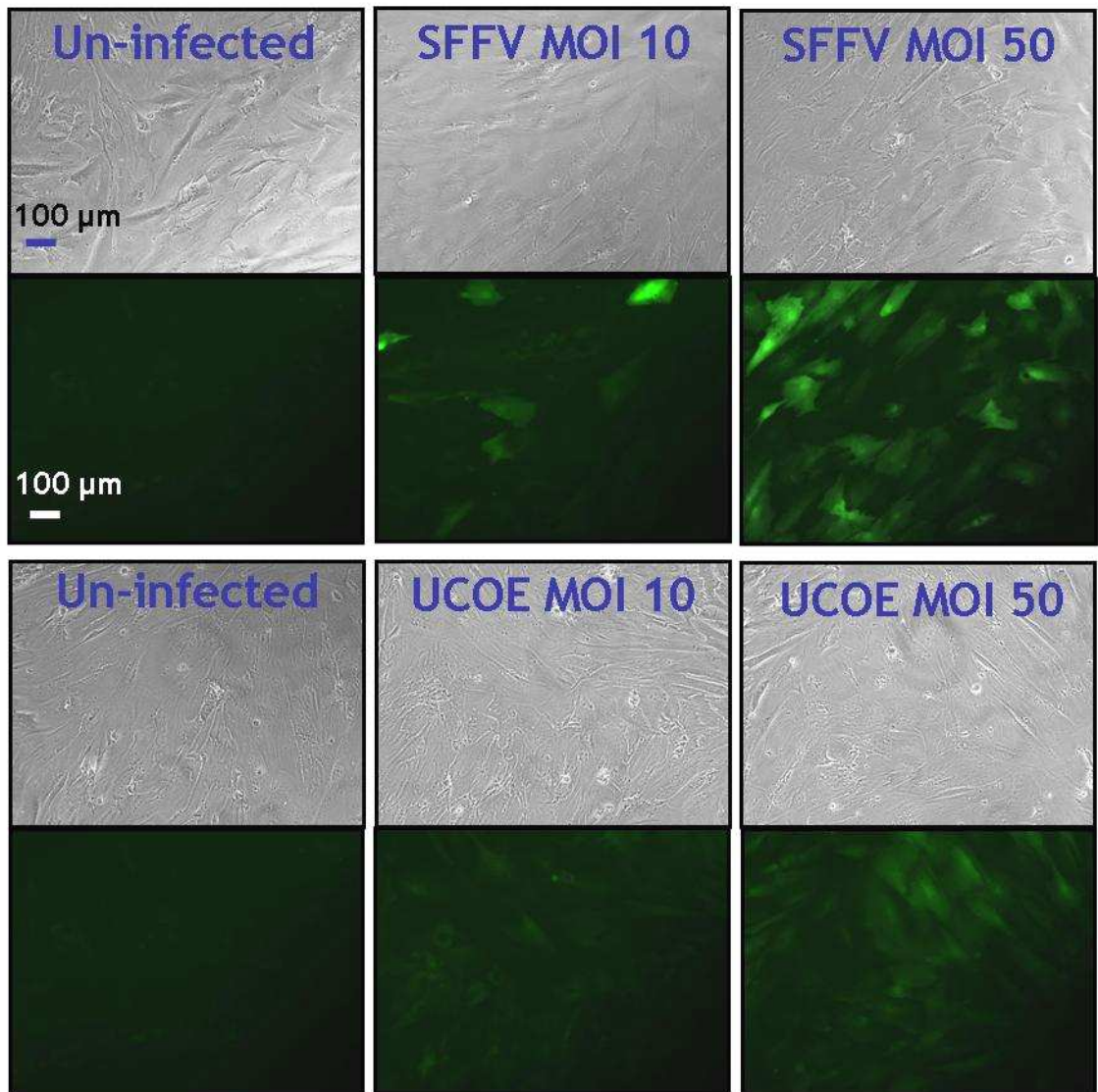


**Figure 3.6. Representative micrographs of the efficiency of eGFP transgene expression in VSMCs mediated by lentiviral vectors under the control of the SFFV or UCOE promoter.** Fluorescent images of eGFP expression in VSMCs infected with int-LV-SFFV or int-LV-UCOE at a MOI of 10 or 50, or un-infected, at 1 w post-infection. 100 µm scale bar applicable to all panels (magnification x 100). Representative of n=1 (cell population/number of individual VSMC preparations used) in triplicate. UCOE, enhancer-less ubiquitously acting chromatin opening element; SFFV, spleen focus forming virus; MOI, multiplicity of infection; int-LV, integrating lentiviral vector; VSMC, vascular smooth muscle cell.

### 3.2.2 Pseudotyping lentiviral vectors

Next, pseudotyped int-LVs were evaluated for transduction efficiency in vascular cells *in vitro* and these included: rabies, RRV, EbolaZ, GP64, MLV-A, MLV-E and HNTV. All envelope plasmids were obtained from Adrian Thrasher's lab (UCL, UK), and have been described elsewhere (Lodge et al., 1998, Demaison et al., 2002, Kang et al., 2002, Sinn et al., 2003, Sinn et al., 2005a, Koch et al., 2006, Qian et al., 2006, Buckley et al., 2008, Rahim et al., 2009). Each pseudotyped-int-LV-eGFP was generated according to the LV production protocol, as described in section 2.9.

#### 3.2.2.1 Pseudotyped-lentiviral transduction efficiency on rat neuronal cells

Based on previous studies which demonstrated that rabies pseudotyped LVs mediated efficient transduction and sustained transgene expression within neuronal cells *in vivo* (Mazarakis et al., 2001, Kato et al., 2007, Rahim et al., 2009); we evaluated the transduction efficiency of rabies pseudotyped int-LVs in comparison to VSV-g pseudotyped int-LVs transduced onto a rat cortical neuronal cell line (B50s), as a positive control for gene transfer. For this transduction efficiency assessment, rabies and VSV-g pseudotyped int-LV visual titres of  $1.08 \times 10^8$  iu/ml and  $4.29 \times 10^8$  iu/ml were used, respectively.

B50s were transduced with rabies or VSV-g pseudotyped int-LVs expressing eGFP at a MOI of 50, or un-transduced. Next, for transduction efficiency and longevity of transgene expression, B50 lysates were assessed for eGFP expression (normalised to mg protein) at 3 d, 6 d and 9 d post-transduction of continuous culture as described before. Here, results demonstrated that LVs pseudotyped with rabies were efficient in transducing B50s (Figure 3.7 and Figure 3.8). Notably, results indicated that VSV-g pseudotyped int-LV mediated an increase eGFP transgene expression, with a greater efficiency and longevity of eGFP expression in B50s at a MOI of 50 in contrast to int-LV pseudotyped with rabies (Figure 3.7) at 3 d [ $10.18 \pm 1.15$  RFU ( $\times 10^4$ )/mg protein vs.  $4.09 \pm 0.09$  RFU ( $\times 10^4$ )/mg protein, respectively], 6 d [ $9.34 \pm 0.58$  RFU ( $\times 10^4$ )/mg protein vs.  $4.33 \pm 0.33$  RFU ( $\times 10^4$ )/mg protein, respectively] and 9 d post-transduction [ $8.39 \pm 0.61$  RFU ( $\times 10^4$ )/mg protein vs.  $4.50 \pm 0.38$  RFU ( $\times 10^4$ )/mg protein,

respectively] (Figure 3.7). Representative fluorescent micrographs also illustrated that VSV-g pseudotyped int-LV transduction on B50s at a MOI of 50 mediated efficient eGFP expression at 9 d post-infection, compared to rabies pseudotyped int-LVs (Figure 3.8).

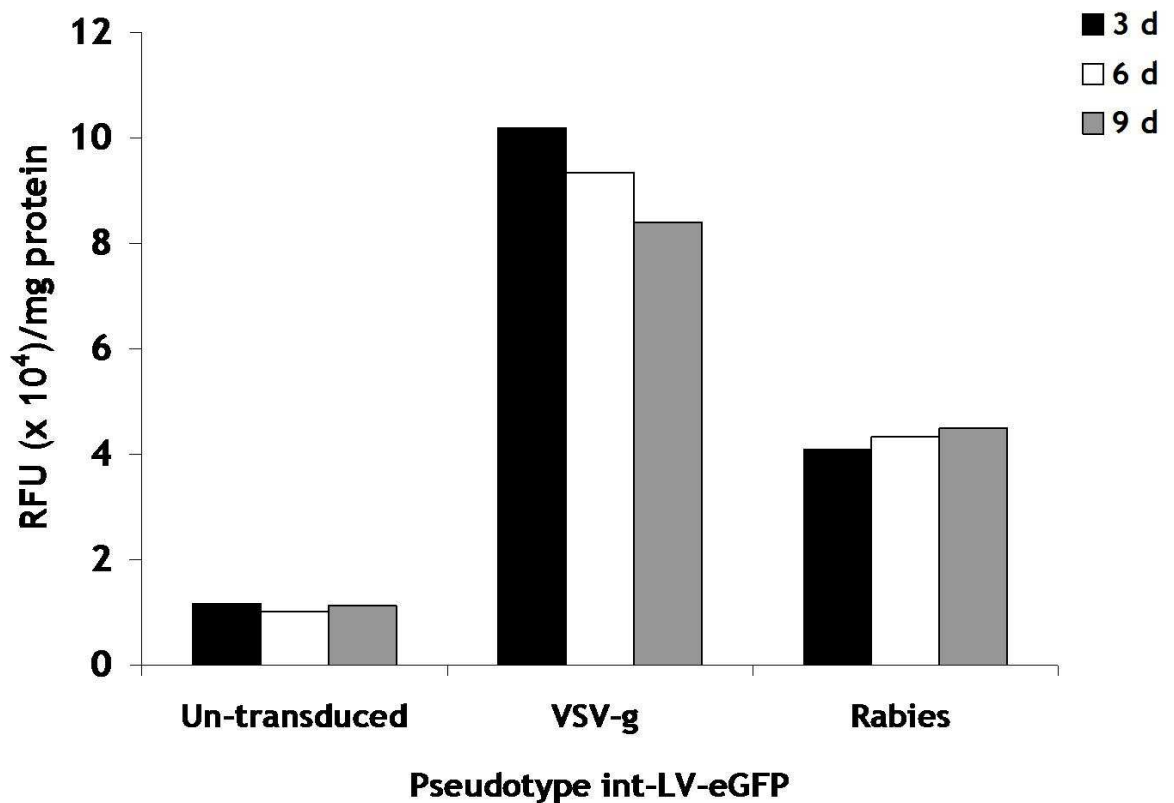


**Figure 3.7. Transduction efficiency of pseudotyped int-LVs on B50s.**

B50s (a rat cortical neuronal cell line) were seeded (cell density of  $3 \times 10^3/\text{well}$  on a 24-well plate) and transduced with either VSV-g (vesicular stomatitis virus- glycoprotein) or rabies pseudotyped-int-LV at a multiplicity of infection (MOI) of 50, or un-transduced (in the presence of  $8 \mu\text{g}/\text{ml}$  of polybrene for an 18 h incubation). Transduction efficiency and longevity of transgene expression mediated by each pseudotype int-LV were assessed 3, 6 & 9 days (d) post-transduction by analysing eGFP expression in VEC lysates by fluorimetry [measured in relative fluorescent units (RFU)], which were then normalised to the total mg of protein (measured by a BCA assay with optical density measured at 570 nm wavelength). Mean value (for technical replicates), repeated in triplicate, and  $n=1$  (cell line population used). Int-LV, integrative lentiviral vector.

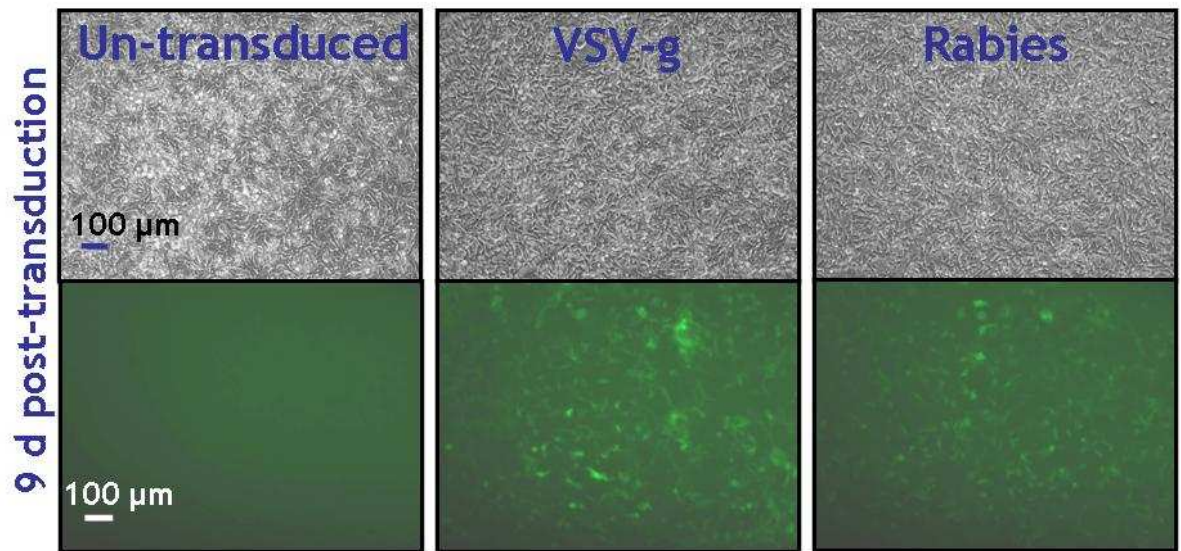


**Figure 3.8.** Representative micrographs of the transduction efficiency and longevity of transgene expression mediated by pseudotyped int-LVs in B50s. Fluorescent micrographs of eGFP expression in B50s (a rat cortical neuronal cell line) transduced with either VSV-g (vesicular stomatitis virus- glycoprotein) or rabies pseudotyped int-LVs at a multiplicity of infection (MOI) of 50, or un-transduced, at 9 days (d) post-transduction. 100 μm scale bar applicable to all panels (magnification x 100). Representative of n=1 (cell line population used) in triplicate. Int-LV, integrating lentiviral vector.

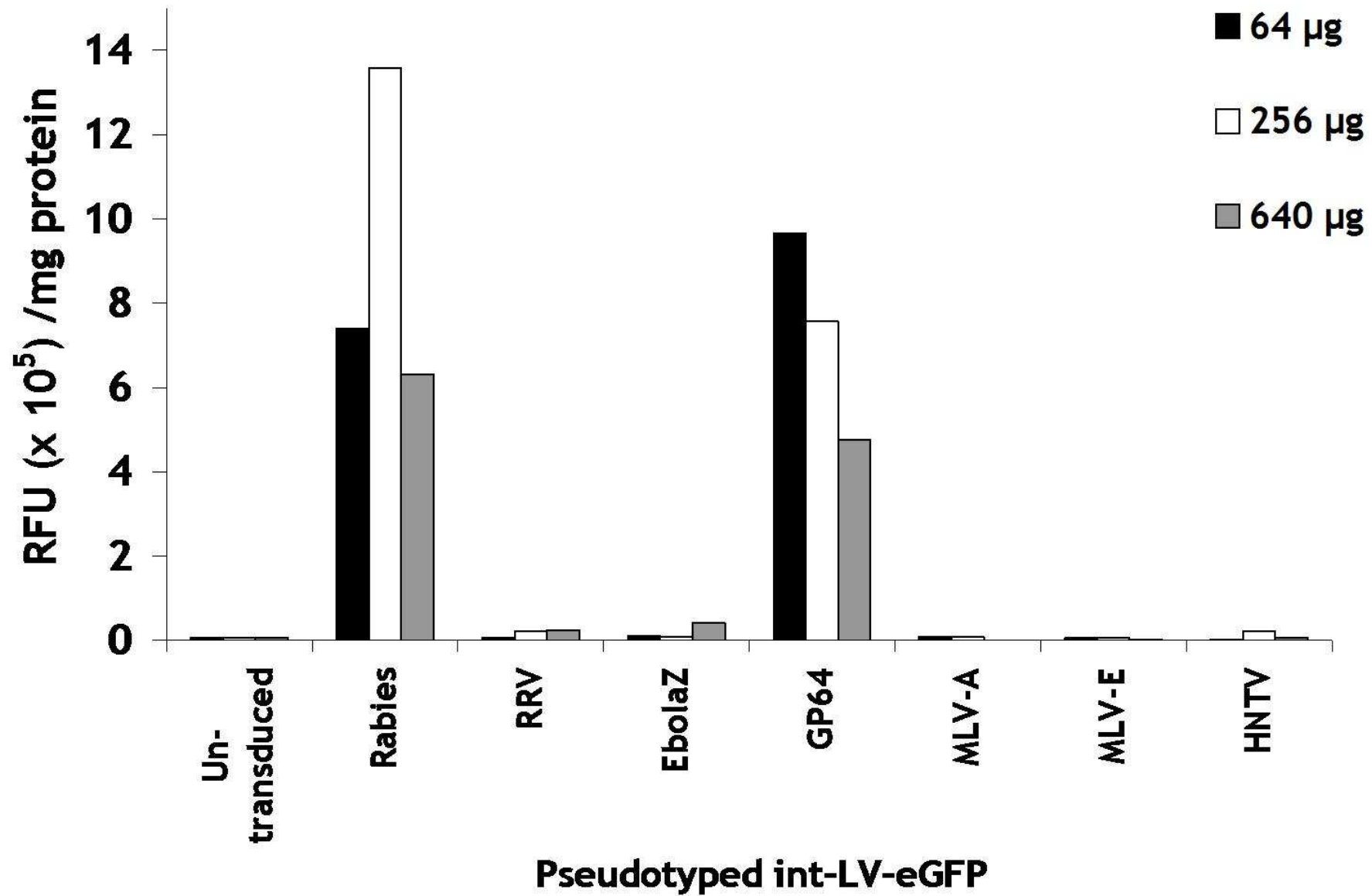
### 3.2.2.2 Pseudotyped-lentiviral transduction efficiency on human vascular cells

The transduction efficiency of each pseudotyped int-LV was assessed in primary human VECs *in vitro*. Titres were measured according to their total protein contents using the microBCA assay (as previously described in section 2.12.1), and protein concentration titres were determined and recorded as described in Table 3.1.

Envelopes for pseudotyping LVs	Protein concentration $\mu\text{g/ml}$
Rabies	3588.04
RRV	3555.38
EbolaZ	4607.56
GP64	3045.47
MLV-A	3634.7
MLV-E	3262.31
HNTV	3392.04

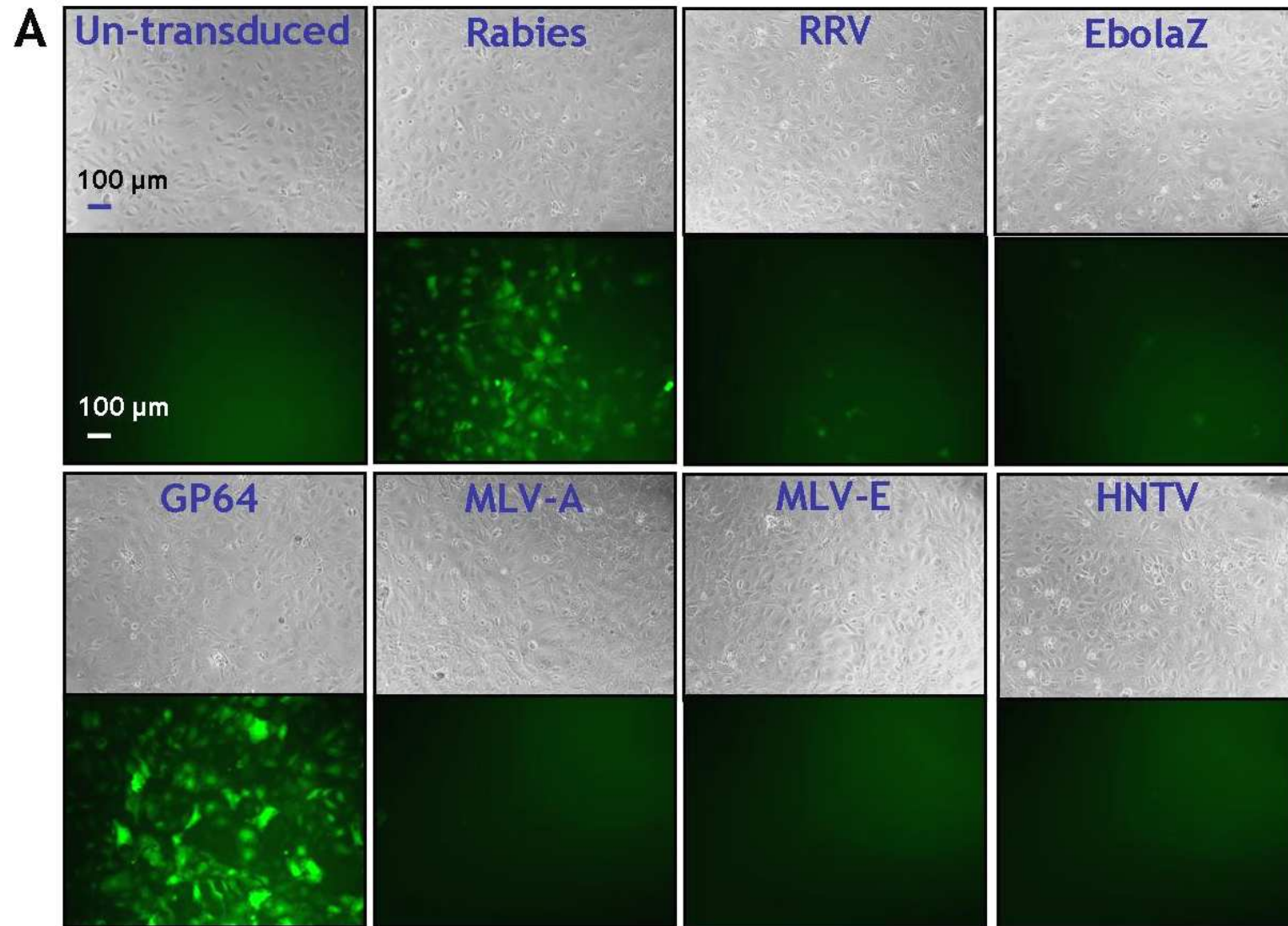
Table 3.1. Pseudotyped LV protein concentration titres.

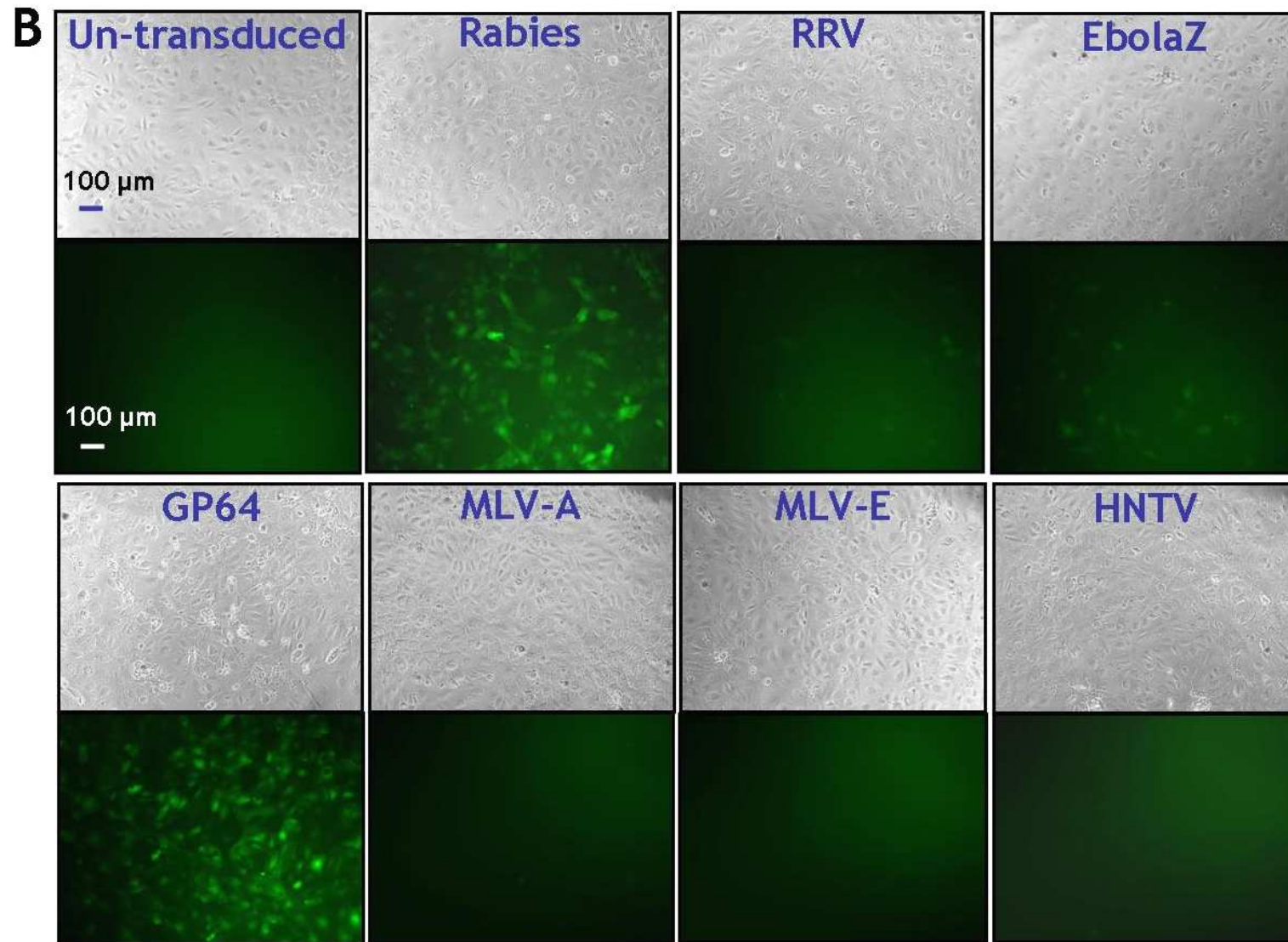
Each pseudotyped int-LV-eGFP was transduced on VECs at 64  $\mu\text{g}$ , 256  $\mu\text{g}$  or 640  $\mu\text{g}$  of LV protein, or un-transduced, and after 5 days post-transduction lysates were assessed for eGFP expression (normalised to mg of protein) to determine transduction efficiency. EGFP expression results and fluorescent images (at 4 d post-infection) indicated that efficient transduction was achieved by GP64 and rabies pseudotyped LVs on VECs (Figure 3.9 and Figure 3.10 A, B & C). Moreover, Figure 3.9 and Figure 3.10 B & C also indicate that EbolaZ pseudotyped LVs have the ability to transduce VECs. However, RRV, MLV-A, MLV-E and HNTV pseudotyped int-LVs did not mediate efficient transduction in VECs (Figure 3.9 and Figure 3.10), the reason being unclear. It was difficult to produce each pseudotyped LV to a high-titre stock, and thereby the evaluation of these pseudotyped LVs for their transduction efficiency in VSMCs was suspended in this study. VSV-g was deemed a suitable envelope and was used in all future LV experiments within the rest of this thesis.



**Figure 3.9. Transduction efficiency of pseudotyped int-LVs on VECs.**

VECs were seeded (cell density of  $3 \times 10^4$ /well on a 48-well plate) and transduced with a pseudotyped-int-LV (in the presence of 8  $\mu\text{g/ml}$  of polybrene for 18 h incubation) at 64  $\mu\text{g}$ , 256  $\mu\text{g}$  or 640  $\mu\text{g}$  of LV protein contents, or un-transduced. Transduction efficiency of each pseudotype int-LV was assessed 5 d post-transduction by analysing eGFP expression in VEC lysates by fluorimetry [measured in relative fluorescent units (RFU)], which was then normalised to the total mg of protein (measured by a BCA assay with optical density measured at 570 nm wavelength). Mean value (for technical replicates) of patient sample repeated in duplicate and  $n=1$  (cell population/number of individual VEC preparations used). VEC, vascular endothelial cell; Int-LV, integrating lentiviral vector; RRV, Ross River virus; EbolaZ, Ebola Zaire; GP64, baculovirus glycoprotein 64; MLV-A, murine leukaemia virus-amphotropic; MLV-E, murine leukaemia virus-ecotropic; HNTV, Hantaan virus.





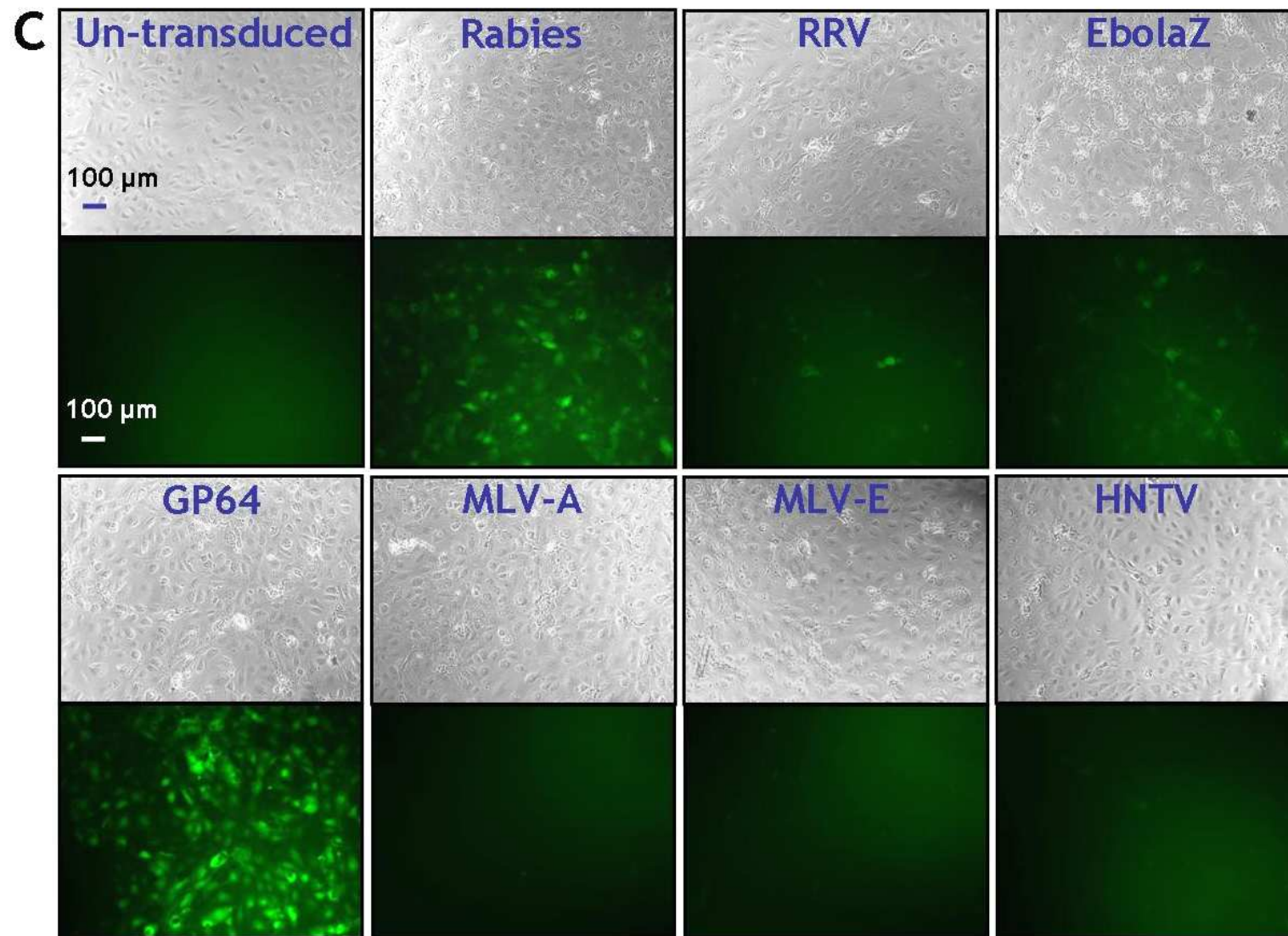


**Figure 3.10. Representative micrographs of the transduction efficiency of pseudotyped int-LVs on VECs.**

Fluorescent micrographs of eGFP expression in VECs transduced with pseudotyped-int-LVs at (A) 64  $\mu\text{g}$  (B) 256  $\mu\text{g}$  or (C) 640  $\mu\text{g}$  of LV protein, or un-transduced, at 4 days post-transduction. 100  $\mu\text{m}$  scale bar applicable to all panels (magnification x 100). Representative of n=1 (cell population/number of individual VEC preparations used) in duplicate. VEC, vascular endothelial cell; RRV, Ross River virus; EbolaZ, Ebola Zaire; GP64, baculovirus glycoprotein 64; MLV-A, murine leukaemia virus-amphotropic; MLV-E, murine leukaemia virus-ecotropic; HNTV, Hantaan virus; int-LV, integrating lentiviral vector.

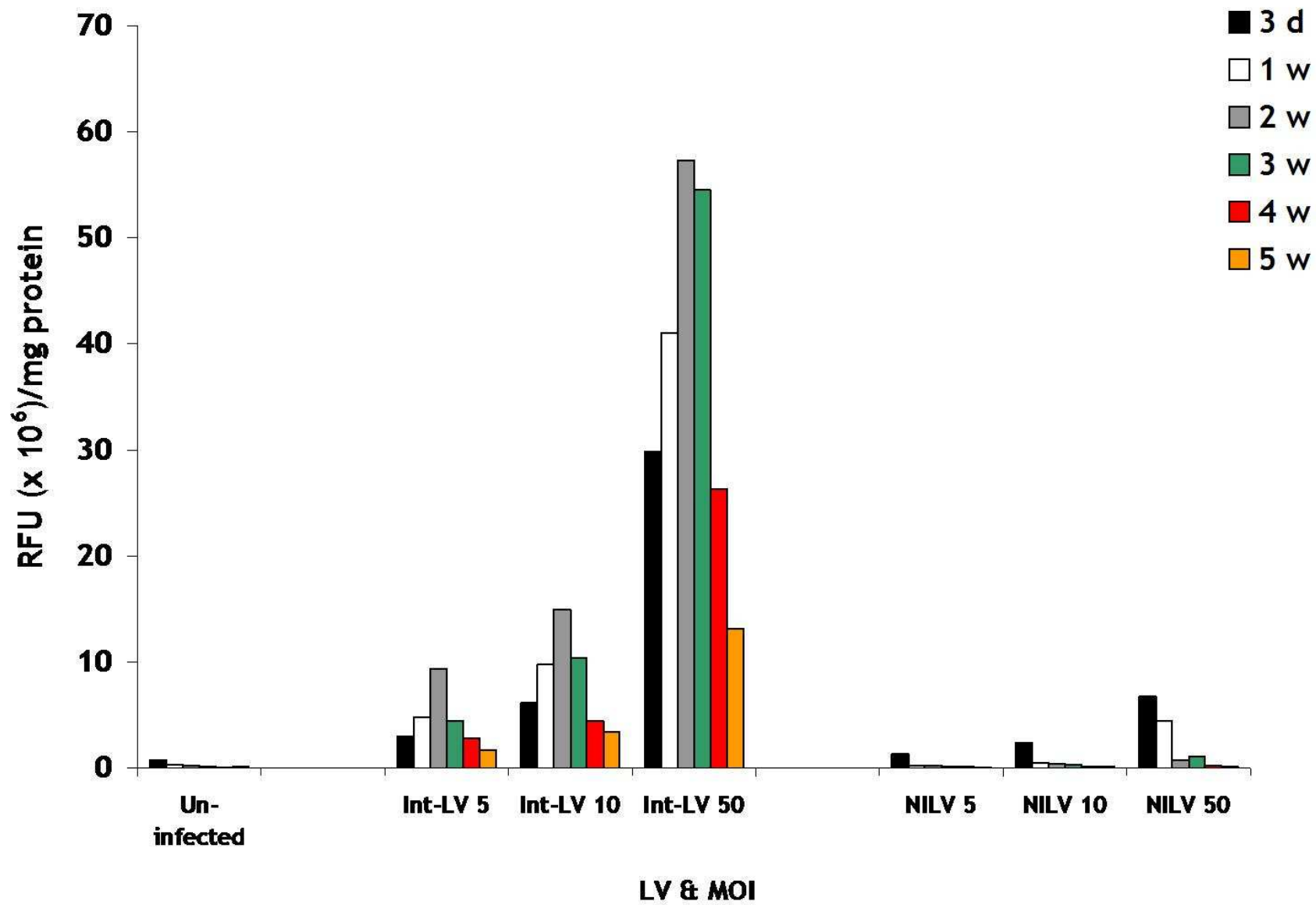
### **3.2.3 Non-integrating lentiviral vectors for gene transfer in vascular cells**

Efficiency and longevity of NILV-mediated eGFP expression in vascular cells were evaluated in comparison to its integrating counterparts. The integration-deficient plasmid (pCMV delta R8.74 D64V mutant integrase) was obtained from Adrian Thrasher's lab (UCL, UK) and has been described previously (Yanez-Munoz et al., 2006, Apolonia et al., 2007) (also see Figure 2.2, Table 2.2 and Table 2.3 for more details on plasmids). For the purpose of this part of the optimisation study, NILV expressing eGFP (NILV-eGFP) and int-LV expressing eGFP (int-LV-eGFP) were produced. Visual eGFP titres of  $1.58 \times 10^8$  iu/ml for NILV-eGFP and  $4.48 \times 10^8$  iu/ml for int-LV-eGFP were used to transduce onto VECs at MOIs of 5, 10 and 50. TaqMan qPCR titres of NILV-eGFP in a range from  $3.36 \times 10^7$  to  $1 \times 10^8$  iu/ml (3 batches) and int-LV-eGFP in a range from  $1 \times 10^8$  to  $1.96 \times 10^9$  iu/ml (3 batches), were used to infect VSMCs at increasing MOIs of 5, 10, 25 and 50. Expression of eGFP in lysates of these vascular cells at specific time points of continuous culture were quantified for eGFP expression, as described before.

#### **3.2.3.1 Non-integrating lentiviral-mediated gene delivery in vascular endothelial cells**

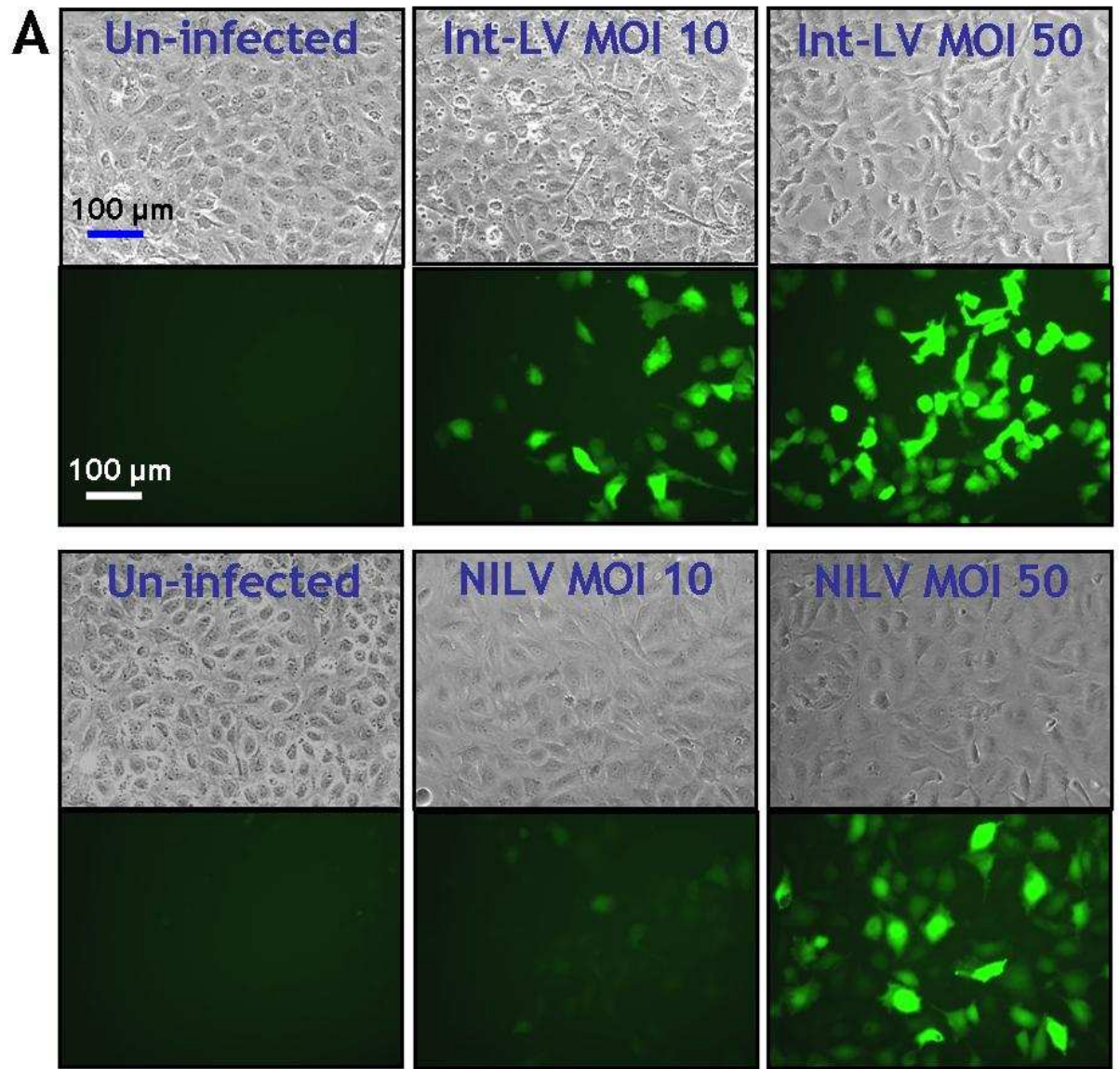
NILV-eGFP mediated efficient eGFP expression in VECs (Figure 3.11 and Figure 3.12). However, int-LV-eGFP induced higher eGFP expression in VECs, compared to NILV-eGFP at matched MOIs of 5, 10 and 50 at 3 d, 1 w, 2 w, 3 w, 4 w and 5 w post-infection (Figure 3.11). For example at a MOI of 50, eGFP expression was greater in VECs mediated by int-LVs compared to NILV-eGFP, at post-infection time points of 3 d [ $29.9 \pm 5.8$  RFU ( $\times 10^6$ )/mg protein vs.  $6.8 \pm 1.7$  RFU ( $\times 10^6$ )/mg protein], 1 w [ $41.1 \pm 4.6$  RFU ( $\times 10^6$ )/mg protein vs.  $4.5 \pm 0.6$  RFU ( $\times 10^6$ )/mg protein, respectively], 2 w [ $57.3 \pm 2.6$  RFU ( $\times 10^6$ )/mg protein vs.  $0.7 \pm 0.1$  RFU ( $\times 10^6$ )/mg protein, respectively], 3 w [ $54.5 \pm 13.1$  RFU ( $\times 10^6$ )/mg protein vs.  $1.1 \pm 0.4$  RFU ( $\times 10^6$ )/mg protein, respectively], 4 w [ $26.3 \pm 1.5$  RFU ( $\times 10^6$ )/mg protein vs.  $0.23 \pm 0.03$  RFU ( $\times 10^6$ )/mg protein, respectively] and 5 w [ $13.2 \pm 1.1$  RFU ( $\times 10^6$ )/mg protein vs.  $0.11 \pm 0.1$  RFU ( $\times 10^6$ )/mg protein, respectively] (Figure 3.11).

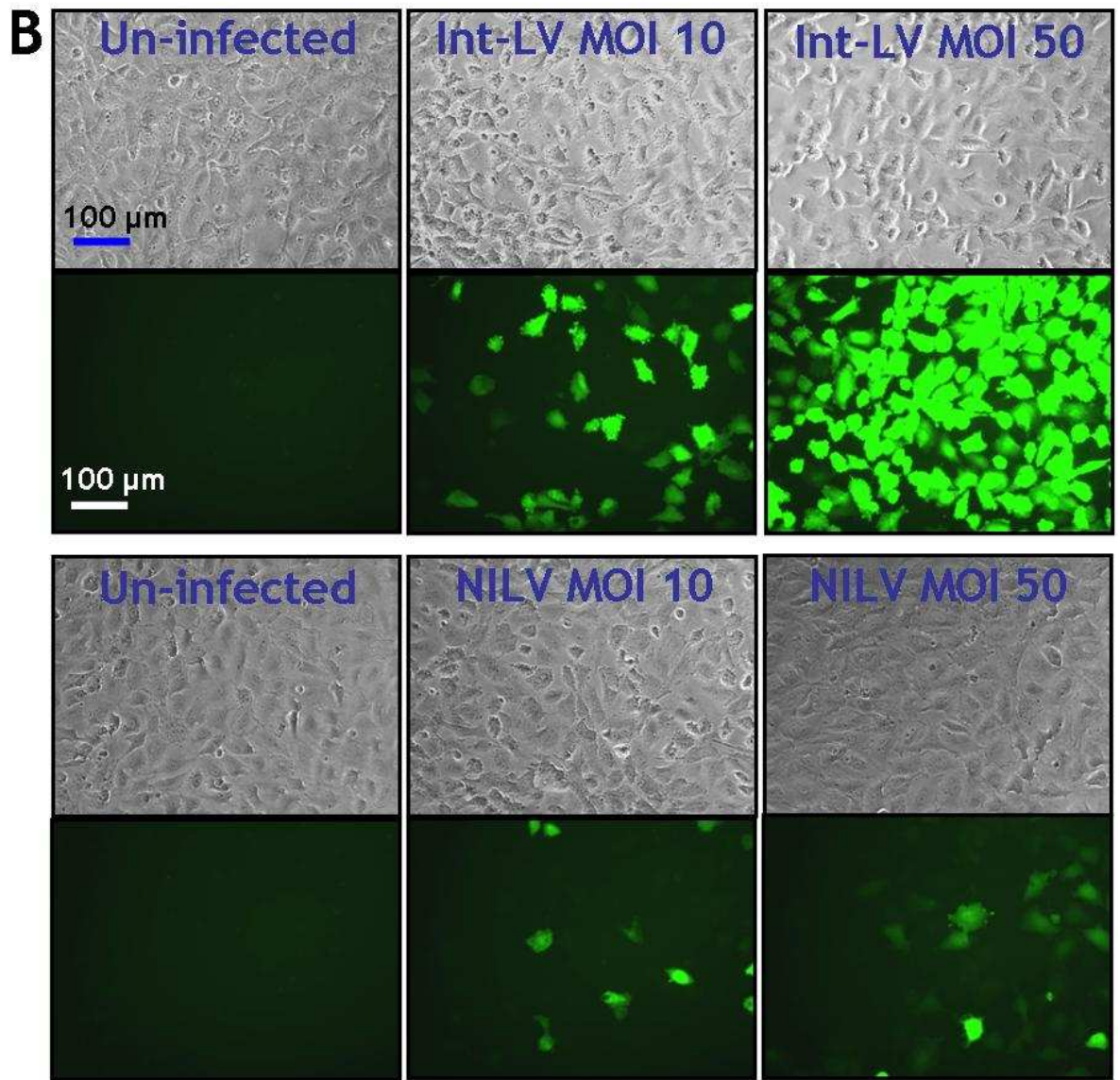
In terms of longevity, data indicated that int-LV-eGFP gene delivery efficiently mediated longevity of transgene expression in VECs at all MOIs from 3 d to 5 w post-infection (Figure 3.11). It was observed that int-LV-eGFP at a MOI of 50 induced long-term transgene expression; however eGFP expression decreased from 3 w to 5 w post-infection, with a greater decrease between 3 w to 4 w post-infection [ $54.5 \pm 13.1$  RFU ( $\times 10^6$ )/mg protein vs.  $26.3 \pm 1.5$  RFU ( $\times 10^6$ )/mg protein, respectively] (Figure 3.11). Importantly, at a MOI of 50, NILV-mediated gene transfer induced sustained transgene expression of eGFP in VECs from 3 d to 3 w post-infection and notably at 3 d to 1 w post-infection (Figure 3.11). However, eGFP expression mediated by NILVs in VECs was greatly down-regulated from 1 w to 2 w post-infection [ $4.5 \pm 0.6$  RFU ( $\times 10^6$ )/mg protein vs.  $0.7 \pm 0.07$  RFU ( $\times 10^6$ )/mg protein, respectively] (Figure 3.11). In relation to this eGFP transgene expression profile, efficient eGFP expression mediated by NILVs was reduced from 3 d to 1 w post-infection at MOIs of 5 [ $1.37 \pm 0.24$  RFU ( $\times 10^6$ )/mg protein vs.  $0.25 \pm 0.054$  RFU ( $\times 10^6$ )/mg protein, respectively] and 10 [ $2.43 \pm 0.028$  RFU ( $\times 10^6$ )/mg protein vs.  $0.45 \pm 0.036$  RFU ( $\times 10^6$ )/mg protein, respectively] (Figure 3.11). Representative micrographs in Figure 3.12 A, B and C illustrated efficient eGFP expression in VECs mediated by NILVs at 3 d, 1 w and 3 w post-infection at MOIs of 10 and 50 (Figure 3.12).



**Figure 3.11. Efficiency and longevity of eGFP expression in VECs mediated by NILVs.**

VECs (vascular endothelial cells) were seeded (at a cell density of  $2 \times 10^4$ /well on a 48-well plate) and infected with int-LV-eGFP or NILV-eGFP (in the presence of  $8 \mu\text{g/ml}$  of polybrene for 18 h incubation) at MOIs of 5, 10 or 50 or un-infected. Efficiency and longevity of eGFP transgene expression were assessed at 3 days (d), 1, 2, 3, 4 and 5 weeks (w) post-infection by analysing eGFP expression in VEC lysates by fluorimetry [measured in relative fluorescent units (RFU)], which were then normalised to the total mg of protein (measured by a BCA assay with optical density measured at 570 nm wavelength). Mean value (for technical replicates) of patient sample repeated in triplicate and  $n=1$  (cell population/number of individual VEC preparations used). MOI, multiplicity of infection; LV, lentiviral vectors; int-LV, integrating lentiviral vector; NILV, non-integrating lentiviral vector.





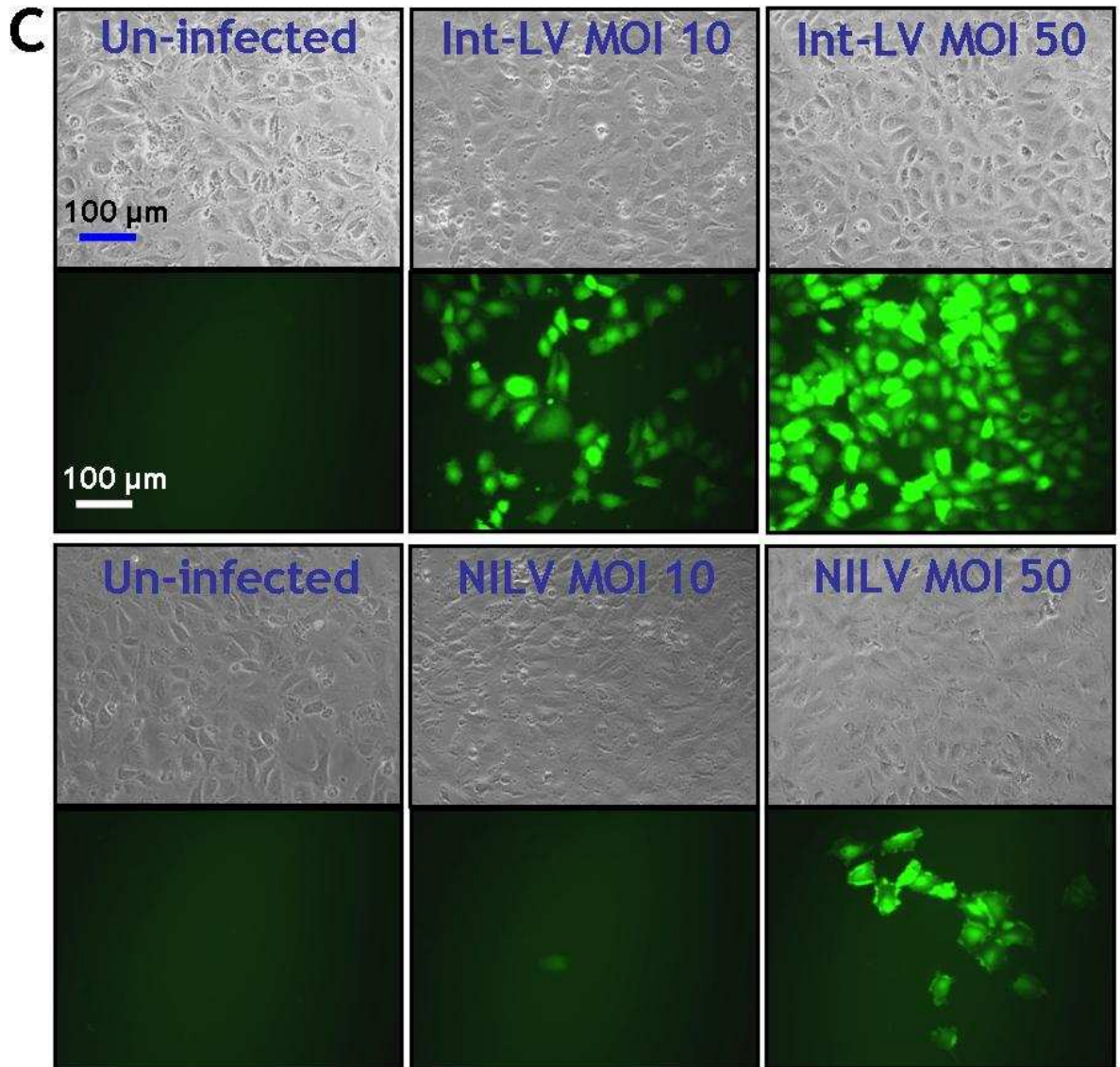


**Figure 3.12. Representative micrographs of the efficiency and long-term eGFP transgene expression in VECs mediated by NILVs.**

Fluorescent images of eGFP expression in VECs (vascular endothelial cells) infected with int-LV-eGFP or NILVs-eGFP at MOIs of 10 and 50 or un-infected, at (A) 3 days, (B) 1 week (w) and (C) 3 w post-infection. 100 μm scale bar applicable to all panels (magnification x 200). Representative of n=1 (cell population/number of individual VEC preparations used) in triplicate. VEC, vascular endothelial cell; MOI, multiplicity of infection; int-LV, integrating lentiviral vector; NILV, non-integrating lentiviral vector.

### 3.2.3.2 Non-integrating lentiviral-mediated gene transfer in vascular smooth muscle cells

Data indicated that NILV-mediated gene transfer of eGFP facilitated efficient and sustained transgene expression at MOIs of 5, 10, 25 and 50, from 3 d to 14 d post-infection in VSMCs (Figure 3.13 and Figure 3.14). However, int-LV-eGFP mediated significantly enhanced eGFP transfer compared to NILV-eGFP in VSMCs (Figure 3.13). For example at a MOI of 50, eGFP expression was significantly induced in VSMCs mediated by int-LVs in contrast to NILV-eGFP, at post-infection time points of 3 d [ $5.60 \pm 0.36$  RFU ( $\times 10^6$ )/mg protein vs.  $2.03 \pm 0.32$  RFU ( $\times 10^6$ )/mg protein, respectively,  $p < 0.001$ ], 7 d [ $7.80 \pm 1.80$  RFU ( $\times 10^6$ )/mg protein vs.  $1.10 \pm 0.40$  RFU ( $\times 10^6$ )/mg protein, respectively,  $p < 0.01$ ] and 14 d [ $3.0 \pm 0.14$  RFU ( $\times 10^6$ )/mg protein vs.  $0.5 \pm 0.042$  RFU ( $\times 10^6$ )/mg protein, respectively,  $p < 0.001$ ] (Figure 3.13). Notably, NILV-eGFP induced efficient eGFP expression in VSMCs, in parallel to int-LV-eGFP (Figure 3.13).

Results demonstrated that int-LV-eGFP gene transfer mediated efficient longevity of transgene expression in VSMCs at all MOIs from 3 d to 14 d post-infection (Figure 3.13). For example, at a MOI of 25 it was observed that int-LV-eGFP facilitated a significant increase in eGFP expression in VSMCs from 3 d to 7 d post-infection [ $3.2 \pm 0.17$  RFU ( $\times 10^6$ )/mg protein vs.  $6.6 \pm 0.83$  RFU ( $\times 10^6$ )/mg protein, respectively,  $p < 0.001$ ]; however transgene expression was significantly down-regulated from 7 d to 14 d post-infection [ $6.6 \pm 0.83$  RFU ( $\times 10^6$ )/mg protein vs.  $2.8 \pm 0.07$  RFU ( $\times 10^6$ )/mg protein, respectively,  $p < 0.001$ ] (Figure 3.13). Moreover, at a MOI of 50 it was observed that int-LV-eGFP induced long-term transgene expression in VSMCs; however eGFP expression was significantly down-regulated from 7 d to 14 d post-infection [ $7.75 \pm 1.81$  RFU ( $\times 10^6$ )/mg protein vs.  $2.95 \pm 0.14$  RFU ( $\times 10^6$ )/mg protein, respectively,  $p < 0.05$ ] (Figure 3.13). Importantly, NILV-mediated gene transfer induced efficient transgene expression of eGFP in parallel to int-LV-eGFP, at all MOIs in VSMCs from 3 d to 14 d post-infection (Figure 3.13). However at each MOI, these transgene expression profiles did decrease overtime, which was significantly indicated from 3 d to 7 d post-infection at MOIs of 5 [ $0.51 \pm 0.058$  RFU ( $\times 10^6$ )/mg protein vs.  $0.174 \pm 0.006$  RFU ( $\times 10^6$ )/mg protein, respectively,  $p < 0.001$ ], 10 [ $0.87 \pm 0.07$  RFU ( $\times 10^6$ )/mg protein vs.  $0.21 \pm 0.07$  RFU ( $\times 10^6$ )/mg protein, respectively,  $p < 0.001$ ]

and 25 [ $1.67 \pm 0.18$  RFU ( $\times 10^6$ )/mg protein vs.  $0.27 \pm 0.03$  RFU ( $\times 10^6$ )/mg protein, respectively,  $p < 0.001$ ] (Figure 3.13). In addition, NILV-eGFP at a MOI of 50 from 3 d to 14 d post-infection mediated a similar down-regulation profile for the longevity of transgene expression in VSMCs; nevertheless this was not significant (Figure 3.13). Representative fluorescent micrographs at 3 d and 7 d post-infection at MOIs of 25 and 50, demonstrated that efficient eGFP expression in VSMCs facilitated by NILVs was achievable (Figure 3.14).

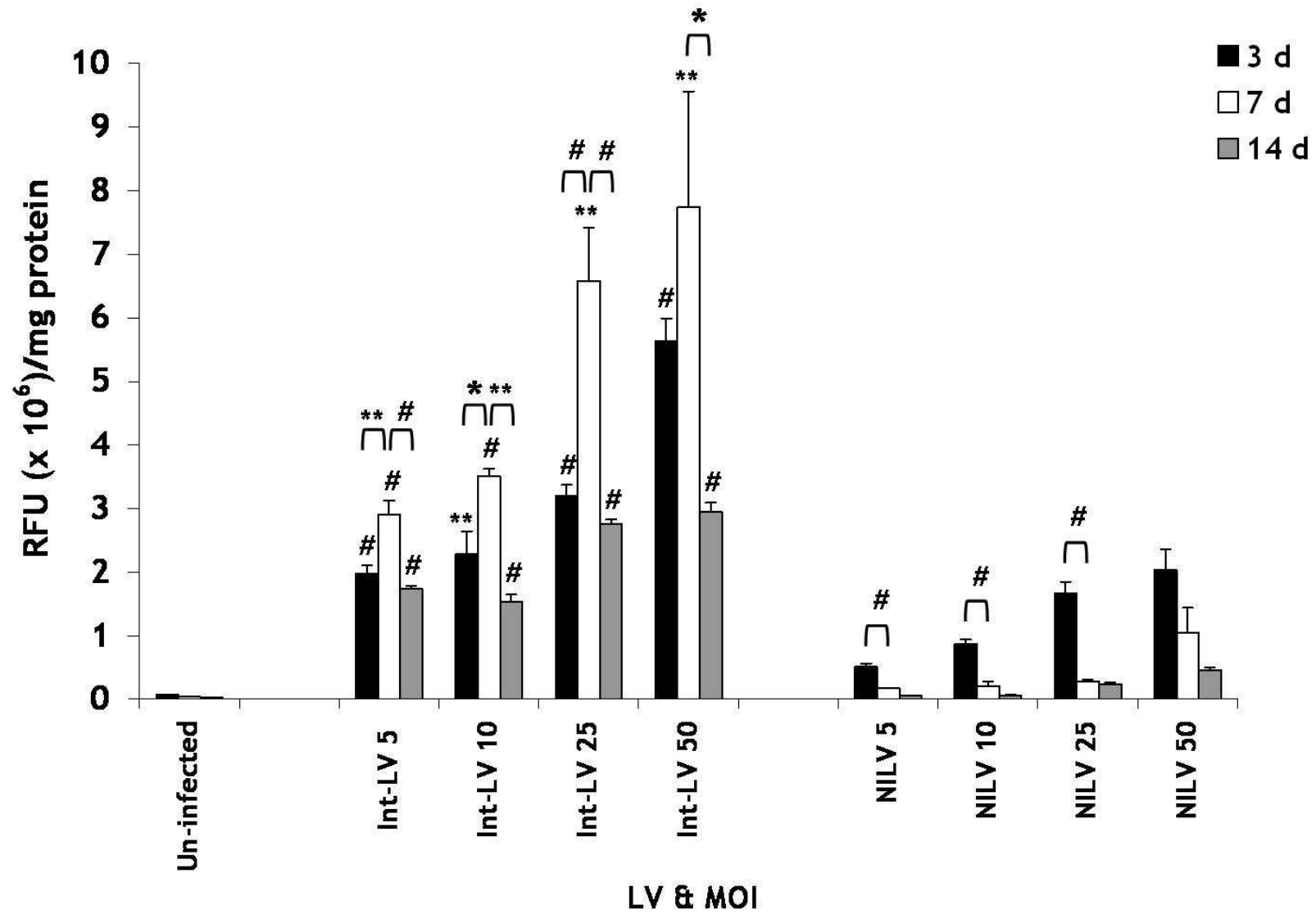


**Figure 3.13. Efficiency and longevity of eGFP expression in VSMCs mediated by NILVs.**

VSMCs (vascular smooth muscle cells) were seeded (at a cell density of  $1 \times 10^4$ /well on a 48-well plate) and infected with int-LV-eGFP or NILV-eGFP (in the presence of 8  $\mu\text{g/ml}$  of polybrene for 18 h incubation) at MOIs of 5, 10, 25 or 50 or un-infected. Efficiency and longevity of eGFP transgene expression were assessed at 3 days (d), 7 d and 14 d post-infection by analysing eGFP expression in VSMC lysates by fluorimetry [measured in relative fluorescent units (RFU)], which were then normalised to the total mg of protein (measured by a BCA assay with optical density measured at 570 nm wavelength). Mean value  $\pm$  S.E.M of patient sample repeated in triplicate. Three independent experiments performed [n=3 (representative of each other), cell population/number of individual VSMC preparations used]. In terms of efficiency, at each matched MOI and time points: \*\* indicates  $p < 0.01$  (int-LV) vs. NILV and # indicates  $p < 0.001$  (int-LV) vs. NILV. Statistical analysis was carried out using a two-tailed unpaired Student's t-test. In terms of longevity: \* indicates  $p < 0.05$  with int-LV at 3 d to 7 d or 7 d to 14 d post-infection, \*\* indicates  $p < 0.01$  with int-LV at 3 d to 7 d or 7 d to 14 d and # indicates  $p < 0.001$  with int-LV at 3 d to 7 d or 7 d to 14 d, or NILV at 3 d to 7 d post-infection. Statistical analysis carried out by one-way ANOVA for Bonferroni's post-hoc analysis. MOI, multiplicity of infection; LV, lentiviral vectors; int-LV, integrating lentiviral vector; NILV, non-integrating lentiviral vector.

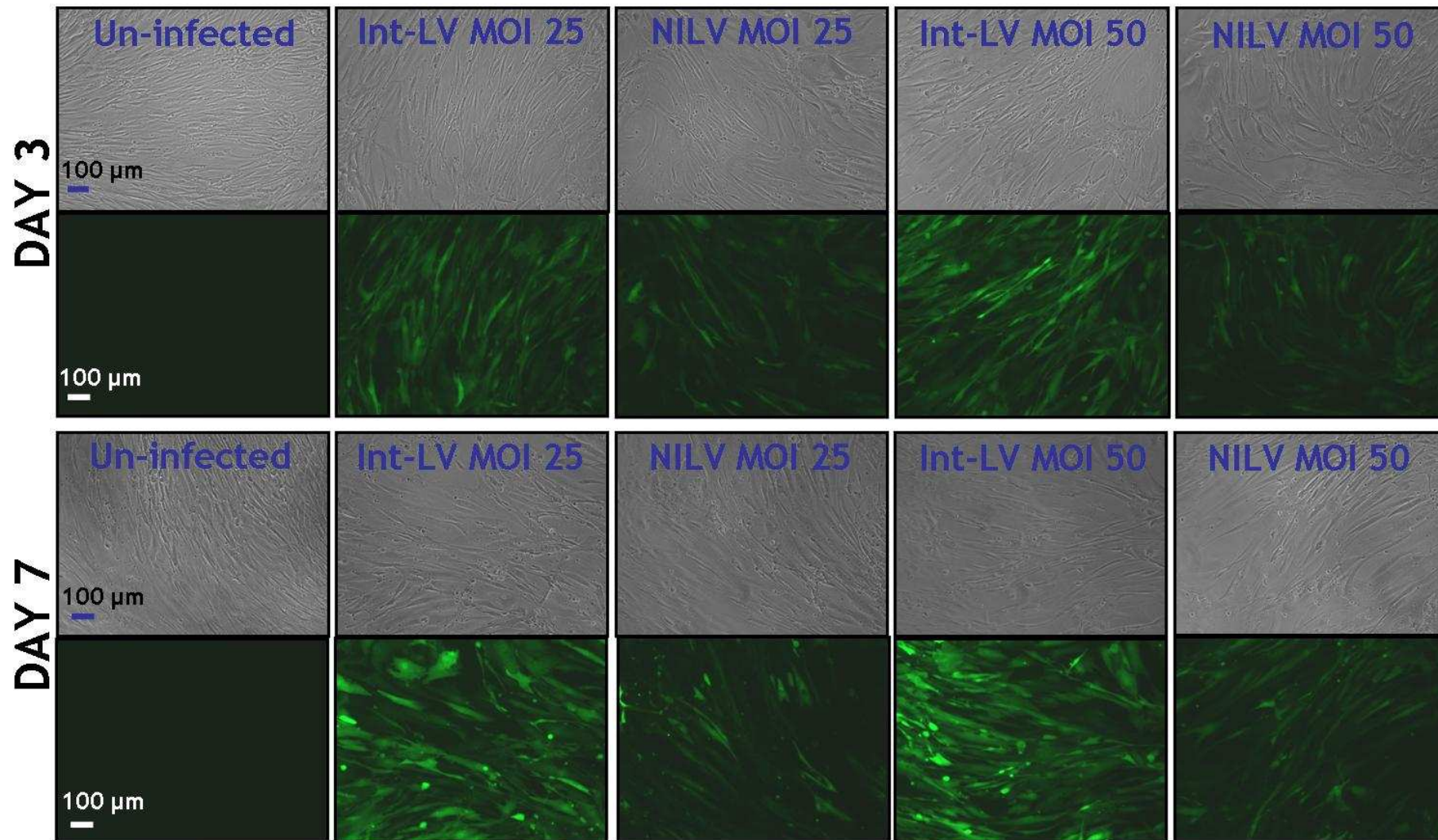


**Figure 3.14. Representative micrographs of the efficiency and long-term eGFP transgene expression in VSMCs mediated by NILVs.**

Fluorescent images of eGFP expression in VSMCs (vascular smooth muscle cells) infected with int-LV-eGFP or NILVs-eGFP at MOIs of 25 and 50 or un-infected, at 3 days (d) and 7 d post-infection. 100  $\mu$ m scale bar applicable to all panels (magnification x 100). Representative of n=3 (cell population/number of individual VSMC preparations used) in triplicate. MOI, multiplicity of infection; int-LV, integrating lentiviral vector; NILV, non-integrating lentiviral vector.

### 3.3 Discussion

In this chapter, second generation SIN LVs were optimised for their therapeutic potential in the context of vascular gene therapy.

- In terms of defining an alternative promoter for LV-mediated vascular cell transgene expression, it was established that both internal heterologous promoters SFFV and UCOE mediated efficient and sustained transgene expression in VECs and VSMCs. Importantly, the SFFV promoter was significantly more active overtime and enhanced transgene expression in VECs and VSMCs compared to UCOE promoter, and therefore was used in subsequent experiments.
- Rabies pseudotyped LVs efficiently transduced and mediated sustained transgene expression in rat neuronal cells, similar to VSV-g pseudotyped LVs. Interestingly, rabies, GP64 and EbolaZ pseudotyped LVs demonstrated their potential utility in VEC transduction through efficient transgene expression. However, these pseudotyped LVs were difficult to produce at high-titres.
- NILVs mediated efficient gene transfer and sustained eGFP transgene expression in VECs and VSMCs.

Taken together, selected SFFV-driven VSV-g enveloped NILVs were used for analysis.

In the context of LV-mediated vascular gene transfer, the CMV promoter has been defined as the most favourable internal heterologous promoter up to date. Importantly, this CMV promoter facilitated sufficient levels of VEGF and TIMP-3 respectively in VSMC and VECs, which modulated their phenotypic effects *in vitro* (Dishart et al., 2003a, Cefai et al., 2005). It is important to continue to define the potential for alternative promoters in LV-mediated transgene expression in vascular cells. This is the first study that has explored the potential use of the SFFV and the UCOE promoter in LV-mediated vascular gene therapy, which successfully induced efficient and long-term transgene

expression of eGFP in HeLa cells, VECs and VSMCs. Indeed, the SFFV promoter has been indicated in various studies to drive strong and sustained transgene expression facilitated by LVs (Demaison et al., 2002, Tschernutter et al., 2005, Yanez-Munoz et al., 2006, Apolonia et al., 2007, Buckley et al., 2008, Rahim et al., 2009, Ward et al., 2011). In relation to these studies, results from this study indicated that the SFFV promoter mediated greater efficiency of transgene expression overtime in HeLa cells, VECs and VSMCs, compared to the UCOE promoter. In contrast to the SFFV and the CMV promoter, UCOE facilitated consistent, stable and reproducible LV-mediated transgene expression in various cell lines; for example HeLa cells and more importantly haematopoietic stem cells, plus induced a more reliable transgene expression per proviral DNA copy. This is due to the fact that the UCOE internal regulatory element is less susceptible to insertion-site position effects (Zhang et al., 2007) and is resistant to DNA methylation-mediated transcriptional silencing (associated with methylation-free CpG islands and the chromatin opening element), unlike the SFFV and the CMV promoter which results in variation of transgene expression among the targeted cell population (Zhang et al., 2007, Zhang et al., 2010). Results from this study indicated that LV-mediated transgene expression in HeLa cells, VECs and VSMCs regulated by the SFFV promoter declined over continuous long-term culture *in vitro* possibly due to transcriptional silencing and insertion-site position effects, whereas the UCOE promoter drove relatively consistent and stable long-term transgene expression in HeLa cells and VECs, which correlates with previous studies (Zhang et al., 2007). Surprisingly, results from VSMC experiments demonstrated that the UCOE promoter was unable to provide stable and consistent LV-mediated transgene expression, in contrary to the results obtained from HeLa cells and VECs. To further support and clarify results, it is important to consider further experiments for example quantifying the variation of transgene expression mediated by each promoter among vascular cells, by assessing the mean vector copy number per cell and mean percentage of eGFP positive cells, to determine the ratio of eGFP expression per copy number as described by Zhang et al., (2007). Moreover, it is worth potentially considering the assessment of the SFFV promoter versus the UCOE promoter alongside the CMV promoter, for completion in these optimisation *in vitro* studies of LV-mediated transgene expression in vascular cells. Although, clinical studies now prefer the use of mammalian promoters, LV-mediated transgene expression

facilitated by the enhancer-less UCOE internal regulatory element would be advantageous in vascular cell gene transfer, but unfortunately it was very hard to produce high-titres of int-LV-UCOE. With the latter taken into consideration as well as int-LV-SFFV facilitating higher efficient long-term transgene compared to int-LV-UCOE in VSMCs; the UCOE promoter was not pursued in this study for assessing the potential of NILV for vascular gene therapy.

With regards to pseudotyping LVs for vascular gene transfer, the most commonly used envelope is the VSV-g (Dishart et al., 2003a, Cefai et al., 2005). It is important to continue to define the potential for alternative pseudotypes in LV-mediated vascular gene delivery for level and selectivity of transgene expression in vascular cells. Here, results interestingly indicated that rabies and GP64 pseudotyped LVs have the potential to efficiently transduce VECs. In relevance to these results, LVs pseudotyped with the GP64 envelope have proven to efficiently transduce a variety of cell lines (Schauber et al., 2004) and respiratory epithelium (Sinn et al., 2005a, Buckley et al., 2008). Rabies pseudotyped LVs have demonstrated their usefulness in gene therapy applications involving the CNS (Mazarakis et al., 2001, Kato et al., 2007, Rahim et al., 2009), however no up to date publications correlate with results obtained in this study, and thus definitively extends the target cell/tissue population of rabies pseudotyped LVs. In addition, EbolaZ pseudotyped LVs indicated their promising utility in transducing these vascular cells, which correlated with previous studies that demonstrated that EbolaZ has the ability to transduce myocytes, cardiomyocytes (MacKenzie et al., 2002), muscle (MacKenzie et al., 2005), skin tissue (Hachiya et al., 2007) and the airway epithelium (Kobinger et al., 2001, Sinn et al., 2003). Surprisingly, HNTV pseudotyped LV VEC transduction did not occur, which does not correlate with results observed by Qian *et al.*, (2006). This may possibly be due to sheer difficulty in producing high titres of HNTV pseudotyped LVs and this can also be suggested for most pseudotyped int-LVs here (Matrai et al., 2010). Unfortunately, difficulty was experienced when determining the titres of all these pseudotyped int-LVs using the same method (this was to allow direct comparison of each pseudotyped LV), such as the eGFP visual titre method and TaqMan PCR titre method, and this was suggested to be due to the occurrence of various tropism statuses among all pseudotyped LVs with the exception of the VSV-g envelope (Cronin et al., 2005,

Kutner et al., 2009). Instead, the microBCA assay was used to determine the total protein concentration of each pseudotype int-LV preparation. Furthermore, with regards to the latter, protein concentrations of each alternative pseudotyped LVs were used in relation to physical titres (however, MOIs could not be determined) for transduction efficiencies on VECs. Whereas, biological/functional titres were determined for rabies pseudotyped LVs versus VSV-g pseudotyped LVs and MOIs were calculated for transduction efficiencies comparison on neuronal cells. Alternatively, the number of vector particles present in a LV preparation can be determined irrespective of its pseudotype, and these include the assessment of reverse transcriptase activity and enzyme-linked immunosorbent assay (ELISA) directed against the p24 capsid protein content (Kutner et al., 2009). Pseudotyped-LV VEC transduction was explored first, due to abundance of VEC preparations from individual human patient saphenous veins. Unfortunately, the evaluation of each pseudotyped LVs (rabies, RRV, EbolaZ, GP64, MLV-A, MLV-E and HNTV) for their transduction efficiency in vascular cells was not followed through in this thesis, due to the sheer effort required to produce high-titre preparations of each pseudotyped LV and as a consequence the VSV-g envelope was continued. Nevertheless, all pseudotype LVs have the potential to be useful in vascular gene therapy and should be considered for future LV optimisation studies.

Preclinical studies have indicated the potential utility of rabies pseudotyped LVs for efficient transduction within cells of the CNS (Mazarakis et al., 2001, Kato et al., 2007, Rahim et al., 2009). In relation to these investigations, results from this *in vitro* study demonstrated that rabies pseudotyped int-LVs mediated efficient transduction and sustained transgene in a rat cortical neuronal cell line. However, in comparison to VSV-g pseudotyped int-LVs, these pseudotyped LVs were not as efficient for these neuronal cells, which confirms previous *in vitro* results by Mazarakis *et al.*, (2001) and *in vivo* results (irrespective of the retrograde transport) by Wong *et al.*, (2004). Therefore, these results indicate that rabies pseudotyped LVs may have the potential for being useful in gene therapy for stroke.

This LV optimisation *in vitro* study addresses for the first time the potential of NILVs for future application in vascular cell gene transfer. Notably, results here demonstrated efficient transgene expression in vascular cells can be facilitated

by NILVs. However, NILVs did not provide efficient and long-term eGFP expression as well as their integrating counterparts in VECs and VSMCs, which correlated with previous studies that indicated transient transgene expression facilitated by NILV-mediated gene transfer in dividing cells (Nightingale et al., 2006, Philippe et al., 2006). This was due to these episomal transgenes (1-LTR and 2-LTR circles) lacking replication signals, and thus diluting as a consequence of cell division (Butler et al., 2002, Pierson et al., 2002, Nightingale et al., 2006, Philippe et al., 2006). NILVs would be highly advantageous in vascular gene therapy. As mentioned previously, indeed many preclinical acute vascular injury models have demonstrated that adenoviral-mediated transient transgene expression can provide sufficient therapeutic benefits, which suggests that longevity is not necessarily an essential requirement in this clinical niche (George et al., 2000, Wan et al., 2004, Johnson et al., 2005, Kritz et al., 2008), and therefore NILVs may have the potential to be useful in this clinical setting.

Previous studies have demonstrated the potential usefulness of LV-mediated gene transfer of therapeutic genes such as TIMP-3 (with the inhibition of migration and increase in apoptosis of VSMCs), VEGF (with the increase of VEC migration and proliferation) and EC-SOD (with the inhibition of the NIF following acute vascular injury associated with reduced VSMC proliferation) (Dishart et al., 2003a, Cefai et al., 2005, Qian et al., 2006). Here in this LV optimisation investigation, results indicate that VSV-g pseudotyped NILV under the control of SFFV promoter are efficient for vascular cell gene transfer and transgene expression; however it is unsure if these vectors have the potential to facilitate sufficient levels of a therapeutic transgene to mediate beneficial effects/phenotypic modulation of vascular cells, and therefore will require more investigation.

It should be noted that this well-established eGFP reporter gene assay of transduced cells (by fluorimetry assessment) (Nicklin et al., 2001, Dishart et al., 2003a) is not without its limitations and measures the total amount of eGFP normalised to total mg of protein present, and thus do not provide information in terms of percentage of eGFP positive cells. In addition, a further eGFP reporter gene experiment should be considered, such as fluorescence-activated cell sorting (FACS) analysis for the percentage of eGFP positive HeLa cells, VECs and VSMCs after LV-mediated gene transfer, which has been widely used in

various LV studies (Demaison et al., 2002, Cefai et al., 2005, Apolonia et al., 2007, Zhang et al., 2007). FACS analysis here would confirm all results within this LV optimisation chapter, especially for the assessment of the potential of NILV gene delivery in vascular cells.

In this chapter, these VSV-g pseudotyped SFFV-driven LVs facilitated efficient gene transfer and transgene expression in VECs and VSMCs, and more broadly have the potential to deliver therapeutic genes into the vasculature which are key to the inhibition of the NIF. However, for the rest of this study, LV transduction on VSMCs will be focused. This is because; vascular injury-induced VSMC phenotypic effects (migration and proliferation) are hallmarks in the NIF (Westerband et al., 1997, Newby and Zaltsman, 2000, Hilker et al., 2002).

Taken together, VSV-g pseudotyped NILVs under the control of the SFFV promoter mediates efficient transgene expression in primary human VSMCs and VECs. In conclusion, these assessments report important implications for the use of NILVs in cardiovascular gene therapy and for its use in acute vascular injury.

#### **4 *In Vitro* Assessment of Lentiviral Gene Transfer of Nogo-B in Human Vascular Smooth Muscle Cells**

## 4.1 Introduction

### 4.1.1 *Nogo-B, a regulator of vascular remodelling*

An ideal therapeutic gene for the reduction of the NIF, would attenuate contributors associated with the acute vascular injury response, such as mediate the modulation of VSMC migration and proliferation, and induce the acceleration of re-endothelialisation (George et al., 2006, Gaffney et al., 2007). Endogenous Nogo-B has been shown to be a regulator in vascular maintenance and remodelling (Figure 1.15). A previous study documented high levels of Nogo-B in blood vessels from mice, and human VECs and VSMCs, with the latter expressing two variants of Nogo-B: Nogo-B1 and Nogo-B2 (Acevedo et al., 2004). Nogo-B has a favourable profile for prevention of the NIF, since this protein mediates negative regulation of VSMC migration (Acevedo et al., 2004, Kritz et al., 2008) and proliferation (Kritz et al., 2008), and positive regulation of VEC migration (Acevedo et al., 2004, Miao et al., 2006, Zhao et al., 2010). Nogo-B mediates its effect through acting as a chemo-attractant for VECs (Acevedo et al., 2004), antagonising of PDGF-BB stimulated VSMC migration (Acevedo et al., 2004, Kritz et al., 2008), and negatively regulating VSMC proliferation in response to serum and PDGF-BB stimulation (Kritz et al., 2008). Moreover, Nogo-B expression was shown to be down-regulated in human arterial atherosclerotic plaques (Rodriguez-Feo et al., 2007, Lee et al., 2009), stenotic lesions (Rodriguez-Feo et al., 2007), and aneurysm lesions (Pan et al., 2007), and thus this reduction may contribute to plaque formation, destabilisation and vascular abnormalities (Pan et al., 2007, Rodriguez-Feo et al., 2007, Lee et al., 2009). The function of Nogo-B has generated a great deal of interest in relation to basic biology and therapeutic potential in the vasculature in order to reduce the NIF following acute vascular injury. Indeed, mice deficient in Nogo-A/B demonstrated accelerated rates of NIF after acute vascular injury, which were attenuated/rescued by adenoviral gene transfer of Nogo-B (Acevedo et al., 2004). It was previously shown that the injury-induced NIF was rescued in a porcine vein graft model and a wire injured murine model by adenoviral gene transfer of Nogo-B (Figure 4.1), and this was also associated with decreased VSMC proliferation (Kritz et al., 2008).



**Figure 4.1. Nogo-B attenuates neointima formation in acute vascular injury.**

Adenoviral-mediated gene delivery of Nogo-B (Ad-Ng-B) reduced neointima formation (NI) in a wire-injury induced murine model (scale bar = 100  $\mu$ m) and a porcine vein graft model (scale bar = 500  $\mu$ m). M, media; A, adventitia (Kritz et al., 2008).

Nogo-B is primarily located in the ER but with a small fraction (approximately 2% of the total Nogo-B protein found in a vascular cell) found within the cell membrane of vascular cells, and with the N-terminus in an extracellular orientation. The N-terminus domain is the major known functional region of Nogo-B in relation to vascular biology. The functional extracellular soluble N-terminal domain comprises of the first 1-200 amino acids of Nogo-B (soluble Nogo-B) and is the important region of Nogo-B for the migration of vascular cells (Acevedo et al., 2004). The N-terminus of Nogo-B is essential for stimulating chemotaxis and morphogenesis of VECs through its engagement with the Ng-BR via Akt signalling (Miao et al., 2006, Zhao et al., 2010). This receptor is presumed to be on the cell surface of VECs (Miao et al., 2006). In cell culture assays, it has been shown that soluble Nogo-B dose-dependently enhanced VEC migration and had a negative effect on VSMC migration (Acevedo et al., 2004, Miao et al., 2006). However, it is unclear whether this soluble Nogo-B is the functional region that mediates a reduction in VSMC proliferation.

Results from chapter three indicate that VSV-g-pseudotyped NILVs are able to mediate efficient transgene expression under the control of the SFFV promoter in human VSMCs. A VSMC has a relatively slow mitotic rate in a disease state (Gordon et al., 1990) and even during the acute vascular injury response (Westerband et al., 1997, Hilker et al., 2002). Therefore, it is possible that NILV-mediated episomal transgene would “dilute” slowly out, but persist for a duration required in this clinical setting to elicit a beneficial effect. NILV-mediated gene transfer of Nogo-B provides a great opportunity to explore these LVs and their anticipated wait, to assess if these vectors mediate a safe and effective delivery strategy of a therapeutic gene key to the inhibition of the NIF.

### Aim of this chapter

- To assess int-LV-mediated gene transfer of full-length Nogo-B and soluble/mutant Nogo-B for over-expression in primary human VSMCs, and its phenotypic effects *in vitro*.
- To evaluate NILV gene delivery of full-length Nogo-B for over-expression and its phenotypic effect on VSMC migration and proliferation *in vitro*.

## 4.2 Results

### ***4.2.1 Cloning of cDNA encoding Nogo-B into a lentiviral vector construct plasmid***

In order to produce LVs expressing the full-length or mutant (soluble) Nogo-B transgene, each cDNA was cloned into a lentiviral construct/transfer plasmid. A lentiviral construct plasmid containing a multiple cloning site (MCS) (consisting of *Bam*HI, *Xho*I, *Kpn*I and *Mlu*I) with an internal heterologous SFFV promoter (pHR'SIN-cPPT-SFFV-MCS-WPRE), was obtained from Adrian Thrasher's lab [from University College London (UCL), UK]. This construct plasmid has been successfully optimised (in terms of biosafety and improved LV performance, see section 1.10.2.1 and Figure 4.2) (Demaison et al., 2002) and evaluated in a number of publications (Demaison et al., 2002, Zhang et al., 2007, Ward et al., 2011).

A strategy for PCR cloning was adopted as described in section 2.8, due to lack of appropriate restriction sites. This was carried out in order to flank cDNA inserts with restriction enzyme recognition sites *Bam*HI and *Xho*I, and therefore facilitate insertion (Figure 4.3). Blunt-ended PCR products of full-length or mutant Nogo-B were purified and sub-cloned into an intermediate plasmid (StrataClone PCR Cloning Vector pSC-B- ampicillin/kanamycin plasmid) (Figure 4.3). Plasmids were DNA sequenced to confirm cDNAs were correct. The full-length and the mutant Nogo-B cDNA were excised from their intermediate plasmid via *Bam*HI and *Xho*I digestion, purified and then cloned into the corresponding restriction enzyme recognition sites in the LV construct plasmid, pHR'SIN-cPPT-SFFV-MCS-WPRE (Figure 4.3). Subsequently, these plasmids [pHR'SIN-cPPT-SFFV-fulllengthNogo-B-WPRE and pHR'SIN-cPPT-SFFV-

mutantNogo-B-WPRE (Figure 4.4)] were confirmed by DNA sequencing (see Appendix 2 and Appendix 3) and restriction digests with the following: *SacII*, *NheI* and *XbaI* for single digestion reactions, and *BamHI* and *XhoI* for a double digestion reaction (see method for Table 2.3 for plasmid fragment sizes) (Figure 4.5). *SacII* single digests generated the following plasmid DNA fragments: linearised the pHR'SIN-cPPT-SFFV-MCS-WPRE (empty) plasmid for a 8931 bp band; 8535 bp & 1549 bp fragments were produced from the pHR'SIN-cPPT-SFFV-fulllengthNogo-B-WPRE (full-length Nogo-B) plasmid and the pHR'SIN-cPPT-SFFV-mutantNogo-B-WPRE (mutant Nogo-B) plasmid gave rise to 8535 bp & 1000 bp fragments (Figure 4.5 A). *NheI* digests produced the following DNA fragments: empty plasmid= 7246 bp & 1685 bp; full-length Nogo-B plasmid = 7246 bp & 2838 bp and mutant Nogo-B plasmid = 7246 bp & 2289 bp (Figure 4.5 B). *XbaI* digests gave rise to the following DNA fragments: empty plasmid = 7970 bp & 961 bp; full-length Nogo-B plasmid = 9123 bp & 961 bp and mutant Nogo-B plasmid = 8574 bp & 961 bp (Figure 4.5 C). *BamHI* and *XhoI* double digests produced the following DNA fragments: empty plasmid = 8921 bp & 10 bp (the latter is not shown); full-length Nogo-B plasmid = 8921 bp & 1163 bp and mutant Nogo-B plasmid = 8921 bp & 614 bp (Figure 4.5 D). A single band of the correct size for full-length Nogo-B and mutant Nogo-B with *BamHI* and *XhoI* double digests confirmed the presence of each cDNA insert (Figure 4.5 D). These completed constructs were then used to produce LVs expressing either full-length Nogo-B or mutant Nogo-B, and subsequently tested in human VSMCs *in vitro*.

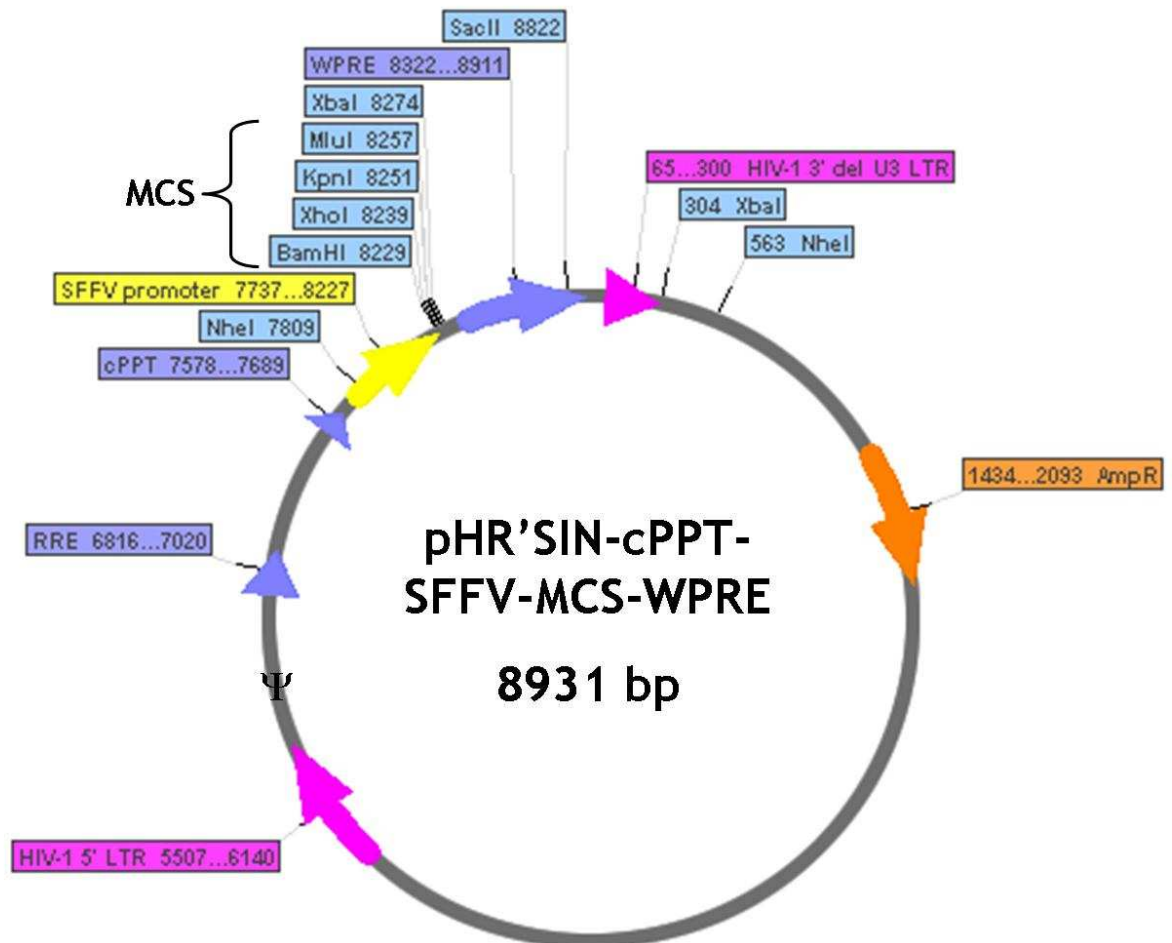


**Figure 4.2. Plasmid map of lentiviral vector construct/transfer plasmid consisting of the multiple cloning site (MCS).**

Schematic diagram illustrates key elements within the lentiviral construct plasmid, these are as follows: HIV-1 5' long terminal repeat (5' LTR); HIV-1 3' partial deletion (del/ $\Delta$ ) in unique 3' region (U3) in the LTR; packaging sequence ( $\Psi$ ); Rev responsive element (RRE); central polypurine tract (cPPT); Spleen focus forming virus (SFFV) promoter; multiple cloning site (MCS) consists of *Bam*HI, *Xho*I, *Kpn*I and *Mlu*I; Woodchuck post-transcriptional regulatory element (WPRE), and ampicillin resistance gene (AmpR).

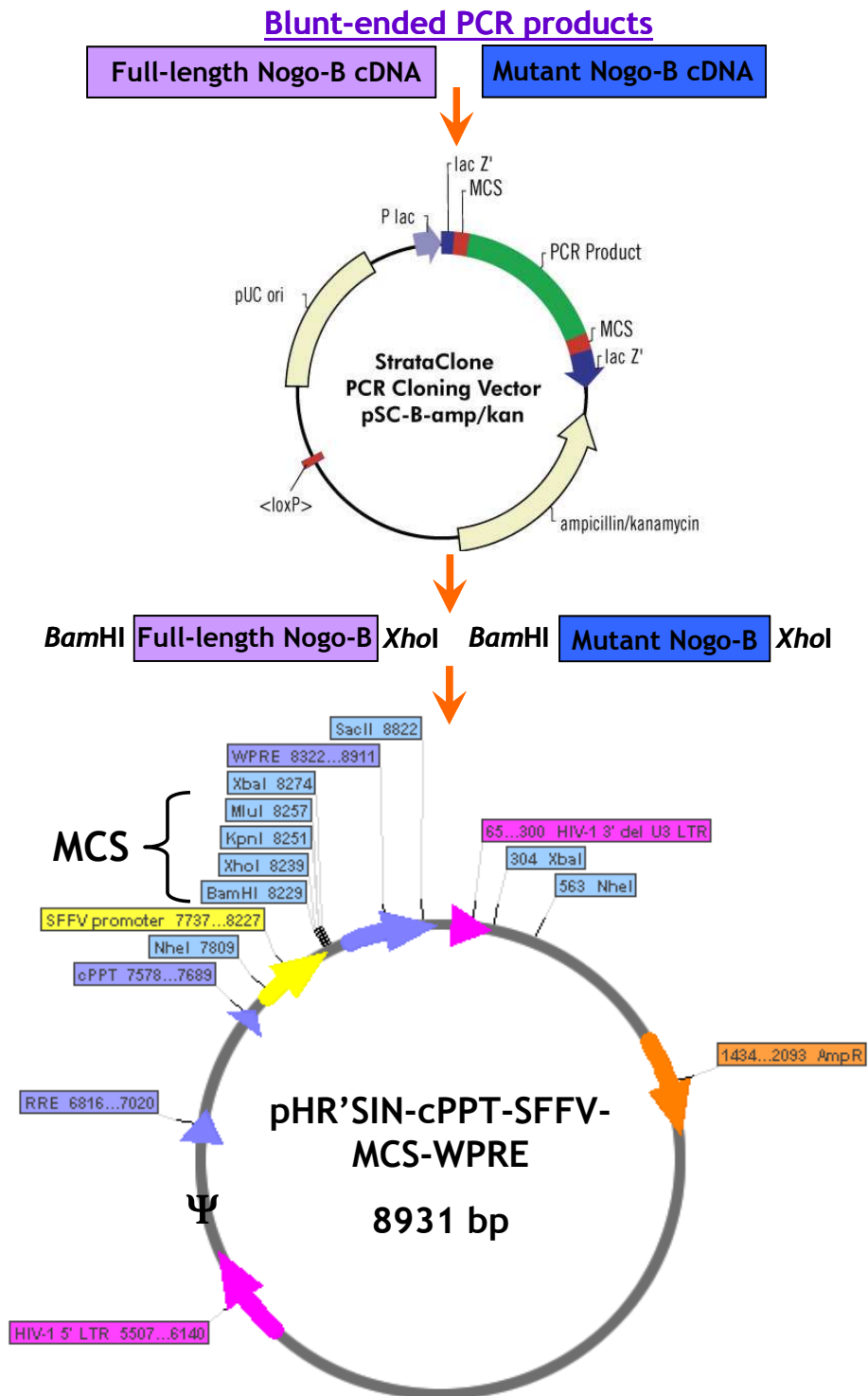


**Figure 4.3. Schematic diagram of the cloning of Nogo-B cDNA into the lentiviral vector construct plasmid.**

Blunt-ended PCR products (containing *Bam*HI and *Xho*I sites) were purified and sub-cloned into the StrataClone PCR cloning vector pSC-B-ampicillin/kanamycin plasmid (intermediate). Full-length and mutant Nogo-B cDNA were released from the intermediate plasmid on *Bam*HI and *Xho*I sites and then cloned into the corresponding sites in the lentiviral vector construct plasmid.

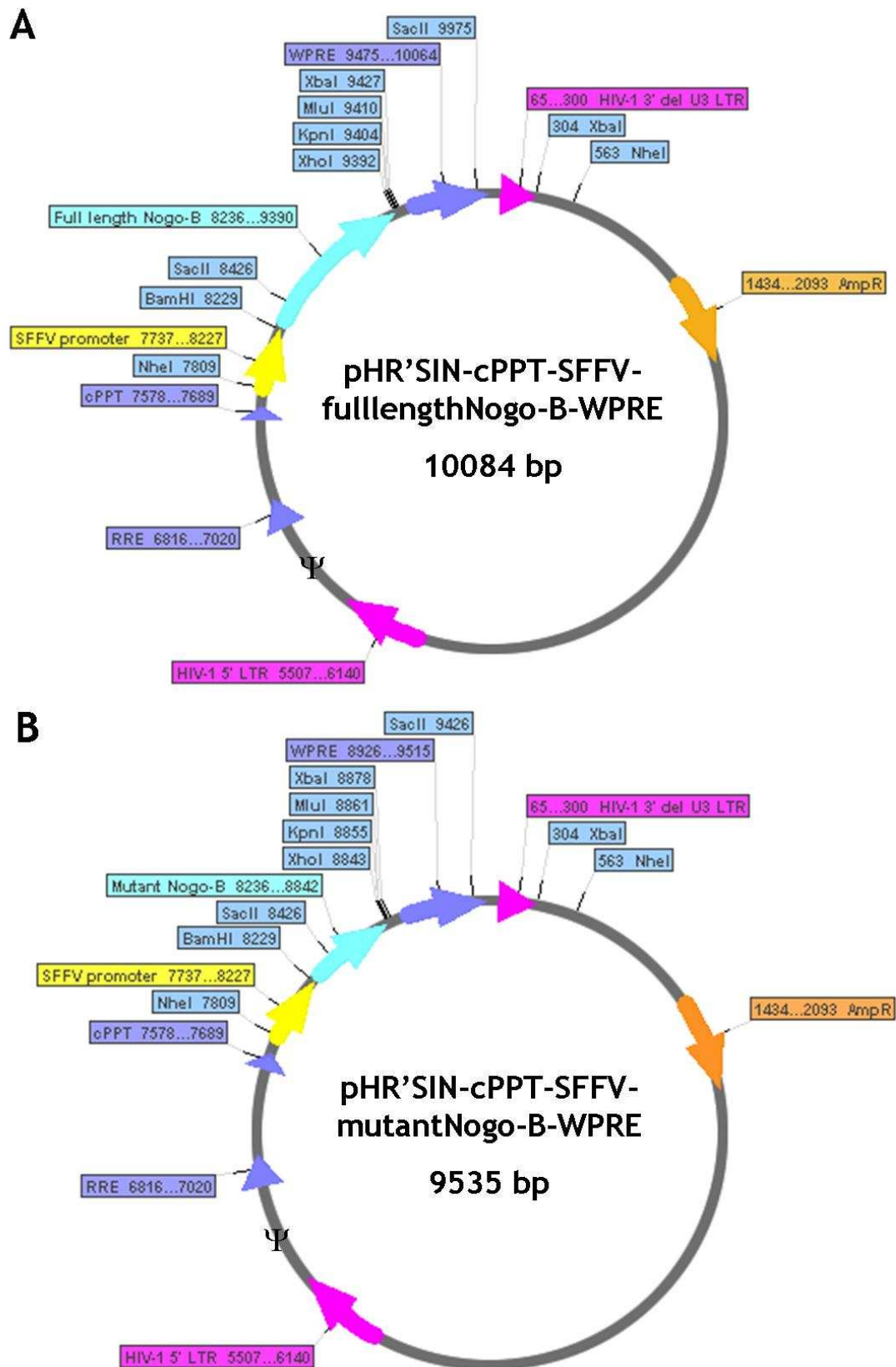
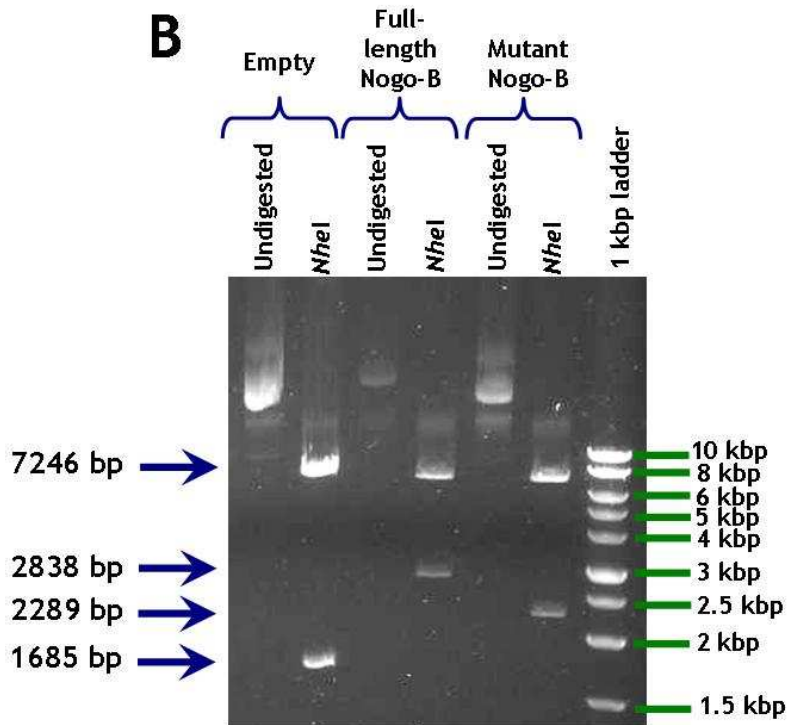
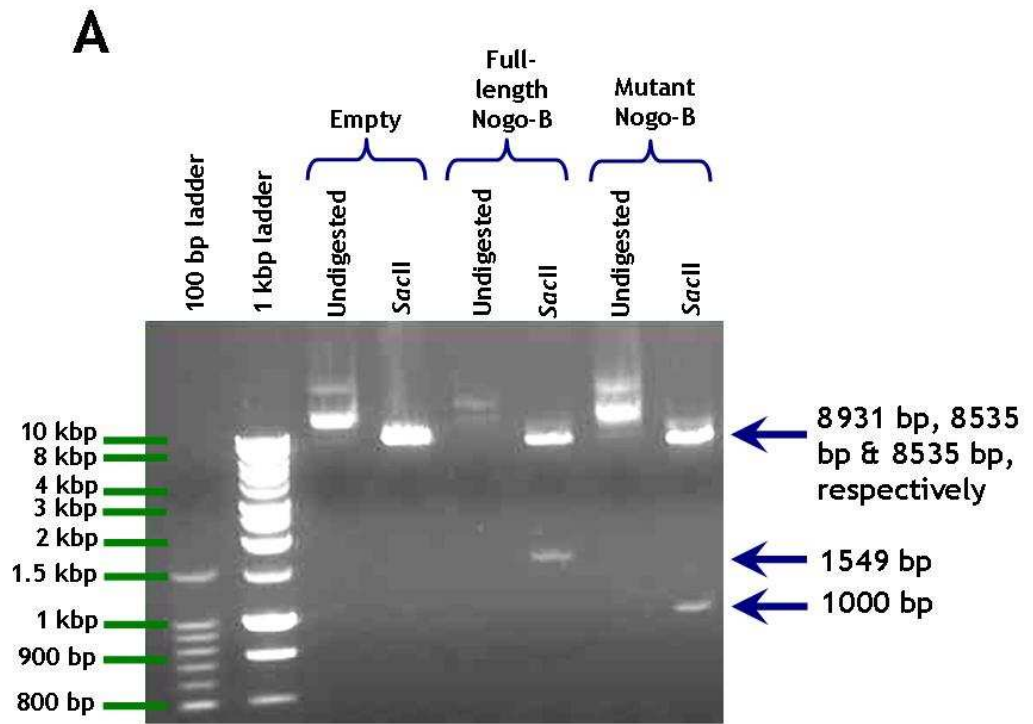


Figure 4.4. Plasmid maps of complete lentiviral construct/transfer plasmids for full-length and mutant Nogo-B.

(A) Illustrates full-length Nogo-B plasmid (pHR'SIN-cPPT-SFFV-fulllengthNogo-B-WPRE) and (B) illustrates mutant Nogo-B plasmid (pHR'SIN-cPPT-SFFV-mutantNogo-B-WPRE).



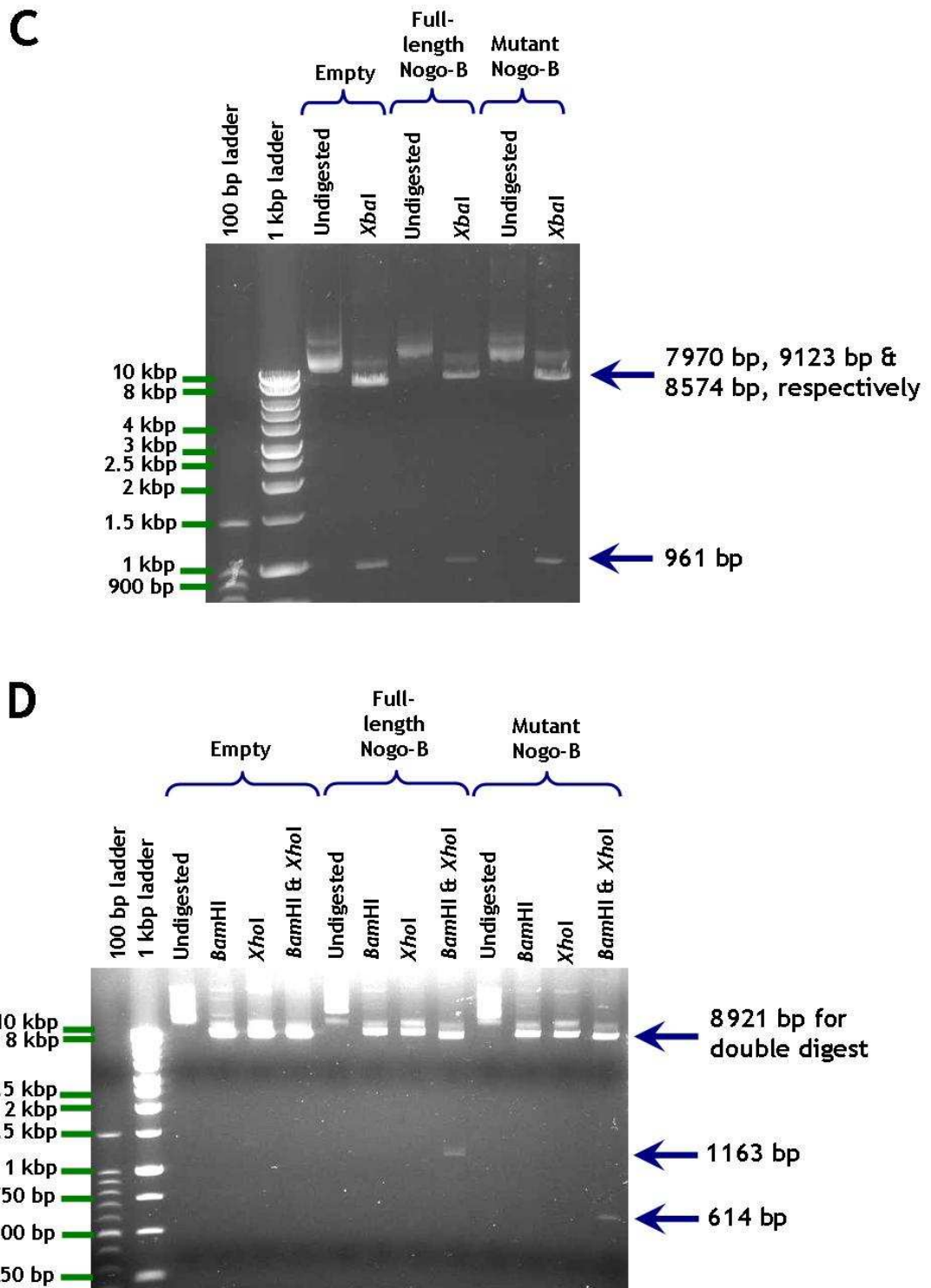


Figure 4.5. Confirmation for the successful cloning of the complete full-length and mutant lentiviral construct/transfer plasmids.

Digestion of 250 ng of each pHR<sup>+</sup>SIN-cPPT-SFFV-MCS-WPRE (empty) plasmid, pHR<sup>+</sup>SIN-cPPT-SFFV-fulllengthNogo-B-WPRE (full-length Nogo-B) plasmid and pHR<sup>+</sup>SIN-cPPT-SFFV-mutantNogo-B-WPRE (mutant Nogo-B) plasmid in 50  $\mu$ l reactions with 10 U of single digests with (A) *Sac*II, (B) *Nhe*I and (C) *Xba*I, and double digests with (D) *Bam*HI and *Xho*I. Undigested= no presence of restriction endonucleases. Kbp, kilo base pairs; bp, base pairs.

#### **4.2.2 Effect of integrating lentiviral gene transfer of Nogo-B on vascular smooth muscle cells migration and proliferation**

The efficiency of int-LV-mediated gene transfer of Nogo-B was assessed in human VSMCs *in vitro*. SFFV-driven, VSV-g pseudotyped second-generation SIN int-LVs expressing either full-length Nogo-B (int-LV-full-length Nogo-B) or mutant Nogo-B (int-LV-mutant Nogo-B) were generated. TaqMan qPCR titres of int-LV-full-length Nogo-B in a range from  $1.27 \times 10^7$  to  $6.58 \times 10^8$  iu/ml (5 batches) and int-LV-mutant Nogo-B in a range from  $7.27 \times 10^8$  to  $8.01 \times 10^8$  iu/ml (2 batches) were used to infect VSMCs.

##### **4.2.2.1 Integrating lentiviral-mediated Nogo-B over-expression**

Western immunoblotting was used to assess the efficiency of int-LV-mediated gene delivery of Nogo-B in HeLa cell and human VSMC lysates and post-cell membrane supernatants, at 4 days (d) or 5 d post-transduction at MOIs of 25 or 50, respectively. Detection of Nogo-B protein was assessed using a goat polyclonal anti-human Nogo IgG antibody. This antibody recognises the N-terminus epitope of Nogo-B, which is common in both full-length and mutant Nogo-B. Full-length Nogo-B (45-50 kDa) over-expression was detected in HeLa cells and VSMCs (in both cell lysates and post-cell membrane supernatants) infected with int-LV-full-length Nogo-B, compared to int-LV-eGFP and un-infected (Figure 4.6 and Figure 4.7). Adenoviral-mediated gene transfer of full-length Nogo-B (Ad-full-length Nogo-B) at 5 d post-transduction at a MOI of 50, was used as a positive control in VSMCs and indicated Nogo-B over-expression [compared to the eGFP control (Ad-eGFP) and un-infected] (Figure 4.7). Mutant Nogo-B (approximately 27-31 kDa) was identified in cell lysates and supernatants of HeLa cells that were transduced with int-LV-mutant Nogo-B, in contrast to int-LV-full-length Nogo-B, int-LV-eGFP and un-infected (Figure 4.6). Surprisingly, mutant Nogo-B protein (27-31 kDa) was not detected in VSMCs (in both cell lysates and supernatants) transduced with int-LV-mutant Nogo-B (Figure 4.7).

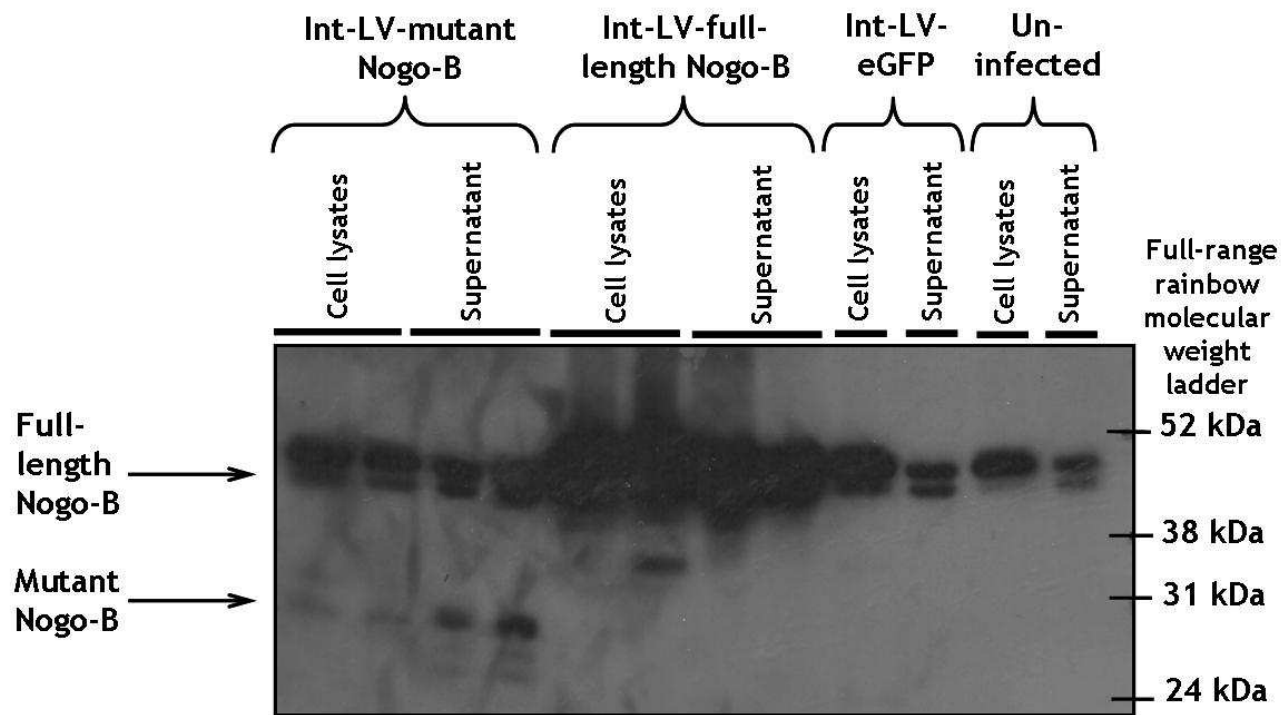


**Figure 4.6. Int-LV-full-length Nogo-B and int-LV-mutant Nogo-B transduction of HeLa cells.**

HeLa cells were seeded (at a cell density of  $1.5 \times 10^5$ /well on a 6-well plate) and transduced with LVs (the presence of  $8 \mu\text{g/ml}$  of polybrene for 18 hours incubation) at a MOI of 25. Cell lysates and post-cell supernatants were collected 4 days post-infection and examined for over-expression of Nogo-B protein by Western immunoblotting [representative of  $n=1$  (cell line populations used)]. All cell lysates and post-cell membrane supernatants were normalised to  $6 \mu\text{g}$  of protein loading (protein concentration determined by BCA assay), and Nogo-B proteins at 45-50 kDa for full-length Nogo-B and 27-31 kDa for mutant Nogo-B were detected using a goat polyclonal anti-human Nogo (used to detect the N-terminus region) IgG antibody ( $0.4 \mu\text{g/ml}$ ). Int-LV, integrating lentiviral vector; kDa, kilo Daltons; MOI, multiplicity of infection.

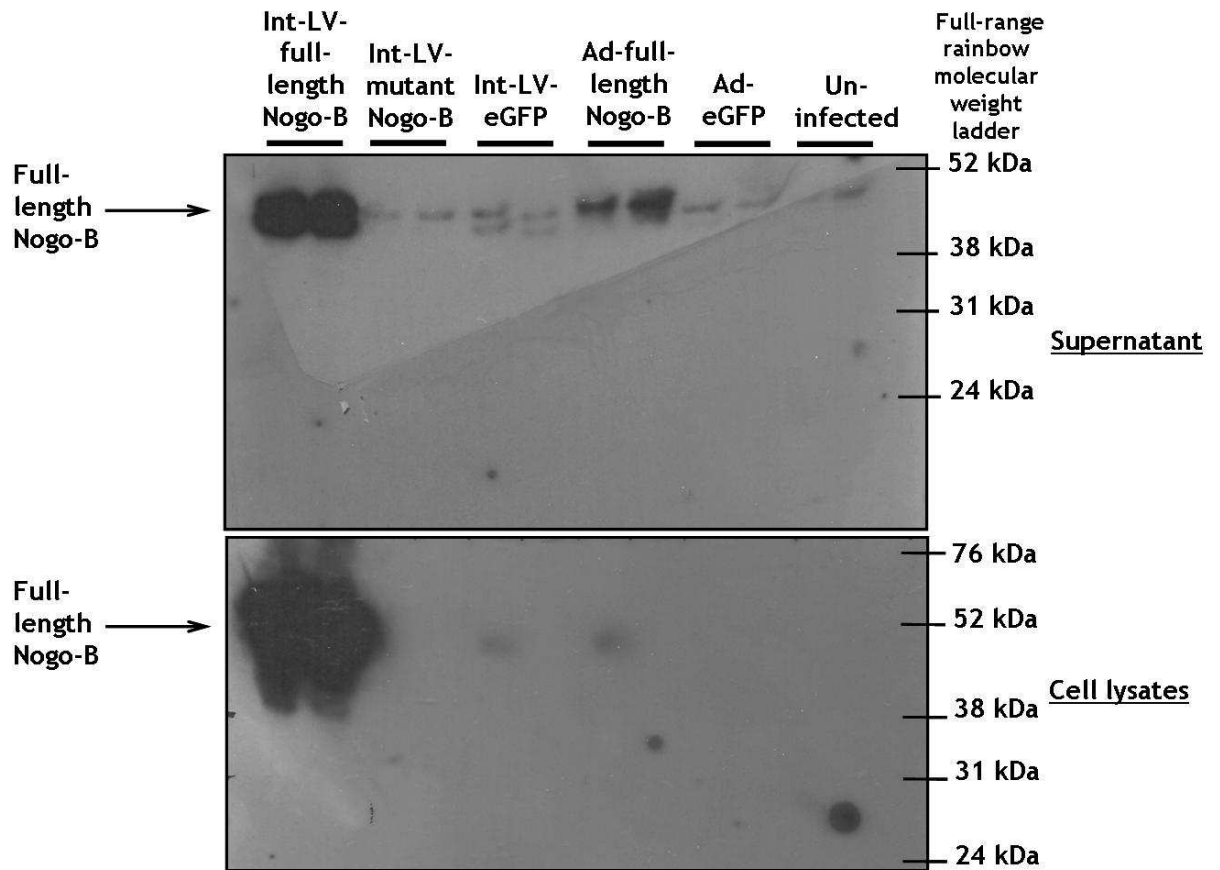


**Figure 4.7. Int-LV-full-length Nogo-B and int-LV-mutant Nogo-B transduction in VSMCs.** VSMCs were seeded (at a cell density of  $2.5 \times 10^5$ /well on a 6-well plate) and transduced with integrating lentiviral vectors (int-LV) or adenoviral vectors (Ad) (in the presence of 8  $\mu\text{g/ml}$  of polybrene or no polybrene, respectively, for 18 hours incubation) at a MOI of 50. Cell lysates and post-cell membrane supernatants were collected 5 days post-infection and examined for over-expression of Nogo-B protein by Western immunoblotting [representative of  $n=1$  (cell population/number of individual VSMC preparations used) in duplicate]. All cell lysates and supernatants were normalised to 6  $\mu\text{g}$  of protein loading (protein concentration determined by BCA assay), and Nogo-B proteins at 45-50 kDa for full-length Nogo-B and 27-31 kDa for mutant Nogo-B were detected using a goat polyclonal anti-human Nogo (used to detect the N-terminus region) IgG antibody (0.4  $\mu\text{g/ml}$ ). VSMC, vascular smooth muscle cell; int-LV, integrating lentiviral vector; kDa, kilo Daltons; MOI, multiplicity of infection.

Over-expression of full-length or mutant Nogo-B in VSMCs following gene transfer mediated by their corresponding int-LVs, were further evaluated by immunocytofluorescent staining for Nogo-B. VSMCs were seeded and then infected with int-LV-full-length Nogo-B, int-LV-mutant Nogo-B or int-LV-eGFP at a MOI of 50, or un-infected. 7 d after transduction VSMCs were assessed for Nogo-B with the same goat polyclonal anti-Nogo IgG antibody used to detect Nogo-B in Western immunoblotting. A corresponding Alexa-Fluor®-555 donkey anti-goat IgG secondary antibody was used and images were taken using fluorescence microscopy. Full-length Nogo-B over-expression and mutant Nogo-B expression was detected (increased red fluorescence) in VSMCs infected by their corresponding int-LVs, in comparison to int-LV-eGFP and endogenous level of Nogo-B observed in un-infected VSMCs (Figure 4.8 A). Isotype-matched negative controls (goat IgG antibody) were carried out for all LV conditions and un-infected VSMCs during immunocytofluorescent staining in parallel. No red immunocytofluorescence was observed and thus no non-specific binding of the anti-Nogo-B antibody occurred (Figure 4.8 B).

Taken together, the over-expression of full-length Nogo-B mediated by int-LV gene delivery was confirmed in HeLa cells and VSMCs. Unfortunately, the expression of mutant Nogo-B mediated by int-LV gene transfer could not be ascertained due to no presence in cell lysates and supernatants of VSMCs by Western immunoblotting; however the presence of this protein was detected in VSMCs by immunocytofluorescence, and in cell lysates and supernatants of HeLa cells. Consequently, further work determining the effects of int-LV gene transfer of mutant Nogo-B on VSMC migration and proliferation was put on hold. For the rest of this thesis int-LV-full-length Nogo-B will be referred to as int-LV-Nogo-B.

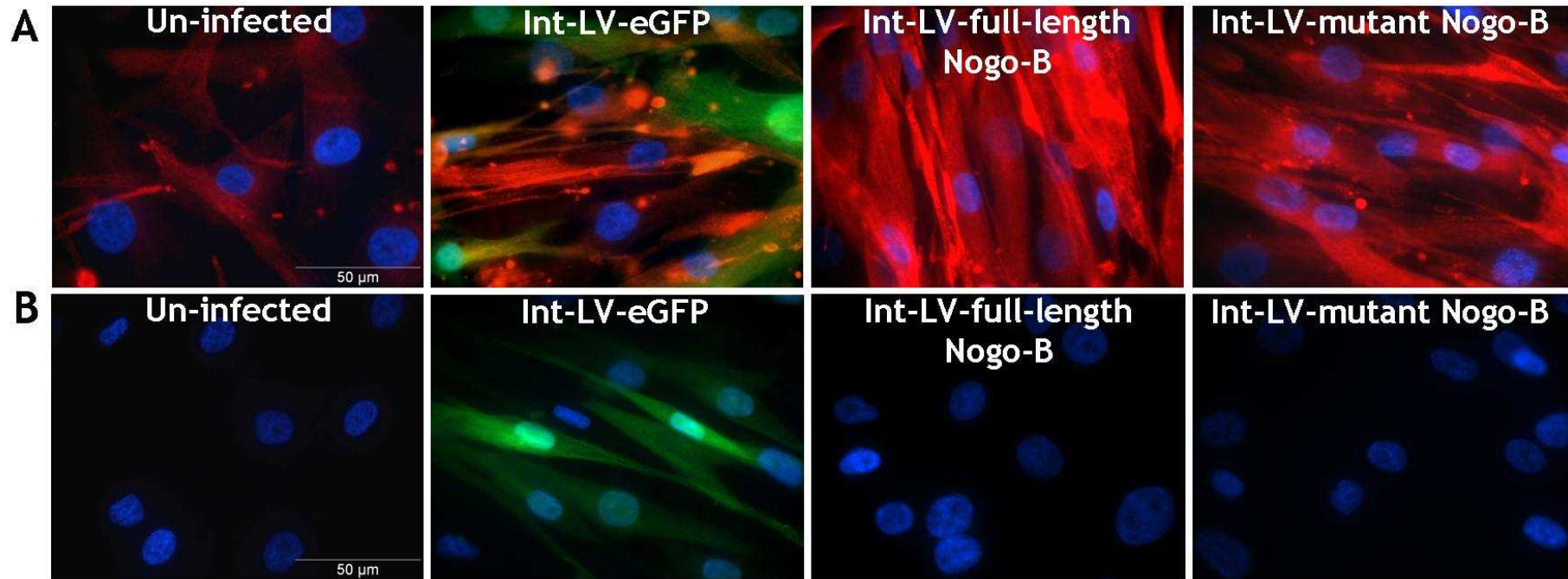


**Figure 4.8. Int-LV-full-length Nogo-B and int-LV-mutant Nogo-B infection in VSMCs indicated by immuno-fluorescence.**

Immunocytofluorescent staining was carried out in VSMCs (seeded at a cell density of  $2.5 \times 10^4$ /well on a 4-well chamber slide) transduced with LVs (in presence of  $0.5 \mu\text{g/ml}$  of polybrene for 18 hours incubation) at a MOI of 50, for 7 days post-infection in permeabilised conditions. **(A)** A goat polyclonal anti-human Nogo (to the N-terminus region) IgG antibody ( $2 \mu\text{g/ml}$ ) along with its corresponding Alexa-Fluor®-555 (red fluorescence) donkey anti-goat IgG secondary antibody ( $4 \mu\text{g/ml}$ ) was used to detect Nogo-B expression. **(B)** Immuno-fluorescent staining using an isotype-matched negative control (goat IgG) antibody.  $50 \mu\text{m}$  scale bar applicable to all panels (magnification x 600). Representative of  $n=1$  (cell population/number of individual VSMC preparations used) in triplicate. VSMC, vascular smooth muscle cell; int-LV, integrating lentiviral vector; MOI, multiplicity of infection.

#### 4.2.2.2 Assessment of the effects of int-LV-Nogo-B on VSMC migration

Kritz et al. (2008) demonstrated adenoviral-mediated over-expression of Nogo-B reduced PDGF-BB-induced migration of VSMCs in a chemotaxis assay. A scratch wound-mediated cell migration assay was implemented to examine the effect of Nogo-B over-expression on VSMC migration, induced by int-LV-mediated gene transfer of Nogo-B. VSMCs were seeded and infected with either int-LV-Nogo-B or int-LV-eGFP at a MOI of 50, or left un-infected as controls. VSMC migration was assessed 3 d post-infection in the presence of 15 % serum. Absolute VSMC migration was measured from the wound edge to the final point of VSMC migration in  $\mu\text{m}$ . VSMCs transduced with int-LV-Nogo-B indicated a significant inhibition in VSMC migration at 22 hours (h) post-wounding, compared to both int-LV-eGFP and un-infected VSMCs [ $310.0 \pm 25.3 \mu\text{m}$  vs.  $1072.2 \pm 54.6 \mu\text{m}$  (70 % significant reduction in VSMC migration) or  $1003.3 \pm 54.6 \mu\text{m}$  (69 %), respectively,  $p < 0.001$ ] (Figure 4.9 A). Representative bright-field micrographs from this migration assay at 0 h and 22 h after wounding also illustrated that int-LV-Nogo-B transduction blocked VSMC migration, compared to int-LV-eGFP and un-infected VSMCs (Figure 4.9 B).

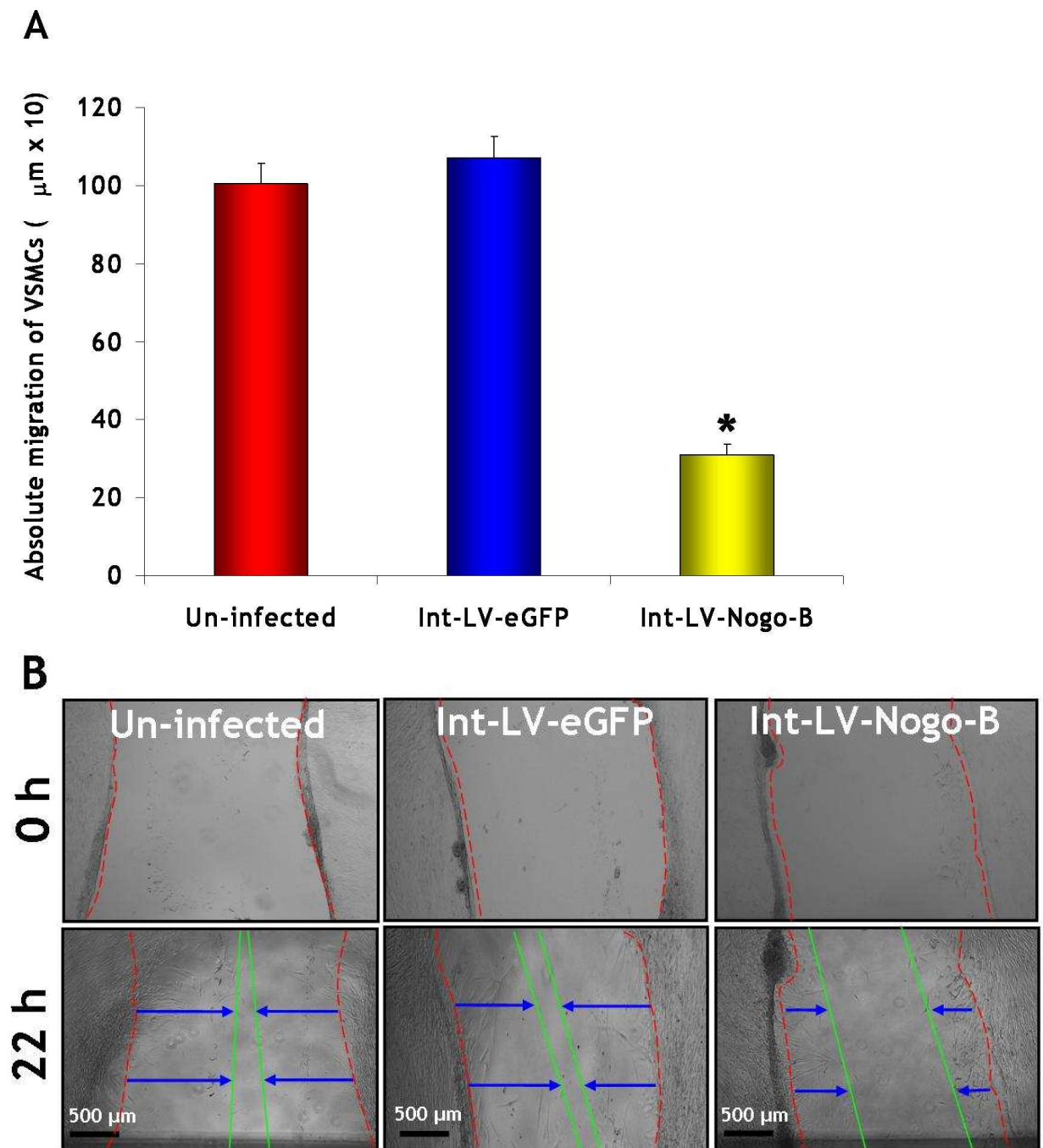


**Figure 4.9. Effect of int-LV-Nogo-B on VSMC migration.**

(A) VSMCs were seeded (cell density of  $0.5 \times 10^4$ /well in an 8-well chamber slide) and infected with LVs [in the presence of  $0.5 \mu\text{g/ml}$  of polybrene for 18 hours (h) incubation] at a MOI of 50. VSMC migration was assessed using a scratch wound-mediated cell migration (using p1000 tip) assay 3 days post-infection and absolute migration (from the wound edge to the final point of VSMC migration) was measured ( $\mu\text{m}$ ) at 22 h post-wounding using ImagePro software. For each condition (repeated in triplicate) = 10 migration distances of 3 fields of view were measured. Mean value  $\pm$  S.E.M of patient sample repeated in triplicate. Two independent experiments performed [n=2 (representative of each other), cell population/number of individual VSMC preparations used]. \* indicates  $p < 0.001$  vs. int-LV-eGFP vector control or un-infected, by one-way ANOVA for Bonferroni's corrections. (B) Representative bright-field micrographs of the scratch wound-mediated cell migration assay at 0 hours and 22 hours post-wound. 500  $\mu\text{m}$  scale bar applicable to all panels (magnification x 40). Representative of n=2 (cell population/number of individual VSMC preparations used) in triplicate. VSMC, vascular smooth muscle cell; int-LV, integrating lentiviral vector; MOI, multiplicity of infection.

#### 4.2.2.3 Assessment of the effects of int-LV-Nogo-B on VSMC proliferation

A proliferation assay was performed to assess the effect of Nogo-B over-expression mediated by int-LV-Nogo-B on VSMC proliferation. VSMCs were seeded and quiescence-induced in serum-free culture media. After 48 h of quiescence, VSMCs were infected with LVs (int-LV-Nogo-B or int-LV-eGFP) at MOIs of 10, 25 and 50, or un-infected, (all conditions in the presence of 15 % serum). VSMC proliferation was quantified using a MTT assay at 5 d post-infection. Results from this proliferation assay demonstrated that int-LV-Nogo-B delivery significantly blocked VSMC proliferation at MOIs of 25 and 50, compared to int-LV-eGFP control vector and un-infected VSMCs [MOI 25:  $0.29 \pm 0.020$  optical density (OD) (at 570 nm) vs.  $0.46 \pm 0.011$  OD (37 % significant inhibition in VSMC proliferation) or  $0.51 \pm 0.026$  OD (43 %), respectively,  $p < 0.001$ . MOI 50:  $0.21 \pm 0.012$  OD vs.  $0.43 \pm 0.017$  OD (51 %) or  $0.51 \pm 0.026$  OD (59 %), respectively,  $p < 0.001$ ] (Figure 4.10). Representative images taken prior to the MTT assay, also illustrated that VSMCs infected with int-LV-Nogo-B 5 d post-transduction at MOIs of 25 and 50 reduced VSMC proliferation, compared to int-LV-eGFP and un-infected VSMCs (Figure 4.11).

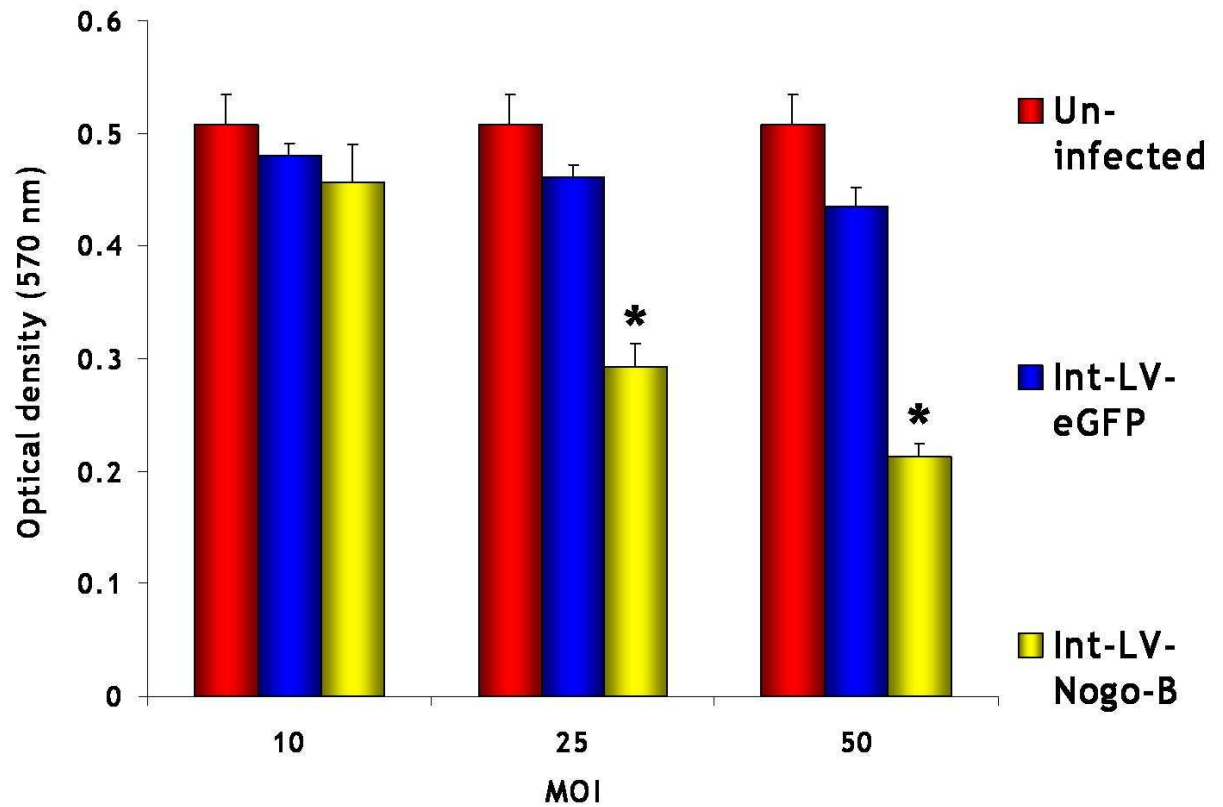


**Figure 4.10. Effect of int-LV-Nogo-B on VSMC proliferation.**

VSMCs were seeded (at a cell density of  $0.5 \times 10^4$ /well on a 48-well plate and quiesced for 48 hours prior to LV infection) and infected with LVs in 15 % serum (in the presence of 8  $\mu\text{g}/\text{ml}$  of polybrene for 18 hours incubation) at MOIs of 10, 25 or 50. VSMC proliferation was assessed using a 3- (4,5-Dimethylthiazol-2-yl)-2, 5- diphenyltetrazolium bromide (MTT) assay, 5 days post-transduction and optical density was measured at 570 nm wavelength. Mean value  $\pm$  S.E.M of patient sample repeated in quadruplicate. Three independent experiments performed [n=3 (representative of each other), cell population/number of individual VSMC preparations used]. \* indicates  $p < 0.001$  vs. int-LV-eGFP vector control or un-infected, by one-way ANOVA for Bonferroni's post-hoc analysis. VSMC, vascular smooth muscle cell; MOI, multiplicity of infection; int-LV, integrating lentiviral vectors.

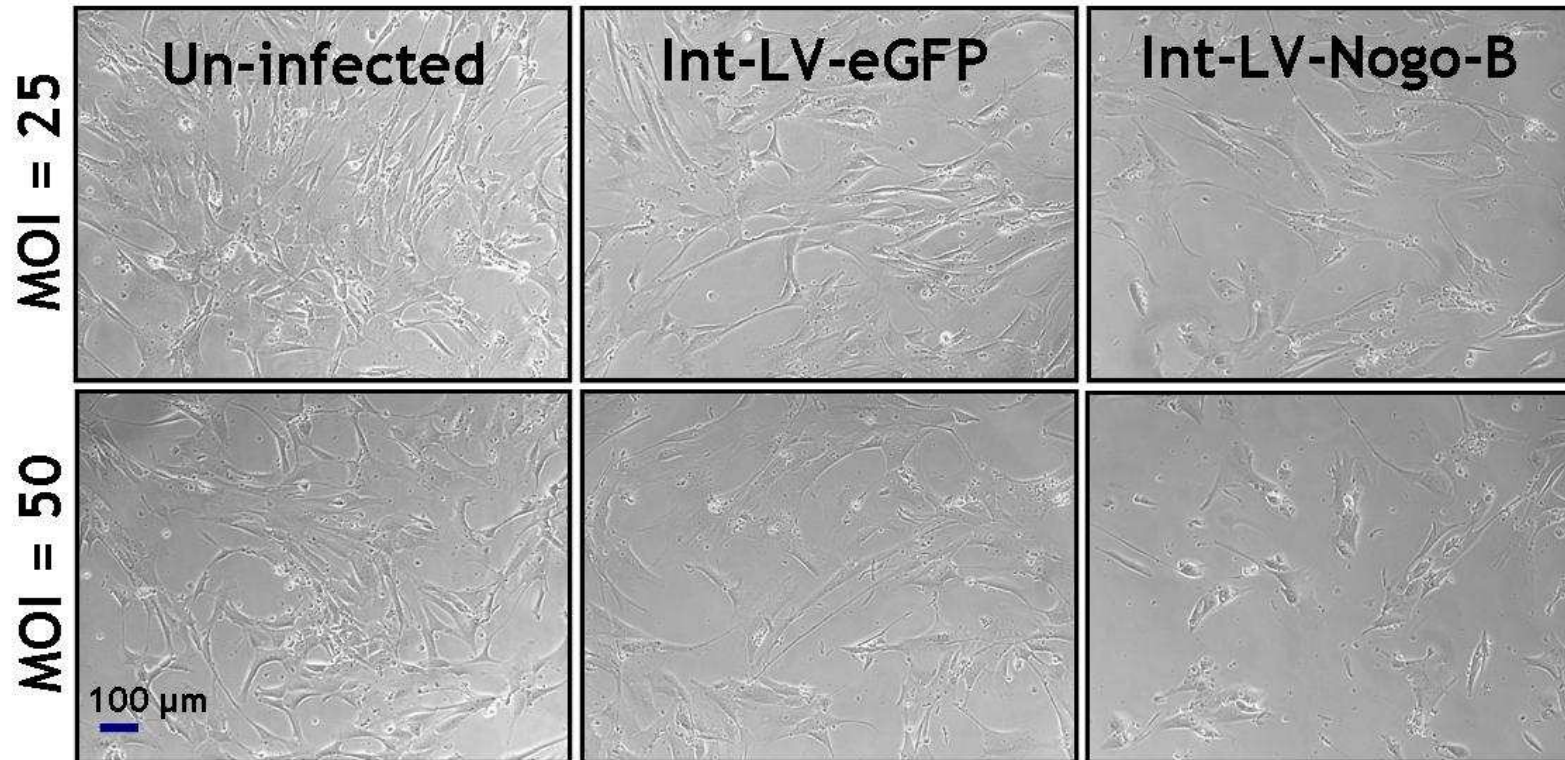


**Figure 4.11. Representative images of the effect of int-LV-Nogo-B on VSMC proliferation.**

Bright-field micrographs of the VSMC proliferation assay 5 days post-infection, prior to the addition of the MTT component. 100 μm scale bar applicable to all panels (magnification x 100). Representative of n=3 (cell population/number of individual VSMC preparations used) in quadruplicate. VSMC, vascular smooth muscle cell; MOI, multiplicity of infection; int-LV, integrating lentiviral vectors.

### 4.2.3 Effect of non-integrating lentiviral gene transfer of Nogo-B on vascular smooth muscle cells migration and proliferation

Based on the data with int-LV-Nogo-B, we next evaluated the effects of NILV-mediated gene transfer of Nogo-B on VSMC migration and proliferation. NILVs (D64V mutants) retain transduction efficiency of their integrating counterparts with minimal host genome integration in cells of the retina (Yanez-Munoz et al., 2006), muscle (Apolonia et al., 2007) and CNS (Rahim et al., 2009). SFFV-driven, VSV-g pseudotyped second-generation SIN NILVs (D64V mutants) expressing full-length Nogo-B (NILV-Nogo-B) (Figure 4.12) were generated and TaqMan qPCR titres were in a range from  $3.54 \times 10^7$  to  $1.18 \times 10^8$  iu/ml (4 batches).

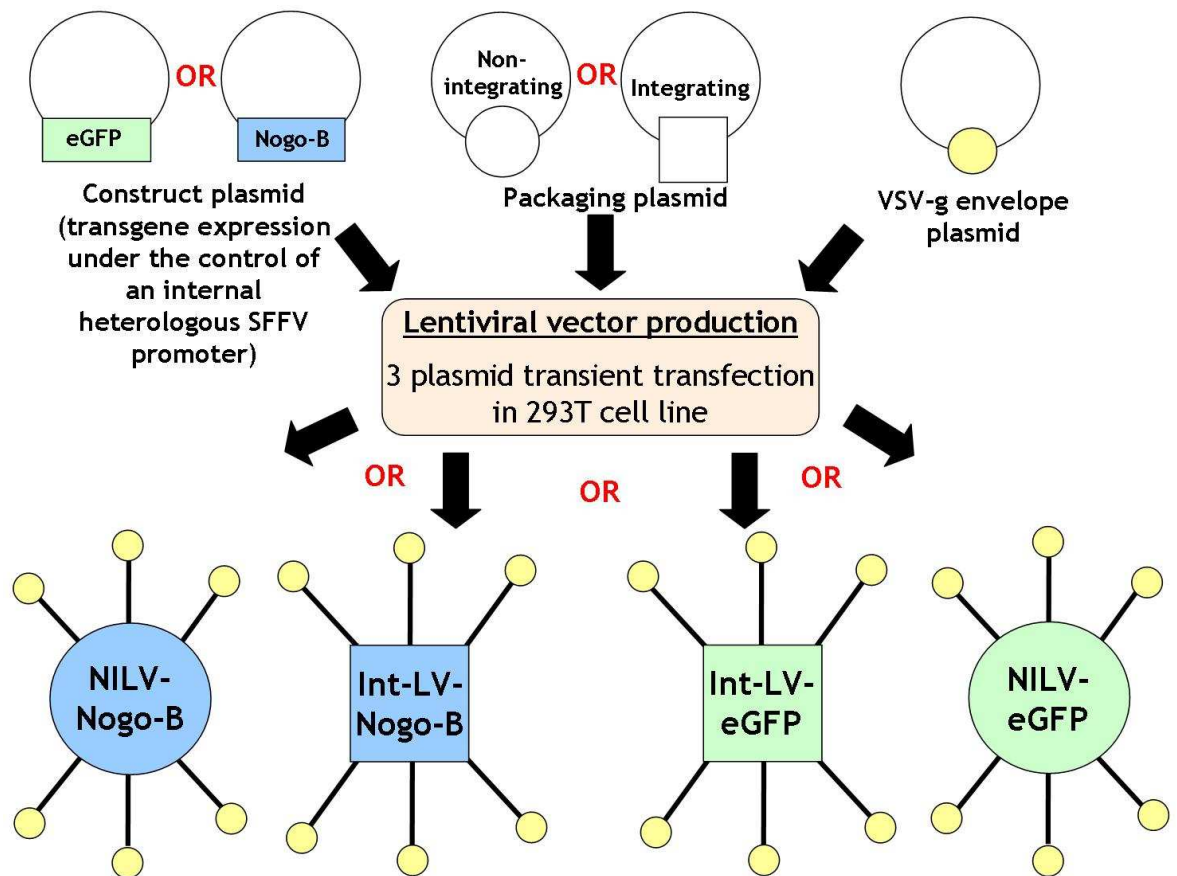


**Figure 4.12. Production of LVs.**

Schematic diagram illustrates the production of vesicular stomatitis virus glycoprotein (VSV-g) pseudotyped NILVs (D64V mutant) expressing full-length Nogo-B (NILV-Nogo-B) under the control of the spleen focus forming virus (SFFV) promoter. Int-LV, integrating lentiviral vector; NILV, non-integrating lentiviral vector.

#### 4.2.3.1 Non-integrating lentiviral-mediated Nogo-B over-expression

As before (section 4.2.2.1), Western immuno-blotting was used to detect the over-expression of Nogo-B in VSMCs following NILVs-mediated gene transfer of Nogo-B, and to assess the transduction efficiency of NILV-Nogo-B compared to int-LV-Nogo-B in VSMCs. VSMCs were seeded and infected with either NILV-Nogo-B, NILV-eGFP, int-LV-Nogo-B or int-LV-eGFP at a MOI of 50 or un-infected. Cell lysates and supernatants were collected at 5 d post-transduction and assessed by Western blot analysis [normalised to 12 µg of protein loading and GAPDH (although weak) indicated equal loading for cell lysates]. Cell lysates and supernatants demonstrated increased Nogo-B protein (45-50 kDa) expression from VSMCs infected with NILV-Nogo-B, compared to NILV-eGFP control vector and un-infected (endogenous Nogo-B levels) (Figure 4.13). In addition, transduction efficiency of NILV-Nogo-B was illustrated to be lower than int-LV-Nogo-B in lysates and supernatants of VSMCs (Figure 4.13), however NILV-Nogo-B was still efficient in mediating Nogo-B over-expression compared to NILV-eGFP vector control.

As before (section 4.2.2.1), immunocytofluorescence was carried out to further illustrate the over-expression of Nogo-B in VSMCs mediated by NILV-Nogo-B. VSMCs were seeded and then infected with the following LVs at a MOI of 50: NILV-Nogo-B, NILV-eGFP, int-LV-Nogo-B and int-LV-eGFP, and un-infected. After 5 d post-infection these VSMCs were examined for visual expression of Nogo-B by immunocytofluorescence. Nogo-B over-expression (increased red fluorescence) was indicated by confocal microscopy in VSMCs infected by NILV-Nogo-B, unlike NILV-eGFP and un-infected VSMCs (endogenous level of Nogo-B) (Figure 4.14 A). Moreover, it was also demonstrated that NILV-Nogo-B mediated efficient transduction and induced Nogo-B over-expression in VSMCs similar to that of int-LV-Nogo-B (Figure 4.14 A). No red immunocytofluorescent staining was observed with either the isotype-matched negative control or the secondary antibody alone (PBS used instead of Nogo-B specific antibody), thus no non-specific binding of the anti-Nogo-B antibody or the secondary antibody was present (Figure 4.14 B).

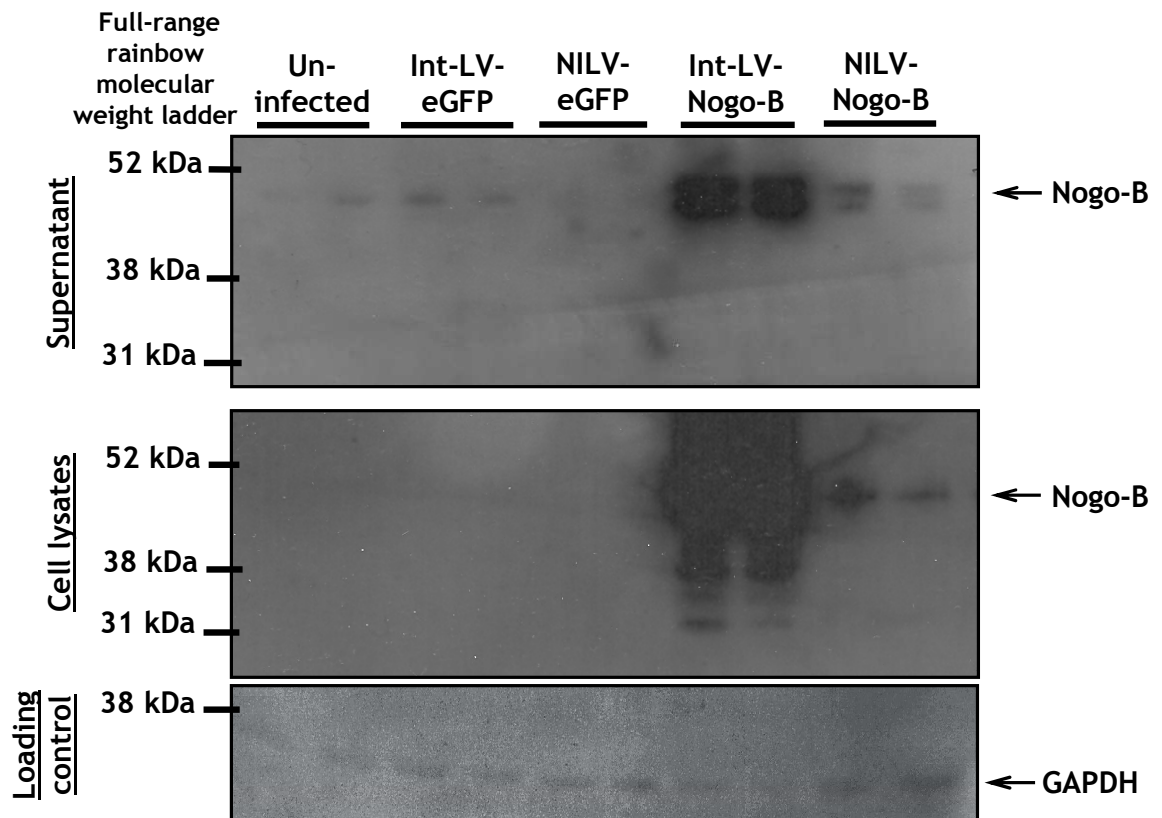


**Figure 4.13. Western blot analysis of NILV-Nogo-B transduction in VSMCs.**

VSMCs were seeded (at a cell density of  $2.5 \times 10^5$ /well on a 6-well plate) and transduced with LVs (in the presence of  $8 \mu\text{g/ml}$  of polybrene, for 18 hours incubation) at a MOI of 50. Cell lysates and post-cell membrane supernatants were collected 5 days post-infection and examined for over-expression of Nogo-B protein by Western immunoblotting [representative of  $n=1$  (cell population/number of individual VSMC preparations used) in duplicate]. All cell lysates and supernatants were normalised to  $12 \mu\text{g}$  of protein loading (protein concentration determined by BCA assay) and Nogo-B protein at 45-50 kDa was detected using a goat polyclonal anti-human Nogo (used to detect the N-terminus region) IgG antibody ( $0.4 \mu\text{g/ml}$ ). A mouse monoclonal anti-human GAPDH antibody ( $0.2 \mu\text{g/ml}$ ) was used to detect GAPDH (36 kDa) in cell lysates for equal loading. VSMC, vascular smooth muscle cell; int-LV, integrating lentiviral vector; NILV, non-integrating lentiviral vector; kDa, kilo Daltons; MOI, multiplicity of infection.

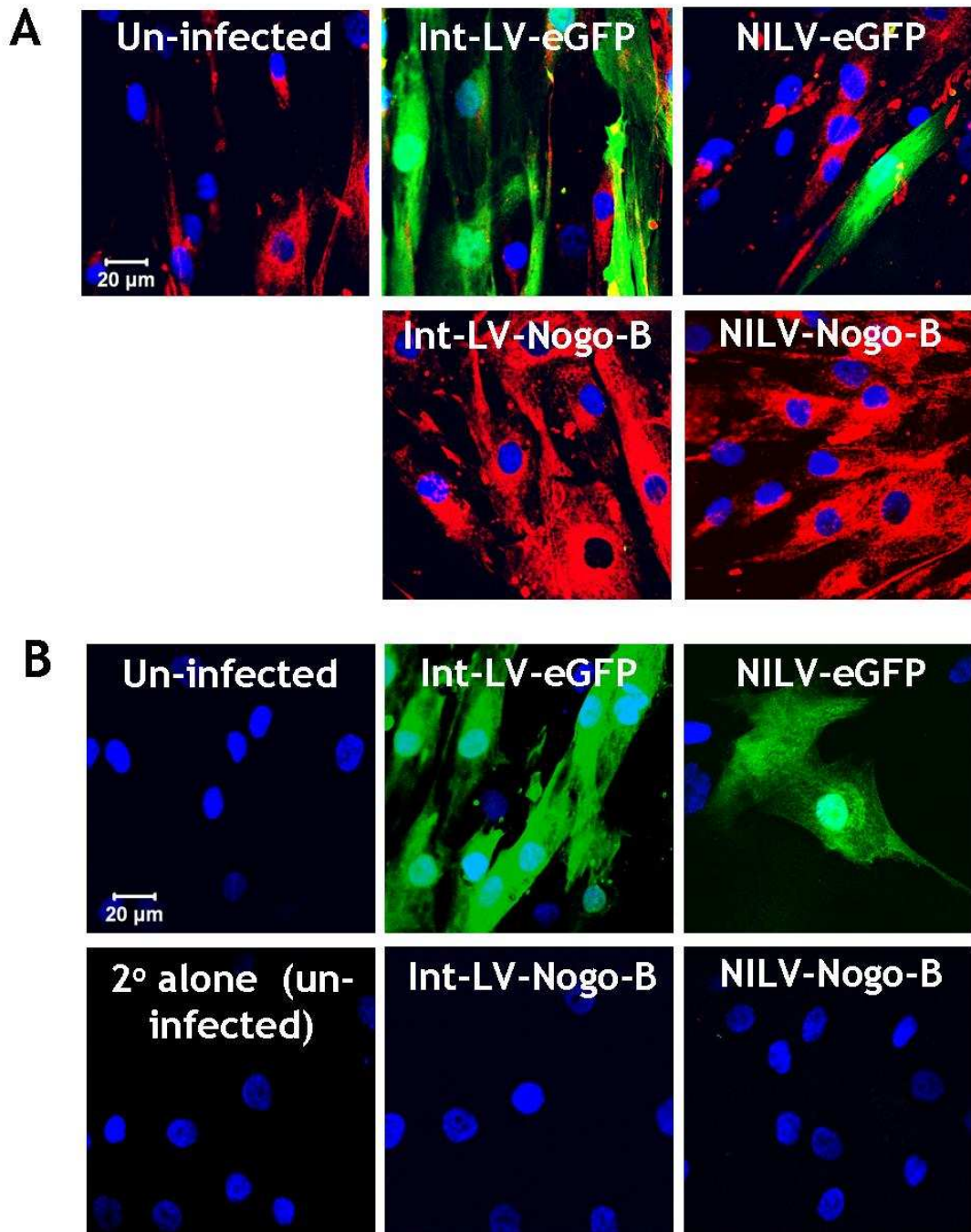


**Figure 4.14.** NILV-Nogo-B transduction in VSMCs indicated by immunocytofluorescence. Immunocytofluorescent staining was carried out in VSMCs (seeded at a cell density of  $0.5 \times 10^4$ /well on an 8-well chamber slide) transduced with LVs (in presence of  $0.5 \mu\text{g/ml}$  of polybrene for 18 hours incubation) at a MOI of 50, for 5 days post-infection in permeabilised conditions. **(A)** A goat polyclonal anti-human Nogo (to the N-terminus region) IgG antibody ( $2 \mu\text{g/ml}$ ) along with its corresponding Alexa-Fluor®-555 (red fluorescence) donkey anti-goat IgG secondary ( $2^\circ$ ) antibody ( $4 \mu\text{g/ml}$ ) was used to detect Nogo-B expression. **(B)** Immunocytofluorescent staining using an isotype-matched negative control (goat IgG) primary antibody or omitting the primary antibody [secondary ( $2^\circ$ ) alone].  $20 \mu\text{m}$  scale bar applicable to all panels (magnification  $\times 630$ ). Representative of  $n=1$  (cell population/number of individual VSMC preparations used) in triplicate. VSMC, vascular smooth muscle cell; int-LV, integrating lentiviral vector; NILV, non-integrating lentiviral vector; MOI, multiplicity of infection.

#### 4.2.3.2 Assessment of the effects of NILV-Nogo-B on VSMC migration

Next to examine was the effect of Nogo-B over-expression on VSMC migration induced by NILV-mediated gene transfer of Nogo-B and as before (section 4.2.2.2) a scratch wound-mediated cell migration assay was carried out. VSMCs were seeded and infected with LVs (with either NILV-Nogo-B, NILV-eGFP, int-LV-Nogo-B or int-LV-eGFP) at MOIs of 25 or 50 or un-infected. VSMC migration was examined using this migration assay at 3 days post-transduction, and VSMC migration was measured ( $\mu\text{m}$ ) at 10 h post-wounding (in the presence of 15% serum). A significant reduction of VSMC migration was observed after infection with NILV-Nogo-B compared to NILV-eGFP and un-infected VSMCs, at 10 h post-wounding at both MOIs [MOI of 25:  $106.24 \pm 7.87 \mu\text{m}$  vs.  $174.16 \pm 6.49 \mu\text{m}$  (39 % significant reduction in VSMC migration) or  $170.15 \pm 8.04 \mu\text{m}$  (38 %),  $p < 0.001$ , respectively, and MOI of 50:  $125.98 \pm 8.66 \mu\text{m}$  vs.  $178.9 \pm 8.78 \mu\text{m}$  (30 %) or  $170.15 \pm 8.04 \mu\text{m}$  (26 %),  $p < 0.001$  or  $p < 0.01$ , respectively] (Figure 4.15). These migration results also reiterated that int-LV-Nogo-B-mediated gene delivery reduced VSMC migration unlike its control vector (at both MOIs) or un-infected VSMCs [MOI of 25:  $101.81 \pm 7.93 \mu\text{m}$  vs.  $163.90 \pm 6.95 \mu\text{m}$  (38 % significant reduction in VSMC migration) or  $170.15 \pm 8.04 \mu\text{m}$  (40 %),  $p < 0.001$ , respectively, and MOI of 50:  $90.88 \pm 2.47 \mu\text{m}$  vs.  $149.55 \pm 4.2 \mu\text{m}$  (39 %) or  $170.15 \pm 8.04 \mu\text{m}$  (47 %),  $p < 0.001$ , respectively] (Figure 4.15). Moreover, these results also demonstrated that NILV-Nogo-B transduction on VSMCs (at both MOIs) was as efficient as int-LV-Nogo-B in mediating a reduction in VSMC migration (MOI of 25:  $106.24 \pm 7.87 \mu\text{m}$  vs.  $101.81 \pm 7.93 \mu\text{m}$ , and MOI of 50:  $125.98 \pm 8.66 \mu\text{m}$  vs.  $90.88 \pm 2.47 \mu\text{m}$ , respectively) (Figure 4.15). Micrographs of this migration assay also illustrated that NILV-Nogo-B infection in VSMCs reduced VSMC migration, compared to NILV-eGFP and no infection (Figure 4.16).

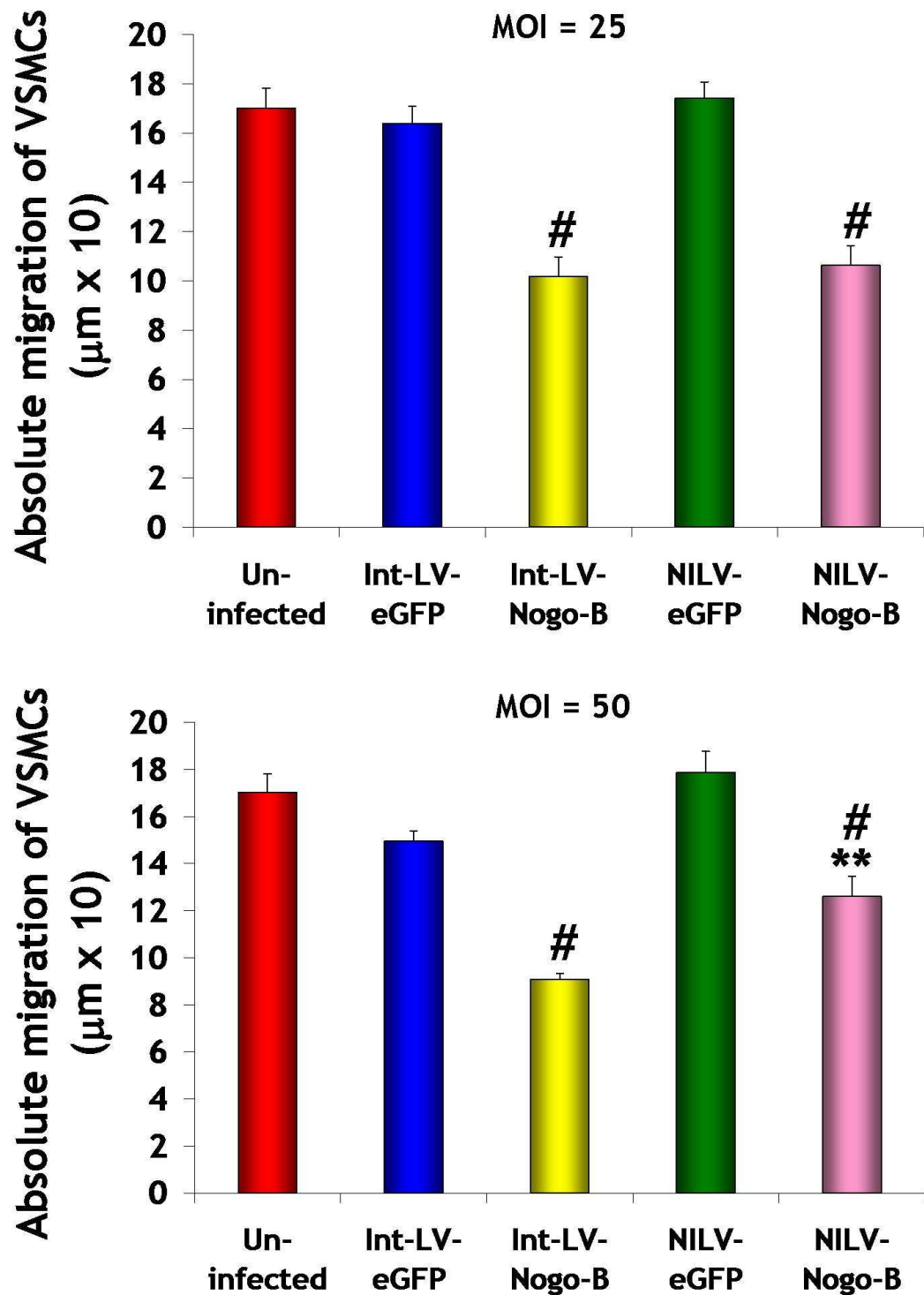


**Figure 4.15. Effect of NILV-Nogo-B on VSMC migration.** VSMCs were seeded (cell density of  $0.5 \times 10^4$ /well in an 8-well chamber slide) and infected with LVs (in the presence of  $0.5 \mu\text{g}/\text{ml}$  of polybrene for an 18 hours incubation) at MOIs of 25 or 50. VSMC migration was assessed using a scratch wound-mediated cell migration (using p200 tip) assay 3 days post-infection and absolute migration (from the wound edge to the final point of VSMC migration) was measured ( $\mu\text{m}$ ) at 10 hours post-wounding using ImagePro software. For each condition (repeated in triplicate) = 10 migration distances of 3 fields of view were measured. Mean value  $\pm$  S.E.M of patient sample repeated in triplicate. Three independent experiments performed [n=3 (representative of each other), cell population/number of individual VSMC preparations used]. \*\* indicates  $p < 0.01$  vs. un-infected, # indicates  $p < 0.001$  vs. their LV-eGFP controls or un-infected at a MOI of 25, # indicates  $p < 0.001$  (int-LV-Nogo-B) vs. un-infected or int-LV-eGFP at a MOI of 50 and # indicates  $p < 0.001$  (NILV-Nogo-B) vs. NILV-eGFP at a MOI of 50. All statistical analysis was carried out by one-way ANOVA for Bonferroni's post-hoc analysis. VSMC, vascular smooth muscle cell; int-LV, integrating lentiviral vector; NILV, non-integrating lentiviral vector; MOI, multiplicity of infection.

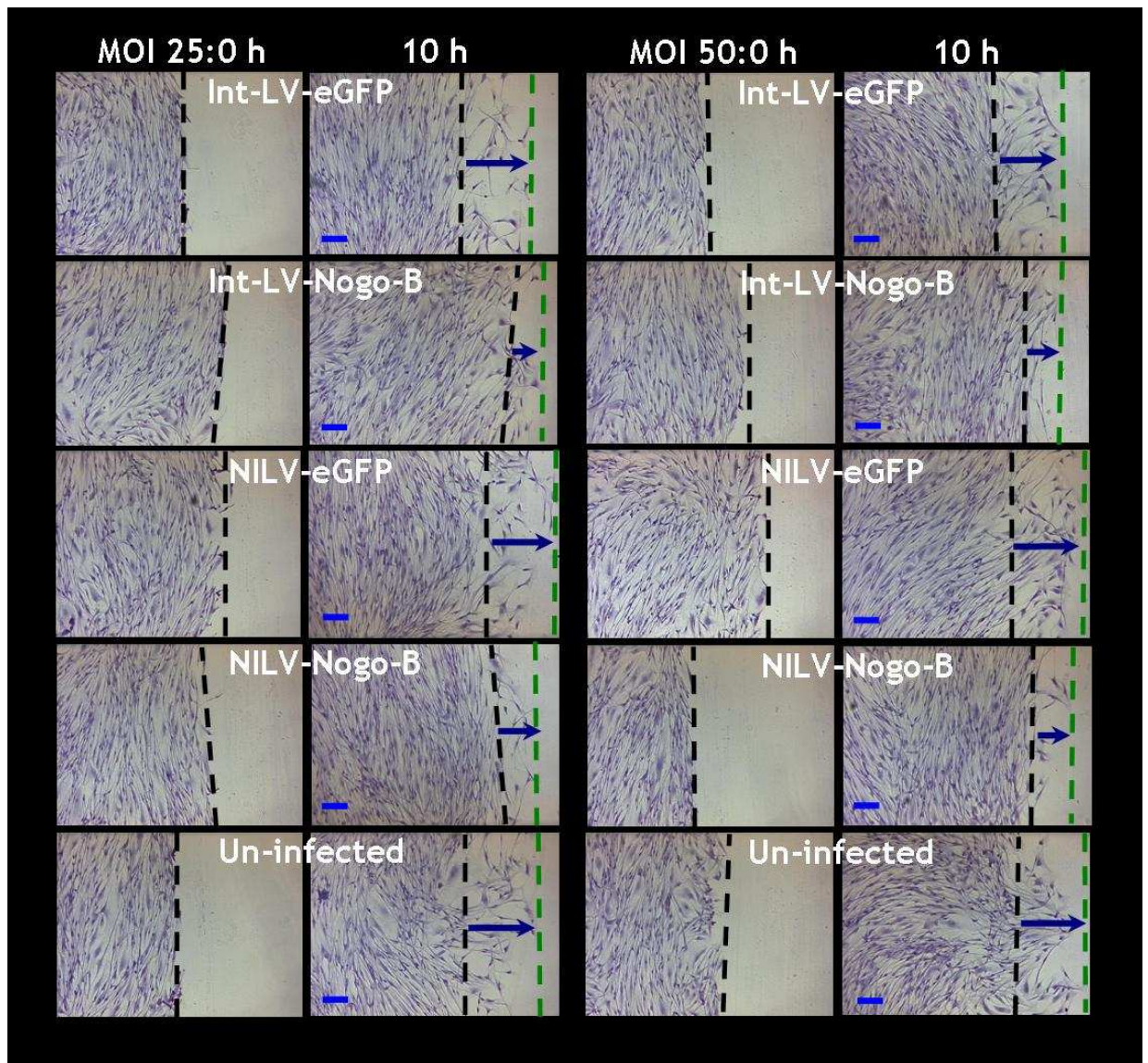


**Figure 4.16. Representative images of the effect of NILV-Nogo-B on VSMC migration.**

Micrographs of the scratch wound-mediated cell migration assay at 0 (hours) h and 10 h post-wound. 100  $\mu\text{m}$  scale bar applicable to all panels (magnification  $\times 100$ ). Representative of  $n=3$  (cell population/number of individual VSMC preparations used) in triplicate. VSMC, vascular smooth muscle cell; int-LV, integrating lentiviral vector; NILV, non-integrating lentiviral vector; MOI, multiplicity of infection.

#### 4.2.3.3 Assessment of the effects of NILV-Nogo-B in VSMC proliferation

Additionally, the effect of NILV-mediated gene delivery of Nogo-B on VSMC proliferation was explored. As before (section 4.2.2.3), a MTT assay was carried out to assess proliferation status in VSMC infected with either NILV-Nogo-B, NILV-eGFP, int-LV-Nogo-B or int-LV-eGFP at MOIs of 10, 25 or 50 or un-infected, at 5 d post-transduction. Results from this VSMC proliferation assay demonstrated that NILV-Nogo-B gene delivery significantly reduced VSMC proliferation at MOIs of 25 and 50, compared to NILV-eGFP control or un-infected VSMCs [MOI 25:  $0.14 \pm 0.0084$  OD vs.  $0.29 \pm 0.01$  OD (52 % significant reduction in VSMC proliferation) or  $0.33 \pm 0.0038$  OD (58 %), respectively,  $p < 0.001$ , and MOI 50:  $0.074 \pm 0.0011$  OD vs.  $0.2 \pm 0.013$  OD (63 %) or  $0.35 \pm 0.015$  OD (79 %), respectively,  $p < 0.001$ ] (Figure 4.17). Representative images (prior to the MTT assay) illustrated this VSMC anti-proliferation effect mediated by NILV-Nogo-B 5 d post-transduction at a MOI of 50 (Figure 4.18). These proliferation results also restated that int-LV-Nogo-B-mediated gene delivery reduced VSMC proliferation unlike its control vector (at MOIs of 25 and 50) or un-infected VSMCs [MOI 25:  $0.24 \pm 0.0031$  OD vs.  $0.32 \pm 0.0064$  OD (25 % significant reduction in VSMC proliferation) or  $0.33 \pm 0.0038$  OD (27 %), respectively,  $p < 0.001$ , and MOI 50:  $0.15 \pm 0.0038$  OD vs.  $0.28 \pm 0.0031$  OD (46 %) or  $0.35 \pm 0.015$  OD (57 %), respectively,  $p < 0.001$ ] (Figure 4.17). In addition, these results also reported that NILV-Nogo-B gene delivery (at MOIs of 25 and 50) was at least as good as int-LV-Nogo-B in mediating a reduction in VSMC proliferation (Figure 4.17).

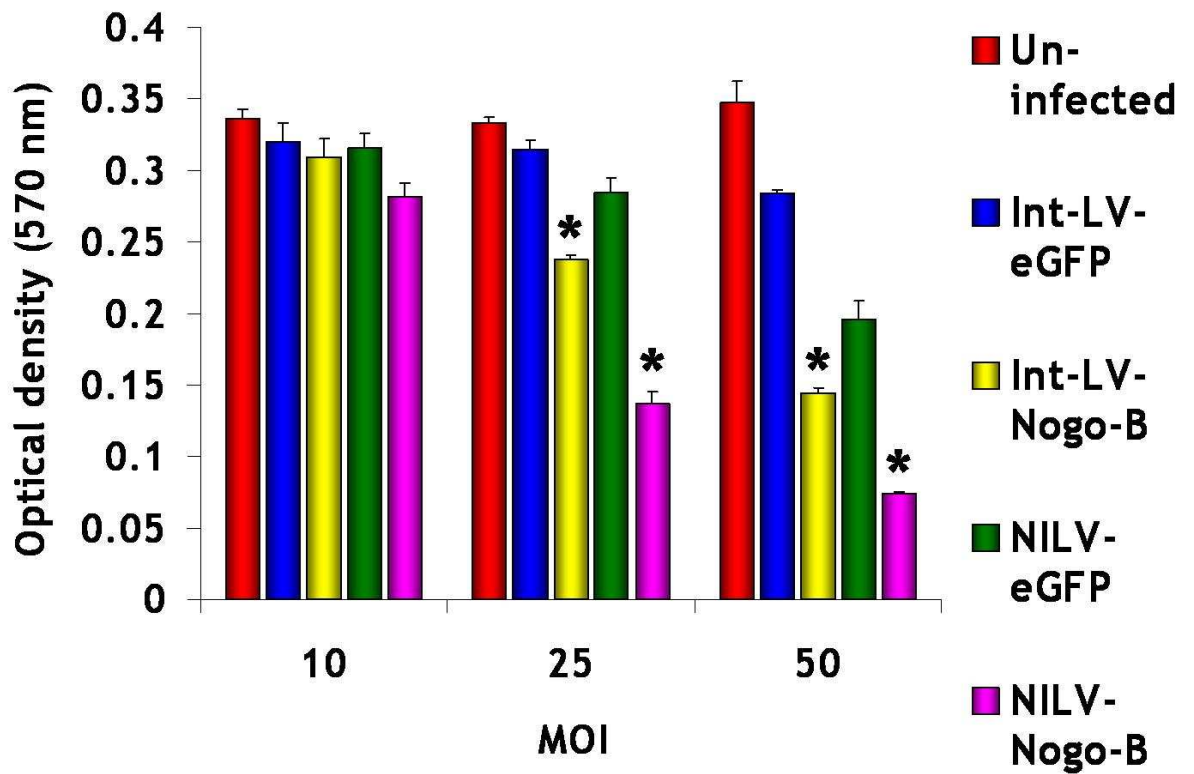


**Figure 4.17. Effect of NILV-Nogo-B on VSMC proliferation.**

VSMCs were seeded (at a cell density of  $0.5 \times 10^4$ /well on a 48-well plate and quiescence of 48 hours in serum-free culture media prior to LV infection) and infected with LVs in 15% serum (in the presence of 8  $\mu\text{g/ml}$  of polybrene for 18 hours incubation) at MOIs of 10, 25 or 50. VSMC proliferation was assessed using a MTT assay, 5 days post-transduction and optical density was measured at 570 nm wavelength. Mean value  $\pm$  S.E.M of patient sample repeated in quadruplicate. Three independent experiments performed [n=3 (representative of each other), cell population/number of individual VSMC preparations used]. \* indicates  $p < 0.001$  vs. their eGFP control vector or un-infected. All statistical analysis was carried out by one-way ANOVA for Bonferroni's post-hoc analysis. VSMC, vascular smooth muscle cell; int-LV, integrating lentiviral vector; NILV, non-integrating lentiviral vector; MOI, multiplicity of infection.

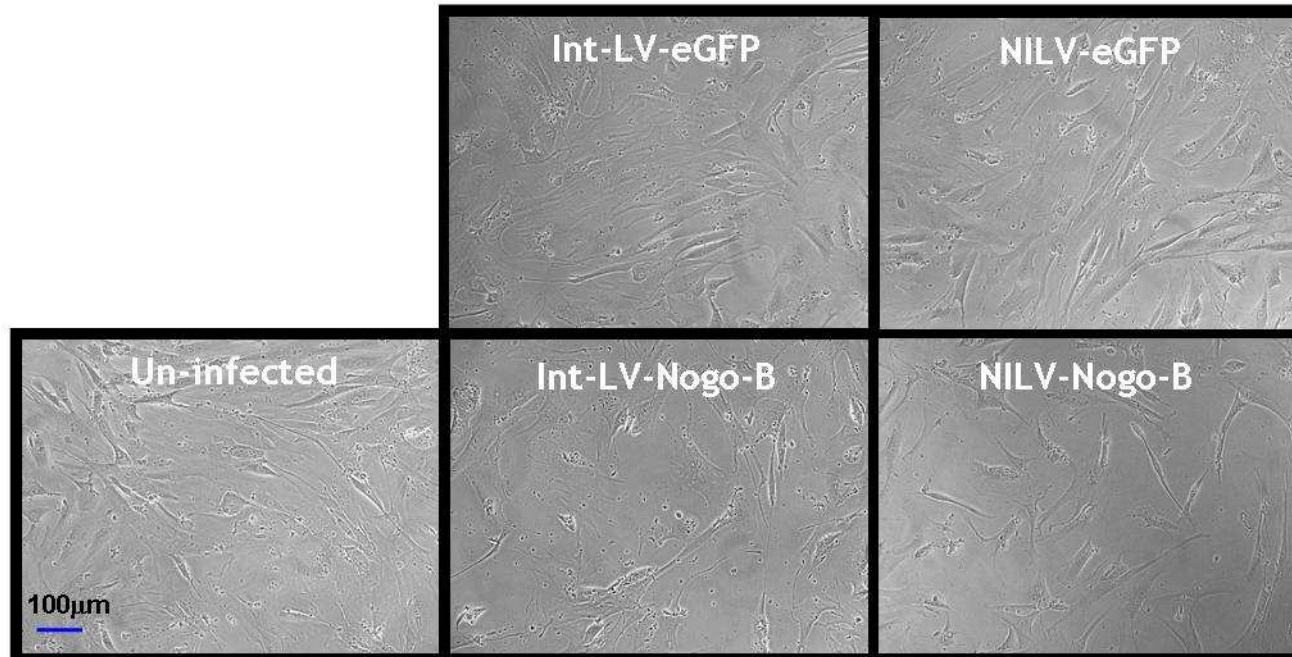


**Figure 4.18. Representative images of the effect of NILV-Nogo-B on VSMC proliferation.**

Bright-field micrographs of the VSMC proliferation assay 5 days post-infection at a MOI 50, prior to the MTT assay. 100  $\mu\text{m}$  scale bar applicable to all panels (magnification  $\times 100$ ). Representative of  $n=3$  (cell population/number of individual VSMC preparations used) in quadruplicate. VSMC, vascular smooth muscle cell; int-LV, integrating lentiviral vector; NILV, non-integrating lentiviral vector; MOI, multiplicity of infection.

### 4.3 Discussion

In this chapter, a new gene delivery vector NILV-Nogo-B was constructed and evaluated for its potential therapeutic utility in the prevention of the NIF following acute vascular injury. Here, successful cloning of Nogo-B cDNA (full-length and mutant) led to the production of VSV-g pseudotyped second-generation SIN int-LV-full-length Nogo-B, int-LV-mutant Nogo-B and NILV-Nogo-B, with transgene expression under the control of an internal heterologous viral promoter SFFV.

- Once it was established that int-LV-Nogo-B (full-length) gene delivery in primary human VSMCs induced efficient Nogo-B up-regulation and mediated phenotypic modulation in VSMC migration and proliferation; subsequently NILV-Nogo-B-mediated gene transfer was then tested. Unfortunately, the expression of mutant (soluble) Nogo-B mediated by int-LV-facilitated gene transfer in VSMCs could not be determined (however, was ascertained in HeLa cells), and thus the effects of int-LV-mutant/soluble Nogo-B transduction on VSMC migration and proliferation were not pursued.
- Most importantly, these experiments demonstrated efficient Nogo-B over-expression in VSMCs transduced with NILV-Nogo-B, and as a consequence successfully reduced VSMC migration and proliferation. NILV-Nogo-B-mediated gene transfer was as efficient as its integrating counterparts by mediating inhibition on VSMC migration and proliferation. Interestingly, NILV-Nogo-B gene delivery appeared better than int-LV-Nogo-B in mediating a reduction on VSMC proliferation.

Adenoviral vectors are the most widely used and extensively studied viral vector gene delivery systems for vascular gene therapy (George et al., 1998a, George et al., 1998b, George et al., 2000, George et al., 2001, Acevedo et al., 2004, Kritiz et al., 2008). Indeed, advances have demonstrated stent-based adenoviral-delivery of TIMP-3 (Johnson et al., 2005) and endothelial nitric oxide synthase (eNOS) (Sharif et al., 2008) reduced ISR *in vivo*. Adenoviral-Nogo-B gene delivery in the vasculature has potential for being a useful therapeutic strategy in rescuing injury-induced NIF following revascularisation (Acevedo et al., 2004,

Kritz et al., 2008). LVs are an alternative and promising gene delivery vector system for the vasculature (Dishart et al., 2003a, Cefai et al., 2005, Qian et al., 2006, Yang et al., 2010). LVs have the potential to mediate gene transfer of a therapeutic gene key to the inhibition of the NIF into the vasculature within a short time exposure, which is required in this clinical setting (Dishart et al., 2003a, Cefai et al., 2005). Firstly, in this study, int-LV-Nogo-B transduction was indicated to be an efficient and effective vector system for Nogo-B over-expression, and its mediated effects on inhibition of VSMC invasion and proliferation in a well-established *in vitro* culture model of VSMCs during vascular injury (used over the years in a large number of vasculature investigations) (Ross et al., 1977). In relevance to these results, Dishart *et al.*, demonstrated that VSV-g pseudotyped int-LV gene delivery of TIMP-3 (another therapeutic gene key to the inhibition of NIF) mediated efficient transduction and over-expression in human VSMCs, which phenotypically modified VSMCs *in vitro* (in terms of reduced chemotaxis and induced apoptosis) (Dishart et al., 2003a). Evidently, LVs are highly efficient in transduction of VSMCs and mediated effective delivery of therapeutic genes key to the inhibition of the NIF.

Before this study, previous investigations had used LVs as their gene transfer vector of choice for the vasculature (Dishart et al., 2003a, Cefai et al., 2005, Qian et al., 2006, Yang et al., 2010), however none had used NILVs. This *in vitro* study addresses the novelty and potential of NILVs for future utility in vascular cell gene delivery in preclinical studies. Permanent transgene expression is not necessarily required in this clinical niche, because indeed many preclinical acute vascular injury models have demonstrated adenoviral-mediated transient transgene expression can provide sufficient therapeutic benefits (George et al., 2000, Wan et al., 2004, Johnson et al., 2005, Kritz et al., 2008). In addition, VSMCs have relatively low rates of proliferation in a disease state (Gordon et al., 1990), and during the acute vascular injury response (Westerband et al., 1997, Hilker et al., 2002) with a proliferative index of approximately 1.34 % (Westerband et al., 1997). Previous studies have shown NILVs especially the D64V mutants to have important aspects relevant for gene transfer into post-mitotic cells within different organs (eye, muscle and CNS of rodents), by retaining transduction efficiency of their wild-type integrase versions with

minimal host genome integration *in vitro* and *in vivo* (Yanez-Munoz et al., 2006, Apolonia et al., 2007, Rahim et al., 2009). In relation to these preclinical reports, results from this *in vitro* study implied efficient gene transfer and transgene expression mediated by NILV-Nogo-B in human VSMCs was similar to that of int-LV-Nogo-B, and as a consequence was as efficient as its integration-proficient counterparts in modulating phenotypic effects of VSMCs. Therefore, data reported in this study denotes the use of NILVs as an alternative and promising gene transfer vector system. It is important to note that even though NILV-Nogo-B is as efficient and effective in modulating VSMC phenotypic effects, it is therefore essential to analyse the following in subsequent studies: quantify the viral copy numbers per cell in contrast to int-LVs and at various matched MOIs by qPCR at a very early time point (Rahim et al., 2009); measure non-integrated viral DNA [containing a junction of the two deleted U3 region in the LTR present in SIN vectors (2d-LTR circles)] copy numbers per total viral DNA copy numbers by qPCR (Yanez-Munoz et al., 2006, Apolonia et al., 2007), to determine that transgene expression in VSMCs transduced with NILVs originates from non-integrated vector templates (transcriptionally proficient episomes) in parallel to int-LVs; detect and determine vector-host DNA junctions mediated by the NILV DNA (due to genomic integration of episomal LV forms could possibly occur through DNA breaks located anywhere in the vector circle) in contrast to int-LVs by linear amplification-mediated (LAM)-PCR (Yanez-Munoz et al., 2006), and furthermore determine residual integration efficiencies in transduced VSMCs with NILVs in contrast to their integrating counterparts (Yanez-Munoz et al., 2006, Apolonia et al., 2007). In summary, all these experiments mentioned are important and should be considered for further experiments involving NILV gene transfer and transgene expression of Nogo-B in VSMCs.

Evidently, the soluble N-terminal domain of Nogo-B (soluble Nogo-B) promotes adhesion to VECs and VSMCs, and modulates migration of these vascular cells (Acevedo et al., 2004), as previously mentioned. Soluble Nogo-B has a high-affinity for the Ng-BR, and as consequence promotes soluble Nogo-B-mediated chemotaxis and tube formation of VECs *in vitro* (Miao et al., 2006). Furthermore, full-length and soluble Nogo-B (both human) rescued defects in intersomitic vessel formation in Nogo-B knock-down zebrafish embryos (Zhao et al., 2010). Taken together, these previous reports support the conclusion that soluble Nogo-

B is the functional domain in VEC migration and VSMC migration. LVs expressing mutant (soluble) Nogo-B were generated in this study, and is a novel vector which has never been tested for its effects on VSMC proliferation and migration *in vitro*. Unfortunately, this int-LV-mutant Nogo-B was undetermined for its mediated expression of mutant (soluble) Nogo-B in VSMC cell lysates and supernatants (however was ascertained in HeLa cells), and therefore was put on hold for optimisation and evaluation on VSMC proliferation and migration.

Nogo-B is presumed to also exert its effects on VEC and VSMC migration through a bystander effect. However, the mechanism of secreting this transmembrane protein is unclear. Secreted Nogo-B (circulating Nogo-B) can be detected in human plasma (Rodriguez-Feo et al., 2007). Results from this study also indicated that secreted Nogo-B can be detected in the conditioned media of un-infected human VSMC (45-50 kDa). Interestingly, enhanced secreted Nogo-B was found present in the supernatant of VSMCs infected with int-LV-Nogo-B or NILV-Nogo-B, in contrast to their control eGFP vector and un-infected VSMCs (endogenous level). In addition, it is important to assess the effects of secreted Nogo-B from its conditioned media on VSMC migration and proliferation *in vitro* and thus further experiments should be considered.

Here, results from this *in vitro* study illustrated that int-LV-Nogo-B and NILV-Nogo-B enhanced Nogo-B expression in VSMC lysates, in contrast to their LV-eGFP controls and un-infected VSMCs, and in contrast to these supernatants. This is plausible since Nogo-B is a reticulon protein with a small fraction found within the cell-membrane of VSMCs (Acevedo et al., 2004). These results don't show whether Nogo-B over-expression is co-localised with the ER and/or cell-membrane, and therefore will require more investigation.

Nogo-B has a favourable profile in the attenuation of the NIF following stenting and vascular bypass grafting. This was determined by adenoviral-mediated over-expression of Nogo-B, reduced the NIF in two acute vascular injury animal models (porcine vein graft model and murine wire-injury model); this notably was achieved by a reduction in VSMC invasion and proliferation (Kritz et al., 2008). In relevance to this, results from this current study further confirmed and extended previous *in vitro* data performed (Kritz et al., 2008). Int-LV-Nogo-B and NILV-Nogo-B mediated gene delivery, reduced VSMC proliferation in a similar

*in vitro* proliferation assay (measured using a MTT assay) implemented by Kritz *et al.*, (2008). This proliferation assay (48 h of VSMC quiescence prior to LVs infections in 15 % serum stimulation) mimics the gene transfer to the vasculature. This is because as mentioned previously at the preferred time of gene delivery during revascularisation, most VSMCs are quiescent with a relatively low rate of proliferation. It should be noted that the MTT assay is not without its limitations, and only measures the reduction of tetrazolium component (MTT) into an insoluble formazan product by the mitochondria of viable cells and not proliferation directly. In addition, further well-established proliferation experiments such as bromodeoxyuridine (BrdU) incorporation analysis and/or Ki67 detection for quantification of proliferating VSMCs, and propidium iodide staining and flow cytometric analysis for quantification of cell-cycle populations, should be considered to confirm VSMC proliferation results observed with NILV-Nogo-B. Determination of int-LV-Nogo-B and NILV-Nogo-B mediated effects on the inhibition of VSMC migration was confirmed using a scratch-wound cell migration assay, which mimics VSMC migration *in vivo* compared to a chemotaxis assay (Liang *et al.*, 2007), and therefore extends previous *in vitro* VSMC findings of adenoviral-Nogo-B over-expression (Kritz *et al.*, 2008). 15 % serum was used to maintain these healthy statuses of LV-infected VSMCs. However, this scratch-wound cell migration assay does not rule out the influence of VSMC proliferation and slightly dilutes these findings. Additionally, the optimisation for the minimal percentage of serum used for this scratch-wound mediated cell migration assay should have been considered (Liang *et al.*, 2007). Furthermore, these migration results could be corrected for proliferation subsequently after the scratch-wound migration assay by measuring for proliferation using the MTT or BrdU assay, and thus further experiments should be considered. Plus, a chemotaxis assay should be considered to support that NILV-Nogo-B-mediated gene transfer reduces VSMC migration.

It is still unknown on the mechanism of how Nogo-B inhibits VSMC migration and proliferation, and therefore will require further investigation. Current results and previous data, demonstrate that Nogo-B is a favourable candidate therapeutic gene in vascular gene therapy for the prevention of NIF following acute vascular injury. This is because of its ability to negatively regulate VSMC migration (Acevedo *et al.*, 2004, Kritz *et al.*, 2008) and proliferation (Kritz *et*

al., 2008), and in addition to its function as a positive regulator of VEC migration as previously demonstrated (Acevedo et al., 2004, Miao et al., 2006, Zhao et al., 2010).

Collectively, these findings report that NILV-Nogo-B retains transduction efficiency of its integrating counterparts in human VSMCs. As a direct result, this vector efficiently induces Nogo-B over-expression, and is as effective as int-LV-Nogo-B in modulating phenotypic effects of VSMC migration and proliferation *in vitro*. Thereby, these data support the use of NILV-Nogo-B as a new candidate for therapeutic application to acute vascular injury. In conclusion, this study addresses the potential of NILVs for future utility in therapeutic gene transfer in the vasculature.

## **5 Analysis of the Mechanism of Action of Nogo-B**

## 5.1 Introduction

Injury-induced NIF was rescued by adenoviral-mediated Nogo-B gene delivery (Acevedo et al., 2004, Kritz et al., 2008), an effect mediated by Nogo-B through the stimulated migration of VECs (Acevedo et al., 2004), and reduced VSMC migration (Acevedo et al., 2004, Kritz et al., 2008) and proliferation (Kritz et al., 2008). Nogo-B is essential for stimulating the chemotaxis and morphogenesis of VECs through its engagement with the Ng-BR [presumed to be on the cell surface of VECs (Miao et al., 2006)] via the Akt signalling pathway (Figure 1.15) (Zhao et al., 2010). In terms of VSMCs, it is speculated that the negative regulation on VSMC migration in response to PDGF-BB by Nogo-B, possibly occurs through the effect of functional repression of PDGF signalling downstream of the receptor or by competitive antagonism of the PDGF receptor (PDGFR) tethering (Acevedo et al., 2004). It is understood that Nogo-B blocks VSMC proliferation (Kritz et al., 2008), however a definitive mechanism is unknown. It has been suggested that the phenotypic effect on VSMC proliferation and/or migration by Nogo-B could be mediated by ER-specific activities (for example modulation of the structure of the ER network in association with cytoskeletal structures and/or ER-stress mediated apoptosis) and/or facilitated through the modulation of intracellular signal transduction pathways (Figure 1.15) (Raines, 2004a). Therefore, it is important to define/validate the mechanism of action of Nogo-B, to help understand its ability to restrict the NIF after acute vascular injury and for possible future use in the clinical setting of vascular gene therapy.

### 5.1.1 Association of Nogo-B with VSMC apoptosis and ER-stress

Nogo-B (reticulon protein) is primarily found co-localised with the ER [due to its ER retention sequence at the C-terminal region (Raines, 2004a, Dodd et al., 2005)] with a small fraction found within the cell-membrane of vascular cells (Acevedo et al., 2004). In chapter 4, it was reported that the over-expression of Nogo-B was greatly enhanced in VSMC lysates mediated by int-LVs or NILVs, in contrary to supernatants. Nogo-B over-expression co-localised with the ER in VSMCs has yet to be explored.

It has been reported that the over-expression of Nogo-B can act as a pro-apoptotic protein in various cancer cells (Li et al., 2001, Tambe et al., 2004),

without any known apoptosis-related motifs (Li et al., 2001). Nogo-B has the ability to interact with anti-apoptotic members of Bcl-2 and Bcl-x<sub>L</sub> and prevent their translocation to the mitochondria from the ER, and thus reducing their anti-apoptotic effect (Tagami et al., 2000, Watari and Yutsudo, 2003). Interestingly, increased amounts of Nogo-B were found in macrophage/foam cell-rich areas of human atherosclerotic plaques (Rodriguez-Feo et al., 2007), and enhanced adventitial Nogo-B expression was reported in macrophages and VSMCs from a rabbit balloon injury-induced NIF model (Paszkwiaik et al., 2007). Both studies suggest that Nogo-B may potentially play a role in macrophage and VSMC induced apoptosis and/or plaque vulnerability/rupture (Paszkwiaik et al., 2007, Rodriguez-Feo et al., 2007). In chapter 4, the potential of NILV-Nogo-B induced over-expression and phenotypic effects on VSMC migration and proliferation *in vitro* was reported. In addition, it is important to assess the possible effects of Nogo-B over-expression on VSMC apoptosis mediated by these vectors.

Oertle *et al.*, (2003c) speculated that highly over-expressed Nogo-B induced ER-stress-mediated apoptosis. In addition, Nogo-B over-expression has been demonstrated to induce ER-stress-mediated apoptosis through ER-specific pathways in HeLa cells (discussed later in this chapter) (Kuang et al., 2006). The ER has essential roles in various cellular processes, for example folding of secretory and membrane proteins, calcium homeostasis and lipid biosynthesis (Minamino and Kitakaze, 2010, Minamino et al., 2010). A variety of factors such as the over-expression of normal and/or incorrectly folded proteins have the potential to mediate the accumulation of un-folded/misfolded/abnormal protein aggregates, which challenges the function of the ER and this is referred to as ER-stress (imbalance between the cellular demand for the ER function and ER capacity). The accumulation of proteins in the ER membrane increases its calcium ion permeability, and thus mediates the disruption of calcium ion homeostasis (calcium ion depletion of ER stores) in the ER lumen. As a consequence, ER-stress induces the onset of an ER protective mechanism such as the unfolded protein response (UPR) to maintain ER homeostasis (Minamino and Kitakaze, 2010, Minamino et al., 2010). However, caspase-12 an ER-specific caspase (specifically localised on the cytoplasmic side of the ER) is activated by prolonged or overwhelming ER-stress and if homeostasis can not be restored. As

a consequence, mediates the sequential activation of the caspase (-9, -7, -6 and -3) cascade, and thus induces apoptosis (Oertle et al., 2003c, Minamino and Kitakaze, 2010, Minamino et al., 2010). In addition, prolonged ER-stress can also induce apoptosis via the transcriptional induction of C/EBP homologous protein (CHOP) and/or c-JUN NH2-terminal kinase (JNK) signal transduction pathway (Myoishi et al., 2007).

UPR signals transient attenuation of protein translation, degradation of abnormal/misfolded proteins, and the induction of resident-ER chaperones and protein folding enzymes (i.e. foldase) to augment the ER capacity for protein folding, assembly of proteins and degradation. UPR signalling pathway is triggered by the activation of three ER transmembrane sensors: the transcriptional factor activating transcription factor 6 (ATF6), protein kinase-like ER kinase (PERK) and inositol-requiring kinase 1 (IRE1) (located with their N-terminus domain inside the lumen of the ER and C-terminus domain in the cytosol). When the cell is not under stress, all three UPR sensors are maintained in an inactive state through the interaction with an ER chaperone protein glucose-regulated protein 78 kDa (GRP78) also known as binding immunoglobulin protein (BiP). BiP is an ER resident protein and is located inside the lumen of the ER. When the UPR occurs, BiP releases these sensors (from their luminal domains) to co-ordinately regulate the UPR signalling (activation and transduction of unfolded protein signals across the ER membrane to the cytosol and the nucleus), involving the up-regulation of transcription of UPR-related genes encoding other resident-ER chaperones and protein folding enzymes to reduce the accumulation of unfolded proteins. Active ATF6 also up-regulates the transcription of BiP. BiP can also associate and form a complex with caspase -7 and -12. Overall, BiP acts as a key regulator in ER-stress signalling and apoptosis, and a monitor of ER-stress (Lee, 2005, Minamino and Kitakaze, 2010, Minamino et al., 2010).

ER-stress and/or UPR have been implicated in patho-physiology of various diseases, in particular CVDs (Hotamisligil, 2010, Minamino and Kitakaze, 2010, Tabas, 2010). Importantly, the presence of oxidised lipids, inflammation and/or metabolic stress in advanced atherosclerotic plaques have been reported to have the potential to mediate ER-stress and/or the UPR (Sanson et al., 2009, Hotamisligil, 2010, Minamino and Kitakaze, 2010), and as a consequence induce

cell death of macrophages and VSMCs, which would contribute to destabilisation and rupture of atherosclerotic and stenotic lesions (Hotamisligil, 2010, Minamino and Kitakaze, 2010). Indeed, it was reported that there was a strong association between ER-stress markers CHOP and BiP, and apoptosis in ruptured atherosclerotic plaques in 152 human coronary artery autopsy specimens. This suggested that ER-stress is likely to play a role in the progression of plaque vulnerability and occurrence of acute complications of coronary atherosclerosis in humans (Myoishi et al., 2007). Importantly, Nogo-B over-expression induced apoptosis in HeLa cells as a consequence of the ER-stress response as indicated in a study by Kuang *et al.*, (2006). Results demonstrated that Nogo-B over-expression initiated the ER overload response (EOR) (unable to adapt to the UPR), and consequently mediated ER-stress (indicated by an increase in BiP) and the disorder of ER calcium ion stores which induced ER-specific apoptotic pathways [caspase-12 activation and CHOP]. In addition, stable transfectants over-expressing Nogo-B were resistant to ER-stress-mediated apoptosis, which was a direct result of the protective UPR, and thus allowed cells to adapt and cope with large amounts of Nogo-B over-expression (Kuang et al., 2006). Taken together, it is important to evaluate the effect of Nogo-B over-expression mediated by NILVs and int-LVs on VSMC ER-stress and apoptosis.

### ***5.1.2 The association of Nogo-B with signal transduction***

VSMC migration and proliferation is a hallmark of NIF associated with acute vascular injury. There are many environmental stimuli that are associated with the activation of multiple intracellular signal transduction cascades in VSMCs (Muto et al., 2007). For example, growth factors such as PDGF-BB, basic fibroblast growth factor (bFGF) and epidermal growth factor (EGF) induce intracellular signal transduction pathways such as mitogen-activated protein kinases (MAPK) and phosphatidylinositol 3-kinase (PI3K)-Akt (Muto et al., 2007, Yu et al., 2007, Morello et al., 2009) in VSMCs. These two pathways have implications in the vascular response to injury and play important roles in the regulation of cell survival, migration, and proliferation and differentiation events in vascular cells (Muto et al., 2007, Yu et al., 2007, Morello et al., 2009). A receptor tyrosine kinase (RTK) (a membrane associated receptor) such as the PDGFR-beta (PDGFR- $\beta$ ) is activated by the binding of its ligand PDGF-BB to its extracellular domains, which subsequently induces proliferation, migration and

cell survival of VSMCs (Ferns et al., 1990, Ferns et al., 1991, Holycross et al., 1992, Jawien et al., 1992). Upon activation, PDGFR- $\beta$  receptors dimerize and are stimulated by auto-phosphorylation of several sites on their cytosolic domains, which then mediates binding of co-factors and activates signal transduction pathways, and subsequently exerts its down-stream effects such as regulation of gene expression and the cell-cycle. The PDGFR not only activates MAPK pathways but also the PI3K-Akt pathway (Muto et al., 2007). MAPK family consists of three sub-families: extracellular signal-regulated kinase (ERK; ERK 1 & 2), c-Jun N-terminal kinase (JNK) and p38-MAPK (Yu et al., 2007). All three MAPK pathways have been demonstrated to participate in PDGF-BB-induced VSMC proliferation and migration, using recombinant adenoviral vectors containing dominant-negative mutants of ERK 1 & 2, p38-MAPK and JNK (Zhan et al., 2003). In addition, it is well-established that ERK 1 & 2 activation is important in PDGF-BB-mediated VSMC migration and proliferation (Bornfeldt et al., 1997, Graf et al., 1997, Nelson et al., 1998, Muto et al., 2007, Yu et al., 2007). Evidently, the activation of the PI3K-Akt pathway also plays a pivotal role in the regulation of VSMC contractility and induced proliferation (Shigematsu et al., 2000, Stabile et al., 2003, Muto et al., 2007, Morello et al., 2009). In terms of bone-marrow-derived monocyte/macrophage (BMM) motility and morphology in a hindlimb ischaemia murine model, Nogo-B does not mediate any difference in the activity of ERK1 & 2, p38-MAPK and PI3K-Akt pathways, as demonstrated in BMM in wild-type mice in contrast to Nogo-A/B knockout mice after stimulation with colony stimulating factor-1 (CSF-1) (Yu et al., 2009). In addition, there are no current reports which have assessed the mechanism of action of Nogo-B in VSMCs association with ERK 1 & 2 and PI3K-Akt pathways.

The aim of this chapter was to assess the effect of Nogo-B over-expression in VSMCs *in vitro*, in terms of the following:

- Apoptosis (caspase-3/7)
- Co-location with the ER
- ER-stress
- Signal transduction of ERK 1 & 2 and Akt activity

## 5.2 Results

### ***5.2.1 Assessment of the effects of lentiviral-mediated Nogo-B over-expression on VSMC apoptosis***

After 48 h of VSMC quiescence (induced by serum-deprivation), VSMCs were infected with either int-LV-Nogo-B, NILV-Nogo-B or their LV-eGFP control at a MOI of 50 or un-infected. VSMC apoptosis quantified using a caspase-3/7 activity assay measuring luminescence at 5 d post-infection and then normalised to mg of total protein. Results demonstrated that int-LV-Nogo-B and NILV-Nogo-B mediated Nogo-B over-expression in VSMCs did not significantly induce caspase-3/7 activation (Figure 5.1). Ad-Nogo-B (as mentioned in chapter 4 as Ad-full-length-Nogo-B but now referred here as Ad-Nogo-B in this chapter) versus ad-eGFP (at MOI of 100) or un-infected (no polybrene) were used as a control for caspase-3/7 activity; indicated no significant increase in caspase-3/7 activation (Figure 5.1).

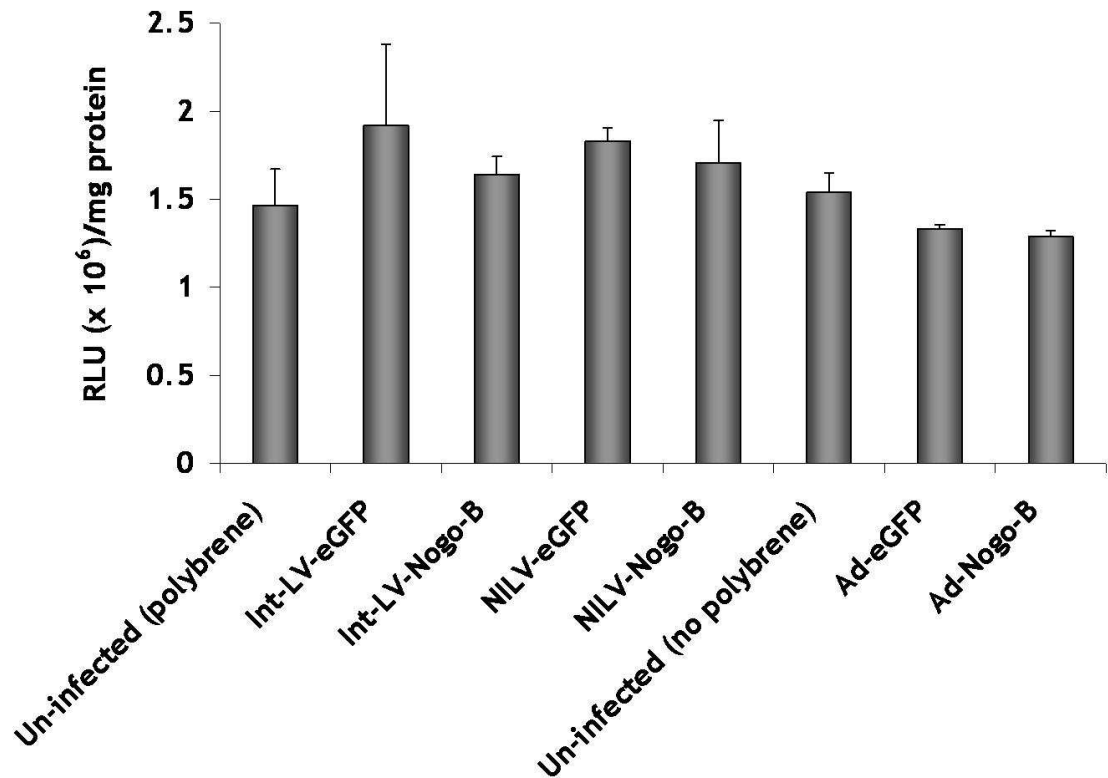


**Figure 5.1. Effect of Nogo-B over-expression mediated by LVs on VSMC apoptosis.**

VSMCs were seeded (at a cell density of  $0.25 \times 10^4$ /well on a 96-well plate and quiescence of 48 h induced by serum-free culture media prior to LV infection) and infected with LVs in 15 % serum (in the presence of 8  $\mu\text{g}/\text{ml}$  of polybrene for 18 h incubation) at a MOI of 50 or un-infected. Additionally, VSMCs were infected with Ad-eGFP or Ad-Nogo-B at MOI of 100 in the presence of no polybrene for 18 h exposure. VSMC apoptosis was assessed using a caspase-3/7 activity assay 5 d post-infection and luminescence was measured in relative luminescence units (RLU) which was then normalised to the total mg of protein (measured by a BCA assay with optical density measured at 570 nm wavelength). Mean value  $\pm$  S.E.M of patient sample repeated in triplicate. Three independent experiments performed [n=3 (representative of each other), cell population/number of individual VSMC preparations used]. No significant difference indicated with: int-LV-Nogo-B vs. int-LV-eGFP or un-infected; NILV-Nogo-B vs. NILV-eGFP or un-infected, and Ad-Nogo-B vs. Ad-eGFP or un-infected. All statistical analysis was carried out by one-way ANOVA for Bonferroni's post-test. VSMC, vascular smooth muscle cell; MOI, multiplicity of infection; Ad, adenoviral vector serotype 5; VSMC, vascular smooth muscle cells; LV, lentiviral vectors; int-LV, integrating-LV; NILV, non-integrating-LV.

### **5.2.2 Over-expression of Nogo-B co-localised with the ER**

The over-expression of Nogo-B co-localisation with the ER in VSMCs mediated by int-LV-Nogo-B at a MOI of 50 was investigated. Immunocytofluorescent staining was performed at 5 d post-infection for the detection of the co-location of ER PDI (mouse monoclonal anti-human ER PDI IgG2a antibody) and Nogo-B (goat polyclonal anti-human Nogo IgG antibody). A corresponding Alexa-Fluor®-594 (donkey anti-mouse IgG antibody, for far red fluorescence) or Alexa-Fluor®-488 (donkey anti-goat IgG secondary antibody, for green fluorescence) secondary antibody was used and confocal microscopy was carried out to observe if the over-expression of Nogo-B co-localised with the ER PDI by yellow fluorescence (green and far red fluorescence merged, respectively). Increased expression levels of Nogo-B were observed co-localised with the ER PDI in VSMCs mediated by int-LV-Nogo-B compared to endogenous levels of Nogo-B in the un-infected VSMCs, as illustrated from fluorescent micrographs in Figure 5.2 A. Isotype-matched negative controls were carried out in parallel. No far red, green and yellow immunocytofluorescent staining was observed with the Isotype-matched negative control, thus no non-specific binding of the anti-Nogo-B antibody and the anti-ER PDI antibody (Figure 5.2 B).

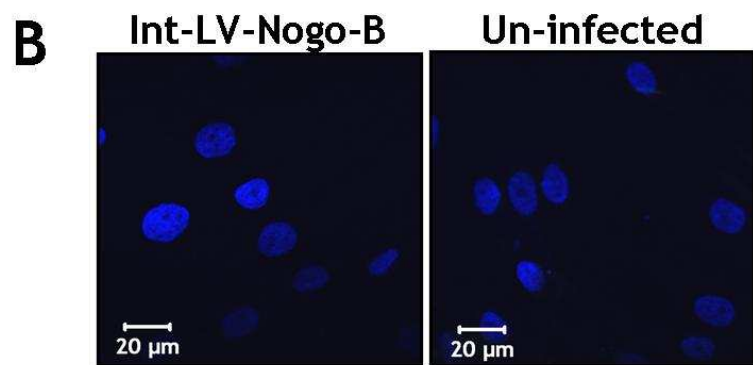
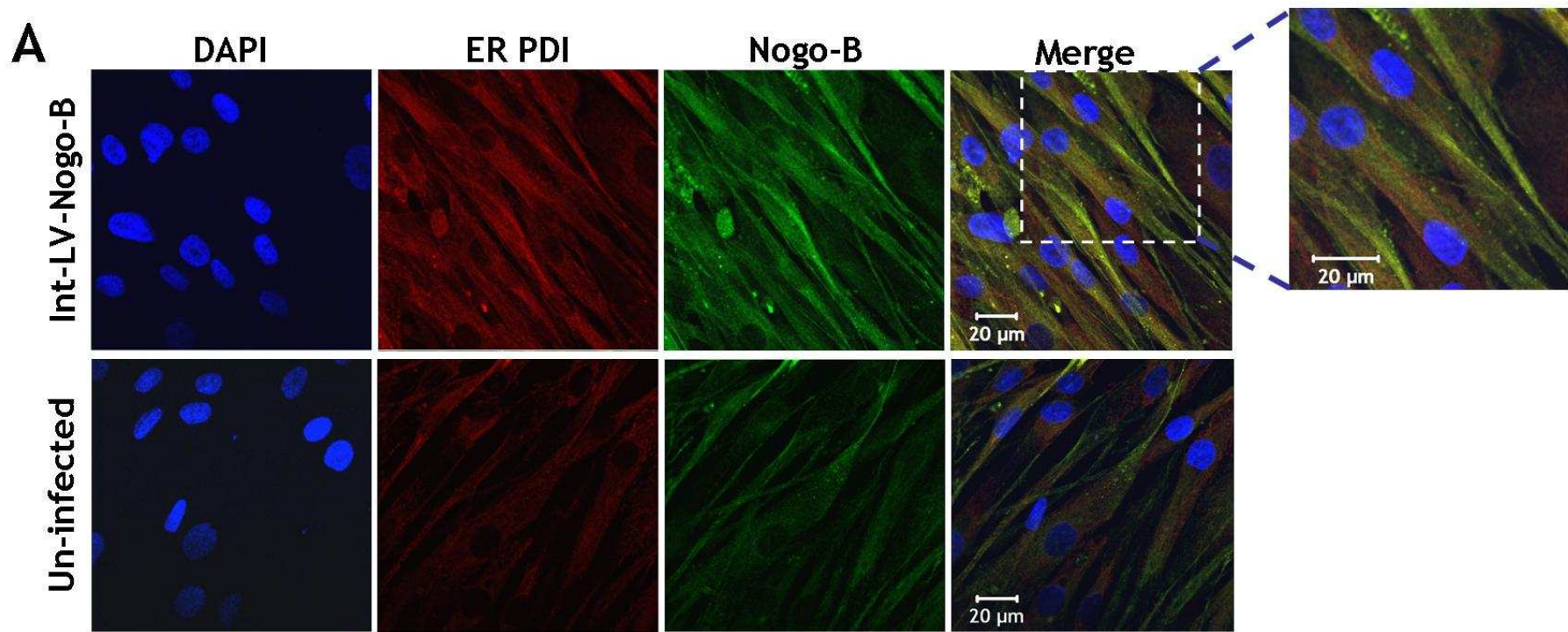


**Figure 5.2. Nogo-B over-expression co-localisation with the ER in VSMCs indicated by immunocytofluorescence.**

Immunocytofluorescent staining was carried out in VSMCs (seeded at a cell density of  $0.5 \times 10^4$ /well on an 8-well chamber slide) at 5 d post-infected with int-LV-Nogo-B (in presence of  $0.5 \mu\text{g/ml}$  of polybrene for 18 h incubation) at a MOI of 50 or un-infected, in permeabilised conditions. **(A)** A mouse monoclonal anti-human ER PDI IgG2a antibody ( $10 \mu\text{g/ml}$ ) and Alexa-Fluor®-594 (far red fluorescence) donkey anti-mouse IgG secondary antibody ( $4 \mu\text{g/ml}$ ) were used to detect ER PDI. A goat polyclonal anti-human Nogo IgG antibody ( $2 \mu\text{g/ml}$ ) and Alexa-Fluor®-488 (green fluorescence) donkey anti-goat IgG secondary antibody ( $4 \mu\text{g/ml}$ ) were used to detect Nogo-B expression. Nogo-B co-localisation with the ER (merge) in VSMCs was illustrated by yellow fluorescence. **(B)** Immunocytofluorescent staining using isotype-matched negative controls (mouse IgG2a and goat IgG) antibodies. Merged fluorescent images illustrated.  $20 \mu\text{m}$  scale bar applicable to all panels (magnification  $\times 630$ ). Representative of  $n=1$  (cell population/number of individual VSMC preparations used) in triplicate. VSMC, vascular smooth muscle cell; int-LV, integrating lentiviral vectors; DAPI, 4', 6-diamidino-2-phenylindole; ER PDI, endoplasmic reticulum protein disulfide isomerase.

### ***5.2.3 Assessment of the effects of Nogo-B over-expression on BiP***

For the rest of this chapter, Ad-Nogo-B was used because low titre preparations of LVs limited their use for assessing the effects of Nogo-B over-expression on VSMC ER-stress signalling and ERK 1 & 2 and PI3K-Akt signal transduction by Western-immunoblotting. However, for mechanistic studies this is not problematic since gene transfer to VSMCs with LV and Ad is very similar (Dishart et al., 2003a). The effect of Nogo-B over-expression in VSMCs on BiP expression levels was evaluated. VSMCs were seeded and infected Ad-Nogo-B or Ad-eGFP at a MOI of 100 or un-infected. VSMC lysates were assessed 5 d post-infection by Western immuno-blotting (normalised to 20 µg of protein loading) to detect BiP expression at approximately 75-78 kDa. Results indicated that the over-expression of Nogo-B mediated by Ad-Nogo-B did not induce BiP expression, compared to the Ad-eGFP control and un-infected VSMCs (SM  $\alpha$ -actin indicated protein loading) (Figure 5.3).

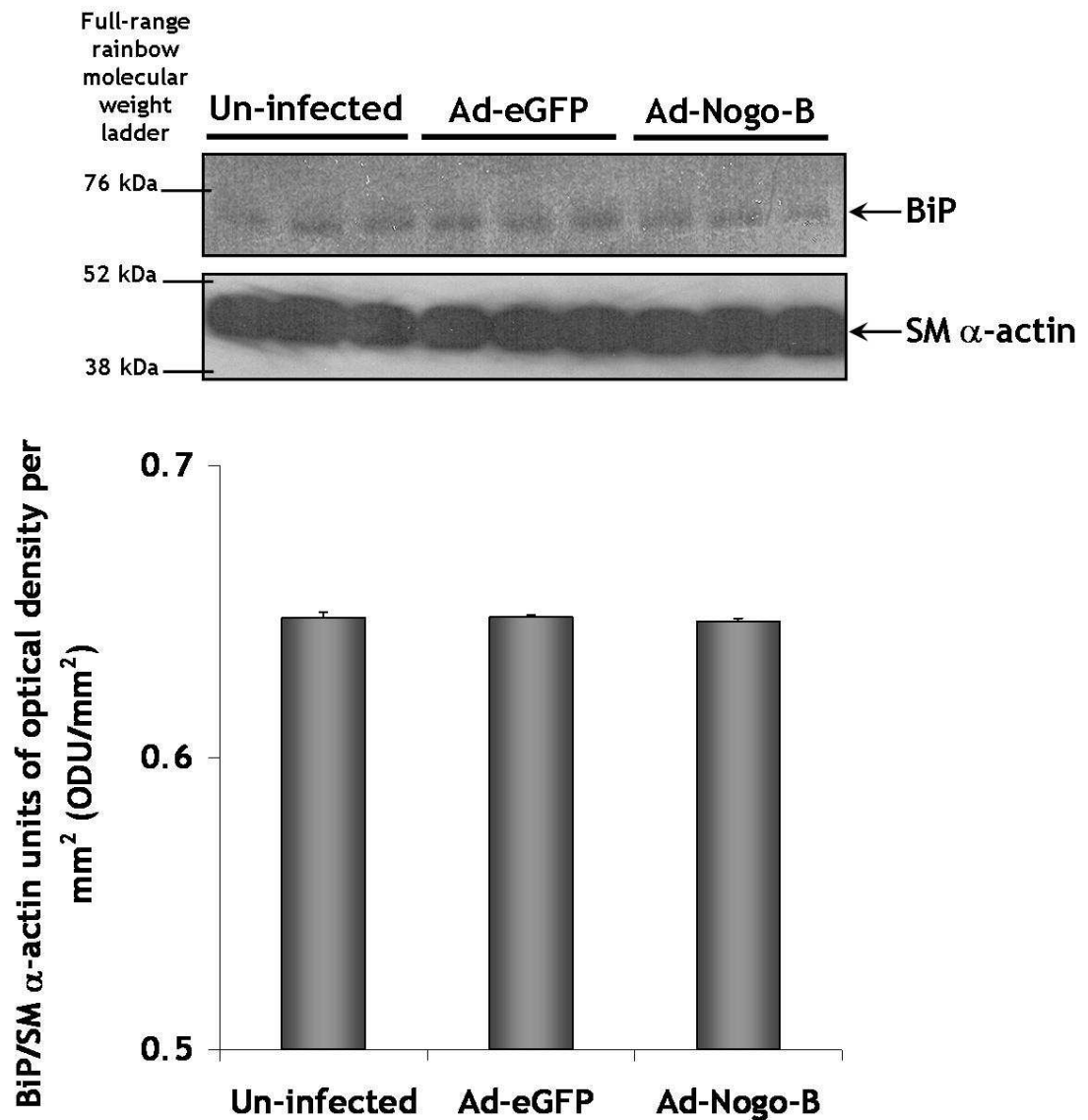
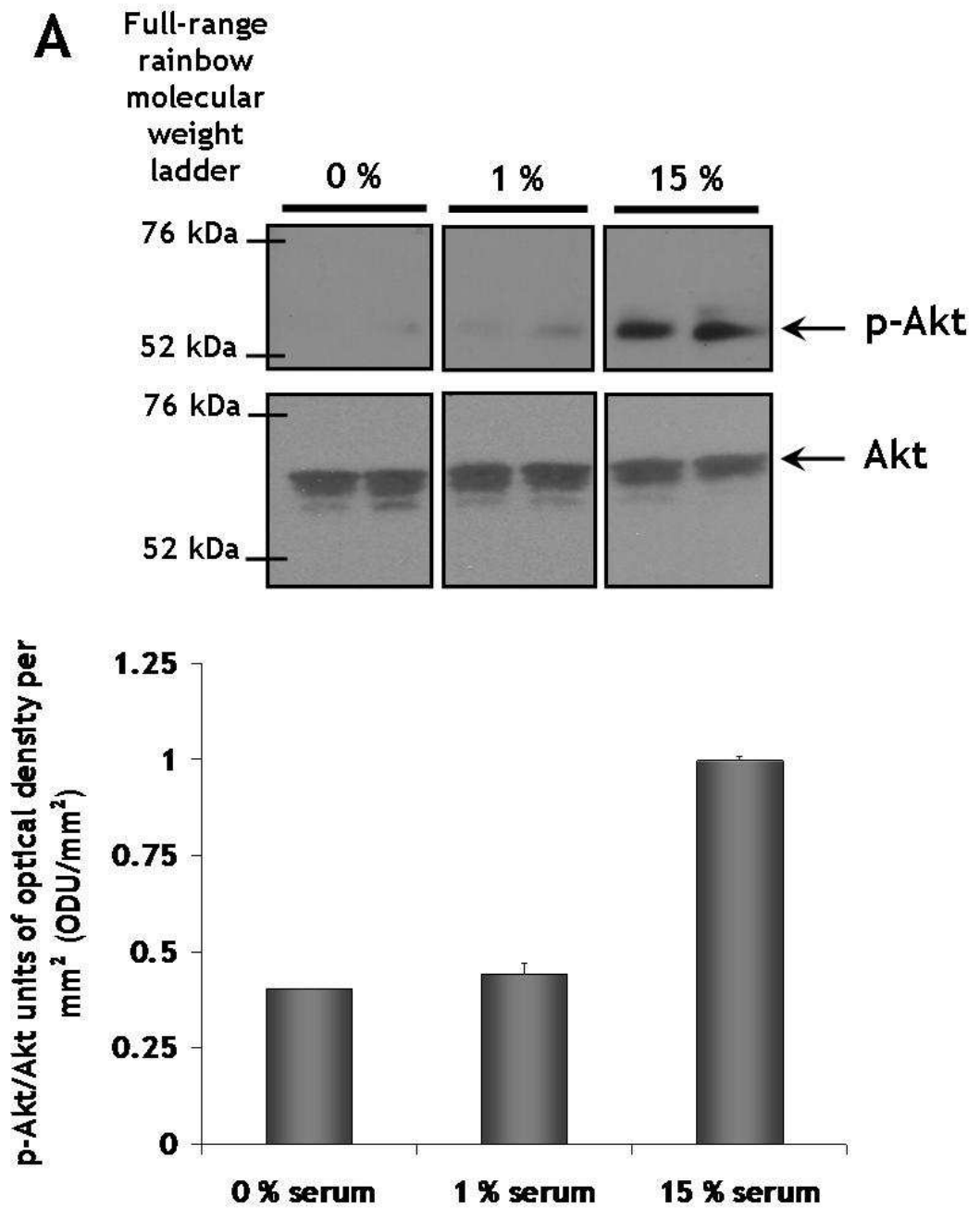


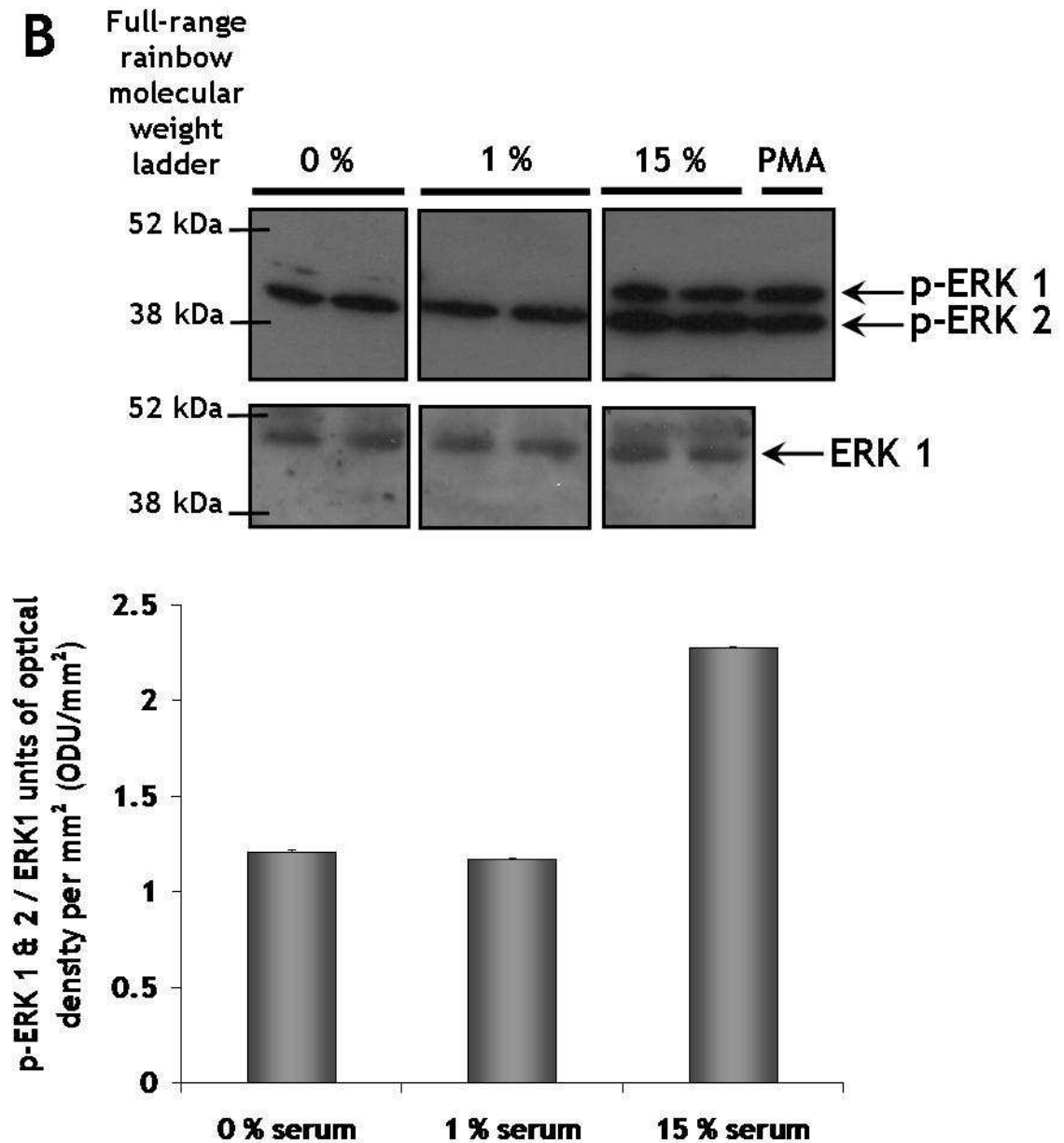
**Figure 5.3.** Effect of Nogo-B over-expression on BiP expression levels in VSMCs.

VSMCs were seeded (at a cell density of  $8 \times 10^4$ /well on a 6-well plate) and infected with Ad-Nogo-B or Ad-eGFP at a MOI of 100 (18 h exposure time), or un-infected. At 5 d post-infection, VSMC lysates [normalised to 20  $\mu$ g of protein loading (protein concentration determined by BCA assay)] were assessed for BiP expression levels (75-78 kDa) by Western immuno-blotting [a rabbit polyclonal anti-human BiP IgG antibody (1  $\mu$ g/ml)]. A mouse monoclonal anti-human SM  $\alpha$ -actin IgG2a antibody was used to detect SM  $\alpha$ -actin (42 kDa) in VSMC lysates for protein loading. BiP expression levels in VSMC lysates were normalised to SM  $\alpha$ -actin using densitometry. Mean value  $\pm$  S.E.M of patient sample repeated in triplicate. Two independent experiments performed [n=2 (representative of each other), cell population/number of individual VSMC preparations used]. No significant difference indicated with Ad-Nogo-B vs. Ad-eGFP or un-infected. All statistical analysis was carried out by one-way ANOVA for Bonferroni's post-hoc analysis. VSMC, vascular smooth muscle cell; Ad, adenoviral vector serotype 5; BiP, binding immunoglobulin protein; SM  $\alpha$ -actin, smooth muscle alpha-actin.

#### **5.2.4 Assessment of the effects of Nogo-B over-expression on VSMC intracellular signalling mechanism**

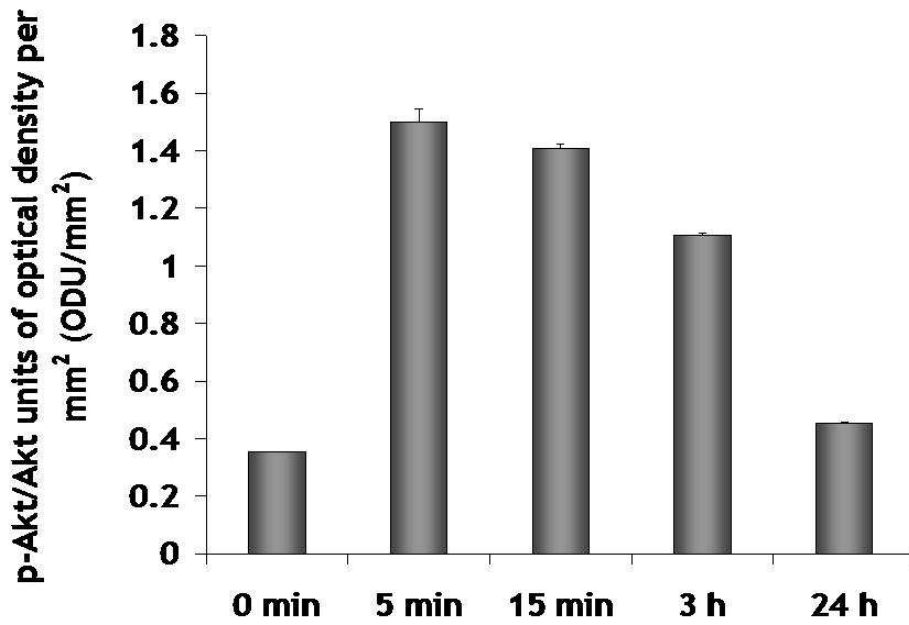
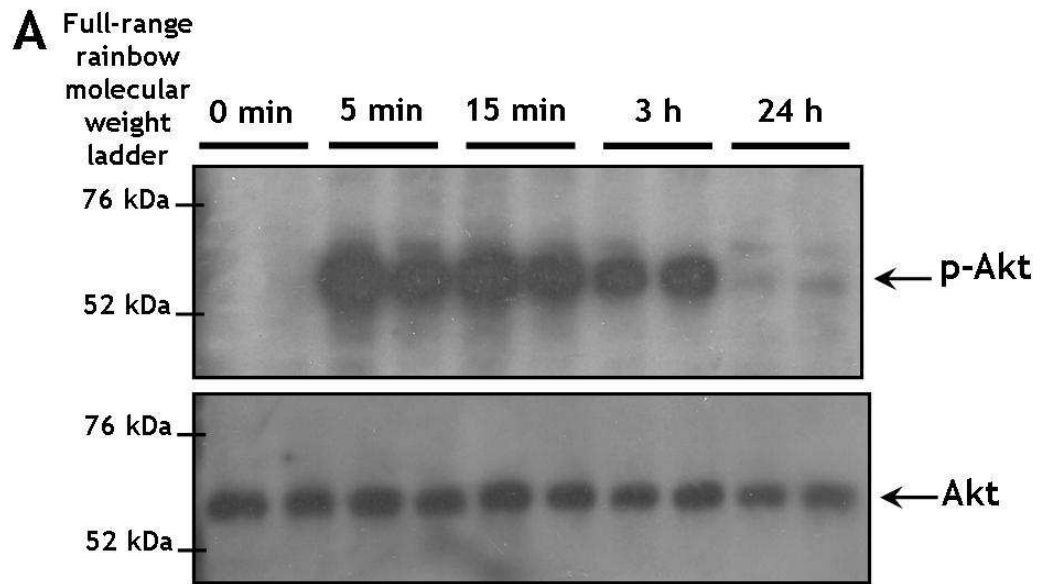
The effects of Nogo-B over-expression on VSMC signal transduction involving phosphorylation of Akt (p-Akt) and ERK 1 & 2 (p-ERK 1 & 2) were assessed. First, the percentage of serum used to cause quiescence in VSMCs which exhibit low Akt and ERK 1 & 2 activity was optimised. VSMCs were cultured in 0 %, 1 % or 15 % serum, and subsequently after 48 h of culture these VSMC lysates were collected and assessed by Western immuno-blotting analysis for Akt and ERK 1 & 2 activity. Results indicated that 1 % serum mediated a low level of p-Akt (60 kDa) and p-ERK 1 (44 kDa), which was similar to 0 % serum but dissimilar to 15 % serum (Figure 5.4). VSMC lysates were normalised to 15 µg of protein loading, and Akt (60 kDa) and ERK1 (44 kDa) indicated equal protein loading, respectively. Phorbol 12-myristate 13-acetate (PMA) was used as a positive control for the activation of ERK 1 & 2 signalling in VSMCs. Second, time points of 15 % serum-stimulation which exhibit high Akt and ERK 1 & 2 activity in VSMCs were optimised. VSMC quiescence was induced with 1 % serum for 48 h and VSMC lysates were collected before serum-stimulation (0 min) and at 5 min, 15 min, 3 h and 24 h after serum-stimulation, and subsequently assessed by Western immuno-blotting analysis. In contrast to un-stimulated VSMCs (0 min), results demonstrated that 15 % serum-stimulation at 5 min, 15 min and 3 h greatly up-regulated p-Akt and p-ERK 1 & 2 levels (44 & 42 kDa, respectively) (Figure 5.5). VSMC lysates were normalised to 15 µg of protein, and Akt and GAPDH (36 kDa) indicated equal protein loading, respectively.

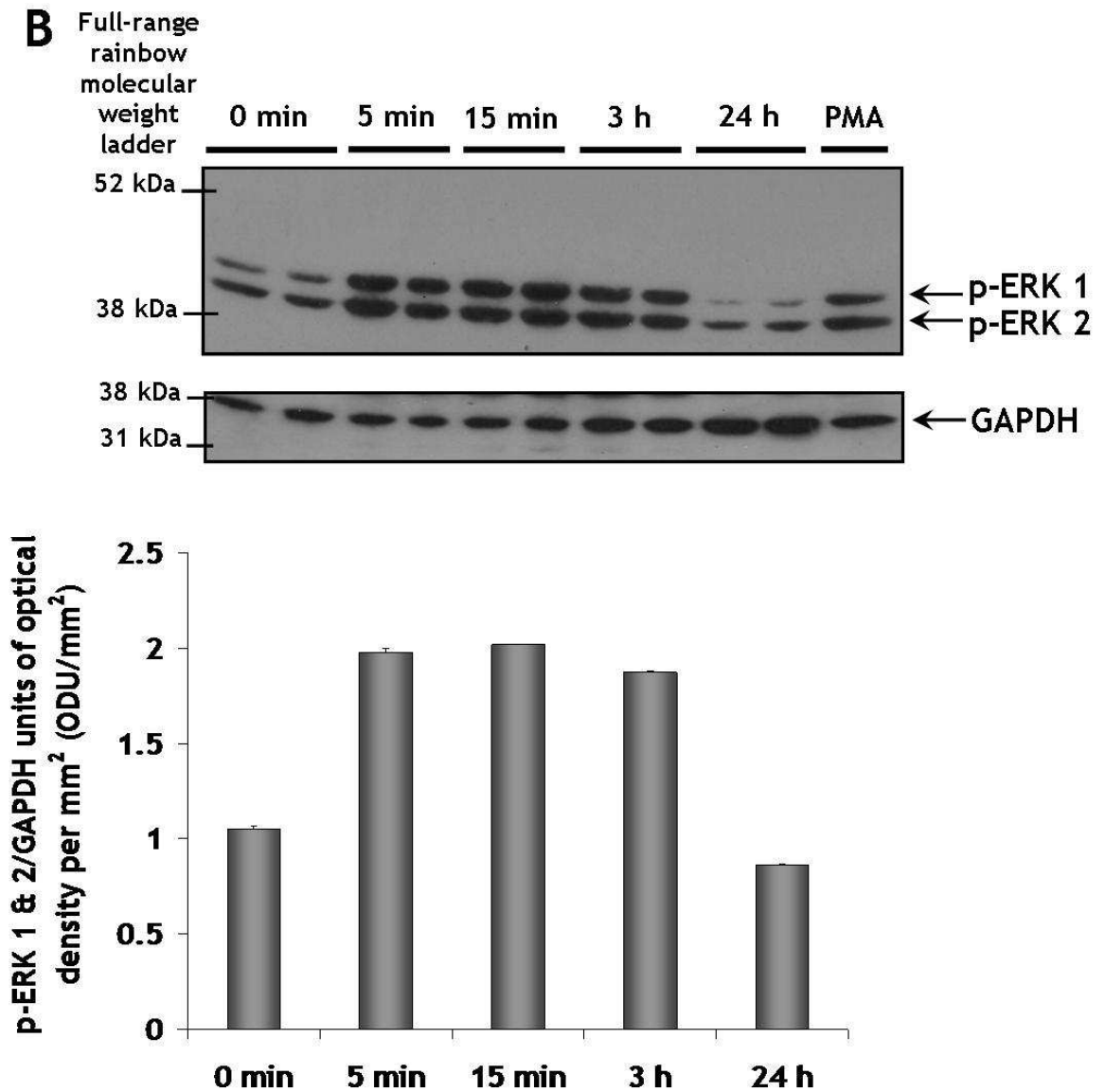




**Figure 5.4.** Optimisation for the percentage of serum to induce VSMC quiescence with low p-Akt and p-ERK 1 & 2 activity.

VSMCs were seeded (at a cell density of  $2.5 \times 10^5$ /well on a 6-well plate), and after 48 h of culture in 0 %, 1 % or 15 % serum, VSMC lysates [normalised to 15  $\mu$ g of protein loading (protein concentration determined by BCA assay)] were assessed for (A) p-Akt (60 kDa) and (B) p-ERK 1 & 2 (44 & 42 kDa) activity by Western immuno-blotting [mouse monoclonal anti-human p-Akt IgG2b antibody (1/1000 dilution) and mouse monoclonal anti-human p-ERK 1/2 IgG1 antibody (1  $\mu$ g/ml)]. A rabbit monoclonal anti-human Akt IgG antibody (1/1000 dilution) was used to detect Akt (60 kDa) and a rabbit polyclonal anti-human ERK 1 IgG antibody (0.4  $\mu$ g/ml) was used to detect ERK 1 (44 kDa) in VSMC lysates for protein loading, respectively. Phorbol 12-myristate 13-acetate (PMA) at 50  $\mu$ M in serum-free culture media was used (30 min incubation) as a positive control for the activation of p-ERK 1 & 2 signalling in VSMCs. (A) p-Akt activity for each percentage serum-stimulation in VSMC lysates was normalised to Akt using densitometry. Mean value  $\pm$  S.E.M (for technical replicates) of patient sample repeated in duplicate and n=1 (cell population/number of individual VSMC preparations used). (B) p-ERK 1 & 2 activity for each percentage serum-stimulation in VSMC lysates was normalised to ERK 1 using densitometry. Mean value  $\pm$  S.E.M (for technical replicates) of patient sample repeated in duplicate and n=1 (cell population/number of individual VSMC preparations used). VSMC, vascular smooth muscle cell; p-Akt, phosphorylated-Akt; p-ERK 1 & 2, phosphorylated-ERK 1 & 2.

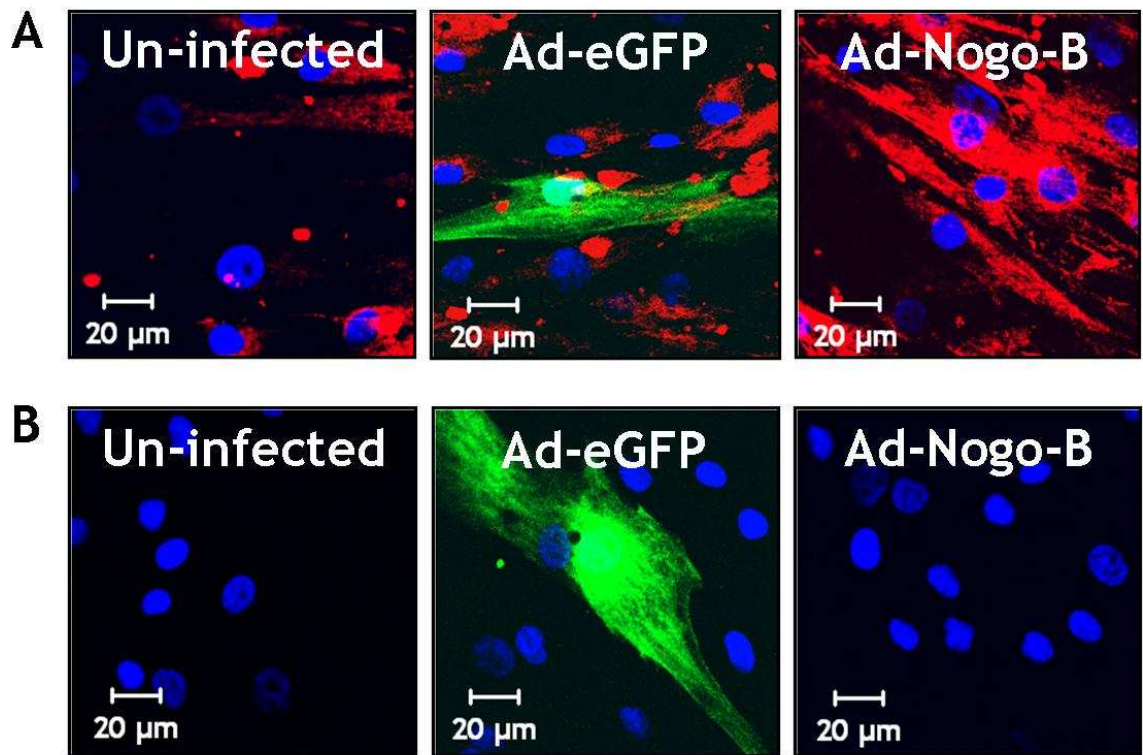




**Figure 5.5.** Optimisation for time points of 15 % serum-stimulation in VSMCs with high p-Akt and p-ERK 1 & 2 activity.

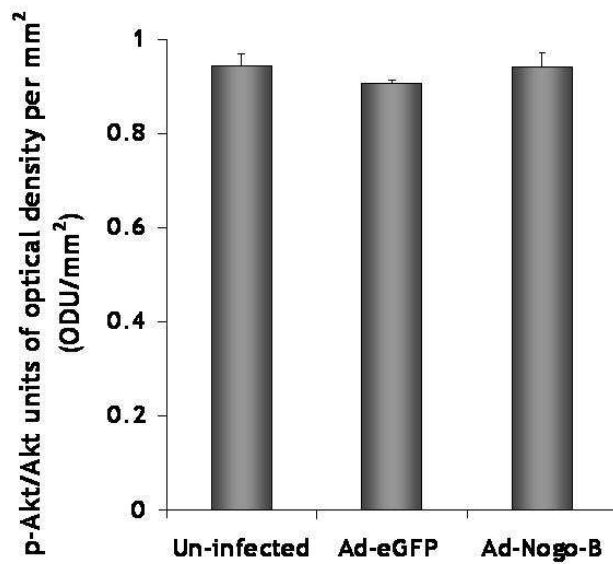
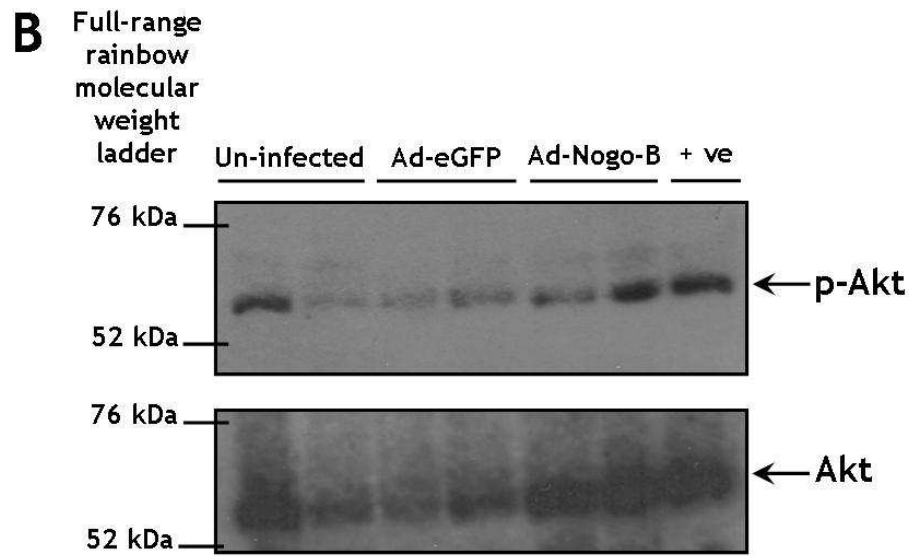
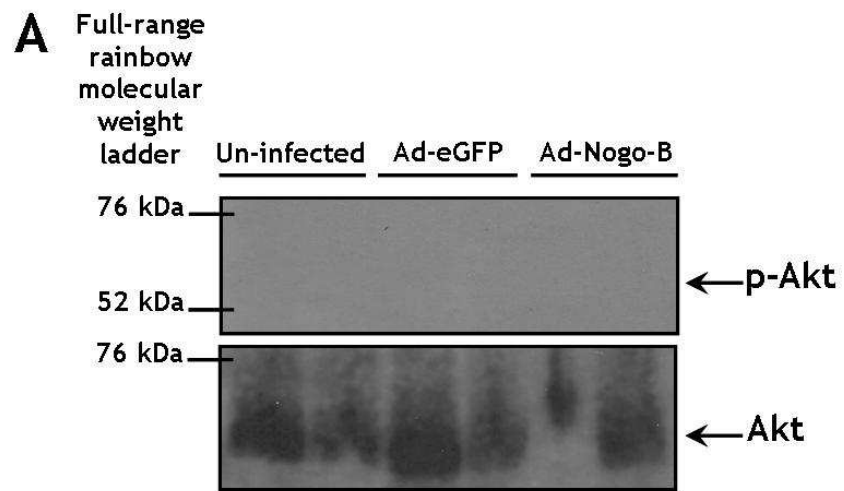
VSMCs were seeded (at a cell density of  $2.5 \times 10^5$ /well on a 6-well plate) and cultured for 48 h in 1 % serum for VSMC quiescence. VSMC lysates [normalised to 15  $\mu$ g of protein loading (protein concentration determined by BCA assay)] of un-stimulated or 15 % serum-stimulated VSMCs at 5 min, 15 min, 3 h or 24 h were assessed for (A) p-Akt (60 kDa) and (B) p-ERK 1 & 2 (44 & 42 kDa) activity by Western immuno-blotting [mouse monoclonal anti-human p-Akt IgG2b antibody (1/1000 dilution) and mouse monoclonal anti-human p-ERK 1/2 IgG1 antibody (1  $\mu$ g/ml)]. A rabbit monoclonal anti-human Akt IgG antibody (1/1000 dilution) was used to detect Akt (60 kDa) and a mouse monoclonal anti-human GAPDH IgG1 antibody (0.2  $\mu$ g/ml) was to detect GAPDH (36 kDa) in VSMC lysates for protein loading, respectively. Phorbol 12-myristate 13-acetate (PMA) at 50  $\mu$ M in serum-free culture media was used (30 min incubation) as a positive control for the activation of p-ERK 1 & 2 signalling in VSMCs. (A) p-Akt activity at each time point of serum-stimulation in VSMC lysates was normalised to Akt using densitometry. Mean value  $\pm$  S.E.M (for technical replicates) of patient sample repeated in duplicate and  $n=1$  (cell population/number of individual VSMC preparations used). (B) p-ERK 1 & 2 activity at each time point of serum-stimulation in VSMC lysates was normalised to GAPDH using densitometry. Mean value  $\pm$  S.E.M (for technical replicates) of patient sample repeated in duplicate and  $n=1$  (cell population/number of individual VSMC preparations used). VSMC, vascular smooth muscle cell; p-Akt, phosphorylated-Akt; p-ERK 1 & 2, phosphorylated-ERK 1 & 2.

As a positive control for adenoviral-mediated gene transfer of Nogo-B, Figure 5.6 indicated Ad-Nogo-B ( $3.27 \times 10^{10}$  pfu/ml) at a MOI 100 mediated over-expression of Nogo-B in VSMCs, in contrast to Ad-eGFP control ( $2.3 \times 10^{10}$  pfu/ml) and uninfected VSMCs (Kritz et al., 2008). Third, VSMCs infected with either Ad-Nogo-B or Ad-eGFP at a MOI of 100 or uninfected were assessed 5 d post-infection. At 3 d post-infection VSMC quiescence was induced with 1 % serum for 48 h, and subsequently 15 % serum-stimulated for 5 min or 3 h or un-stimulated (0 min). VSMC lysates were assessed for Akt and ERK 1 & 2 activity by Western immunoblotting. Results indicated that Ad-Nogo-B had no effect on the level of p-Akt in VSMCs after serum-stimulation of 5 min and 3 h, compared to Ad-eGFP control and uninfected VSMCs (Akt indicated protein loading) (Figure 5.7). With regards to the ERK 1 & 2 signal transduction pathway, results demonstrated that Ad-Nogo-B significantly down-regulated p-ERK 1 & 2 after 3 h of serum-stimulation, in contrast to Ad-eGFP control and uninfected VSMCs ( $1.13 \pm 0.030$  p-ERK 1 & 2/SM  $\alpha$ -actin ODU/mm<sup>2</sup> vs.  $1.48 \pm 0.013$  p-ERK 1 & 2/SM  $\alpha$ -actin ODU/mm<sup>2</sup> or  $1.53 \pm 0.074$  p-ERK 1 & 2/SM  $\alpha$ -actin ODU/mm<sup>2</sup>, respectively,  $p < 0.01$ ) (Figure 5.8 B). VSMCs lysates were normalised to 20  $\mu$ g of protein loading, and SM  $\alpha$ -actin (42 kDa) indicated protein loading (Figure 5.8).



**Figure 5.6. Ad-Nogo-B transduction in VSMCs indicated by immunocytofluorescence.**

Immunocytofluorescent staining was carried out in VSMCs (seeded at a cell density of  $0.5 \times 10^4$ /well on an 8-well chamber slide) transduced with Ad-eGFP, Ad-Nogo-B or un-infected (18 h exposure) at a MOI of 100 for 5 d post-infection in permeabilised conditions. **(A)** A goat polyclonal anti-human Nogo (to the N-terminus region) IgG antibody (2  $\mu\text{g}/\text{ml}$ ) along with its corresponding Alexa-Fluor®-555 (red fluorescence) donkey anti-goat IgG secondary antibody (4  $\mu\text{g}/\text{ml}$ ) was used to detect Nogo-B expression. **(B)** Immunocytofluorescent staining using an isotype-matched negative control (goat IgG) primary antibody. 20  $\mu\text{m}$  scale bar (magnification  $\times 630$ ). Representative of  $n=1$  (cell population/number of individual VSMC preparations used) in triplicate. VSMC, vascular smooth muscle cell; Ad, adenoviral vector serotype 5.



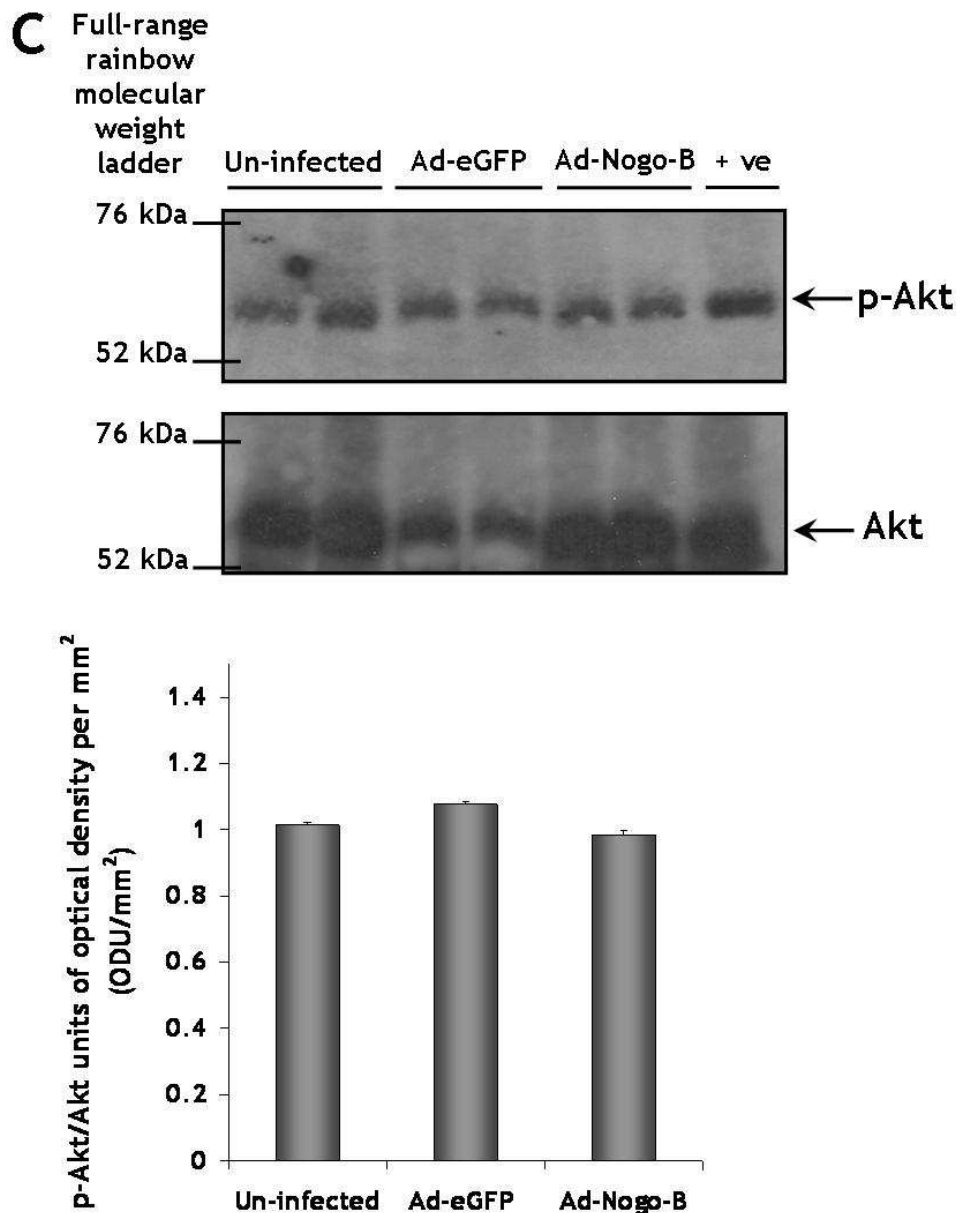


**Figure 5.7. Effect of Nogo-B over-expression on p-Akt activity levels in VSMCs.**

VSMCs were seeded (at a cell density of  $8 \times 10^4$ /well on a 6-well plate) and infected with Ad-Nogo-B or Ad-eGFP at a multiplicity of infection (MOI) of 100 (18 h exposure time), or un-infected. At 3 d post-infection, VSMC quiescence was induced using 1 % serum for 48 h. Subsequently at 5 d post-infection, VSMC lysates were collected (A) at 0 min (un-stimulated) or 15 % serum-stimulation at (B) 5 min or (C) 3 h (protein concentration determined by BCA assay), and assessed for p-Akt (60 kDa) activity by Western immuno-blotting [mouse monoclonal anti-human p-Akt IgG2b antibody (1/1000 dilution)]. A rabbit monoclonal anti-human Akt IgG antibody (1/1000 dilution) was used to detect Akt (60 kDa) in VSMC lysates for protein loading. Lysates from VSMCs serum-stimulated for 5 min from the optimisation experiment were used as a positive control (+ ve) for p-Akt Western immuno-blotting [(A) un-stimulated and (B) 5 min serum-stimulated VSMC lysates were from the same Western immuno-blot]. At (B) 5 min and (C) 3 h of serum-stimulation, p-Akt activity levels in VSMC lysates was normalised to Akt using densitometry. Mean value  $\pm$  S.E.M (for technical replicates) of patient sample repeated in duplicate and  $n=1$  (cell population/number of individual VSMC preparations used). No significant difference with Ad-Nogo-B vs. Ad-eGFP or un-infected at 5 min or 3 h serum-stimultaion. All statistical analysis was carried out by one-way ANOVA for Bonferroni's post-hoc analysis. VSMC, vascular smooth muscle cell; Ad, adenoviral vector serotype 5; p-Akt, phosphorylated-Akt.

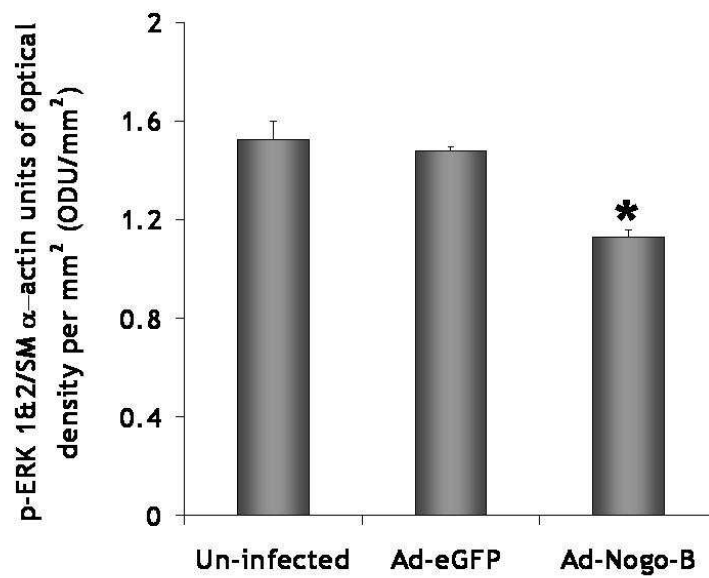
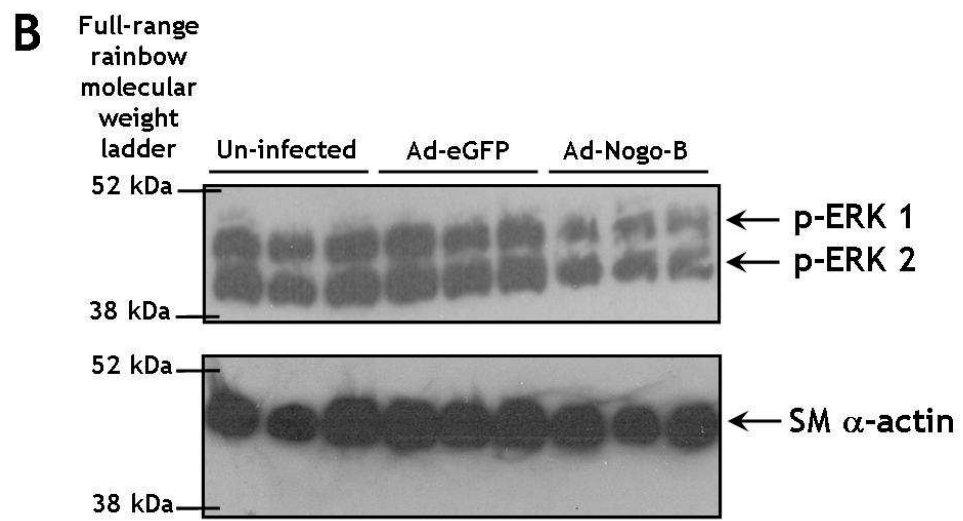
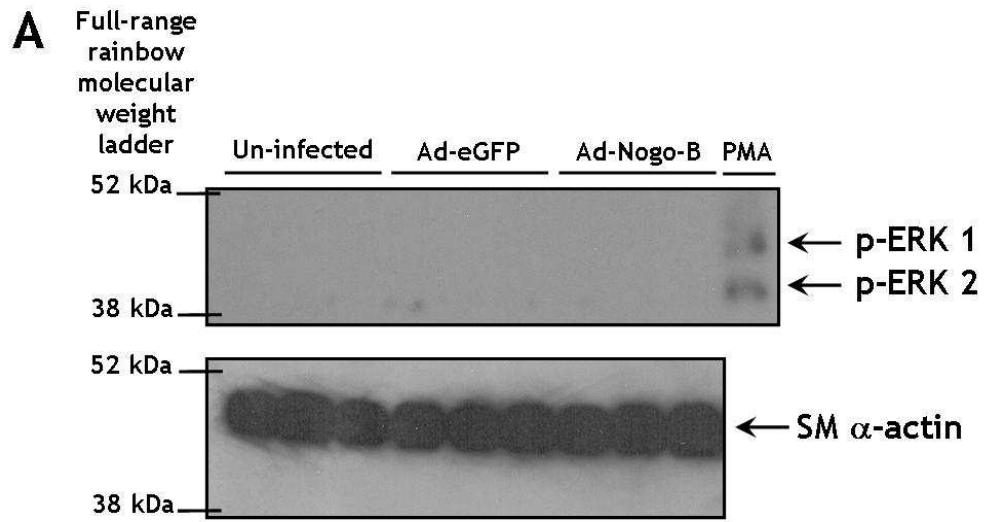


**Figure 5.8. Effect of Nogo-B over-expression on p-ERK 1 & 2 activity levels in VSMCs.**

VSMCs were seeded (at a cell density of  $8 \times 10^4$ /well on a 6-well plate) and infected with Ad-Nogo-B or Ad-eGFP at a multiplicity of infection (MOI) of 100 (18 h exposure time), or uninfected. At 3 d post-infection, VSMC quiescence was induced with 1 % serum for 48 h. Subsequently after 5 d post-infection, VSMCs were (A) un-stimulated at 0 min or (B) 15 % serum-stimulated at 3 h, and lysates [normalised to 20  $\mu$ g of protein loading (protein concentration determined by BCA assay)] were assessed for p-ERK 1 & 2 (44 & 42 kDa) activity by Western immuno-blotting [mouse monoclonal anti-human p-ERK 1 & 2 IgG1 antibody (1  $\mu$ g/ml)]. A mouse monoclonal anti-human SM  $\alpha$ -actin IgG2a antibody (0.4  $\mu$ g/ml) was used to detect SM  $\alpha$ -actin (42 kDa) in VSMC lysates for protein loading. Phorbol 12-myristate 13-acetate (PMA) at 50  $\mu$ M in serum-free culture media was used (30 min incubation) as a positive control for the activation of p-ERK 1 & 2 signalling in VSMCs. At (B) 3 h of serum-stimulation, p-ERK 1 & 2 activity levels in VSMC lysates was normalised to SM  $\alpha$ -actin using densitometry. Mean value  $\pm$  S.E.M of patient sample repeated in triplicate. Two independent experiments performed [n=2 (representative of each other), cell population/number of individual VSMC preparations used]. \* indicates  $p < 0.01$  vs. Ad-eGFP or un-infected. All statistical analysis was carried out by one-way ANOVA for Bonferroni's post-hoc analysis. VSMC, vascular smooth muscle cell; Ad, adenoviral vector serotype 5; p-ERK 1 & 2, phosphorylated-ERK 1 & 2; SM  $\alpha$ -actin, smooth muscle alpha-actin.

### 5.3 Discussion

In this chapter, the mechanism of action of Nogo-B on VSMCs was explored.

- It was established that Nogo-B over-expression mediated by int-LVs or NILVs did not induce VSMC apoptosis.
- Over-expression of Nogo-B mediated by int-LV was observed co-localised with the ER in VSMCs.
- In addition, results suggested that Nogo-B over-expression in VSMCs did not mediate ER-stress signalling.
- Interestingly, results demonstrated that Nogo-B over-expression in VSMCs did not have an effect on Akt activity; however ERK 1 & 2 activation was significantly down-regulated.

Previously it was reported by Kritz *et al.*, (2008) that the over-expression of Nogo-B mediated by adenoviral gene transfer reduced VSMC migration and proliferation *in vitro*, and did not induce VSMC apoptosis assessed by trypan blue exclusion assay and caspase-3/7 assay. Moreover, in a porcine vein graft bypass grafting model, Ad-Nogo-B rescued the injury-induced NIF associated with a reduction in VSMC proliferation, and no effect on VSMC apoptosis which was evaluated with terminal deoxynucleotidyl transferase dUTP nick end labelling (TUNEL) staining (Kritz *et al.*, 2008). In relevance to this, results from a caspase-3/7 activity assay in this study indicated that Nogo-B over-expression mediated by int-LVs and NILVs in VSMCs *in vitro* did not induce apoptosis in these vascular cells. However, it should be noted that this caspase-3/7 assay carried out in this study is not without its limitations, and only measures caspase-3/7 activity in VSMCs transduced with int-LV-Nogo-B, NILV-Nogo-B or LV-eGFP controls or untransduced VSMCs in parallel to Ad-Nogo-B and Ad-eGFP [used as a negative control for caspase-3/7 activity mediated by Nogo-B over-expression (Kritz *et al.*, 2008)]. Additionally, positive controls for VSMC apoptosis possibly should have been considered in this assay, for example the combination of interleukin-1 beta (IL-1 $\beta$ ), tumour necrosis factor-alpha (TNF- $\alpha$ ) and interferon-gamma (IFN- $\gamma$ ) which are known to induce VSMC apoptosis (Geng *et al.*, 1996). Furthermore,

results were deduced using only a caspase-3/7 activity assay, therefore it is worth considering further apoptosis assays such as Annexin V and/or TUNEL staining to strongly confirm these results observed with int-LV-Nogo-B and NILV-Nogo-B. Taken together, both studies evidently confirm that regulation of apoptosis is not a mechanism for Nogo-B in VSMCs. In correlation to this, previous publications have indicated that non-cancerous cells are resistant to apoptosis induced by Nogo-B over-expression (Li et al., 2001), and stable over-expression of Nogo-B in certain types of cancer did not significantly induce a pro-apoptotic effect compared to wild-type control (Oertle et al., 2003c).

Interestingly, results demonstrated that the over-expression of Nogo-B mediated by int-LV was observed co-localised with the PDI ER in VSMCs. It is possible that Nogo-B exerts its phenotypic effects on VSMCs in association with ER-specific pathways, such as the regulation of the structure of the ER network in association with cytoskeletal structures (Raines, 2004a), and therefore this would need further investigation. It is important to consider completing this *in vitro* study by determining NILV-Nogo-B mediated over-expression co-localisation with the ER in VSMCs. In addition, 2 % of the total Nogo-B protein associated with vascular cells is found within the cell-membrane (Acevedo et al., 2004). Therefore, it is also worth considering assessing int-LV-Nogo-B, NILV-Nogo-B and Ad-Nogo-B mediated over-expression and its co-localisation with the cell-membrane (in parallel to un-infected VSMCs) by immunocytofluorescence, which may also help with defining the mechanism of action of Nogo-B with regards to phenotypic effects on VSMC proliferation and migration.

Here, results indicated that the amount of BiP protein did not change after Nogo-B over-expression in VSMCs. Therefore, it can be suggested that the over-expression of Nogo-B does not induce ER-stress in VSMCs, which is an apparent contradiction to findings previously reported by Kuang et al., (2006), as previously discussed. BiP is a key ER chaperone, regulator in ER-stress/UPR signalling and a monitor of cells under ER-stress (Lee, 2005). However, there are other markers of ER-stress such as of ATF6, IRE1, PERK and/or CHOP, which could have been considered to fully establish that Nogo-B over-expression does not induce ER-stress in VSMCs. Additionally, positive controls for ER-stress induction could have been considered in this assay, for example tunicamycin and staurosporine, which are well-established ER-stress inducers. In addition, it is

important to evaluate the effects of Nogo-B over-expression mediated by NILV-Nogo-B and int-LV-Nogo-B on ER-stress in VSMCs *in vitro*, and thus further experiments should be considered.

Indeed, Nogo-B over-expression mediated by Ad-Nogo-B inhibited PDGF-BB-induced VSMC migration (Acevedo et al., 2004, Kritz et al., 2008) and proliferation, and blocked serum-stimulated VSMC proliferation (Kritz et al., 2008). In chapter 4, it was reported that int-LV-Nogo-B and NILV-Nogo-B mediated Nogo-B over-expression and reduced serum-stimulated human VSMC migration and proliferation *in vitro*. As mentioned previously, it is speculated that Nogo-B's mechanism of action leading to phenotypic effects on VSMC migration and/or proliferation may be governed through intracellular signal transduction cascades (Acevedo et al., 2004, Raines, 2004a), such as ERK 1 & 2 and PI3K-Akt pathways [both cascades are well known signal transduction pathways for VSMC migration and proliferation (Bornfeldt et al., 1997, Graf et al., 1997, Nelson et al., 1998, Shigematsu et al., 2000, Stabile et al., 2003, Zhan et al., 2003, Muto et al., 2007, Yu et al., 2007, Morello et al., 2009)]. In relation to this, results in this chapter demonstrated that the over-expression of Nogo-B in VSMC reduced the activation of ERK 1 & 2 signalling cascade induced by serum-stimulation unlike the PI3K-Akt pathway, and therefore could have implications in phenotypic effects on VSMC migration and proliferation. No difference in PI3K-Akt activation possibly correlates with the fact that the Ng-BR has been described to be necessary for Nogo-B and VEGF induced chemotaxis and morphogenesis of VECs, in vascular maintenance and remodelling and angiogenesis (Miao et al., 2006, Zhao et al., 2010). This mechanistic effect is mediated by the activation of the PI3K pathway, via the phosphorylation of Akt (Zhao et al., 2010). Results in this current study, were determined using a well-established signal transduction activity assay (Nelson et al., 1998, Kaplan-Albuquerque et al., 2003) followed by Western-immunoblotting. These results were determined by Western immunoblotting for p-ERK 1 & 2 normalised to  $SM\alpha$ -actin. This was because, problems were encountered with the total ERK antibody used in the optimisation study for the percentage of serum. However, it is important to normalise to the total ERK, in order to understand the proportion of ERK which is phosphorylated and to verify the total ERK present was equal in all VSMC populations, and therefore should be corrected in further work carried

out. Additionally, ELISA assays assessing the levels of total and phosphorylated ERK 1 & 2 and PI3K-Akt should be considered for confirming these results obtained with Ad-Nogo-B. Furthermore for completeness, it is important to assess the effects of int-LV-Nogo-B and NILV-Nogo-B on VSMC ERK 1 & 2 and PI3K-Akt activation, and therefore will require further investigation.

Taken together, all results here in this chapter provide the beginning of a long investigation into Nogo-B's mechanism of action on phenotypic effects on VSMC migration and proliferation. Indeed, it has been speculated that Nogo-B may potentially exert its effect on inhibition of VSMC migration and proliferation by competitive antagonism of the PDGFR binding (Acevedo et al., 2004, Kritz et al., 2008), and thus further experiments such as pull-down assays should be considered. VEC function of Nogo-B is mediated via the Ng-BR (Miao et al., 2006, Zhao et al., 2010) which is highly expressed in VECs (Miao et al., 2006). The Ng-BR is presumed to reside at the cell surface of VECs as a receptor for Nogo-B (Miao et al., 2006), and evidently is localised with the ER in HeLa cells (Harrison et al., 2009). Interestingly, the Ng-BR consists of an intrinsically unstructured ectodomain (no secondary and tertiary structures) and a partially folded cytoplasmic domain (with secondary structures but no tertiary structures). It has been suggested these unusual properties of Ng-BR could be advantageous and important for its biological functions, including signal transduction, cytoskeletal organisation, ER-specific pathways and maintenance of membrane structure (Li and Song, 2007). Nogo-B mediated VSMC phenotypic modulation could potentially be facilitated via the Ng-BR; however this is currently unknown and will require further investigation.

The Rho kinase family monomer G proteins, Cdc42 (cell division control protein 42 homolog), Rac (Ras-related C3 botulinum toxin substrate) and Rho (Ras homolog gene family protein) and their activation, play a pivotal role in induced cell migration by the control of the intracellular cytoskeletal architecture, such as reconstruction of the actin filaments (actin polymerisation) (Muto et al., 2007). In relation to this, Nogo-B has been reported to co-localise with Rac in the ER and plasma membrane of monocytes/macrophages, and is necessary for motility. The loss of Nogo-B in macrophages derived from Nogo-A/B knock-out mice demonstrated reduced macrophage migration due to impaired Rac activation (Yu et al., 2009). Furthermore, another study indicated the

association of Nogo-B with cytoskeletal structures in human monocyte-derived macrophages. Nogo-B was found co-localised in cell protrusions of migrating macrophages as well as with actin/Rho/Rac regions and the tubulin network (Schanda et al., 2011). Both studies support that Nogo-B has a possible influence on cytoskeletal organisation and regulation in cell migration (Yu et al., 2009, Schanda et al., 2011). Therefore, it is possible that the Rho kinase family pathway could have implications to Nogo-B's function in the inhibition of VSMC migration, and thus will require additional analysis.

Collectively, Nogo-B over-expression does not induce VSMC apoptosis and ER-stress. Moreover, the over-expression of Nogo-B reduces ERK 1 & 2 activation in VSMCs, unlike Akt signalling; this may have possible implications in VSMC migration and proliferation. Figure 5.9 illustrates the working hypothesis of the mechanism of action of Nogo-B on VSMC phenotypic modulation. These results provide for the first time, an insight into Nogo-B's possible mechanisms of action leading to phenotypic effects on VSMC migration and proliferation.

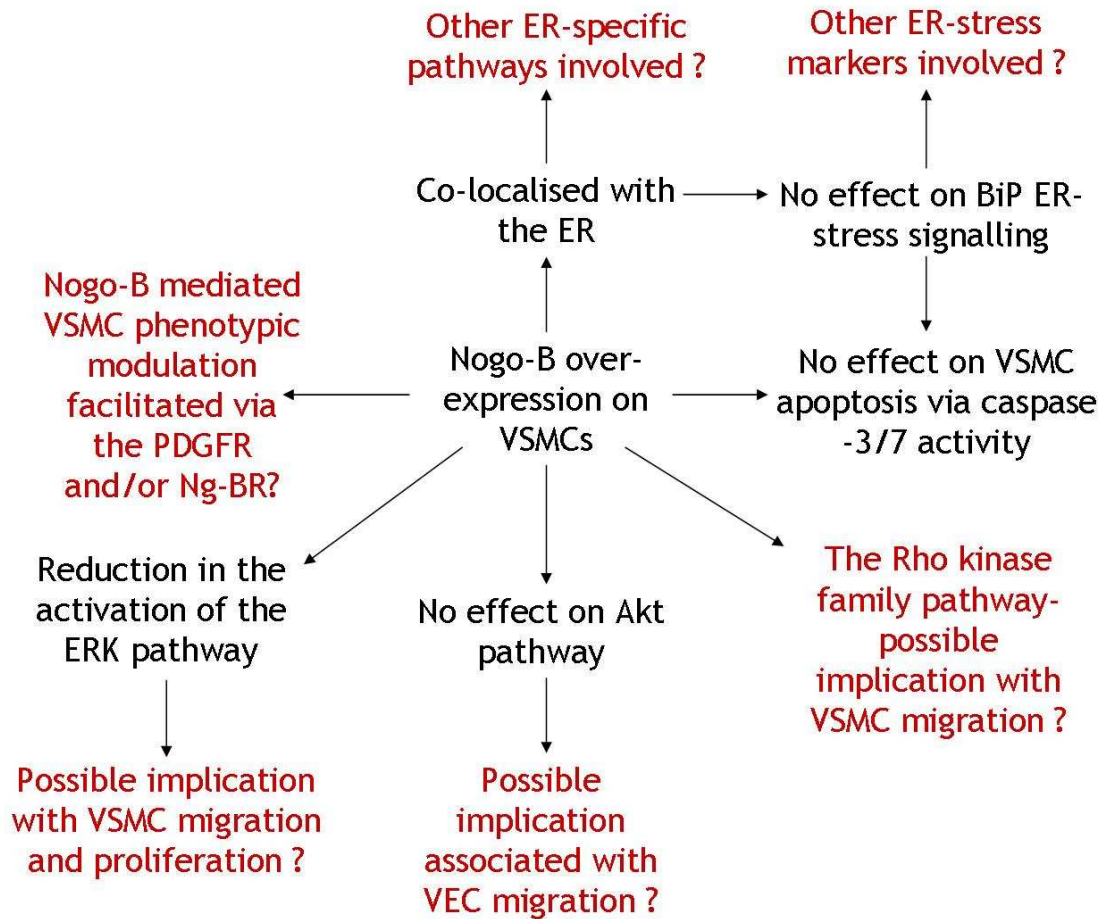


**Figure 5.9. Mechanism of action of Nogo-B on VSMC phenotypic effects.**

This is a schematic diagram illustrating the working hypothesis on Nogo-B’s mechanism of action on VSMC phenotypic effects and for future work that could be subsequently addressed/investigated (in red).

## 6 General Discussion

The main focus of this thesis was to construct and assess a suitable candidate NILV for potential application to vascular gene therapy in the setting of acute vascular injury. Undoubtedly, LVs are highly efficient for vascular cell gene transfer (Dishart et al., 2003a, Cefai et al., 2005, Qian et al., 2006, Yang et al., 2010). A hypothesis for this body of work was to test whether NILVs could have the potential to be very useful for vascular gene delivery (George et al., 2006, White et al., 2007), due to the reduction of host genome integration (Yanez-Munoz et al., 2006, Apolonia et al., 2007). For the first time, this thesis reported the feasibility of NILVs for use in vascular cell gene transfer studies, especially the optimised SFFV-driven VSV-g pseudotyped NILV, which provided efficient transgene expression in VECs and VSMCs *in vitro*. To follow on from this, these selected VSV-g pseudotyped NILVs were then used for therapeutic gene transfer analysis in VSMCs *in vitro*. This thesis supports the use of NILV-Nogo-B as a candidate for therapeutic application to acute vascular injury. Similar to int-LV-Nogo-B, NILV-Nogo-B was an efficient vector system for Nogo-B gene transfer to VSMCs, which led to phenotypic effects on migration and proliferation *in vitro*. Results in this thesis confirm previous studies (Acevedo et al., 2004, Kritz et al., 2008), demonstrating that Nogo-B is a favourable candidate therapeutic gene for the prevention of NIF associated with acute vascular injury. Therefore, more broadly, NILVs have the potential to deliver other therapeutic genes which are relevant for the prevention of vascular abnormalities in the context of ISR and/or vein graft failure, and for example these include: eNOS (Janssens et al., 1998, Varenne et al., 1998); inducible nitric oxide synthase (iNOS) (Kibbe et al., 2001); TIMP-1 (George et al., 1998b, Ramirez Correa et al., 2004); TIMP-2 (George et al., 1998a, Hu et al., 2001); TIMP-3 (George et al., 2000, Akowuah et al., 2005, Johnson et al., 2005) and p53 (George et al., 2001, Wan et al., 2004).

### **Clinical and future implications**

This work addressed the potential of this new candidate NILV-Nogo-B for future use in vascular cell gene delivery studies, with justification to take forward to *in vivo* models. For example, to assess the potential effectiveness of NILV-Nogo-B (in parallel to int-LV-Nogo-B and along with their LV-eGFP controls) mediated gene delivery in appropriate preclinical acute vascular injury models, such as a human saphenous vein *ex vivo* organ culture model (George et al., 2000, George

et al., 2001), a saphenous vein interposition graft *in vivo* porcine model (George et al., 2000, Kritz et al., 2008) and a porcine in-stent *in vivo* model.

Catheter-mediated *in vivo* gene delivery method has been used in numerous investigations, which have reported efficient and effective intravascular therapeutic gene transfer in preclinical animal models of PCI, and as a result mediated the prevention of the NIF (Luo et al., 2004, Numaguchi et al., 2004, Gao et al., 2006, Qian et al., 2006, Nakano et al., 2007). A study by Nakano *et al.*, (2007) demonstrated that a percutaneous catheter-based vector delivery system of adenoviral-mediated anti-monocyte chemoattractant gene transfer attenuated the NIF in a primate ISR model. With regards to a porcine in-stent *in vivo* model, the proposed delivery for NILV-Nogo-B would be to directly deliver the vector to the inner vessel/artery wall using a microporous balloon infusion catheter during stent intervention (Coats et al., 2008). This infusion catheter-based gene delivery has previously been used, and successfully delivered lentiviral-mediated gene transfer of VEGF to porcine femoral arteries (Gao et al., 2006) and EC-SOD to rabbit carotid arteries (Qian et al., 2006) during acute vascular injury *in vivo*.

First to be addressed would be the assessment of efficiency and longevity of eGFP expression mediated by SFFV-driven VSV-g pseudotyped int-LV and NILV in a porcine in-stent *in vivo* model, delivered via this microporous balloon catheter-based delivery system (as described above) immediately following coronary artery stenting. Each LV-eGFP would be administered at various doses (units in iu/ml). In terms of efficiency, vessels would be harvested at an early post-infection time point [for example, 7 days (Qian et al., 2006)] and coronary artery sections assessed for detection of eGFP co-localised with SM- $\alpha$  actin using standard immunohistochemical techniques. This would define the optimised dose of LV and also whether NILV mediated efficient gene transfer at this early time point. The optimised dose would then be used for a subsequent study to quantify longevity. Here, vessels would be harvested at a late time-point post-infection [for example 28 days (Johnson et al., 2005, Kritz et al., 2008)] and coronary artery sections assessed as previously mentioned. This would confirm the longevity of int-LV and define the potential longevity of NILV.

Once optimised, next to be investigated would be the effect of over-expression of Nogo-B mediated by NILV or int-LV compared to their LV-eGFP controls on the status of ISR in this porcine *in vivo* model. Arteries would be assessed 7 days post-infection/stent deployment for the detection of Nogo-B over-expression (Johnson et al., 2005, Kritz et al., 2008). For the status of the vascular injury-induced NIF, vessels would be evaluated at 28 days post-transduction/stenting using quantitative morphometry measurements (quantification of neointimal, medial, lumen and total vessel areas) in the stented region (Johnson et al., 2005). These arteries would also be assessed for Nogo-B over-expression, proliferation and apoptosis indices and endothelial re-growth over the stented area of the vasculature (Kritz et al., 2008). One can speculate that Nogo-B's effect on the inhibition of VSMC proliferation would also assist with the longevity of transgene expression mediated by NILVs.

DESs represent drug reservoirs during PCIs and thus in addition, a stent placement is an ideal platform for gene elution for local vector delivery into the vasculature. The proof of principle of gene-eluting stents has emerged in preclinical studies using non-viral vectors, adenoviral vectors or AAVs. These studies have demonstrated successful gene transfer following stent deployment (Ye et al., 1998, Klugherz et al., 2000, Klugherz et al., 2002, Takahashi et al., 2003, Walter et al., 2004, Johnson et al., 2005, Fishbein et al., 2006, Sharif et al., 2006, Egashira et al., 2007, Sharif et al., 2008, Brito et al., 2010). Furthermore, some of these studies have shown promise in therapeutic gene transfer mediated ISR reduction, and these include eNOS (Sharif et al., 2008, Brito et al., 2010), VEGF (Walter et al., 2004), TIMP-3 (Johnson et al., 2005) and anti-monocyte chemoattractant protein-1 (Egashira et al., 2007). Indeed, gene-eluting stents have the potential to be very useful in vascular gene therapy, but this technology is still in its infancy. Stent-based delivery of Nogo-B mediated by NILV or int-LV would be a novel and compelling gene delivery system, and should be considered for future utility in a porcine *in vivo* model.

The production of int-Nogo-B, NILV-Nogo-B and their LV-eGFP controls would need to be scaled-up for use in this porcine in-stent *in vivo* model. High-titre LV production remains an important challenge, particularly in quantities sufficient for pre-clinical and clinical studies, plus it is also difficult and expensive (Matrai et al., 2010). Attempts have been made to ease the LV production scale-up using

stable, inducible packaging or producer cell lines (Klages et al., 2000, Ikeda et al., 2003, Ni et al., 2005, Broussau et al., 2008) and alternatively by the transient transfection method on an industrial bioreactor scale (Ansorge et al., 2009); however these LV titres remain relatively low (from a range between  $10^9$ - $10^{11}$  iu/ml) in comparison to other viral vector titres (Matrai et al., 2010). Efforts are being made to overcome these shortcomings. A recent publication reported an easy and inexpensive method to increase the LV titres (both NILVs and int-LVs) up to 8-fold, for both research and clinical use. This involves the transient transfection method with the addition of 2-4 mM of caffeine, from 17 hours to 41 hours post-transfection which mediates optimal titres (Ellis et al., 2011). High-titre production of NILV-Nogo-B and int-LV-Nogo-B for future use in these acute vascular injury preclinical models could be problematic, and therefore it is imperative to consider the addition of caffeine during LV production.

Despite the difficulty in producing high-titre HNTV pseudotyped LVs which was encountered in chapter 3, it would be advantageous to evaluate HNTV pseudotyped NILV-Nogo-B for its targeted gene delivery and transgene expression in the vasculature (Qian et al., 2006) of these mentioned *in vivo* and *ex vivo* acute vascular injury models.

LV-mediated transduction in vascular cells in relation to integration site profiles has not been explored. Unfortunately, both retroviral vector and LV mediated gene transfer have the potential risk of genotoxicity associated with integration and activation of adjacent proto-oncogenes (also known as insertional mutagenesis/oncogenesis). Evidently, uncontrolled clonal T-lymphocyte proliferation (T-lymphocyte leukaemia) occurred in 2 out of 10 patients after gene therapy for X-linked SCID. This was a consequence of retroviral (gammaretroviral) vector integration in proximity to the *LMO2* (LIM domain-only 2) proto-oncogene promoter, and thereby led to aberrant transcription and up-regulation of *LMO2* (Hacein-Bey-Abina et al., 2003b). A further 2 patients developed adverse events of insertional oncogenesis (T-lymphocyte leukaemia), which was reported as a consequence of integration near the *LMO2*, *BMI1* (*BMI1* polycomb ring finger oncogene) and/or *CCND2* (*G1/S*-specific cyclin-D2) proto-oncogenes in these patients' blast cells (Hacein-Bey-Abina et al., 2008). In a retroviral-mediated gene therapy trial for X-linked chronic granulomatous disease in 2 patients (granulocytes colony-stimulating factor mobilised

peripheral blood haematopoietic cells), non-malignant amplification of myeloid clones facilitated therapeutic efficacy, which was augmented by insertional activation of *MDS1-EVI1* (myelodysplasia syndrome 1-ecotropic viral integration site 1), *PRDM16* (PR domain containing 16) and/or *SETBP1* (SET binding protein 1) genes (integration near or within these PR domain-containing zinc-finger genes). However, these results do raise concerns that these myeloid clones could lead to uncontrolled proliferation, abnormal haematopoiesis and eventually leukemogenesis (Ott et al., 2006). Collectively, retroviral-mediated integrative gene transfer is semi-random and most harbour common integration sites (CIS) (Hacein-Bey-Abina et al., 2003b, Ott et al., 2006, Deichmann et al., 2007, Schwarzwaelder et al., 2007, Hacein-Bey-Abina et al., 2008). Clinical success occurred in a one patient gene therapy trial for  $\beta$ -thalassaemia by HSC transduction with a LV-mediated gene transfer of  $\beta$ -globin. Long-term therapeutic benefit derived from a dominant myeloid-biased cell clone, with the patient remaining healthy. With similarities to gammaretroviral vectors, integration site analysis indicated that LV integration was most commonly located within the *HMG2* (high-mobility group AT-hook 2) proto-oncogene (accounted for approximately 30 % of all integration sites in erythroid cells and thus known as the CIS) and as a consequence induced transcriptional activation of this gene. However, this therapeutic efficacy mediated by clonal dominance, could have resulted from benign cell expansion caused by dysregulation of the *HMG2* gene in stem/progenitor cells (Cavazzana-Calvo et al., 2010). Therefore, this suggestion does raise concerns with possible insertional oncogenesis, because the *HMG2* gene is linked with abnormal proliferation, malignant epithelial tumours and leukaemia (Cleynen and Van de Ven, 2008). Moreover, this study raises concerns of LV safety, because the detection of CIS within proto-oncogenes is a well-established hallmark of genotoxicity (Cavazzana-Calvo et al., 2010). However, a recent study demonstrated that LV-mediated CIS were found in specific genomic regions, instead of oncogenic selection (Biffi et al., 2011). Doubtlessly, it is important to detect and characterise these CIS (the integration profile) of int-LV, in parallel to their integration-deficient counterparts in vascular cells [NILV D64V mutant has a residual integration frequency of approximately  $10^3$ -fold lower than the integrative wild-type vector (Apolonia et al., 2007), and genomic integration of episomal LV form could possibly occur through DNA nicks located anywhere in the vector circle (Yanez-

Munoz et al., 2006)]. Currently, integration site analysis for int-LV-mediated gene transfer of eGFP, in parallel to NILV-eGFP in human primary VSMCs is underway using highly-sensitive LAM-PCR. This is a nested PCR designed specially to amplify integration sites. Amplified integration sites are cloned and sequenced, to provide information on the quantity and position on integration in the host genome (Schmidt et al., 2007). Additionally, Bartholomae et al., (2011) reported that LVs integrate less frequently in actively transcribed genes of post-mitotic cells, compared to rapidly dividing cells. This could have implications in LV-transduced VSMCs, which have low mitotic rates in a disease state (Gordon et al., 1990) and even during the acute vascular injury response (Westerband et al., 1997, Hilker et al., 2002), and thus possible lesser likelihood of genotoxicity (Bartholomae et al., 2011).

Results obtained in chapter 5, which explored the mechanism of action of Nogo-B on VSMCs, was just the start of a long investigation. MicroRNAs (MiRs) are highly conserved, endogenous, short non-coding RNAs of about 22 nucleotides in length. MiRs regulate gene expression at the post-transcriptional level [directly regulate about 30 % of encoding genes of the human genome (Lewis et al., 2005)], generally by either degradation or translational inhibition of their target mRNAs through Watson-Crick base pairing between the miR and the seed sequence located in the 3' untranslated region (UTR) of the specific mRNA (Small and Olson, 2011). There are certainly numerous miRs that are involved and important in phenotypic modulation of VSMCs. Several reports have indicated miR-21, 143, 145, 221 and 222 are highly enriched in VSMCs, and evidently have critical roles in the regulation of VSMC differentiation, migration, proliferation and/or apoptosis in the NIF during the vascular response to injury (Ji et al., 2007, Davis et al., 2008, Boettger et al., 2009, Cheng et al., 2009, Cordes et al., 2009, Davis et al., 2009, Liu et al., 2009, Xin et al., 2009). MiR bioinformatics databases, [microrna.org](http://microrna.org) (John et al., 2004, Betel et al., 2010) and MicroCosm Targets (Griffiths-Jones et al., 2006, Griffiths-Jones et al., 2008) were utilised to identify putative MiR binding sites within the 3' UTR of Nogo-B. In relevance to this, there is presumed to be a seed sequence for miR-21 and 143 in Nogo-B, and therefore these miRs could have involvement in direct post-transcriptional regulation of endogenous Nogo-B associated with phenotypic modulation of VSMCs. In addition, there are many pathways involved in the

regulation of VSMC migration and proliferation, and thus there could be an indirect casual effect of Nogo-B with regards to miR-21, 143, 145, 221 and 222 (Selbach et al., 2008) during phenotypic modulation. Therefore, it would be interesting to study if Nogo-B over-expression mediates changes in these MiRs in VSMCs and their importance with regards to SM differentiation markers (SM-MHC, calponin and SM- $\alpha$  actin). Taken together, experiments investigating the association of Nogo-B with these miRs in VSMCs should be considered.

VSMCs used within this thesis were obtained from patients undergoing bypass surgery. Consideration should be given to the fact that LV transduction may differ in VSMCs from atherosclerotic plaques (Deng et al., 2006), which is important for stent-based delivery, and thus should be considered for investigation *in vitro* and *in vivo*. Furthermore, LV transduction could vary among each VSMC patient preparation depending on drug regime that the individual is undertaking and/or the individual's biological variability.

### **Conclusion**

Collectively, this thesis addresses the hypothesis that SFFV-driven VSV-g pseudotyped NILVs are efficient in vascular cell gene transfer. Additionally, this thesis supports the use of NILV-Nogo-B as a new candidate for therapeutic application in the prevention of NIF associated with acute vascular injury following revascularisation. In conclusion, this thesis reports important implications for the use of NILVs as a potential therapeutic vector for application to vascular gene therapy.

## List of References

- ABORDO-ADESIDA, E., FOLLENZI, A., BARCIA, C., SCIASCIA, S., CASTRO, M. G., NALDINI, L. & LOWENSTEIN, P. R. 2005. Stability of lentiviral vector-mediated transgene expression in the brain in the presence of systemic antivector immune responses. *Hum Gene Ther*, 16: 741-51.
- ACEVEDO, L., YU, J., ERDJUMENT-BROMAGE, H., MIAO, R. Q., KIM, J. E., FULTON, D., TEMPST, P., STRITTMATTER, S. M. & SESSA, W. C. 2004. A new role for Nogo as a regulator of vascular remodeling. *Nat Med*, 10: 382-8.
- AKOWUAH, E. F., GRAY, C., LAWRIE, A., SHERIDAN, P. J., SU, C. H., BETTINGER, T., BRISKEN, A. F., GUNN, J., CROSSMAN, D. C., FRANCIS, S. E., BAKER, A. H. & NEWMAN, C. M. 2005. Ultrasound-mediated delivery of TIMP-3 plasmid DNA into saphenous vein leads to increased lumen size in a porcine interposition graft model. *Gene Ther*, 12: 1154-7.
- ALEXANDER, J. H., FERGUSON, T. B., JR., JOSEPH, D. M., MACK, M. J., WOLF, R. K., GIBSON, C. M., GENNEVOIS, D., LORENZ, T. J., HARRINGTON, R. A., PETERSON, E. D., LEE, K. L., CALIFF, R. M. & KOUCHOUKOS, N. T. 2005a. The PProject of Ex-vivo Vein graft ENgineering via Transfection IV (PREVENT IV) trial: study rationale, design, and baseline patient characteristics. *Am Heart J*, 150: 643-9.
- ALEXANDER, J. H., HAFLEY, G., HARRINGTON, R. A., PETERSON, E. D., FERGUSON, T. B., JR., LORENZ, T. J., GOYAL, A., GIBSON, M., MACK, M. J., GENNEVOIS, D., CALIFF, R. M. & KOUCHOUKOS, N. T. 2005b. Efficacy and safety of edifoligide, an E2F transcription factor decoy, for prevention of vein graft failure following coronary artery bypass graft surgery: PREVENT IV: a randomized controlled trial. *Jama*, 294: 2446-54.
- ALI, Z. A., BURSILL, C. A., HU, Y., CHOUDHURY, R. P., XU, Q., GREAVES, D. R. & CHANNON, K. M. 2005. Gene transfer of a broad spectrum CC-chemokine inhibitor reduces vein graft atherosclerosis in apolipoprotein E-knockout mice. *Circulation*, 112: 1235-41.
- ALMARZA, E., ZHANG, F., SANTILLI, G., BLUNDELL, M. P., HOWE, S. J., THORNHILL, S. I., BUEREN, J. A. & THRASHER, A. J. 2011. Correction of SCID-X1 using an enhancerless Vav promoter. *Hum Gene Ther*, 22: 263-70.
- ANGELINI, G. D., BRYAN, A. J., WILLIAMS, H. M., SOYOMBO, A. A., WILLIAMS, A., TOVEY, J. & NEWBY, A. C. 1992. Time-course of medial and intimal thickening in pig venous arterial grafts: relationship to endothelial injury and cholesterol accumulation. *J Thorac Cardiovasc Surg*, 103: 1093-103.
- ANSORGE, S., LANTHIER, S., TRANFIGURACION, J., DUROCHER, Y., HENRY, O. & KAMEN, A. 2009. Development of a scalable process for high-yield lentiviral vector production by transient transfection of HEK293 suspension cultures. *J Gene Med*, 11: 868-76.

- APOLONIA, L., WADDINGTON, S. N., FERNANDES, C., WARD, N. J., BOUMA, G., BLUNDELL, M. P., THRASHER, A. J., COLLINS, M. K. & PHILPOTT, N. J. 2007. Stable gene transfer to muscle using non-integrating lentiviral vectors. *Mol Ther*, 15: 1947-54.
- BAHR, U., MURANYI, W., MULLER, S., KEHM, R., HANDERMANN, M., DARAI, G. & ZEIER, M. 2004. Bovine aortic endothelial cells are susceptible to Hantaan virus infection. *Virology*, 321: 1-7.
- BAKER, A. H. 2004. Designing gene delivery vectors for cardiovascular gene therapy. *Prog Biophys Mol Biol*, 84: 279-99.
- BAKER, A. H., EDWARDS, D. R. & MURPHY, G. 2002. Metalloproteinase inhibitors: biological actions and therapeutic opportunities. *J Cell Sci*, 115: 3719-27.
- BAKER, A. H., KRITZ, A., WORK, L. M. & NICKLIN, S. A. 2005. Cell-selective viral gene delivery vectors for the vasculature. *Exp Physiol*, 90: 27-31.
- BAKER, A. H., YIM, A. P. & WAN, S. 2006. Opportunities for gene therapy in preventing vein graft failure after coronary artery bypass surgery. *Diabetes Obes Metab*, 8: 119-24.
- BAKER, A. H., ZALTSMAN, A. B., GEORGE, S. J. & NEWBY, A. C. 1998. Divergent effects of tissue inhibitor of metalloproteinase-1, -2, or -3 overexpression on rat vascular smooth muscle cell invasion, proliferation, and death in vitro. TIMP-3 promotes apoptosis. *J Clin Invest*, 101: 1478-87.
- BANASIK, M. B. & MCCRAY, P. B., JR. 2010. Integrase-defective lentiviral vectors: progress and applications. *Gene Ther*, 17: 150-7.
- BARTHOLOMAE, C. C., ARENS, A., BALAGGAN, K. S., YANEZ-MUNOZ, R. J., MONTINI, E., HOWE, S. J., PARUZYNSKI, A., KORN, B., APPELT, J. U., MACNEIL, A., CESANA, D., ABEL, U., GLIMM, H., NALDINI, L., ALI, R. R., THRASHER, A. J., VON KALLE, C. & SCHMIDT, M. 2011. Lentiviral vector integration profiles differ in rodent postmitotic tissues. *Mol Ther*, 19: 703-10.
- BARTHOLOMAE, C. C., KIRSTEN, R., GLIMM, H., SCHMIDT, M. & VON KALLE, C. 2010. Retroviral Vectors and Integration Analysis. In: [ZOLOTUKHIN, R. W. H. S. (ed.) *A Guide to Human Gene Therapy*. First ed. World Scientific publishing Co.Pte.Ltd. p.37-49.
- BERK, B. C. 2001. Vascular smooth muscle growth: autocrine growth mechanisms. *Physiol Rev*, 81: 999-1030.
- BETEL, D., KOPPAL, A., AGIUS, P., SANDER, C. & LESLIE, C. 2010. Comprehensive modeling of microRNA targets predicts functional non-conserved and non-canonical sites. *Genome Biol*, 11: R90.
- BIFFI, A., BARTOLOMAE, C. C., CESANA, D., CARTIER, N., AUBOURG, P., RANZANI, M., CESANI, M., BENEDECENTI, F., PLATI, T., RUBAGOTTI, E., MERELLA, S., CAPOTONDO, A., SGUALDINO, J., ZANETTI, G., VON KALLE, C., SCHMIDT, M., NALDINI, L. & MONTINI, E. 2011. Lentiviral-vector common integration sites in preclinical models and a clinical trial reflect

- a benign integration bias and not oncogenic selection. *Blood*, 117: 5332-5339.
- BOETTGER, T., BEETZ, N., KOSTIN, S., SCHNEIDER, J., KRUGER, M., HEIN, L. & BRAUN, T. 2009. Acquisition of the contractile phenotype by murine arterial smooth muscle cells depends on the Mir143/145 gene cluster. *J Clin Invest*, 119: 2634-47.
- BORNFELDT, K. E., CAMPBELL, J. S., KOYAMA, H., ARGAST, G. M., LESLIE, C. C., RAINES, E. W., KREBS, E. G. & ROSS, R. 1997. The mitogen-activated protein kinase pathway can mediate growth inhibition and proliferation in smooth muscle cells. Dependence on the availability of downstream targets. *J Clin Invest*, 100: 875-85.
- BRITO, L. A., CHANDRASEKHAR, S., LITTLE, S. R. & AMIJI, M. M. 2010. Non-viral eNOS gene delivery and transfection with stents for the treatment of restenosis. *Biomed Eng Online*, 9: 56.
- BROUSSAU, S., JABBOUR, N., LACHAPPELLE, G., DUROCHER, Y., TOM, R., TRANFIGURACION, J., GILBERT, R. & MASSIE, B. 2008. Inducible packaging cells for large-scale production of lentiviral vectors in serum-free suspension culture. *Mol Ther*, 16: 500-7.
- BROWN, T. A. 2010. *Gene Cloning and DNA Analysis. An Introduction*. Sixth ed. Wiley-Blackwell. p.166-169.
- BRYAN, A. J. & ANGELINI, G. D. 1994. The biology of saphenous vein graft occlusion: etiology and strategies for prevention. *Curr Opin Cardiol*, 9: 641-9.
- BUCHSCHACHER, G. L., JR. 2001. Introduction to retroviruses and retroviral vectors. *Somat Cell Mol Genet*, 26: 1-11.
- BUCHSCHACHER, G. L., JR. & WONG-STAAAL, F. 2000. Development of lentiviral vectors for gene therapy for human diseases. *Blood*, 95: 2499-504.
- BUCKLEY, S. M., HOWE, S. J., SHEARD, V., WARD, N. J., COUTELLE, C., THRASHER, A. J., WADDINGTON, S. N. & MCKAY, T. R. 2008. Lentiviral transduction of the murine lung provides efficient pseudotype and developmental stage-dependent cell-specific transgene expression. *Gene Ther*, 15: 1167-75.
- BULLARD, T. A., PROTACK, T. L., AGUILAR, F., BAGWE, S., MASSEY, H. T. & BLAXALL, B. C. 2008. Identification of Nogo as a novel indicator of heart failure. *Physiol Genomics*, 32: 182-9.
- BURSILL, C. A., MCNEILL, E., WANG, L., HIBBITT, O. C., WADE-MARTINS, R., PATERSON, D. J., GREAVES, D. R. & CHANNON, K. M. 2009. Lentiviral gene transfer to reduce atherosclerosis progression by long-term CC-chemokine inhibition. *Gene Ther*, 16: 93-102.
- BUTLER, S. L., HANSEN, M. S. & BUSHMAN, F. D. 2001. A quantitative assay for HIV DNA integration in vivo. *Nat Med*, 7: 631-4.

- BUTLER, S. L., JOHNSON, E. P. & BUSHMAN, F. D. 2002. Human immunodeficiency virus cDNA metabolism: notable stability of two-long terminal repeat circles. *J Virol*, 76: 3739-47.
- BUXTON, B. F. & FULLER, J. 2004. Clinical trials and graft patency data in coronary artery surgery--a 30-year perspective. *Heart Lung Circ*, 13 Suppl 3: S7-S12.
- CANDOTTI, F., JOHNSTON, J. A., PUCK, J. M., SUGAMURA, K., O'SHEA, J. J. & BLAESE, R. M. 1996. Retroviral-mediated gene correction for X-linked severe combined immunodeficiency. *Blood*, 87: 3097-102.
- CANN, A. J. 2005. *Principles of Molecular Virology*. Fourth ed. Elsevier Academic Press Inc. p.292.
- CARTIER, N., HACEIN-BEY-ABINA, S., BARTHOLOMAE, C. C., VERES, G., SCHMIDT, M., KUTSCHERA, I., VIDAUD, M., ABEL, U., DAL-CORTIVO, L., CACCAVELLI, L., MAHLAOU, N., KIERMER, V., MITTELSTAEDT, D., BELLESME, C., LAHLOU, N., LEFRERE, F., BLANCHE, S., AUDIT, M., PAYEN, E., LEBOULCH, P., L'HOMME, B., BOUGNERES, P., VON KALLE, C., FISCHER, A., CAVAZZANA-CALVO, M. & AUBOURG, P. 2009. Hematopoietic stem cell gene therapy with a lentiviral vector in X-linked adrenoleukodystrophy. *Science*, 326: 818-23.
- CAVAZZANA-CALVO, M., HACEIN-BEY, S., DE SAINT BASILE, G., DE COENE, C., SELZ, F., LE DEIST, F. & FISCHER, A. 1996. Role of interleukin-2 (IL-2), IL-7, and IL-15 in natural killer cell differentiation from cord blood hematopoietic progenitor cells and from gamma c transduced severe combined immunodeficiency X1 bone marrow cells. *Blood*, 88: 3901-9.
- CAVAZZANA-CALVO, M., HACEIN-BEY, S., DE SAINT BASILE, G., GROSS, F., YVON, E., NUSBAUM, P., SELZ, F., HUE, C., CERTAIN, S., CASANOVA, J. L., BOUSSO, P., DEIST, F. L. & FISCHER, A. 2000. Gene therapy of human severe combined immunodeficiency (SCID)-X1 disease. *Science*, 288: 669-72.
- CAVAZZANA-CALVO, M., PAYEN, E., NEGRE, O., WANG, G., HEHIR, K., FUSIL, F., DOWN, J., DENARO, M., BRADY, T., WESTERMAN, K., CAVALLESCO, R., GILLET-LEGRAND, B., CACCAVELLI, L., SGARRA, R., MAOUCHE-CHRETIEN, L., BERNAUDIN, F., GIROT, R., DORAZIO, R., MULDER, G. J., POLACK, A., BANK, A., SOULIER, J., LARGHERO, J., KABBARA, N., DALLE, B., GOURMEL, B., SOCIE, G., CHRETIEN, S., CARTIER, N., AUBOURG, P., FISCHER, A., CORNETTA, K., GALACTEROS, F., BEUZARD, Y., GLUCKMAN, E., BUSHMAN, F., HACEIN-BEY-ABINA, S. & LEBOULCH, P. 2010. Transfusion independence and HMG2 activation after gene therapy of human beta-thalassaemia. *Nature*, 467: 318-22.
- CEFAI, D., SIMEONI, E., LUDUNGE, K. M., DRISCOLL, R., VON SEGESSER, L. K., KAPPENBERGER, L. & VASSALLI, G. 2005. Multiply attenuated, self-inactivating lentiviral vectors efficiently transduce human coronary artery cells in vitro and rat arteries in vivo. *J Mol Cell Cardiol*, 38: 333-44.
- CHAMLEY-CAMPBELL, J., CAMPBELL, G. R. & ROSS, R. 1979. The smooth muscle cell in culture. *Physiol Rev*, 59: 1-61.

- CHANG, C. W., LAI, Y. S., PAWLIK, K. M., LIU, K., SUN, C. W., LI, C., SCHOEB, T. R. & TOWNES, T. M. 2009. Polycistronic lentiviral vector for "hit and run" reprogramming of adult skin fibroblasts to induced pluripotent stem cells. *Stem Cells*, 27: 1042-9.
- CHARRIER, S., DUPRE, L., SCARAMUZZA, S., JEANSON-LEH, L., BLUNDELL, M. P., DANOS, O., CATTANEO, F., AIUTI, A., ECKENBERG, R., THRASHER, A. J., RONCAROLO, M. G. & GALY, A. 2007. Lentiviral vectors targeting WASp expression to hematopoietic cells, efficiently transduce and correct cells from WAS patients. *Gene Ther*, 14: 415-28.
- CHEN, M. S., HUBER, A. B., VAN DER HAAR, M. E., FRANK, M., SCHNELL, L., SPILLMANN, A. A., CHRIST, F. & SCHWAB, M. E. 2000. Nogo-A is a myelin-associated neurite outgrowth inhibitor and an antigen for monoclonal antibody IN-1. *Nature*, 403: 434-9.
- CHENG, Y., LIU, X., YANG, J., LIN, Y., XU, D. Z., LU, Q., DEITCH, E. A., HUO, Y., DELPHIN, E. S. & ZHANG, C. 2009. MicroRNA-145, a novel smooth muscle cell phenotypic marker and modulator, controls vascular neointimal lesion formation. *Circ Res*, 105: 158-66.
- CHO, K. R., KIM, J. S., CHOI, J. S. & KIM, K. B. 2006. Serial angiographic follow-up of grafts one year and five years after coronary artery bypass surgery. *Eur J Cardiothorac Surg*, 29: 511-6.
- CLEYNEN, I. & VAN DE VEN, W. J. 2008. The HMGA proteins: a myriad of functions (Review). *Int J Oncol*, 32: 289-305.
- COATS, P., KENNEDY, S., PYNE, S., WAINWRIGHT, C. L. & WADSWORTH, R. M. 2008. Inhibition of non-Ras protein farnesylation reduces in-stent restenosis. *Atherosclerosis*, 197: 515-23.
- COCHRANE, A. W., CHEN, C. H. & ROSEN, C. A. 1990. Specific interaction of the human immunodeficiency virus Rev protein with a structured region in the env mRNA. *Proc Natl Acad Sci U S A*, 87: 1198-202.
- COCKRELL, A. S. & KAFRI, T. 2007. Gene delivery by lentivirus vectors. *Mol Biotechnol*, 36: 184-204.
- CONTE, M. S., BANDYK, D. F., CLOWES, A. W., MONETA, G. L., SEELY, L., LORENZ, T. J., NAMINI, H., HAMDAN, A. D., RODDY, S. P., BELKIN, M., BERCELI, S. A., DEMASI, R. J., SAMSON, R. H. & BERMAN, S. S. 2006. Results of PREVENT III: a multicenter, randomized trial of edifoligide for the prevention of vein graft failure in lower extremity bypass surgery. *J Vasc Surg*, 43: 742-751; discussion 751.
- CONTE, M. S., LORENZ, T. J., BANDYK, D. F., CLOWES, A. W., MONETA, G. L. & SEELY, B. L. 2005. Design and rationale of the PREVENT III clinical trial: edifoligide for the prevention of infrainguinal vein graft failure. *Vasc Endovascular Surg*, 39: 15-23.
- CORDES, K. R., SHEEHY, N. T., WHITE, M. P., BERRY, E. C., MORTON, S. U., MUTH, A. N., LEE, T. H., MIANO, J. M., IVEY, K. N. & SRIVASTAVA, D.

2009. miR-145 and miR-143 regulate smooth muscle cell fate and plasticity. *Nature*, 460: 705-10.
- COSTA, M. A. & SIMON, D. I. 2005. Molecular basis of restenosis and drug-eluting stents. *Circulation*, 111: 2257-73.
- CRONIN, J., ZHANG, X. Y. & REISER, J. 2005. Altering the tropism of lentiviral vectors through pseudotyping. *Curr Gene Ther*, 5: 387-98.
- DAVIS, B. N., HILYARD, A. C., LAGNA, G. & HATA, A. 2008. SMAD proteins control DROSHA-mediated microRNA maturation. *Nature*, 454: 56-61.
- DAVIS, B. N., HILYARD, A. C., NGUYEN, P. H., LAGNA, G. & HATA, A. 2009. Induction of microRNA-221 by platelet-derived growth factor signaling is critical for modulation of vascular smooth muscle phenotype. *J Biol Chem*, 284: 3728-38.
- DE SCHEERDER, I., WANG, K., ZHOU, X. R., VERBEKEN, E., PING, Q. B., YANMING, H., JIANHUA, H., SZILARD, M. & VAN DE WERF, F. 1999. Neointimal hyperplasia and late pathologic remodeling in a porcine coronary stent model. *J Invasive Cardiol*, 11: 9-12.
- DEICHMANN, A., HACEIN-BEY-ABINA, S., SCHMIDT, M., GARRIGUE, A., BRUGMAN, M. H., HU, J., GLIMM, H., GYAPAY, G., PRUM, B., FRASER, C. C., FISCHER, N., SCHWARZWAELDER, K., SIEGLER, M. L., DE RIDDER, D., PIKE-OVERZET, K., HOWE, S. J., THRASHER, A. J., WAGEMAKER, G., ABEL, U., STAAL, F. J., DELABESSE, E., VILLEVAL, J. L., ARONOW, B., HUE, C., PRINZ, C., WISSLER, M., KLANKE, C., WEISSENBACH, J., ALEXANDER, I., FISCHER, A., VON KALLE, C. & CAVAZZANA-CALVO, M. 2007. Vector integration is nonrandom and clustered and influences the fate of lymphopoiesis in SCID-X1 gene therapy. *J Clin Invest*, 117: 2225-32.
- DEMAISON, C., PARSLEY, K., BROUNS, G., SCHERR, M., BATTMER, K., KINNON, C., GREZ, M. & THRASHER, A. J. 2002. High-level transduction and gene expression in hematopoietic repopulating cells using a human immunodeficiency [correction of imunodeficiency] virus type 1-based lentiviral vector containing an internal spleen focus forming virus promoter. *Hum Gene Ther*, 13: 803-13.
- DENG, D. X., SPIN, J. M., TSALENKO, A., VAILAYA, A., BEN-DOR, A., YAKHINI, Z., TSAO, P., BRUHN, L. & QUERTERMOUS, T. 2006. Molecular signatures determining coronary artery and saphenous vein smooth muscle cell phenotypes: distinct responses to stimuli. *Arterioscler Thromb Vasc Biol*, 26: 1058-65.
- DI LORENZO, A., MANES, T. D., DAVALOS, A., WRIGHT, P. L. & SESSA, W. C. 2010. Endothelial Reticulon-4B (Nogo-B) regulates ICAM-1-mediated leukocyte transmigration and acute inflammation. *Blood*, 117: 2284-2295.
- DISHART, K. L., DENBY, L., GEORGE, S. J., NICKLIN, S. A., YENDLURI, S., TUERK, M. J., KELLEY, M. P., DONAHUE, B. A., NEWBY, A. C., HARDING, T. & BAKER, A. H. 2003a. Third-generation lentivirus vectors efficiently transduce and phenotypically modify vascular cells: implications for gene therapy. *J Mol Cell Cardiol*, 35: 739-48.

- DISHART, K. L., WORK, L. M., DENBY, L. & BAKER, A. H. 2003b. Gene Therapy for Cardiovascular Disease. *J Biomed Biotechnol*, 2003: 138-148.
- DODD, D. A., NIEDEROEST, B., BLOECHLINGER, S., DUPUIS, L., LOEFFLER, J. P. & SCHWAB, M. E. 2005. Nogo-A, -B, and -C are found on the cell surface and interact together in many different cell types. *J Biol Chem*, 280: 12494-502.
- DULL, T., ZUFFEREY, R., KELLY, M., MANDEL, R. J., NGUYEN, M., TRONO, D. & NALDINI, L. 1998. A third-generation lentivirus vector with a conditional packaging system. *J Virol*, 72: 8463-71.
- EDELSTEIN, M. L., ABEDI, M. R. & WIXON, J. 2007. Gene therapy clinical trials worldwide to 2007--an update. *J Gene Med*, 9: 833-42.
- EDELSTEIN, M. L., ABEDI, M. R., WIXON, J. & EDELSTEIN, R. M. 2004. Gene therapy clinical trials worldwide 1989-2004-an overview. *J Gene Med*, 6: 597-602.
- EGASHIRA, K., NAKANO, K., OHTANI, K., FUNAKOSHI, K., ZHAO, G., IHARA, Y., KOGA, J., KIMURA, S., TOMINAGA, R. & SUNAGAWA, K. 2007. Local delivery of anti-monocyte chemoattractant protein-1 by gene-eluting stents attenuates in-stent stenosis in rabbits and monkeys. *Arterioscler Thromb Vasc Biol*, 27: 2563-8.
- EHSAN, A. & MANN, M. J. 2000. Antisense and gene therapy to prevent restenosis. *Vasc Med*, 5: 103-14.
- EHSAN, A., MANN, M. J., DELL'ACQUA, G. & DZAU, V. J. 2001. Long-term stabilization of vein graft wall architecture and prolonged resistance to experimental atherosclerosis after E2F decoy oligonucleotide gene therapy. *J Thorac Cardiovasc Surg*, 121: 714-22.
- ELLIS, B. L., POTTS, P. R. & PORTEUS, M. H. 2011. Creating higher titer lentivirus with caffeine. *Hum Gene Ther*, 22: 93-100.
- ESCORS, D. & BRECKPOT, K. 2010. Lentiviral vectors in gene therapy: their current status and future potential. *Arch Immunol Ther Exp (Warsz)*, 58: 107-19.
- FAGER, G., HANSSON, G. K., OTTOSSON, P., DAHLLOF, B. & BONDJERS, G. 1988. Human arterial smooth muscle cells in culture. Effects of platelet-derived growth factor and heparin on growth in vitro. *Exp Cell Res*, 176: 319-35.
- FEDERICO, M. 2003. From lentiviruses to lentivirus vectors. *Methods Mol Biol*, 229: 3-15.
- FERNS, G. A., RAINES, E. W., SPRUGEL, K. H., MOTANI, A. S., REIDY, M. A. & ROSS, R. 1991. Inhibition of neointimal smooth muscle accumulation after angioplasty by an antibody to PDGF. *Science*, 253: 1129-32.
- FERNS, G. A., SPRUGEL, K. H., SEIFERT, R. A., BOWEN-POPE, D. F., KELLY, J. D., MURRAY, M., RAINES, E. W. & ROSS, R. 1990. Relative platelet-derived

growth factor receptor subunit expression determines cell migration to different dimeric forms of PDGF. *Growth Factors*, 3: 315-24.

- FINN, A. V., NAKAZAWA, G., JONER, M., KOLODIE, F. D., MONT, E. K., GOLD, H. K. & VIRMANI, R. 2007. Vascular responses to drug eluting stents: importance of delayed healing. *Arterioscler Thromb Vasc Biol*, 27: 1500-10.
- FISHBEIN, I., ALFERIEV, I. S., NYANGUILE, O., GASTER, R., VOHS, J. M., WONG, G. S., FELDERMAN, H., CHEN, I. W., CHOI, H., WILENSKY, R. L. & LEVY, R. J. 2006. Bisphosphonate-mediated gene vector delivery from the metal surfaces of stents. *Proc Natl Acad Sci U S A*, 103: 159-64.
- GABRIEL, R., ECKENBERG, R., PARUZYNSKI, A., BARTHOLOMAE, C. C., NOWROUZI, A., ARENS, A., HOWE, S. J., RECCHIA, A., CATTOGLIO, C., WANG, W., FABER, K., SCHWARZWAELDER, K., KIRSTEN, R., DEICHMANN, A., BALL, C. R., BALAGGAN, K. S., YANEZ-MUNOZ, R. J., ALI, R. R., GASPAR, H. B., BIASCO, L., AIUTI, A., CESANA, D., MONTINI, E., NALDINI, L., COHEN-HAGUENAUER, O., MAVILIO, F., THRASHER, A. J., GLIMM, H., VON KALLE, C., SAURIN, W. & SCHMIDT, M. 2009. Comprehensive genomic access to vector integration in clinical gene therapy. *Nat Med*, 15: 1431-6.
- GAFFNEY, M. M., HYNES, S. O., BARRY, F. & O'BRIEN, T. 2007. Cardiovascular gene therapy: current status and therapeutic potential. *Br J Pharmacol*, 152: 175-88.
- GALY, A., RONCAROLO, M. G. & THRASHER, A. J. 2008. Development of lentiviral gene therapy for Wiskott Aldrich syndrome. *Expert Opin Biol Ther*, 8: 181-90.
- GAO, F., QIU, B., KAR, S., ZHAN, X., HOFMANN, L. V. & YANG, X. 2006. Intravascular magnetic resonance/radiofrequency may enhance gene therapy for prevention of in-stent neointimal hyperplasia. *Acad Radiol*, 13: 526-30.
- GASPAR, H. B., PARSLEY, K. L., HOWE, S., KING, D., GILMOUR, K. C., SINCLAIR, J., BROUNS, G., SCHMIDT, M., VON KALLE, C., BARINGTON, T., JAKOBSEN, M. A., CHRISTENSEN, H. O., AL GHONAIUM, A., WHITE, H. N., SMITH, J. L., LEVINSKY, R. J., ALI, R. R., KINNON, C. & THRASHER, A. J. 2004. Gene therapy of X-linked severe combined immunodeficiency by use of a pseudotyped gammaretroviral vector. *Lancet*, 364: 2181-7.
- GENG, Y. J., WU, Q., MUSZYNSKI, M., HANSSON, G. K. & LIBBY, P. 1996. Apoptosis of vascular smooth muscle cells induced by in vitro stimulation with interferon-gamma, tumor necrosis factor-alpha, and interleukin-1 beta. *Arterioscler Thromb Vasc Biol*, 16: 19-27.
- GEORGE, S. J., ANGELINI, G. D., CAPOGROSSI, M. C. & BAKER, A. H. 2001. Wild-type p53 gene transfer inhibits neointima formation in human saphenous vein by modulation of smooth muscle cell migration and induction of apoptosis. *Gene Ther*, 8: 668-76.
- GEORGE, S. J., BAKER, A. H., ANGELINI, G. D. & NEWBY, A. C. 1998a. Gene transfer of tissue inhibitor of metalloproteinase-2 inhibits

metalloproteinase activity and neointima formation in human saphenous veins. *Gene Ther*, 5: 1552-60.

GEORGE, S. J., CHANNON, K. M. & BAKER, A. H. 2006. Gene therapy and coronary artery bypass grafting: current perspectives. *Curr Opin Mol Ther*, 8: 288-94.

GEORGE, S. J., JOHNSON, J. L., ANGELINI, G. D., NEWBY, A. C. & BAKER, A. H. 1998b. Adenovirus-mediated gene transfer of the human TIMP-1 gene inhibits smooth muscle cell migration and neointimal formation in human saphenous vein. *Hum Gene Ther*, 9: 867-77.

GEORGE, S. J., LLOYD, C. T., ANGELINI, G. D., NEWBY, A. C. & BAKER, A. H. 2000. Inhibition of late vein graft neointima formation in human and porcine models by adenovirus-mediated overexpression of tissue inhibitor of metalloproteinase-3. *Circulation*, 101: 296-304.

GLASS, C. K. & WITZTUM, J. L. 2001. Atherosclerosis. the road ahead. *Cell*, 104: 503-16.

GORDON, D., REIDY, M. A., BENDITT, E. P. & SCHWARTZ, S. M. 1990. Cell proliferation in human coronary arteries. *Proc Natl Acad Sci U S A*, 87: 4600-4.

GRAF, K., XI, X. P., YANG, D., FLECK, E., HSUEH, W. A. & LAW, R. E. 1997. Mitogen-activated protein kinase activation is involved in platelet-derived growth factor-directed migration by vascular smooth muscle cells. *Hypertension*, 29: 334-9.

GRIFFITHS-JONES, S., GROCOCK, R. J., VAN DONGEN, S., BATEMAN, A. & ENRIGHT, A. J. 2006. miRBase: microRNA sequences, targets and gene nomenclature. *Nucleic Acids Res*, 34: D140-4.

GRIFFITHS-JONES, S., SAINI, H. K., VAN DONGEN, S. & ENRIGHT, A. J. 2008. miRBase: tools for microRNA genomics. *Nucleic Acids Res*, 36: D154-8.

GROPP, M., ITSYKSON, P., SINGER, O., BEN-HUR, T., REINHARTZ, E., GALUN, E. & REUBINOFF, B. E. 2003. Stable genetic modification of human embryonic stem cells by lentiviral vectors. *Mol Ther*, 7: 281-7.

GROVES, P. H., BANNING, A. P., PENNY, W. J., LEWIS, M. J., CHEADLE, H. A. & NEWBY, A. C. 1995. Kinetics of smooth muscle cell proliferation and intimal thickening in a pig carotid model of balloon injury. *Atherosclerosis*, 117: 83-96.

HACEIN-BEY-ABINA, S., GARRIGUE, A., WANG, G. P., SOULIER, J., LIM, A., MORILLON, E., CLAPPIER, E., CACCAVELLI, L., DELABESSE, E., BELDJORD, K., ASNAFI, V., MACINTYRE, E., DAL CORTIVO, L., RADFORD, I., BROUSSE, N., SIGAUX, F., MOSHOUS, D., HAUER, J., BORKHARDT, A., BELOHRADSKY, B. H., WINTERGERST, U., VELEZ, M. C., LEIVA, L., SORENSEN, R., WULFFRAAT, N., BLANCHE, S., BUSHMAN, F. D., FISCHER, A. & CAVAZZANA-CALVO, M. 2008. Insertional oncogenesis in 4 patients after retrovirus-mediated gene therapy of SCID-X1. *J Clin Invest*, 118: 3132-42.

- HACEIN-BEY-ABINA, S., HAUER, J., LIM, A., PICARD, C., WANG, G. P., BERRY, C. C., MARTINACHE, C., RIEUX-LAUCAT, F., LATOUR, S., BELOHRADSKY, B. H., LEIVA, L., SORENSEN, R., DEBRE, M., CASANOVA, J. L., BLANCHE, S., DURANDY, A., BUSHMAN, F. D., FISCHER, A. & CAVAZZANA-CALVO, M. 2010. Efficacy of gene therapy for X-linked severe combined immunodeficiency. *N Engl J Med*, 363: 355-64.
- HACEIN-BEY-ABINA, S., LE DEIST, F., CARLIER, F., BOUNEAUD, C., HUE, C., DE VILLARTAY, J. P., THRASHER, A. J., WULFFRAAT, N., SORENSEN, R., DUPUIS-GIROD, S., FISCHER, A., DAVIES, E. G., KUIS, W., LEIVA, L. & CAVAZZANA-CALVO, M. 2002. Sustained correction of X-linked severe combined immunodeficiency by ex vivo gene therapy. *N Engl J Med*, 346: 1185-93.
- HACEIN-BEY-ABINA, S., VON KALLE, C., SCHMIDT, M., LE DEIST, F., WULFFRAAT, N., MCINTYRE, E., RADFORD, I., VILLEVAL, J. L., FRASER, C. C., CAVAZZANA-CALVO, M. & FISCHER, A. 2003a. A serious adverse event after successful gene therapy for X-linked severe combined immunodeficiency. *N Engl J Med*, 348: 255-6.
- HACEIN-BEY-ABINA, S., VON KALLE, C., SCHMIDT, M., MCCORMACK, M. P., WULFFRAAT, N., LEBOULCH, P., LIM, A., OSBORNE, C. S., PAWLIUK, R., MORILLON, E., SORENSEN, R., FORSTER, A., FRASER, P., COHEN, J. I., DE SAINT BASILE, G., ALEXANDER, I., WINTERGERST, U., FREBOURG, T., AURIAS, A., STOPPA-LYONNET, D., ROMANA, S., RADFORD-WEISS, I., GROSS, F., VALENSI, F., DELABESSE, E., MACINTYRE, E., SIGAUX, F., SOULIER, J., LEIVA, L. E., WISSLER, M., PRINZ, C., RABBITTS, T. H., LE DEIST, F., FISCHER, A. & CAVAZZANA-CALVO, M. 2003b. LMO2-associated clonal T cell proliferation in two patients after gene therapy for SCID-X1. *Science*, 302: 415-9.
- HACEIN-BEY, H., CAVAZZANA-CALVO, M., LE DEIST, F., DAUTRY-VARSAT, A., HIVROZ, C., RIVIERE, I., DANOS, O., HEARD, J. M., SUGAMURA, K., FISCHER, A. & DE SAINT BASILE, G. 1996. gamma-c gene transfer into SCID X1 patients' B-cell lines restores normal high-affinity interleukin-2 receptor expression and function. *Blood*, 87: 3108-16.
- HACEIN-BEY, S., BASILE, G. D., LEMERLE, J., FISCHER, A. & CAVAZZANA-CALVO, M. 1998. gammac gene transfer in the presence of stem cell factor, FLT-3L, interleukin-7 (IL-7), IL-1, and IL-15 cytokines restores T-cell differentiation from gammac(-) X-linked severe combined immunodeficiency hematopoietic progenitor cells in murine fetal thymic organ cultures. *Blood*, 92: 4090-7.
- HACHIYA, A., SRIWIRIYANONT, P., PATEL, A., SAITO, N., OHUCHI, A., KITAHARA, T., TAKEMA, Y., TSUBOI, R., BOISSY, R. E., VISSCHER, M. O., WILSON, J. M. & KOBINGER, G. P. 2007. Gene transfer in human skin with different pseudotyped HIV-based vectors. *Gene Ther*, 14: 648-56.
- HANAWA, H., KELLY, P. F., NATHWANI, A. C., PERSONS, D. A., VANDERGRUFF, J. A., HARGROVE, P., VANIN, E. F. & NIENHUIS, A. W. 2002. Comparison of various envelope proteins for their ability to pseudotype lentiviral vectors and transduce primitive hematopoietic cells from human blood. *Mol Ther*, 5: 242-51.

- HARRISON, K. D., MIAO, R. Q., FERNANDEZ-HERNANDO, C., SUAREZ, Y., DAVALOS, A. & SESSA, W. C. 2009. Nogo-B receptor stabilizes Niemann-Pick type C2 protein and regulates intracellular cholesterol trafficking. *Cell Metab*, 10: 208-18.
- HARRISON, K. D., PARK, E. J., GAO, N., KUO, A., RUSH, J. S., WAECHTER, C. J., LEHRMAN, M. A. & SESSA, W. C. 2011. Nogo-B receptor is necessary for cellular dolichol biosynthesis and protein N-glycosylation. *EMBO J*, 30: 2490-2500.
- HEDMAN, M., HARTIKAINEN, J., SYVANNE, M., STJERNVALL, J., HEDMAN, A., KIVELA, A., VANNINEN, E., MUSSALO, H., KAUPPILA, E., SIMULA, S., NARVANEN, O., RANTALA, A., PEUHKURINEN, K., NIEMINEN, M. S., LAAKSO, M. & YLA-HERTTUALA, S. 2003. Safety and feasibility of catheter-based local intracoronary vascular endothelial growth factor gene transfer in the prevention of postangioplasty and in-stent restenosis and in the treatment of chronic myocardial ischemia: phase II results of the Kuopio Angiogenesis Trial (KAT). *Circulation*, 107: 2677-83.
- HEDMAN, M., HARTIKAINEN, J. & YLA-HERTTUALA, S. 2011. Progress and prospects: hurdles to cardiovascular gene therapy clinical trials. *Gene Ther*, 18: 743-749.
- HEDMAN, M., MUONA, K., HEDMAN, A., KIVELA, A., SYVANNE, M., ERANEN, J., RANTALA, A., STJERNVALL, J., NIEMINEN, M. S., HARTIKAINEN, J. & YLA-HERTTUALA, S. 2009. Eight-year safety follow-up of coronary artery disease patients after local intracoronary VEGF gene transfer. *Gene Ther*, 16: 629-34.
- HEINZINGER, N. K., BUKINSKY, M. I., HAGGERTY, S. A., RAGLAND, A. M., KEWALRAMANI, V., LEE, M. A., GENDELMAN, H. E., RATNER, L., STEVENSON, M. & EMERMAN, M. 1994. The Vpr protein of human immunodeficiency virus type 1 influences nuclear localization of viral nucleic acids in nondividing host cells. *Proc Natl Acad Sci U S A*, 91: 7311-5.
- HIGASHIKAWA, F. & CHANG, L. 2001. Kinetic analyses of stability of simple and complex retroviral vectors. *Virology*, 280: 124-31.
- HILKER, M., TELLMANN, G., BUERKE, M., GLOGER, K., MOERSIG, W., OELERT, H., HAKE, U. & LEHR, H. A. 2002. Proliferative activity in stenotic human aortocoronary bypass grafts. *Cardiovasc Pathol*, 11: 284-90.
- HOLYCROSS, B. J., BLANK, R. S., THOMPSON, M. M., PEACH, M. J. & OWENS, G. K. 1992. Platelet-derived growth factor-BB-induced suppression of smooth muscle cell differentiation. *Circ Res*, 71: 1525-32.
- HOTAMISLIGIL, G. S. 2010. Endoplasmic reticulum stress and atherosclerosis. *Nat Med*, 16: 396-9.
- HOWE, S. J., MANSOUR, M. R., SCHWARZWAELDER, K., BARTHOLOMAE, C., HUBANK, M., KEMPSKI, H., BRUGMAN, M. H., PIKE-OVERZET, K., CHATTERS, S. J., DE RIDDER, D., GILMOUR, K. C., ADAMS, S., THORNHILL, S. I., PARSLEY, K. L., STAAL, F. J., GALE, R. E., LINCH, D. C., BAYFORD,

J., BROWN, L., QUAYE, M., KINNON, C., ANCLIFF, P., WEBB, D. K., SCHMIDT, M., VON KALLE, C., GASPAR, H. B. & THRASHER, A. J. 2008. Insertional mutagenesis combined with acquired somatic mutations causes leukemogenesis following gene therapy of SCID-X1 patients. *J Clin Invest*, 118: 3143-50.

[HTTP://WWW.BHF.ORG.UK](http://www.bhf.org.uk) 2008. Cardiovascular (heart and circulatory) disease. *British Heart Foundation Coronary Heart Disease Statistics*. BHF.

[HTTP://WWW.BHF.ORG.UK](http://www.bhf.org.uk) 2010a. Treatment: coronary angioplasty and stents. *Heart Health*. British Heart Foundation.

[HTTP://WWW.BHF.ORG.UK](http://www.bhf.org.uk) 2010b. Treatment: coronary bypass surgery. *Heart Health*. British Heart Foundation.

[HTTP://WWW.DH.GOV.UK/AB/GTAC/GENETHERAPY/](http://www.dh.gov.uk/ab/gtac/genetherapy/) 2011. Gene Therapy Advisory Committee, Gene Therapy. Department of Health, Gene Therapy Advisory Committee (GTAC).

[HTTP://WWW.HEARTSTATS.ORG](http://www.heartstats.org) 2009a. Heart and circulatory disease is the biggest killer. *British Heart Foundation statistics*. British Heart Foundation.

[HTTP://WWW.HEARTSTATS.ORG](http://www.heartstats.org) 2009b. Number of CABGs and PCIs, 1977 to 2008, United Kingdom. *British Heart Foundation Statistics Website*. British Heart Foundation.

[HTTP://WWW.HEARTSTATS.ORG](http://www.heartstats.org) 2010a. Coronary heart disease statistics: mortality. *Coronary heart disease statistics, seventeenth edition*. British Heart Foundation.

[HTTP://WWW.HEARTSTATS.ORG](http://www.heartstats.org) 2010b. Coronary heart disease statistics: summary. *Coronary heart disease statistics, seventeenth edition*. British Heart Foundation.

[HTTP://WWW.HEARTSTATS.ORG](http://www.heartstats.org) 2010c. Treatment: revascularisation procedures. *Coronary heart disease statistics*. British Heart Foundation.

[HTTP://WWW.OXFORDBIOMEDICA.CO.UK/](http://www.oxfordbiomedica.co.uk/) 2011. Oxford BioMedica's LentiVector® gene delivery technology *Oxford BioMedica, gene-delivery technologies*. Oxford BioMedica.

[HTTP://WWW.WHO.INT](http://www.who.int) 2009. Cardiovascular diseases (CVDs): fact sheets. *WHO: Cardiovascular diseases*. World Health Organisation (WHO).

[HTTP://WWW.WILEY.COM/LEGACY/WILEYCHI/GENMED/CLINICAL/](http://www.wiley.com/legacy/wileychi/genmed/clinical/) 2011a. Indications addressed by gene therapy clinical trials. *Journal of Gene Medicine*. Wiley.

[HTTP://WWW.WILEY.COM/LEGACY/WILEYCHI/GENMED/CLINICAL/](http://www.wiley.com/legacy/wileychi/genmed/clinical/) 2011b. Number of gene therapy clinical trials approved worldwide 1989-2010. *Journal of Gene Medicine*. Wiley.

- HTTP://WWW.WILEY.COM/LEGACY/WILEYCHI/GENMED/CLINICAL/ 2011c.  
Vectors used in gene therapy clinical trials. *Journal of Gene Medicine*.  
Wiley.
- HU, Y., BAKER, A. H., ZOU, Y., NEWBY, A. C. & XU, Q. 2001. Local gene transfer of tissue inhibitor of metalloproteinase-2 influences vein graft remodeling in a mouse model. *Arterioscler Thromb Vasc Biol*, 21: 1275-80.
- HUBER, A. B., WEINMANN, O., BROSAMLE, C., OERTLE, T. & SCHWAB, M. E. 2002. Patterns of Nogo mRNA and protein expression in the developing and adult rat and after CNS lesions. *J Neurosci*, 22: 3553-67.
- HUEB, W., LOPES, N., GERSH, B. J., SOARES, P. R., RIBEIRO, E. E., PEREIRA, A. C., FAVARATO, D., ROCHA, A. S., HUEB, A. C. & RAMIRES, J. A. 2010. Ten-year follow-up survival of the Medicine, Angioplasty, or Surgery Study (MASS II): a randomized controlled clinical trial of 3 therapeutic strategies for multivessel coronary artery disease. *Circulation*, 122: 949-57.
- HUEB, W., LOPES, N. H., GERSH, B. J., SOARES, P., MACHADO, L. A., JATENE, F. B., OLIVEIRA, S. A. & RAMIRES, J. A. 2007. Five-year follow-up of the Medicine, Angioplasty, or Surgery Study (MASS II): a randomized controlled clinical trial of 3 therapeutic strategies for multivessel coronary artery disease. *Circulation*, 115: 1082-9.
- IACCARINO, G., SMITHWICK, L. A., LEFKOWITZ, R. J. & KOCH, W. J. 1999. Targeting Gbeta gamma signaling in arterial vascular smooth muscle proliferation: a novel strategy to limit restenosis. *Proc Natl Acad Sci U S A*, 96: 3945-50.
- IKEDA, Y., TAKEUCHI, Y., MARTIN, F., COSSET, F. L., MITROPHANOUS, K. & COLLINS, M. 2003. Continuous high-titer HIV-1 vector production. *Nat Biotechnol*, 21: 569-72.
- JAFFE, E. A., NACHMAN, R. L., BECKER, C. G. & MINICK, C. R. 1973. Culture of human endothelial cells derived from umbilical veins. Identification by morphologic and immunologic criteria. *J Clin Invest*, 52: 2745-56.
- JAKOBSSON, J., NIELSEN, T. T., STAFILIN, K., GEORGIEVSKA, B. & LUNDBERG, C. 2006. Efficient transduction of neurons using Ross River glycoprotein-pseudotyped lentiviral vectors. *Gene Ther*, 13: 966-73.
- JANSSENS, S., FLAHERTY, D., NONG, Z., VARENNE, O., VAN PELT, N., HAUSTERMANS, C., ZOLDHELYI, P., GERARD, R. & COLLEN, D. 1998. Human endothelial nitric oxide synthase gene transfer inhibits vascular smooth muscle cell proliferation and neointima formation after balloon injury in rats. *Circulation*, 97: 1274-81.
- JAWIEN, A., BOWEN-POPE, D. F., LINDNER, V., SCHWARTZ, S. M. & CLOWES, A. W. 1992. Platelet-derived growth factor promotes smooth muscle migration and intimal thickening in a rat model of balloon angioplasty. *J Clin Invest*, 89: 507-11.
- JENSEN, L. O., MAENG, M., KALTOFT, A., THAYSSSEN, P., HANSEN, H. H., BOTTCHER, M., LASSEN, J. F., KRUSSEL, L. R., RASMUSSEN, K., HANSEN,

- K. N., PEDERSEN, L., JOHNSEN, S. P., SOERENSEN, H. T. & THUESEN, L. 2007. Stent thrombosis, myocardial infarction, and death after drug-eluting and bare-metal stent coronary interventions. *J Am Coll Cardiol*, 50: 463-70.
- JI, R., CHENG, Y., YUE, J., YANG, J., LIU, X., CHEN, H., DEAN, D. B. & ZHANG, C. 2007. MicroRNA expression signature and antisense-mediated depletion reveal an essential role of MicroRNA in vascular neointimal lesion formation. *Circ Res*, 100: 1579-88.
- JOHN, B., ENRIGHT, A. J., ARAVIN, A., TUSCHL, T., SANDER, C. & MARKS, D. S. 2004. Human MicroRNA targets. *PLoS Biol*, 2: e363.
- JOHNSON, T. W., WU, Y. X., HERDEG, C., BAUMBACH, A., NEWBY, A. C., KARSCH, K. R. & OBERHOFF, M. 2005. Stent-based delivery of tissue inhibitor of metalloproteinase-3 adenovirus inhibits neointimal formation in porcine coronary arteries. *Arterioscler Thromb Vasc Biol*, 25: 754-9.
- JONER, M., FINN, A. V., FARB, A., MONT, E. K., KOLODGIE, F. D., LADICH, E., KUTYS, R., SKORIJA, K., GOLD, H. K. & VIRMANI, R. 2006. Pathology of drug-eluting stents in humans: delayed healing and late thrombotic risk. *J Am Coll Cardiol*, 48: 193-202.
- KANG, Y., STEIN, C. S., HETH, J. A., SINN, P. L., PENISTEN, A. K., STABER, P. D., RATLIFF, K. L., SHEN, H., BARKER, C. K., MARTINS, I., SHARKEY, C. M., SANDERS, D. A., MCCRAY, P. B., JR. & DAVIDSON, B. L. 2002. In vivo gene transfer using a nonprimate lentiviral vector pseudotyped with Ross River Virus glycoproteins. *J Virol*, 76: 9378-88.
- KAPLAN-ALBUQUERQUE, N., GARAT, C., DESSEVA, C., JONES, P. L. & NEMENOFF, R. A. 2003. Platelet-derived growth factor-BB-mediated activation of Akt suppresses smooth muscle-specific gene expression through inhibition of mitogen-activated protein kinase and redistribution of serum response factor. *J Biol Chem*, 278: 39830-8.
- KARVINEN, H. & YLA-HERTTUALA, S. 2010. New aspects in vascular gene therapy. *Curr Opin Pharmacol*, 10: 208-11.
- KATO, S., INOUE, K., KOBAYASHI, K., YASOSHIMA, Y., MIYACHI, S., INOUE, S., HANAWA, H., SHIMADA, T., TAKADA, M. & KOBAYASHI, K. 2007. Efficient gene transfer via retrograde transport in rodent and primate brains using a human immunodeficiency virus type 1-based vector pseudotyped with rabies virus glycoprotein. *Hum Gene Ther*, 18: 1141-51.
- KIBBE, M. R., TZENG, E., GLEIXNER, S. L., WATKINS, S. C., KOVESDI, I., LIZONOVA, A., MAKAROUN, M. S., BILLIAR, T. R. & RHEE, R. Y. 2001. Adenovirus-mediated gene transfer of human inducible nitric oxide synthase in porcine vein grafts inhibits intimal hyperplasia. *J Vasc Surg*, 34: 156-65.
- KING, S. B., 3RD, SMITH, S. C., JR., HIRSHFELD, J. W., JR., JACOBS, A. K., MORRISON, D. A., WILLIAMS, D. O., FELDMAN, T. E., KERN, M. J., O'NEILL, W. W., SCHAFF, H. V., WHITLOW, P. L., ADAMS, C. D., ANDERSON, J. L., BULLER, C. E., CREAGER, M. A., ETTINGER, S. M., HALPERIN, J. L., HUNT,

- S. A., KRUMHOLZ, H. M., KUSHNER, F. G., LYTLE, B. W., NISHIMURA, R., PAGE, R. L., RIEGEL, B., TARKINGTON, L. G. & YANCY, C. W. 2008. 2007 Focused Update of the ACC/AHA/SCAI 2005 Guideline Update for Percutaneous Coronary Intervention: a report of the American College of Cardiology/American Heart Association Task Force on Practice Guidelines: 2007 Writing Group to Review New Evidence and Update the ACC/AHA/SCAI 2005 Guideline Update for Percutaneous Coronary Intervention, Writing on Behalf of the 2005 Writing Committee. *Circulation*, 117: 261-95.
- KLAGES, N., ZUFFEREY, R. & TRONO, D. 2000. A stable system for the high-titer production of multiply attenuated lentiviral vectors. *Mol Ther*, 2: 170-6.
- KLUGHERZ, B. D., JONES, P. L., CUI, X., CHEN, W., MENEVEAU, N. F., DEFELICE, S., CONNOLLY, J., WILENSKY, R. L. & LEVY, R. J. 2000. Gene delivery from a DNA controlled-release stent in porcine coronary arteries. *Nat Biotechnol*, 18: 1181-4.
- KLUGHERZ, B. D., SONG, C., DEFELICE, S., CUI, X., LU, Z., CONNOLLY, J., HINSON, J. T., WILENSKY, R. L. & LEVY, R. J. 2002. Gene delivery to pig coronary arteries from stents carrying antibody-tethered adenovirus. *Hum Gene Ther*, 13: 443-54.
- KOBINGER, G. P., WEINER, D. J., YU, Q. C. & WILSON, J. M. 2001. Filovirus-pseudotyped lentiviral vector can efficiently and stably transduce airway epithelia in vivo. *Nat Biotechnol*, 19: 225-30.
- KOCH, P., SIEMEN, H., BIEGLER, A., ITSKOVITZ-ELDOR, J. & BRUSTLE, O. 2006. Transduction of human embryonic stem cells by ecotropic retroviral vectors. *Nucleic Acids Res*, 34: e120.
- KRITZ, A. B., YU, J., WRIGHT, P. L., WAN, S., GEORGE, S. J., HALLIDAY, C., KANG, N., SESSA, W. C. & BAKER, A. H. 2008. In vivo modulation of Nogo-B attenuates neointima formation. *Mol Ther*, 16: 1798-804.
- KUANG, E., WAN, Q., LI, X., XU, H., ZOU, T. & QI, Y. 2006. ER stress triggers apoptosis induced by Nogo-B/ASY overexpression. *Exp Cell Res*, 312: 1983-8.
- KUMAR, A. & LINDNER, V. 1997. Remodeling with neointima formation in the mouse carotid artery after cessation of blood flow. *Arterioscler Thromb Vasc Biol*, 17: 2238-44.
- KUMAR, M., BRADOW, B. P. & ZIMMERBERG, J. 2003. Large-scale production of pseudotyped lentiviral vectors using baculovirus GP64. *Hum Gene Ther*, 14: 67-77.
- KUMAR, M., KELLER, B., MAKALOU, N. & SUTTON, R. E. 2001. Systematic determination of the packaging limit of lentiviral vectors. *Hum Gene Ther*, 12: 1893-905.
- KUNICHER, N., FALK, H., YAACOV, B., TZUR, T. & PANET, A. 2008. Tropism of lentiviral vectors in skin tissue. *Hum Gene Ther*, 19: 255-66.

- KUSHNER, F. G., HAND, M., SMITH, S. C., JR., KING, S. B., 3RD, ANDERSON, J. L., ANTMAN, E. M., BAILEY, S. R., BATES, E. R., BLANKENSHIP, J. C., CASEY, D. E., JR., GREEN, L. A., HOCHMAN, J. S., JACOBS, A. K., KRUMHOLZ, H. M., MORRISON, D. A., ORNATO, J. P., PEARLE, D. L., PETERSON, E. D., SLOAN, M. A., WHITLOW, P. L. & WILLIAMS, D. O. 2009. 2009 Focused Updates: ACC/AHA Guidelines for the Management of Patients With ST-Elevation Myocardial Infarction (updating the 2004 Guideline and 2007 Focused Update) and ACC/AHA/SCAI Guidelines on Percutaneous Coronary Intervention (updating the 2005 Guideline and 2007 Focused Update): a report of the American College of Cardiology Foundation/American Heart Association Task Force on Practice Guidelines. *Circulation*, 120: 2271-306.
- KUTNER, R. H., ZHANG, X. Y. & REISER, J. 2009. Production, concentration and titration of pseudotyped HIV-1-based lentiviral vectors. *Nat Protoc*, 4: 495-505.
- LAITINEN, M., HARTIKAINEN, J., HILTUNEN, M. O., ERANEN, J., KIVINIEMI, M., NARVANEN, O., MAKINEN, K., MANNINEN, H., SYVANNE, M., MARTIN, J. F., LAAKSO, M. & YLA-HERTTUALA, S. 2000. Catheter-mediated vascular endothelial growth factor gene transfer to human coronary arteries after angioplasty. *Hum Gene Ther*, 11: 263-70.
- LAITINEN, M., ZACHARY, I., BREIER, G., PAKKANEN, T., HAKKINEN, T., LUOMA, J., ABEDI, H., RISAU, W., SOMA, M., LAAKSO, M., MARTIN, J. F. & YLA-HERTTUALA, S. 1997. VEGF gene transfer reduces intimal thickening via increased production of nitric oxide in carotid arteries. *Hum Gene Ther*, 8: 1737-44.
- LANGE, R. A. & HILLIS, L. D. 2010. Second-generation drug-eluting coronary stents. *N Engl J Med*, 362: 1728-30.
- LEAVITT, A. D., ROBLES, G., ALESANDRO, N. & VARMUS, H. E. 1996. Human immunodeficiency virus type 1 integrase mutants retain in vitro integrase activity yet fail to integrate viral DNA efficiently during infection. *J Virol*, 70: 721-8.
- LEE, A. S. 2005. The ER chaperone and signaling regulator GRP78/BiP as a monitor of endoplasmic reticulum stress. *Methods*, 35: 373-81.
- LEE, W. S., KIM, S. W., HONG, S. A., LEE, T. J., PARK, E. S., KIM, H. J., LEE, K. J., KIM, T. H., KIM, C. J. & RYU, W. S. 2009. Atherosclerotic progression attenuates the expression of Nogo-B in autopsied coronary artery: pathology and virtual histology intravascular ultrasound analysis. *J Korean Med Sci*, 24: 596-604.
- LEWIS, B. P., BURGE, C. B. & BARTEL, D. P. 2005. Conserved seed pairing, often flanked by adenosines, indicates that thousands of human genes are microRNA targets. *Cell*, 120: 15-20.
- LI, M. & SONG, J. 2007. Nogo-B receptor possesses an intrinsically unstructured ectodomain and a partially folded cytoplasmic domain. *Biochem Biophys Res Commun*, 360: 128-34.

- LI, Q., QI, B., OKA, K., SHIMAKAGE, M., YOSHIOKA, N., INOUE, H., HAKURA, A., KODAMA, K., STANBRIDGE, E. J. & YUTSUDO, M. 2001. Link of a new type of apoptosis-inducing gene ASY/Nogo-B to human cancer. *Oncogene*, 20: 3929-36.
- LIANG, C. C., PARK, A. Y. & GUAN, J. L. 2007. In vitro scratch assay: a convenient and inexpensive method for analysis of cell migration in vitro. *Nat Protoc*, 2: 329-33.
- LIBBY, P. & O'BRIEN, K. V. 1983. Culture of quiescent arterial smooth muscle cells in a defined serum-free medium. *J Cell Physiol*, 115: 217-23.
- LIBBY, P., RIDKER, P. M. & HANSSON, G. K. 2011. Progress and challenges in translating the biology of atherosclerosis. *Nature*, 473: 317-25.
- LIBBY, P. & THEROUX, P. 2005. Pathophysiology of coronary artery disease. *Circulation*, 111: 3481-8.
- LINDNER, V., FINGERLE, J. & REIDY, M. A. 1993. Mouse model of arterial injury. *Circ Res*, 73: 792-6.
- LIU, X., CHENG, Y., ZHANG, S., LIN, Y., YANG, J. & ZHANG, C. 2009. A necessary role of miR-221 and miR-222 in vascular smooth muscle cell proliferation and neointimal hyperplasia. *Circ Res*, 104: 476-87.
- LO, M., BLOOM, M. L., IMADA, K., BERG, M., BOLLENBACHER, J. M., BLOOM, E. T., KELSALL, B. L. & LEONARD, W. J. 1999. Restoration of lymphoid populations in a murine model of X-linked severe combined immunodeficiency by a gene-therapy approach. *Blood*, 94: 3027-36.
- LODGE, R., SUBBRAMANIAN, R. A., FORGET, J., LEMAY, G. & COHEN, E. A. 1998. MuLV-based vectors pseudotyped with truncated HIV glycoproteins mediate specific gene transfer in CD4<sup>+</sup> peripheral blood lymphocytes. *Gene Ther*, 5: 655-64.
- LOGAN, A. C., NIGHTINGALE, S. J., HAAS, D. L., CHO, G. J., PEPPER, K. A. & KOHN, D. B. 2004. Factors influencing the titer and infectivity of lentiviral vectors. *Hum Gene Ther*, 15: 976-88.
- LOMBARDO, A., GENOVESE, P., BEAUSEJOUR, C. M., COLLEONI, S., LEE, Y. L., KIM, K. A., ANDO, D., URNOV, F. D., GALLI, C., GREGORY, P. D., HOLMES, M. C. & NALDINI, L. 2007. Gene editing in human stem cells using zinc finger nucleases and integrase-defective lentiviral vector delivery. *Nat Biotechnol*, 25: 1298-306.
- LUO, Z., PALASIS, M., YAMAKAWA, M., LIU, L. X., VINCENT, K. A., TRUDELL, L., AKITA, G. A., KOCH, W. J., CHENG, S. H., GREGORY, R. J. & JIANG, C. 2004. Catheter-mediated delivery of adenoviral vectors expressing beta-adrenergic receptor kinase C-terminus inhibits intimal hyperplasia and luminal stenosis in rabbit iliac arteries. *J Gene Med*, 6: 1061-8.
- LUSIS, A. J. 2000. Atherosclerosis. *Nature*, 407: 233-41.

- MACKENZIE, T. C., KOBINGER, G. P., KOOTSTRA, N. A., RADU, A., SENA-ESTEVEZ, M., BOUCHARD, S., WILSON, J. M., VERMA, I. M. & FLAKE, A. W. 2002. Efficient transduction of liver and muscle after in utero injection of lentiviral vectors with different pseudotypes. *Mol Ther*, 6: 349-58.
- MACKENZIE, T. C., KOBINGER, G. P., LOUBOUTIN, J. P., RADU, A., JAVAZON, E. H., SENA-ESTEVEZ, M., WILSON, J. M. & FLAKE, A. W. 2005. Transduction of satellite cells after prenatal intramuscular administration of lentiviral vectors. *J Gene Med*, 7: 50-8.
- MAKINEN, K., MANNINEN, H., HEDMAN, M., MATSI, P., MUSSALO, H., ALHAVA, E. & YLA-HERTTUALA, S. 2002. Increased vascularity detected by digital subtraction angiography after VEGF gene transfer to human lower limb artery: a randomized, placebo-controlled, double-blinded phase II study. *Mol Ther*, 6: 127-33.
- MANN, M. J. & DZAU, V. J. 2000. Therapeutic applications of transcription factor decoy oligonucleotides. *J Clin Invest*, 106: 1071-5.
- MANN, M. J., WHITTEMORE, A. D., DONALDSON, M. C., BELKIN, M., CONTE, M. S., POLAK, J. F., ORAV, E. J., EHSAN, A., DELL'ACQUA, G. & DZAU, V. J. 1999. Ex-vivo gene therapy of human vascular bypass grafts with E2F decoy: the PREVENT single-centre, randomised, controlled trial. *Lancet*, 354: 1493-8.
- MARANGONI, F., BOSTICARDO, M., CHARRIER, S., DRAGHICI, E., LOCCI, M., SCARAMUZZA, S., PANARONI, C., PONZONI, M., SANVITO, F., DOGLIONI, C., LIABEU, M., GJATA, B., MONTUS, M., SIMINOVITCH, K., AIUTI, A., NALDINI, L., DUPRE, L., RONCAROLO, M. G., GALY, A. & VILLA, A. 2009. Evidence for long-term efficacy and safety of gene therapy for Wiskott-Aldrich syndrome in preclinical models. *Mol Ther*, 17: 1073-82.
- MARIN, E. P., MOECKEL, G., AL-LAMKI, R., BRADLEY, J., YAN, Q., WANG, T., WRIGHT, P. L., YU, J. & SESSA, W. C. 2010. Identification and Regulation of Reticulon 4B (Nogo-B) in Renal Tubular Epithelial Cells. *Am J Pathol*, 177: 2765-2773.
- MATRAI, J., CANTORE, A., BARTHOLOMAE, C. C., ANNONI, A., WANG, W., ACOSTA-SANCHEZ, A., SAMARA-KUKO, E., DE WAELE, L., MA, L., GENOVESE, P., DAMO, M., ARENS, A., GOUDY, K., NICHOLS, T. C., VON KALLE, C., MK, L. C., RONCAROLO, M. G., SCHMIDT, M., VANDENDRIESSCHE, T. & NALDINI, L. 2011. Hepatocyte-targeted expression by integrase-defective lentiviral vectors induces antigen-specific tolerance in mice with low genotoxic risk. *Hepatology*, 53: 1696-707.
- MATRAI, J., CHUAH, M. K. & VANDENDRIESSCHE, T. 2010. Recent advances in lentiviral vector development and applications. *Mol Ther*, 18: 477-90.
- MATRAI, J., CHUAH, M. K. L. & VANDENDRIESSCHE, T. 2010. Lentiviral Vectors In: [HERZOG, R. W. & ZOLOTUKHIN, S. (eds.)] *A Guide to Human Gene Therapy*. First ed. World Scientific Publishing Co.Pte.Ltd. p.53-64.

- MAZARAKIS, N. D., AZZOUZ, M., ROHLL, J. B., ELLARD, F. M., WILKES, F. J., OLSEN, A. L., CARTER, E. E., BARBER, R. D., BABAN, D. F., KINGSMAN, S. M., KINGSMAN, A. J., O'MALLEY, K. & MITROPHANOUS, K. A. 2001. Rabies virus glycoprotein pseudotyping of lentiviral vectors enables retrograde axonal transport and access to the nervous system after peripheral delivery. *Hum Mol Genet*, 10: 2109-21.
- MEHTA, D., IZZAT, M. B., BRYAN, A. J. & ANGELINI, G. D. 1997. Towards the prevention of vein graft failure. *Int J Cardiol*, 62 Suppl 1: S55-63.
- MIAO, R. Q., GAO, Y., HARRISON, K. D., PRENDERGAST, J., ACEVEDO, L. M., YU, J., HU, F., STRITTMATTER, S. M. & SESSA, W. C. 2006. Identification of a receptor necessary for Nogo-B stimulated chemotaxis and morphogenesis of endothelial cells. *Proc Natl Acad Sci U S A*, 103: 10997-1002.
- MINAMINO, T. & KITAKAZE, M. 2010. ER stress in cardiovascular disease. *J Mol Cell Cardiol*, 48: 1105-10.
- MINAMINO, T., KOMURO, I. & KITAKAZE, M. 2010. Endoplasmic reticulum stress as a therapeutic target in cardiovascular disease. *Circ Res*, 107: 1071-82.
- MITRA, A. K., GANGAHAR, D. M. & AGRAWAL, D. K. 2006. Cellular, molecular and immunological mechanisms in the pathophysiology of vein graft intimal hyperplasia. *Immunol Cell Biol*, 84: 115-24.
- MODLICH, U., NAVARRO, S., ZYCHLINSKI, D., MAETZIG, T., KNOESS, S., BRUGMAN, M. H., SCHAMBACH, A., CHARRIER, S., GALY, A., THRASHER, A. J., BUEREN, J. & BAUM, C. 2009. Insertional transformation of hematopoietic cells by self-inactivating lentiviral and gammaretroviral vectors. *Mol Ther*, 17: 1919-28.
- MONTINI, E., CESANA, D., SCHMIDT, M., SANVITO, F., PONZONI, M., BARTHOLOMAE, C., SERGI SERGI, L., BENEDICENTI, F., AMBROSI, A., DI SERIO, C., DOGLIONI, C., VON KALLE, C. & NALDINI, L. 2006. Hematopoietic stem cell gene transfer in a tumor-prone mouse model uncovers low genotoxicity of lentiviral vector integration. *Nat Biotechnol*, 24: 687-96.
- MORELLO, F., PERINO, A. & HIRSCH, E. 2009. Phosphoinositide 3-kinase signalling in the vascular system. *Cardiovasc Res*, 82: 261-71.
- MORICE, M. C., SERRUYS, P. W., SOUSA, J. E., FAJADET, J., BAN HAYASHI, E., PERIN, M., COLOMBO, A., SCHULER, G., BARRAGAN, P., GUAGLIUMI, G., MOLNAR, F. & FALOTICO, R. 2002. A randomized comparison of a sirolimus-eluting stent with a standard stent for coronary revascularization. *N Engl J Med*, 346: 1773-80.
- MORISHITA, R., GIBBONS, G. H., HORIUCHI, M., ELLISON, K. E., NAKAMA, M., ZHANG, L., KANEDA, Y., OGIHARA, T. & DZAU, V. J. 1995. A gene therapy strategy using a transcription factor decoy of the E2F binding site inhibits smooth muscle proliferation in vivo. *Proc Natl Acad Sci U S A*, 92: 5855-9.
- MORTELLARO, A., HERNANDEZ, R. J., GUERRINI, M. M., CARLUCCI, F., TABUCCHI, A., PONZONI, M., SANVITO, F., DOGLIONI, C., DI SERIO, C., BIASCO, L.,

- FOLLENZI, A., NALDINI, L., BORDIGNON, C., RONCAROLO, M. G. & AIUTI, A. 2006. Ex vivo gene therapy with lentiviral vectors rescues adenosine deaminase (ADA)-deficient mice and corrects their immune and metabolic defects. *Blood*, 108: 2979-88.
- MURANYI, W., KEHM, R., BAHR, U., MULLER, S., HANDERMANN, M., DARAI, G. & ZEIER, M. 2004. Bovine aortic endothelial cells are susceptible to hantavirus infection; a new aspect in hantavirus ecology. *Virology*, 318: 112-22.
- MUTO, A., FITZGERALD, T. N., PIMIENTO, J. M., MALONEY, S. P., TESO, D., PASZKOWIAK, J. J., WESTVIK, T. S., KUDO, F. A., NISHIBE, T. & DARDIK, A. 2007. Smooth muscle cell signal transduction: implications of vascular biology for vascular surgeons. *J Vasc Surg*, 45 Suppl A: A15-24.
- MUTO, A., MODEL, L., ZIEGLER, K., EGHBALIEH, S. D. & DARDIK, A. 2010. Mechanisms of vein graft adaptation to the arterial circulation: insights into the neointimal algorithm and management strategies. *Circ J*, 74: 1501-12.
- MYOISHI, M., HAO, H., MINAMINO, T., WATANABE, K., NISHIHARA, K., HATAKEYAMA, K., ASADA, Y., OKADA, K., ISHIBASHI-UEDA, H., GABBIANI, G., BOCHATON-PIALLAT, M. L., MOCHIZUKI, N. & KITAKAZE, M. 2007. Increased endoplasmic reticulum stress in atherosclerotic plaques associated with acute coronary syndrome. *Circulation*, 116: 1226-33.
- NABEL, E. G., PLAUTZ, G., BOYCE, F. M., STANLEY, J. C. & NABEL, G. J. 1989. Recombinant gene expression in vivo within endothelial cells of the arterial wall. *Science*, 244: 1342-4.
- NABEL, E. G., PLAUTZ, G. & NABEL, G. J. 1990. Site-specific gene expression in vivo by direct gene transfer into the arterial wall. *Science*, 249: 1285-8.
- NABEL, E. G., PLAUTZ, G. & NABEL, G. J. 1991. Gene transfer into vascular cells. *J Am Coll Cardiol*, 17: 189B-194B.
- NAKANO, K., EGASHIRA, K., OHTANI, K., ZHAO, G., FUNAKOSHI, K., IHARA, Y. & SUNAGAWA, K. 2007. Catheter-based adenovirus-mediated anti-monocyte chemoattractant gene therapy attenuates in-stent neointima formation in cynomolgus monkeys. *Atherosclerosis*, 194: 309-16.
- NALDINI, L., BLOMER, U., GAGE, F. H., TRONO, D. & VERMA, I. M. 1996a. Efficient transfer, integration, and sustained long-term expression of the transgene in adult rat brains injected with a lentiviral vector. *Proc Natl Acad Sci U S A*, 93: 11382-8.
- NALDINI, L., BLOMER, U., GALLAY, P., ORY, D., MULLIGAN, R., GAGE, F. H., VERMA, I. M. & TRONO, D. 1996b. In vivo gene delivery and stable transduction of nondividing cells by a lentiviral vector. *Science*, 272: 263-7.
- NELSON, P. R., YAMAMURA, S., MUREEBE, L., ITOH, H. & KENT, K. C. 1998. Smooth muscle cell migration and proliferation are mediated by distinct

phases of activation of the intracellular messenger mitogen-activated protein kinase. *J Vasc Surg*, 27: 117-25.

- NEWBY, A. C. 2006. Matrix metalloproteinases regulate migration, proliferation, and death of vascular smooth muscle cells by degrading matrix and non-matrix substrates. *Cardiovasc Res*, 69: 614-24.
- NEWBY, A. C. 2007. Metalloproteinases and vulnerable atherosclerotic plaques. *Trends Cardiovasc Med*, 17: 253-8.
- NEWBY, A. C. & ZALTSMAN, A. B. 2000. Molecular mechanisms in intimal hyperplasia. *J Pathol*, 190: 300-9.
- NI, Y., SUN, S., OPARAOCHA, I., HUMEAU, L., DAVIS, B., COHEN, R., BINDER, G., CHANG, Y. N., SLEPUSHKIN, V. & DROPULIC, B. 2005. Generation of a packaging cell line for prolonged large-scale production of high-titer HIV-1-based lentiviral vector. *J Gene Med*, 7: 818-34.
- NICKLIN, S. A. & BAKER, A. H. 1999. Simple Method for Preparing Recombinant Adenoviruses for High-Efficiency Transduction of Vascular Cells. In: [BAKER, A. H. (ed.) *Methods in Molecular Medicine, Vascular Disease: Molecular Biology and Gene Therapy Protocols*. First ed. Human Press Inc., . p.271-283.
- NICKLIN, S. A., BUENING, H., DISHART, K. L., DE ALWIS, M., GIROD, A., HACKER, U., THRASHER, A. J., ALI, R. R., HALLEK, M. & BAKER, A. H. 2001. Efficient and selective AAV2-mediated gene transfer directed to human vascular endothelial cells. *Mol Ther*, 4: 174-81.
- NIGHTINGALE, S. J., HOLLIS, R. P., PEPPER, K. A., PETERSEN, D., YU, X. J., YANG, C., BAHNER, I. & KOHN, D. B. 2006. Transient gene expression by nonintegrating lentiviral vectors. *Mol Ther*, 13: 1121-32.
- NUMAGUCHI, Y., OKUMURA, K., HARADA, M., NARUSE, K., YAMADA, M., OSANAI, H., MATSUI, H., ITO, M. & MUROHARA, T. 2004. Catheter-based prostacyclin synthase gene transfer prevents in-stent restenosis in rabbit atheromatous arteries. *Cardiovasc Res*, 61: 177-85.
- OERTLE, T., HUBER, C., VAN DER PUTTEN, H. & SCHWAB, M. E. 2003a. Genomic structure and functional characterisation of the promoters of human and mouse nogo/rtn4. *J Mol Biol*, 325: 299-323.
- OERTLE, T., KLINGER, M., STUERMER, C. A. & SCHWAB, M. E. 2003b. A reticular rhapsody: phylogenetic evolution and nomenclature of the RTN/Nogo gene family. *Faseb J*, 17: 1238-47.
- OERTLE, T., MERKLER, D. & SCHWAB, M. E. 2003c. Do cancer cells die because of Nogo-B? *Oncogene*, 22: 1390-9.
- OERTLE, T. & SCHWAB, M. E. 2003. Nogo and its paRTNers. *Trends Cell Biol*, 13: 187-94.
- OTT, M. G., SCHMIDT, M., SCHWARZWAELDER, K., STEIN, S., SILER, U., KOEHL, U., GLIMM, H., KUHLCHE, K., SCHILZ, A., KUNKEL, H., NAUNDORF, S.,

- BRINKMANN, A., DEICHMANN, A., FISCHER, M., BALL, C., PILZ, I., DUNBAR, C., DU, Y., JENKINS, N. A., COPELAND, N. G., LUTHI, U., HASSAN, M., THRASHER, A. J., HOELZER, D., VON KALLE, C., SEGER, R. & GREZ, M. 2006. Correction of X-linked chronic granulomatous disease by gene therapy, augmented by insertional activation of MDS1-EVI1, PRDM16 or SETBP1. *Nat Med*, 12: 401-9.
- OWENS, G. K. 1995. Regulation of differentiation of vascular smooth muscle cells. *Physiol Rev*, 75: 487-517.
- PALU, G., PAROLIN, C., TAKEUCHI, Y. & PIZZATO, M. 2000. Progress with retroviral gene vectors. *Rev Med Virol*, 10: 185-202.
- PAN, J. W., WEI, M., YANG, P. Y., ZHENG, X., LI, J. B., LU, Z. G., ZHAO, X. X., WU, H., KANG, H. & RUI, Y. C. 2007. Regulation of Nogo-B expression in the lesion of aortic aneurysms. *Clin Exp Pharmacol Physiol*, 34: 856-60.
- PARRY, T. J., BROSIUS, R., THYAGARAJAN, R., CARTER, D., ARGENTIERI, D., FALOTICO, R. & SIEKIERKA, J. 2005. Drug-eluting stents: sirolimus and paclitaxel differentially affect cultured cells and injured arteries. *Eur J Pharmacol*, 524: 19-29.
- PASZKOWIAK, J. J., MALONEY, S. P., KUDO, F. A., MUTO, A., TESO, D., RUTLAND, R. C., WESTVIK, T. S., PIMIENTO, J. M., TELLIDES, G., SESSA, W. C. & DARDIK, A. 2007. Evidence supporting changes in Nogo-B levels as a marker of neointimal expansion but not adaptive arterial remodeling. *Vascul Pharmacol*, 46: 293-301.
- PHILIPPE, S., SARKIS, C., BARKATS, M., MAMMERI, H., LADROUE, C., PETIT, C., MALLET, J. & SERGUERA, C. 2006. Lentiviral vectors with a defective integrase allow efficient and sustained transgene expression in vitro and in vivo. *Proc Natl Acad Sci U S A*, 103: 17684-9.
- PHILPOTT, N. J. & THRASHER, A. J. 2007. Use of nonintegrating lentiviral vectors for gene therapy. *Hum Gene Ther*, 18: 483-9.
- PIERSON, T. C., KIEFFER, T. L., RUFF, C. T., BUCK, C., GANGE, S. J. & SILICIANO, R. F. 2002. Intrinsic stability of episomal circles formed during human immunodeficiency virus type 1 replication. *J Virol*, 76: 4138-44.
- POPOV, A. F., DORGE, H., HINZ, J., SCHMITTO, J. D., STOJANOVIC, T., SEIPELT, R., DIDILIS, V. & SCHOENDUBE, F. A. 2008. Accelerated intimal hyperplasia in aortocoronary internal mammary vein grafts in minipigs. *J Cardiothorac Surg*, 3: 20.
- QIAN, Z., HAESSLER, M., LEMOS, J. A., ARSENAULT, J. R., AGUIRRE, J. E., GILBERT, J. R., BOWLER, R. P. & PARK, F. 2006. Targeting vascular injury using Hantavirus-pseudotyped lentiviral vectors. *Mol Ther*, 13: 694-704.
- RAFFETTO, J. D. & KHALIL, R. A. 2008. Matrix metalloproteinases and their inhibitors in vascular remodeling and vascular disease. *Biochem Pharmacol*, 75: 346-59.

- RAHIM, A. A., WONG, A. M., HOWE, S. J., BUCKLEY, S. M., ACOSTA-SALTOS, A. D., ELSTON, K. E., WARD, N. J., PHILPOTT, N. J., COOPER, J. D., ANDERSON, P. N., WADDINGTON, S. N., THRASHER, A. J. & RAIVICH, G. 2009. Efficient gene delivery to the adult and fetal CNS using pseudotyped non-integrating lentiviral vectors. *Gene Ther*, 16: 509-20.
- RAINES, E. W. 2004a. Nogo puts the brakes on vascular lesions. *Nature Medicine*, 10: 348-349.
- RAINES, E. W. 2004b. PDGF and cardiovascular disease. *Cytokine Growth Factor Rev*, 15: 237-54.
- RAMIREZ CORREA, G. A., ZACCHIGNA, S., ARSIC, N., ZENTILIN, L., SALVI, A., SINAGRA, G. & GIACCA, M. 2004. Potent inhibition of arterial intimal hyperplasia by TIMP1 gene transfer using AAV vectors. *Mol Ther*, 9: 876-84.
- RISSANEN, T. T. & YLA-HERTTUALA, S. 2007. Current status of cardiovascular gene therapy. *Mol Ther*, 15: 1233-47.
- RODRIGUEZ-FEO, J. A., HELLINGS, W. E., VERHOEVEN, B. A., MOLL, F. L., DE KLEIJN, D. P., PRENDERGAST, J., GAO, Y., VAN DER GRAAF, Y., TELLIDES, G., SESSA, W. C. & PASTERKAMP, G. 2007. Low levels of Nogo-B in human carotid atherosclerotic plaques are associated with an atheromatous phenotype, restenosis, and stenosis severity. *Arterioscler Thromb Vasc Biol*, 27: 1354-60.
- ROSS, R. 1993. The pathogenesis of atherosclerosis: a perspective for the 1990s. *Nature*, 362: 801-9.
- ROSS, R. 1995. Cell biology of atherosclerosis. *Annu Rev Physiol*, 57: 791-804.
- ROSS, R. 1999. Atherosclerosis--an inflammatory disease. *N Engl J Med*, 340: 115-26.
- ROSS, R., GLOMSET, J. & HARKER, L. 1977. Response to injury and atherogenesis. *Am J Pathol*, 86: 675-84.
- SANDERS, D. A. 2004. Ebola virus glycoproteins: guidance devices for targeting gene therapy vectors. *Expert Opin Biol Ther*, 4: 329-36.
- SANSON, M., AUGÉ, N., VINDIS, C., MULLER, C., BANDO, Y., THIERS, J. C., MARACHET, M. A., ZARKOVIC, K., SAWA, Y., SALVAYRE, R. & NEGRE-SALVAYRE, A. 2009. Oxidized low-density lipoproteins trigger endoplasmic reticulum stress in vascular cells: prevention by oxygen-regulated protein 150 expression. *Circ Res*, 104: 328-36.
- SANTILLI, G., THORNHILL, S. I., KINNON, C. & THRASHER, A. J. 2008. Gene therapy of inherited immunodeficiencies. *Expert Opin Biol Ther*, 8: 397-407.
- SASTRY, L., JOHNSON, T., HOBSON, M. J., SMUCKER, B. & CORNETTA, K. 2002. Titering lentiviral vectors: comparison of DNA, RNA and marker expression methods. *Gene Ther*, 9: 1155-62.

- SCHANDA, K., HERMANN, M., STEFANOVA, N., GREDLER, V., BANDTLOW, C. & REINDL, M. 2011. Nogo-B is associated with cytoskeletal structures in human monocyte-derived macrophages. *BMC Res Notes*, 4: 6.
- SCHAUBER, C. A., TUERK, M. J., PACHECO, C. D., ESCARPE, P. A. & VERES, G. 2004. Lentiviral vectors pseudotyped with baculovirus gp64 efficiently transduce mouse cells in vivo and show tropism restriction against hematopoietic cell types in vitro. *Gene Ther*, 11: 266-75.
- SCHMIDT, M., SCHWARZWAELDER, K., BARTHOLOMAE, C., ZAOUI, K., BALL, C., PILZ, I., BRAUN, S., GLIMM, H. & VON KALLE, C. 2007. High-resolution insertion-site analysis by linear amplification-mediated PCR (LAM-PCR). *Nat Methods*, 4: 1051-7.
- SCHMIDT, M., SCHWARZWAELDER, K., BARTHOLOMAE, C. C., GLIMM, H. & VON KALLE, C. 2009. Detection of retroviral integration sites by linear amplification-mediated PCR and tracking of individual integration clones in different samples. *Methods Mol Biol*, 506: 363-72.
- SCHOFER, J., SCHLUTER, M., GERSHLICK, A. H., WIJNS, W., GARCIA, E., SCHAMPAERT, E. & BREITHARDT, G. 2003. Sirolimus-eluting stents for treatment of patients with long atherosclerotic lesions in small coronary arteries: double-blind, randomised controlled trial (E-SIRIUS). *Lancet*, 362: 1093-9.
- SCHWAB, M. E. 2010. Functions of Nogo proteins and their receptors in the nervous system. *Nat Rev Neurosci*, 11: 799-811.
- SCHWARTZ, R. S., CHRONOS, N. A. & VIRMANI, R. 2004. Preclinical restenosis models and drug-eluting stents: still important, still much to learn. *J Am Coll Cardiol*, 44: 1373-85.
- SCHWARTZ, R. S. & HENRY, T. D. 2002. Pathophysiology of coronary artery restenosis. *Rev Cardiovasc Med*, 3 Suppl 5: S4-9.
- SCHWARZWAELDER, K., HOWE, S. J., SCHMIDT, M., BRUGMAN, M. H., DEICHMANN, A., GLIMM, H., SCHMIDT, S., PRINZ, C., WISSLER, M., KING, D. J., ZHANG, F., PARSLEY, K. L., GILMOUR, K. C., SINCLAIR, J., BAYFORD, J., PERAJ, R., PIKE-OVERZET, K., STAAL, F. J., DE RIDDER, D., KINNON, C., ABEL, U., WAGEMAKER, G., GASPAR, H. B., THRASHER, A. J. & VON KALLE, C. 2007. Gammaretrovirus-mediated correction of SCID-X1 is associated with skewed vector integration site distribution in vivo. *J Clin Invest*, 117: 2241-9.
- SEELAMGARI, A., MADDUKURI, A., BERRO, R., DE LA FUENTE, C., KEHN, K., DENG, L., DADGAR, S., BOTTAZZI, M. E., GHEDIN, E., PUMFERY, A. & KASHANCHI, F. 2004. Role of viral regulatory and accessory proteins in HIV-1 replication. *Front Biosci*, 9: 2388-413.
- SELBACH, M., SCHWANHAUSSER, B., THIERFELDER, N., FANG, Z., KHANIN, R. & RAJEWSKY, N. 2008. Widespread changes in protein synthesis induced by microRNAs. *Nature*, 455: 58-63.

- SHAH, P. J., GORDON, I., FULLER, J., SEEVANAYAGAM, S., ROSALION, A., TATOULIS, J., RAMAN, J. S. & BUXTON, B. F. 2003. Factors affecting saphenous vein graft patency: clinical and angiographic study in 1402 symptomatic patients operated on between 1977 and 1999. *J Thorac Cardiovasc Surg*, 126: 1972-7.
- SHARIF, F., HYNES, S. O., COONEY, R., HOWARD, L., MCMAHON, J., DALY, K., CROWLEY, J., BARRY, F. & O'BRIEN, T. 2008. Gene-eluting stents: adenovirus-mediated delivery of eNOS to the blood vessel wall accelerates re-endothelialization and inhibits restenosis. *Mol Ther*, 16: 1674-80.
- SHARIF, F., HYNES, S. O., MCMAHON, J., COONEY, R., CONROY, S., DOCKERY, P., DUFFY, G., DALY, K., CROWLEY, J., BARTLETT, J. S. & O'BRIEN, T. 2006. Gene-eluting stents: comparison of adenoviral and adeno-associated viral gene delivery to the blood vessel wall in vivo. *Hum Gene Ther*, 17: 741-50.
- SHIGEMATSU, K., KOYAMA, H., OLSON, N. E., CHO, A. & REIDY, M. A. 2000. Phosphatidylinositol 3-kinase signaling is important for smooth muscle cell replication after arterial injury. *Arterioscler Thromb Vasc Biol*, 20: 2373-8.
- SINN, P. L., BURNIGHT, E. R., HICKEY, M. A., BLISSARD, G. W. & MCCRAY, P. B., JR. 2005a. Persistent gene expression in mouse nasal epithelia following feline immunodeficiency virus-based vector gene transfer. *J Virol*, 79: 12818-27.
- SINN, P. L., HICKEY, M. A., STABER, P. D., DYLLA, D. E., JEFFERS, S. A., DAVIDSON, B. L., SANDERS, D. A. & MCCRAY, P. B., JR. 2003. Lentivirus vectors pseudotyped with filoviral envelope glycoproteins transduce airway epithelia from the apical surface independently of folate receptor alpha. *J Virol*, 77: 5902-10.
- SINN, P. L., SAUTER, S. L. & MCCRAY, P. B., JR. 2005b. Gene therapy progress and prospects: development of improved lentiviral and retroviral vectors--design, biosafety, and production. *Gene Ther*, 12: 1089-98.
- SIRVEN, A., PFLUMIO, F., ZENNOU, V., TITEUX, M., VAINCHENKER, W., COULOMBEL, L., DUBART-KUPPERSCHMITT, A. & CHARNEAU, P. 2000. The human immunodeficiency virus type-1 central DNA flap is a crucial determinant for lentiviral vector nuclear import and gene transduction of human hematopoietic stem cells. *Blood*, 96: 4103-10.
- SMALL, E. M. & OLSON, E. N. 2011. Pervasive roles of microRNAs in cardiovascular biology. *Nature*, 469: 336-42.
- SORELLE, R. 2001. Late-breaking clinical trials at the American Heart Association's scientific sessions 2001. *Circulation*, 104: E9046-8.
- SOUDAIS, C., SHIHO, T., SHARARA, L. I., GUY-GRAND, D., TANIGUCHI, T., FISCHER, A. & DI SANTO, J. P. 2000. Stable and functional lymphoid reconstitution of common cytokine receptor gamma chain deficient mice by retroviral-mediated gene transfer. *Blood*, 95: 3071-7.

- SOUTHGATE, K. & NEWBY, A. C. 1990. Serum-induced proliferation of rabbit aortic smooth muscle cells from the contractile state is inhibited by 8-Br-cAMP but not 8-Br-cGMP. *Atherosclerosis*, 82: 113-23.
- STABILE, E., ZHOU, Y. F., SAJI, M., CASTAGNA, M., SHOU, M., KINNAIRD, T. D., BAFFOUR, R., RINGEL, M. D., EPSTEIN, S. E. & FUCHS, S. 2003. Akt controls vascular smooth muscle cell proliferation in vitro and in vivo by delaying G1/S exit. *Circ Res*, 93: 1059-65.
- STEWART, H. J., FONG-WONG, L., STRICKLAND, I., CHIPCHASE, D., KELLEHER, M., STEVENSON, L., THOREE, V., MCCARTHY, J., RALPH, G. S., MITROPHANOUS, K. A. & RADCLIFFE, P. A. 2011. A stable producer cell line for the manufacture of a lentiviral vector for gene therapy of Parkinson's disease. *Hum Gene Ther*, 22: 357-69.
- STONE, G. W., ELLIS, S. G., COX, D. A., HERMILLER, J., O'SHAUGHNESSY, C., MANN, J. T., TURCO, M., CAPUTO, R., BERGIN, P., GREENBERG, J., POPMA, J. J. & RUSSELL, M. E. 2004a. One-year clinical results with the slow-release, polymer-based, paclitaxel-eluting TAXUS stent: the TAXUS-IV trial. *Circulation*, 109: 1942-7.
- STONE, G. W., ELLIS, S. G., COX, D. A., HERMILLER, J., O'SHAUGHNESSY, C., MANN, J. T., TURCO, M., CAPUTO, R., BERGIN, P., GREENBERG, J., POPMA, J. J. & RUSSELL, M. E. 2004b. A polymer-based, paclitaxel-eluting stent in patients with coronary artery disease. *N Engl J Med*, 350: 221-31.
- STONE, G. W., RIZVI, A., NEWMAN, W., MASTALI, K., WANG, J. C., CAPUTO, R., DOOSTZADEH, J., CAO, S., SIMONTON, C. A., SUDHIR, K., LANSKY, A. J., CUTLIP, D. E. & KEREIAKES, D. J. 2010. Everolimus-eluting versus paclitaxel-eluting stents in coronary artery disease. *N Engl J Med*, 362: 1663-74.
- TABAS, I. 2010. The role of endoplasmic reticulum stress in the progression of atherosclerosis. *Circ Res*, 107: 839-50.
- TAGAMI, S., EGUCHI, Y., KINOSHITA, M., TAKEDA, M. & TSUJIMOTO, Y. 2000. A novel protein, RTN-XS, interacts with both Bcl-XL and Bcl-2 on endoplasmic reticulum and reduces their anti-apoptotic activity. *Oncogene*, 19: 5736-46.
- TAKAHASHI, A., PALMER-OPOLSKI, M., SMITH, R. C. & WALSH, K. 2003. Transgene delivery of plasmid DNA to smooth muscle cells and macrophages from a biostable polymer-coated stent. *Gene Ther*, 10: 1471-8.
- TALBOT, G. E., WADDINGTON, S. N., BALES, O., TCHEN, R. C. & ANTONIOU, M. N. 2010. Desmin-regulated lentiviral vectors for skeletal muscle gene transfer. *Mol Ther*, 18: 601-8.
- TAMBE, Y., ISONO, T., HARAGUCHI, S., YOSHIOKA-YAMASHITA, A., YUTSUDO, M. & INOUE, H. 2004. A novel apoptotic pathway induced by the drs tumor suppressor gene. *Oncogene*, 23: 2977-87.
- TAYLOR, N., URIBE, L., SMITH, S., JAHN, T., KOHN, D. B. & WEINBERG, K. 1996. Correction of interleukin-2 receptor function in X-SCID lymphoblastoid

- cells by retrovirally mediated transfer of the gamma-c gene. *Blood*, 87: 3103-7.
- TENG, F. Y. & TANG, B. L. 2008. Cell autonomous function of Nogo and reticulons: The emerging story at the endoplasmic reticulum. *J Cell Physiol*, 216: 303-8.
- THOMAS, C. E., EHRHARDT, A. & KAY, M. A. 2003. Progress and problems with the use of viral vectors for gene therapy. *Nat Rev Genet*, 4: 346-58.
- TRONC, F., WASSEF, M., ESPOSITO, B., HENRION, D., GLAGOV, S. & TEDGUI, A. 1996. Role of NO in flow-induced remodeling of the rabbit common carotid artery. *Arterioscler Thromb Vasc Biol*, 16: 1256-62.
- TSCHERNUTTER, M., SCHLICHTENBREDE, F. C., HOWE, S., BALAGGAN, K. S., MUNRO, P. M., BAINBRIDGE, J. W., THRASHER, A. J., SMITH, A. J. & ALI, R. R. 2005. Long-term preservation of retinal function in the RCS rat model of retinitis pigmentosa following lentivirus-mediated gene therapy. *Gene Ther*, 12: 694-701.
- TSUI, J. C. & DASHWOOD, M. R. 2002. Recent strategies to reduce vein graft occlusion: a need to limit the effect of vascular damage. *Eur J Vasc Endovasc Surg*, 23: 202-8.
- VANDENDRIESSCHE, T., THORREZ, L., NALDINI, L., FOLLENZI, A., MOONS, L., BERNEMAN, Z., COLLEN, D. & CHUAH, M. K. 2002. Lentiviral vectors containing the human immunodeficiency virus type-1 central polypurine tract can efficiently transduce nondividing hepatocytes and antigen-presenting cells in vivo. *Blood*, 100: 813-22.
- VARENNE, O., PISLARU, S., GILLIJNS, H., VAN PELT, N., GERARD, R. D., ZOLDHELYI, P., VAN DE WERF, F., COLLEN, D. & JANSSENS, S. P. 1998. Local adenovirus-mediated transfer of human endothelial nitric oxide synthase reduces luminal narrowing after coronary angioplasty in pigs. *Circulation*, 98: 919-26.
- VARGAS, J., JR., GUSELLA, G. L., NAJFELD, V., KLOTMAN, M. E. & CARA, A. 2004. Novel integrase-defective lentiviral episomal vectors for gene transfer. *Hum Gene Ther*, 15: 361-72.
- VERMA, I. M. & SOMIA, N. 1997. Gene therapy -- promises, problems and prospects. *Nature*, 389: 239-42.
- VIGNA, E. & NALDINI, L. 2000. Lentiviral vectors: excellent tools for experimental gene transfer and promising candidates for gene therapy. *J Gene Med*, 2: 308-16.
- VOELTZ, G. K., PRINZ, W. A., SHIBATA, Y., RIST, J. M. & RAPOPORT, T. A. 2006. A class of membrane proteins shaping the tubular endoplasmic reticulum. *Cell*, 124: 573-86.
- VON SEGGERN, D. J., KEHLER, J., ENDO, R. I. & NEMEROW, G. R. 1998. Complementation of a fibre mutant adenovirus by packaging cell lines

- stably expressing the adenovirus type 5 fibre protein. *J Gen Virol*, 79 ( Pt 6): 1461-8.
- WAEHLER, R., RUSSELL, S. J. & CUIEL, D. T. 2007. Engineering targeted viral vectors for gene therapy. *Nat Rev Genet*, 8: 573-87.
- WAKI, K. & FREED, E. O. 2010. Macrophages and Cell-Cell Spread of HIV-1. *Viruses*, 2: 1603-1620.
- WALTER, D. H., CEJNA, M., DIAZ-SANDOVAL, L., WILLIS, S., KIRKWOOD, L., STRATFORD, P. W., TIETZ, A. B., KIRCHMAIR, R., SILVER, M., CURRY, C., WECKER, A., YOON, Y. S., HEIDENREICH, R., HANLEY, A., KEARNEY, M., TIO, F. O., KUENZLER, P., ISNER, J. M. & LOSORDO, D. W. 2004. Local gene transfer of phVEGF-2 plasmid by gene-eluting stents: an alternative strategy for inhibition of restenosis. *Circulation*, 110: 36-45.
- WAN, S., GEORGE, S. J., NICKLIN, S. A., YIM, A. P. & BAKER, A. H. 2004. Overexpression of p53 increases lumen size and blocks neointima formation in porcine interposition vein grafts. *Mol Ther*, 9: 689-98.
- WANISCH, K. & YANEZ-MUNOZ, R. J. 2009. Integration-deficient lentiviral vectors: a slow coming of age. *Mol Ther*, 17: 1316-32.
- WARD, N. J., BUCKLEY, S. M., WADDINGTON, S. N., VANDENDRIESSCHE, T., CHUAH, M. K., NATHWANI, A. C., MCINTOSH, J., TUDDENHAM, E. G., KINNON, C., THRASHER, A. J. & MCVEY, J. H. 2011. Codon optimization of human factor VIII cDNAs leads to high-level expression. *Blood*, 117: 798-807.
- WATARI, A. & YUTSUDO, M. 2003. Multi-functional gene ASY/Nogo/RTN-X/RTN4: apoptosis, tumor suppression, and inhibition of neuronal regeneration. *Apoptosis*, 8: 5-9.
- WATSON, D. J., KOBINGER, G. P., PASSINI, M. A., WILSON, J. M. & WOLFE, J. H. 2002. Targeted transduction patterns in the mouse brain by lentivirus vectors pseudotyped with VSV, Ebola, Mokola, LCMV, or MuLV envelope proteins. *Mol Ther*, 5: 528-37.
- WEINTRAUB, W. S. 2007. The pathophysiology and burden of restenosis. *Am J Cardiol*, 100: 3K-9K.
- WESTERBAND, A., MILLS, J. L., MAREK, J. M., HEIMARK, R. L., HUNTER, G. C. & WILLIAMS, S. K. 1997. Immunocytochemical determination of cell type and proliferation rate in human vein graft stenoses. *J Vasc Surg*, 25: 64-73.
- WHITE, K., BUNING, H., KRITZ, A., JANICKI, H., MCVEY, J., PERABO, L., MURPHY, G., ODENTHAL, M., WORK, L. M., HALLEK, M., NICKLIN, S. A. & BAKER, A. H. 2008. Engineering adeno-associated virus 2 vectors for targeted gene delivery to atherosclerotic lesions. *Gene Ther*, 15: 443-51.
- WHITE, K., NICKLIN, S. A. & BAKER, A. H. 2007. Novel vectors for in vivo gene delivery to vascular tissue. *Expert Opin Biol Ther*, 7: 809-21.

- WHITWAM, T., HASKINS, M. E., HENTHORN, P. S., KRASZEWSKI, J. N., KLEIMAN, S. E., SEIDEL, N. E., BODINE, D. M. & PUCK, J. M. 1998. Retroviral marking of canine bone marrow: long-term, high-level expression of human interleukin-2 receptor common gamma chain in canine lymphocytes. *Blood*, 92: 1565-75.
- WILLIAMS, S., MUSTOE, T., MULCAHY, T., GRIFFITHS, M., SIMPSON, D., ANTONIOU, M., IRVINE, A., MOUNTAIN, A. & CROMBIE, R. 2005. CpG-island fragments from the HNRPA2B1/CBX3 genomic locus reduce silencing and enhance transgene expression from the hCMV promoter/enhancer in mammalian cells. *BMC Biotechnol*, 5: 17.
- WILLS, K. N., MANO, T., AVANZINI, J. B., NGUYEN, T., ANTELMAN, D., GREGORY, R. J., SMITH, R. C. & WALSH, K. 2001. Tissue-specific expression of an anti-proliferative hybrid transgene from the human smooth muscle alpha-actin promoter suppresses smooth muscle cell proliferation and neointima formation. *Gene Ther*, 8: 1847-54.
- WONG, L. F., AZZOUZ, M., WALMSLEY, L. E., ASKHAM, Z., WILKES, F. J., MITROPHANOUS, K. A., KINGSMAN, S. M. & MAZARAKIS, N. D. 2004. Transduction patterns of pseudotyped lentiviral vectors in the nervous system. *Mol Ther*, 9: 101-11.
- WRIGHT, P. L., YU, J., DI, Y. P., HOMER, R. J., CHUPP, G., ELIAS, J. A., COHN, L. & SESSA, W. C. 2010. Epithelial reticulon 4B (Nogo-B) is an endogenous regulator of Th2-driven lung inflammation. *J Exp Med*, 207: 2595-2607.
- XIN, M., SMALL, E. M., SUTHERLAND, L. B., QI, X., MCANALLY, J., PLATO, C. F., RICHARDSON, J. A., BASSEL-DUBY, R. & OLSON, E. N. 2009. MicroRNAs miR-143 and miR-145 modulate cytoskeletal dynamics and responsiveness of smooth muscle cells to injury. *Genes Dev*, 23: 2166-78.
- XU, W., HONG, W., SHAO, Y., NING, Y., CAI, Z. & LI, Q. 2011. Nogo-B regulates migration and contraction of airway smooth muscle cells by decreasing ARPC 2/3 and increasing MYL-9 expression. *Respir Res*, 12: 14.
- YAMAJI, K., KIMURA, T., MORIMOTO, T., NAKAGAWA, Y., INOUE, K., SOGA, Y., ARITA, T., SHIRAI, S., ANDO, K., KONDO, K., SAKAI, K., GOYA, M., IWABUCHI, M., YOKOI, H., NOSAKA, H. & NOBUYOSHI, M. 2010. Very Long-Term (15 to 20 Years) Clinical and Angiographic Outcome After Coronary Bare Metal Stent Implantation. *Circ Cardiovasc Interv*, 3: 468-475.
- YAN, R., SHI, Q., HU, X. & ZHOU, X. 2006. Reticulon proteins: emerging players in neurodegenerative diseases. *Cell Mol Life Sci*, 63: 877-89.
- YANEZ-MUNOZ, R. J., BALAGGAN, K. S., MACNEIL, A., HOWE, S. J., SCHMIDT, M., SMITH, A. J., BUCH, P., MACLAREN, R. E., ANDERSON, P. N., BARKER, S. E., DURAN, Y., BARTHOLOMAE, C., VON KALLE, C., HECKENLIVELY, J. R., KINNON, C., ALI, R. R. & THRASHER, A. J. 2006. Effective gene therapy with nonintegrating lentiviral vectors. *Nat Med*, 12: 348-53.
- YANG, J., JIANG, H., CHEN, S. S., CHEN, J., LI, W. Q., XU, S. K. & WANG, J. C. 2010. Lentivirus-mediated RNAi targeting CREB binding protein attenuates

neointimal formation and promotes re-endothelialization in balloon injured rat carotid artery. *Cell Physiol Biochem*, 26: 441-8.

- YANG, Y. S. & STRITTMATTER, S. M. 2007. The reticulons: a family of proteins with diverse functions. *Genome Biol*, 8: 234.
- YE, Y. W., LANDAU, C., WILLARD, J. E., RAJASUBRAMANIAN, G., MOSKOWITZ, A., AZIZ, S., MEIDELL, R. S. & EBERHART, R. C. 1998. Bioresorbable microporous stents deliver recombinant adenovirus gene transfer vectors to the arterial wall. *Ann Biomed Eng*, 26: 398-408.
- YOSHIDA, T. & OWENS, G. K. 2005. Molecular determinants of vascular smooth muscle cell diversity. *Circ Res*, 96: 280-91.
- YU, J., FERNANDEZ-HERNANDO, C., SUAREZ, Y., SCHLEICHER, M., HAO, Z., WRIGHT, P. L., DILORENZO, A., KYRIAKIDES, T. R. & SESSA, W. C. 2009. Reticulon 4B (Nogo-B) is necessary for macrophage infiltration and tissue repair. *Proc Natl Acad Sci U S A*, 106: 17511-6.
- YU, P. J., FERRARI, G., PIRELLI, L., GULKAROV, I., GALLOWAY, A. C., MIGNATTI, P. & PINTUCCI, G. 2007. Vascular injury and modulation of MAPKs: a targeted approach to therapy of restenosis. *Cell Signal*, 19: 1359-71.
- ZHAN, Y., KIM, S., IZUMI, Y., IZUMIYA, Y., NAKAO, T., MIYAZAKI, H. & IWAO, H. 2003. Role of JNK, p38, and ERK in platelet-derived growth factor-induced vascular proliferation, migration, and gene expression. *Arterioscler Thromb Vasc Biol*, 23: 795-801.
- ZHANG, D., UTSUMI, T., HUANG, H. C., GAO, L., SANGWUNG, P., CHUNG, C., SHIBAO, K., OKAMOTO, K., YAMAGUCHI, K., GROSZMANN, R. J., JOZSEF, L., HAO, Z., SESSA, W. C. & IWAKIRI, Y. 2011. Reticulon 4B (Nogo-B) is a novel regulator of hepatic fibrosis. *Hepatology*, 53: 1306-15.
- ZHANG, F., FROST, A. R., BLUNDELL, M. P., BALES, O., ANTONIOU, M. N. & THRASHER, A. J. 2010. A ubiquitous chromatin opening element (UCOE) confers resistance to DNA methylation-mediated silencing of lentiviral vectors. *Mol Ther*, 18: 1640-9.
- ZHANG, F., THORNHILL, S. I., HOWE, S. J., ULAGANATHAN, M., SCHAMBACH, A., SINCLAIR, J., KINNON, C., GASPAR, H. B., ANTONIOU, M. & THRASHER, A. J. 2007. Lentiviral vectors containing an enhancer-less ubiquitously acting chromatin opening element (UCOE) provide highly reproducible and stable transgene expression in hematopoietic cells. *Blood*, 110: 1448-57.
- ZHAO, B., CHUN, C., LIU, Z., HORSWILL, M. A., PRAMANIK, K., WILKINSON, G. A., RAMCHANDRAN, R. & MIAO, R. Q. 2010. Nogo-B receptor is essential for angiogenesis in zebrafish via Akt pathway. *Blood*, 116: 5423-33.
- ZHOU, S., MODY, D., DRAVIN, S. S., HAUER, J., LU, T., MA, Z., HACEIN-BEY ABINA, S., GRAY, J. T., GREENE, M. R., CAVAZZANA-CALVO, M., MALECH, H. L. & SORRENTINO, B. P. 2010. A self-inactivating lentiviral vector for SCID-X1 gene therapy that does not activate LMO2 expression in human T cells. *Blood*, 116: 900-8.

- ZUFFEREY, R., DONELLO, J. E., TRONO, D. & HOPE, T. J. 1999. Woodchuck hepatitis virus posttranscriptional regulatory element enhances expression of transgenes delivered by retroviral vectors. *J Virol*, 73: 2886-92.
- ZUFFEREY, R., DULL, T., MANDEL, R. J., BUKOVSKY, A., QUIROZ, D., NALDINI, L. & TRONO, D. 1998. Self-inactivating lentivirus vector for safe and efficient in vivo gene delivery. *J Virol*, 72: 9873-80.
- ZUFFEREY, R., NAGY, D., MANDEL, R. J., NALDINI, L. & TRONO, D. 1997. Multiply attenuated lentiviral vector achieves efficient gene delivery in vivo. *Nat Biotechnol*, 15: 871-5.

## Appendices

## DNA sequencing results

### *Complete full-length and mutant Nogo-B cDNA sequences*

Complete (full-length) human Nogo-B-haemagglutinin tagged ~ 1.2 kb Nogo-B

ATGGAAGACCTGGACCAGTCTCCTCTGGTCTCGTCCTCGGACAGCCCACCCCGGCCGCA  
 GCCCCGCTTCAAGTACCAGTTCGTGAGGGAGCCCGAGGACGAGGAGGAAGAAGAGGAG  
 GAGGAAGAGGAGGACGAGGACGAAGACCTGGAGGAGCTGGAGGTGCTGGAGAGGAAG  
 CCCGCCGCCGGGCTGTCCGCGGCCCCAGTGCCCACCGCCCCTGCCGCCGGCGCGCCCCCT  
 GATGGACTTCGGAAATGACTTCGTGCCGCGGCCCGGGGACCCCTGCCGGCCGCT  
 CCCCCGTCGCCCCGGAGCGGCAGCCGTCTTGGGACCCGAGCCCGGTGTCGTCGACCG  
 TGCCCGCGCCATCCCCGCTGTCTGCTGCCGCAGTCTCGCCCTCCAAGCTCCCTGAGGAC  
 GACGAGCCTCCGGCCCCGGCCTCCCCCTCCTCCCCCGGCCAGCGTGAGCCCCCAGGCAGA  
 GCCCCGTGTGGACCCCGCCAGCCCCGGCTCCCGCCGCGCCCCCTCCACCCCGGCCGCGC  
 CCAAGCGCAGGGGCTCCTCGGGCTCAGTGGTTGTTGACCTCCTGTACTGGAGAGACATT  
 AAGAAGACTGGAGTGGTGTGGTGGTGCCAGCCTATTCCTGCTGCTTTTCATTGACAGTATT  
 CAGCATTGTGAGCGTAACAGCCTACATTGCCTTGGCCCTGCTCTCTGTGACCATCAGCTT  
 TAGGATATAACAAGGGTGTGATCCAAGCTATCCAGAAATCAGATGAAGGCCACCCATTAG  
 GGCATATCTGGAATCTGAAGTTGCTATATCTGAGGAGTTGGTTCAGAAGTACAGTAATT  
 CTGCTCTTGGTCATGTGAACTGCACGATAAAGGAACTCAGGCGCCTCTTCTTAGTTGAT  
 GATTTAGTTGATTCTCTGAAGTTTGCAGTGTGATGTGGGTATTTACCTATGTTGGTGC  
 CTTGTTTAATGGTCTGACACTACTGATTTTGGCTCTCATTTCACTCTTCAGTGTTCCCTGT  
 TATTTATGAACGGCATCAGGCACAGATAGATCATTATCTAGGACTTGCAAATAAGAATGT  
 TAAAGATGCTATGGCTAAAATCCAAGCAAAAATCCCTGGATTGAAGCGCAAAGCTGAAGG  
 TGGCTACCCATACGACGTCCCAGACTACGCTTGA

Full-length Nogo-B = 384 amino acids in length

MEDLDQSPLV SSSDSPRPQ PAFKYQFVRE PEDEEEEEEE EEEDEDEDLE ELEVLERKPA  
 AGLSAAPVPT APAAGAPLMD FGNDVFPAP RGPLPAAPPV APERQPSWDP SPVSSTVPAP  
 SPLSAAVSP SKLPEDDEPP ARPPPPPPAS VSPQAEPVWT PPAPAPAAPP STPAAPKRRG  
 SSGSVVDLL YWRDIKKTGV VFGASLFLLL SLTVFSIVSV TAYIALALLS VTISFRIYKG  
 VIQAIQKSDE GHPFRAYLES EVAISEELVQ KYSNSALGHV NCTIKELRRL FLVDDLVDL  
 KFAVLMWVFT YVGALFNGLT LLILALISLF SVPVIYERHQ AQIDHYLGLA NKNVKDAMAK  
 IQAKIPGLKR KAEGGYDYDV PDYA

Human mutant (soluble) Nogo-B ~ 600 bp

ATGGAAGACCTGGACCAGTCTCCTCTGGTCTCGTCCTCGGACAGCCCACCCCGGCCGCA  
 GCCCCGCGTTCAAGTACCAGTTCGTGAGGGAGCCCGAGGACGAGGAGGAAGAAGAGGAG  
 GAGGAAGAGGAGGACGAGGACGAAGACCTGGAGGAGCTGGAGGTGCTGGAGAGGAAG  
 CCCGCCGCCGGGCTGTCCGCGGCCCCAGTGCCCACCGCCCCTGCCGCCGGCGCGCCCCT  
 GATGGACTTCGGAAATGACTTCGTGCCGCGGCGCCCCGGGGACCCCTGCCGGCCGCT  
 CCCCCGTCGCCCCGGAGCGGCAGCCGTCTTGGGACCCGAGCCCGGTGTCGTCGACCG  
 TGCCCGCGCCATCCCCGCTGTCTGCTGCCGCAGTCTCGCCCTCCAAGCTCCCTGAGGAC  
 GACGAGCCTCCGGCCCCGGCCTCCCCCTCCTCCCCCGGCCAGCGTGAGCCCCCAGGCAGA  
 GCCCGTGTGGACCCCGCCAGCCCCGGCTCCCGCCGCGCCCCCTCCACCCCGGCCGCGC  
 CCAAGCGCAGGGGCTCCTCGGGCTCAGTGGTTGTTGACCTCCTGTACTGGAGAGACATT  
 AAGAAGACTGGAGTGGTGTGA

Mutant Nogo-B = 200 amino acids in length

MEDLDQSPLV SSSDSPRPQ PAFKYQFVRE PEDEEEEEEE EEEDEDEDLE ELEVLERKPA  
 AGLSAAPVPT APAAGAPLMD FGNDVFPPAP RGPLPAAPPV APERQPSWDP SPVSSTVPAP  
 SPLSAAVSP SKLPEDEPP ARPPPPPPAS VSPQAEPVWT PPAPAPAAPP STPAAPKRRG  
 SSGSVVDLL YWRDIKKTGV V

Appendix 1. Sequences for full-length Nogo-B and mutant (soluble) Nogo-B.

***DNA sequencing for full-length Nogo-B in the lentiviral construct plasmid***

**Forward primer 5'-CAATCAGCCTGCTTCTCG-3'**

CCCACCCCGGCCGAGCCCGCGTTCAAGTACCAGTTCGTGAGGGAGCCCGAGGACGAG  
GAGGAAGAAGAGGAGGAGGAAGAGGAGGACGAGGACGAAGACCTGGAGGAGCTGGAG  
GTGCTGGAGAGGAAGCCCGCCGCGGGCTGTCCGCGGCCCCAGTGCCACCCGCCCTG  
CCGCCGGCGCGCCCCTGATGGACTTCGGAAATGACTTCGTGCCGCGGCGCCCGGGG  
ACCCCTGCCGGCCGCTCCCCCGTCGCCCCGGAGCGGCAGCCGTCTTGGGACCCGAGCC  
CGGTGTCGTCGACCGTGCCCGCGCCATCCCCGCTGTCTGCTGCCGAGTCTCGCCCTCC  
AAGCTCCCTGAGGACGACGAGCCTCCGGCCCGGCCTCCCCCTCTCCCCGGCCAGCGT  
GAGCCCCAGGCAGAGCCCGTGTGGACCCCGCCAGCCCGGCTCCCGCCGCGCCCCCT  
CCACCCCGGCCGCGCCCAAGCGC

TCTGTTGCGCGCTTCTGCTTCCCGAGCTCTATAAAAGAGCTCACAACCCCTCACTCGG  
CGCGCCAGTCCTCCGACAGACTGAGTCGCCCCGGGGGGGATCCATGGAAGACCTGGAC  
CAGTCTCCTCTGGTCTCGTCCTCGGACAGCCCACCCCGGCCGAGCCCGCGTTCAAGTA  
CCAGTTCGTGAGGGAGCCCGAGGACGAGGAG

CACAACCCCTCACTCGGCGCGCCAGTCCTCCGACAGACTGAGTCGCCCCGGGGGGGATCC  
TATGGAAGACCTGGACCAGTCTCCTCTGGTCTCGTCCTCGGACAGCCCACCCCGGCCG  
AGCCCGCGTTCAAGTACCAGTTCGTGAGGGAGCCCGAGGACGAGGAGG

MEDLDQSPLV SSSDSPRPQ PAFKYQFVRE PEDEEEEEEE EEEDEDEDLE ELEVLERKPA  
AGLSAAPVPT APAAGAPLMD FGNDVFPAP RGPLPAAPPV APERQPSWDP SPVSSTVPAP  
SPLSAAAVSP SKLPEDDEPP ARPPPPPPAS VSPQAEPVWT PPAPAPAAPP STPAAPKR

**Reverse primer 5'-GAGAGCCAAAATCAGTAGTGTCAG-3'**

ACCCACATCAACACTGCAAACCTTCAGAGAATCAACTAAATCATCAACTAAGAAGAGGCGC  
CTGAGTTCCTTTATCGTGCAGTTCACATGACCAAGAGCAGAATTACTGTACTTCTGAACC  
AACTCCTCAGATATAGCAAACCTTCAGATTCCAGATATGCCCTGAATGGGTGGCCTTCATCT  
GATTTCTGGATAGCTTGGATCACACCCTTGTATATCCTAAAGCTGATGGTCACAGAGAGC  
AGGGCCAAGGCAATGTAGGCTGTTACGCTCACAATGCTGAATACTGTCAATGAAAGCAG  
CAGGAATAGGCTGGCACCAAACACCACTCCAGTCTTCTTAATGTCTCTCCAGTACAGGAG

GTCAACAACCACTGAGCCCGAGGAGCCCCTGCGCTTGGGCGCGGCCGGGGTGGAGGGG  
 GGCGCGGGGAGCCGGGGCTGGCGGGGTCCACACGGGCTCTGCCTGGGGGCTCACG  
 CTGGCCGGGGGAGGAGGGGGAGGCCGGGCCGAGGCTCGTCGTCTCAGGGAGCTTG  
 GAGGGCGAGACTGCGGCAGCAGACAGCGGGGATGGCGCGGGCACGGTCGACGACACC  
 GGGCTCGGGTCCCAAGACGGCTGCCGCTCCGGGGCGACGGGGGGAGCGGCCGGCAGG  
 GGTCCCCGGGGCGCCGGCGGCACGAAGTCATTTCCGAAGTCCAT

**AGGCCTCTCGAGT**TCAAGCGTAGTCTGGGACGTCGTATGGGTAGCCACCTTCAGCTTTG  
 CGTTCAATCCAGGGATTTTTGCTTGGATTTTAGCCATAGCATCTTTAACATTCTTATTT  
 GCAAGTCCTAGATAATGATCTATCTGTGCCTGATGCCGTTCATAAATAACAGGAACACTG  
 AAGAGTGAAATGAGAGCCAAAATCAGTAGTGTGACACCATTAAACAAGGCACCAACATAG  
 GTAAATACCCACATCAACACTGCAAATTCAGAGAATCAACTAAATCATCAACTAAGAAGA  
 GGCGCCTGAGTTCCTTTATCGTGCAGTTCACATGACCAAGAGCAGAATTACTGTACTTCT  
 GAACCAACTCCTCAGATATAGCAACTTCAGATTCCAGATATGCCCTGAATGGGTGGCCTT  
 CATCTGATTTCTGGATAGCTTGGATCACACCCTTGTATATCCTAAAGCTGATGGTCACAG  
 AGAGCAGGGCCAAGGCAATGTAGGCTGTTACGCTCACAATGCTGAATACTGTCAATGAA  
 AGCAGCAGGAATAGGCTGGCACCAAACACCACTCCAGTCTTCTTAATGTCTCTCCAGTAC  
 AGGAGGTCAACAACCACTGAGCCCGAGGAGCCCCTGCGCTTGGGCGCGGCCGGGGTGG  
 AGGGGGGCGCGGGGAGCC

**GGCCTCTCGAGT**TCAAGCGTAGTCTGGGACGTCGTATGGGTAGCCACCTTCAGCTTTGC  
 GCTTCAATCCAGGGATTTTTGCTTGGATTTTAGCCATAGCATCTTTAACATTCTTATTTG  
 CAAGTCCTAGATAATGATCTATCTGTGCCTGATGCCGTTCATAAATAACAGGAACACTGA  
 AGAGTGAAATGAGAGCCAAAATCAGTAGTGTGACACCATTAAACAAGGCACCAACATAG  
 GTAAATACCCACATCAACACTGCAAATTCAGAGAATCAACTAAATCATCAACTAAGAAGA  
 GGCGCCTGAGTTCCTTTATCGTGCAGTTCACATGACCAAGAGCAGAATTACTGTACTTCT  
 GAACCAACTCCTCAGATATAGCAACTTCAGATTCCAGATATGCCCTGAATGGGTGGCCTT  
 CATCTGATTTCTGGATAGCTTGGATCACACCCTTGTATATCCTAAAGCTGATGGTCACAG  
 AGAGCAGGGCCAAGGCAATGTAGGCTGTTACGCTCACAATGCTGAATACTGTCAATGAA  
 AGCAGCAGGAATAGGCTGGCACCAAACACCACTCCAGTCTTCTTAATGTCTCTCCAGTAC  
 AGGAGGTCAACAACCACTGAGCCCGAGGAGCCCCTGCGCTTGGGCGCGGCCGGGGTGG  
 AGGGG

VVDLL YWRDIKKTGV VFGASLFLLL SLTVFSIVSV TAYIALALLS VTISFRIYKG  
 VIQAIQKSD E GHPFRAYLES EVAISEELVQ KYSNSALGHV NCTIKELRRL FLVDDLVDLSL

KFAVLMWVFT YVGALFNGLT LLILALISLF SVPVIYERHQ AQIDHYLGLA NKNVKDAMAK  
 IQAKIPGLKR KAEGGYPYDV PDYA

**Forward primer 5'-GCAGTCTCGCCCTCCAAG-3'**

CTCCCCCTCCTCCCCGGCCAGCGTGAGCCCCAGGCAGAGCCCGTGTGGACCCGCCA  
 GCCCCGGCTCCCGCCGCGCCCCCTCACCCCGGCCGCGCCCAAGCGCAGGGGCTCCTC  
 GGGCTCAGTGGTTGTTGACCTCCTGTACTGGAGAGACATTAAGAAGACTGGAGTGGTGT  
 TTGGTGCCAGCCTATTCCTGCTGCTTTCATTGACAGTATTCAGCATTGTGAGCGTAACAG  
 CCTACATTGCCTTGGCCCTGCTCTCTGTGACCATCAGCTTTAGGATATAACAAGGGTGTGA  
 TCCAAGCTATCCAGAAATCAGATGAAGGCCACCCATTCAGGGCATATCTGGAATCTGAAG  
 TTGCTATATCTGAGGAGTTGGTTCAGAAGTACAGTAATTCTGCTCTTGGTCATGTGAACT  
 GCACGATAAAGGAACTCAGGCGCCTCTTCTTAGTTGATGATTTAGTTGATTCTCTGAAGT  
 TTGCAGTGTGATGTGGGTATTTACCTATG

GTACTGGAGAGACATTAAGAAGACTGGAGTGGTGTGGTGCCAGCCTATTCCTGCTGC  
 TTTTCATTGACAGTATTCAGCATTGTGAGCGTAACAGCCTACATTGCCTTGGCCCTGCTCT  
 CTGTGACCATCAGCTTTAGGATATAACAAGGGTGTGATCCAAGCTATCCAGAAATCAGATG  
 AAGGCCACCCATTCAGGGCATATCTGGAATCTGAAGTTGCTATATCTGAGGAGTTGGTT  
 CAGAAGTACAGTAATTCTGCTCTTGGTCATGTGAACTGCACGATAAAGGAACTCAGGCG  
 CCTCTTCTTAGTTGATGATTTAGTTGATTCTCTGAAGTTTGCAGTGTGATGTGGGTATT  
 TACCTATGTTGGTGCCTTGTTAATGGTCTGACACTACTGATTTTGGCTCTCATTTCACT  
 CTTCAGTGTTCCTGTTA

**Reverse primer 5'-GAGAGCCAAAATCAGTAGTGTCAG-3'**

TCAACACTGCAAACCTTCAGAGAATCAACTAAATCATCAACTAAGAAGAGGCGCCTGAGTT  
 CCTTTATCGTGCAGTTCACATGACCAAGAGCAGAATTACTGTACTTCTGAACCAACTCCT  
 CAGATATAGCAACTTCAGATTCCAGATATGCCCTGAATGGGTGGCCTTCATCTGATTTCT  
 GGATAGCTTGGATCACACCCTTGATATCCTAAAGCTGATGGTCACAGAGAGCAGGGCC  
 AAGGCAATGTAGGCTGTTACGCTCACAATGCTGAATACTGTCAATGAAAGCAGCAGGAA  
 TAGGCTGGCACCAAACACCACTCCAGTCTTCTTAATGTCTCTCCAGTACAGGAGGTCAAC  
 AACCACTGAGCCCGAGGAGCCCCTGCGCTTGGGCGCGGCCGGGGTGGAGGGGGGCGC  
 GGCGGGAGCCGGGGCTGGCGGGGTCCACACGGGCTCTGCCTGGGGGCTCACGCTGGC  
 CGGGGGAGGAGGGGGAGGCCGGGCCGGAGGCTCGTCGTCCTCAGGGAGCTTGGAGGG  
 CGAGACTGCGGCAGCAGACAGCGGGGATGGCGCGGGCACGGTTCGACGACACCGGGCTC

GGGTCCCAAGACGGCTGCCGCTCCGGGGCGACGGGGGAGCGGCCGGCAGGGGTCCC  
 CGGGGCGCCGGCGGCACGAAGTCATTTCCGAAGTCCATCAGGGGCGCGCCGGCGGCAG  
 GG

ACACTGCAAACCTTCAGAGAATCAACTAAATCATCAACTAAGAAGAGGGCGCCTGAGTTCCT  
 TTATCGTGCAGTTCACATGACCAAGAGCAGAATTACTGTACTTCTGAACCAACTCCTCAG  
 ATATAGCAAACCTTCAGATTCCAGATATGCCCTGAATGGGTGGCCTTCATCTGATTTCTGGA  
 TAGCTTGGATCACACCCTTGTATATCCTAAAGCTGATGGTCACAGAGAGCAGGGCCAAG  
 GCAATGTAGGCTGTTACGCTACAATGCTGAATACTGTCAATGAAAGCAGCAGGAATAG  
 GCTGGCACCAAACACCACTCCAGTCTTCTTAATGTCTCTCCAGTACAGGAGGTCAACAAC  
 CACTGAGCCCGAGGAGCCCCTGCGCTTGGGCGCGGCCGGGGTGGAGGGGGGCGCGGC  
 GGGAGCCGGGGCTGGCGGGGTCCACACGGGCTCTGCCTGGGGGCTCACGCTGGCCGG  
 GGGAGGAGGGGGAGGCCGGGCCGGAGGCTCGTCGTCCTCAGGGAGCTTGGAGGGCGA  
 GACTGCGGCAGCAGACAGCGGGGATGGCGCGGGCACGGTCGACGACACCGGGCTCGG  
 GTCCCAAGACGGCTGC

**Appendix 2. DNA sequencing for the full-length Nogo-B lentiviral construct plasmid.**

DNA sequencing was carried out on pHR'SIN-cPPT-SFFV-fulllengthNogo-B-WPRE plasmid. Italic labelling = lentiviral construct sequence, blue and underlined labelling = restriction enzyme recognition sites *Bam*HI or *Xho*I and red labelling = Nogo-B sequence.

***DNA sequencing for mutant (soluble) Nogo-B in the lentiviral construct plasmid***

**Forward primer 5'-CAATCAGCCTGCTTCTCG-3'**

TCCTCCGACAGACTGAGTCGCCCGGGGGGGGATCCTATGGAAGACCTGGACCAGTCTCCT  
 CTGGTCTCGTCTCGGACAGCCACCCCGGCCGAGCCCGCGTTCAAGTACCAGTTCGT  
 GAGGGAGCCCGAGGACGAGGAGGAAGAAGAGGAGGAGGAAGAGGAGGACGAGGACGA  
 AGACCTGGAGGAGCTGGAGGTGCTGGAGAGGAAGCCCGCCCGGGCTGTCCGCGGCC  
 CCAGTGCCACCGCCCCTGCCGCCGGCGCGCCCTGATGGACTTCGGAATGACTTCGT  
 GCCGCCGGCGCCCCGGGACCCCTGCCGGCCGCTCCCCCGTCGCCCGGAGCGGCAG  
 CCGTCTTGGGACCCGAGCCCGGTGTCGTCGACCGTGCCCGCGCCATCCCCGCTGTCTGC  
 TGCCGCAGTCTCGCCCTCCAAGCTCCCTGAGGACGACGAGCCTCCGGCCCGGCCTCCCC  
 CTCCTCCCCGGCCAGCGTGAGCCCCAGGCAGAGCCCGTGTGGACCCCGCCAGCCCCG  
 GCTCCCGCCGCGCCCCCTCCACCCCGGCCGCGCCCAAGCGCAGGGGCTCCTCGGGCTC  
 AGTGGTTGTTGACCTCCTGTACTGGAGAGACATTAAGAAGACTGGAGTGGTG

GCGCCAGTCCTCCGACAGACTGAGTCGCCCGGGGGGGGATCCTATGGAAGACCTGGACC  
 AGTCTCCTCTGGTCTCGTCTCGGACAGCCACCCCGGCCGAGCCCGCGTTCAAGTAC  
 CAGTTCGTGAGGGAGCCCGAGGACGAGGAGGAAGAAGAGGAGGAGGAAGAGGAGGAC  
 GAGGACGAAGACCTGGAGGAGCTGGAGGTGCTGGAGAGGAAGCCCGCCCGGGCTGT  
 CCGCGGCCCCAGTGCCACCGCCCCTGCCGCCGGCGCGCCCTGATGGACTTCGGAAT  
 GACTTCGTGCCGCCGGCGCCCCGGGACCCCTGCCGGCCGCTCCCCCGTCGCCCGG  
 AGCGGCAGCCGTCTTGGGACCCGAGCCCGGTGTCGTCGACCGTGCCCGC

MEDLDQSPLV SSSDSPRPQ PAFKYQFVRE PEDEEEEEEE EEEDEDEDLE ELEVLERKPA  
 AGLSAAPVPT APAAGAPLMD FGNDVFPAP RGPLPAAPPV APERQPSWDP SPVSSTVPAP  
 SPLSAAAVSP SKLPEDEPP ARPPPPPPAS VSPQAEPVWT PPAPAPAAPP STPAAPKRRG  
 SSGSVVDLL YWRDIKKTGV V

**Reverse primer 5'-ATGCCTGCAGGTCGACTCTAG-3'**

GGCCTCTCGAGATCACACCACTCCAGTCTTCTTAATGTCTCTCCAGTACAGGAGGTCAAC  
 AACCACTGAGCCCGAGGAGCCCCTGCGCTTGGGCGCGGCCGGGGTGGAGGGGGGCGC  
 GGCGGGAGCCGGGGCTGGCGGGGTCCACACGGGCTCTGCCTGGGGGCTCACGCTGGC  
 CGGGGGAGGAGGGGGAGGCCGGGCCGGAGGCTCGTCGTCCTCAGGGAGCTTGGAGGG

CGAGACTGCGGCAGCAGACAGCGGGGATGGCGCGGGCACGGTTCGACGACACCGGGGCTC  
GGGTCCCAAGACGGCTGCCGCTCCGGGGCGACGGGGGAGCGGCCGGCAGGGGTCCC  
CGGGGCGCCGGCGGCACGAAGTCATTTCCGAAGTCCATCAGGGGCGCGCCGGCGGCAG  
GGGCGGTGGGCACTGGGGCCGCGGACAGCCCGGCGGGGCTTCCTCTCCAGCACCTC  
CAGCTCCTCCAGGTCTTCGTCTCGTCCTCCTCCTCCTCCTCCTCCTCCTCCTCCTCGTCC  
TCGGGCTCCCTCACGAAGTGGTACTTGAACGCGGGCTGCGGCCGGGGTGGGCTGTCCG  
AGGACGAGACCAGAGGAGACTGGTCCAGGTCTTCCATAGGA

*GGCT*CTCGAGATCACACCACTCCAGTCTTCTTAATGTCTCTCCAGTACAGGAGGTCAAC  
AACCACTGAGCCCGAGGAGCCCCTGCGCTTGGGCGCGGCCGGGGTGGAGGGGGGCGC  
GGCGGGAGCCGGGGCTGGCGGGGTCCACACGGGCTCTGCCTGGGGGCTCACGCTGGC  
CGGGGAGGAGGGGGAGGCCGGGCCGAGGCTCGTCGTCTCAGGGAGCTTGGAGGG  
CGAGACTGCGGCAGCAGACAGCGGGGATGGCGCGGGCACGGTTCGACGACACCGGGGCTC  
GGGTCCCAAGACGGCTGCCGCTCCGGGGCGACGGGGGAGCGGCCGGCAGGGGTCCC  
CGGGGCGCCGGCGGCACGAAGTCATTTCCGAAGTCCATCAGGGGCGCGCCGGCGGCAG  
GGGCGGTGGGCACTGGGGCCGCGGACAGCCCGGCGGGGCTTCCTCTCCAGCACCTC  
CAGCTCCTCCAGGTCTTCGTCTCGTCCTCCTCCTCCTCCTCCTCCTCCTCCTCCTCGTCC  
TCGGGCTCCCTCACGAAGTGGTACTTGAACGCGGGCTGCGGCCGGGGTGGGCTGTCCG  
AGGACGAGACCAGAGGAGACTGGTCCAGGTCTTCCATAGGATCCCCCGGGCGACTCA  
GTCTGTGCGGAGGACTGGCGCGCCGAGT

MEDLDQSPLV SSSDSPRPQ PAFKYQFVRE PEDEEEEEEE EEEDEDEDLE ELEVLERKPA  
AGLSAAPVPT APAAGAPLMD FGNDVFPAP RGPLPAAPPV APERQPSWDP SPVSSTVPAP  
SPLSAAVSP SKLPEDEPP ARPPPPPPAS VSPQAEPVWT PPAPAPAAPP STPAAPKRRG  
SSGSVVVDLL YWRDIKKTGV V

**Appendix 3. DNA sequencing for the mutant (soluble) Nogo-B lentiviral construct plasmid.**

DNA sequencing was carried out on pHR'SIN-cPPT-SFFV-mutant Nogo-B-WPRE plasmid. Italic labelling = lentiviral construct sequence, blue and underlined labelling = restriction enzyme recognition sites *Bam*HI or *Xho*I and red labelling = Nogo-B sequence.